Metabolic transport blockade enhances chimeric antigen receptors T cell therapy against B cell lymphoma.

Submitted by:

Ernesto López Cabrera

Cancer institute PhD

Haematology department, Cancer Institute

University College London

July 2023

Declaration.

UCL Research Paper Declaration Form

referencing the doctoral candidate's own published work(s)

1. **For a research manuscript that has already been published** (if not yet published, please skip to section 2)

a) **What is the title of the manuscript?**

Inhibition of lactate transport by MCT-1 blockade improves chimeric antigen receptor T cell therapy against B cell malignancies.

b) **Please include a link to or doi for the work**

http://dx.doi.org/10.1136/jitc-2022-006287

c) **Where was the work published?**

Journal of ImmunoTherapy of Cancer

d) **Who published the work?** (e.g. OUP)

BJM

e) **When was the work published?**

July 2023

f) **List the manuscript's authors in the order they appear on the publication**

Ernesto López, Rajesh Karattil, Francesco Nannini, Gordon Weng-Kit Cheung, Lilian Denzler, Felipe Gálvez-Cancino, Sergio Quezada, Martin Pule.

g) **Was the work peer reviewed?**

Yes

h) **Have you retained the copyright?**

Yes

i) **Was an earlier form of the manuscript uploaded to a preprint server?** (e.g. medRxiv). If 'Yes', please give a link or doi)

No

If 'No', please seek permission from the relevant publisher and check the box next to the below statement:

☒

I acknowledge permission of the publisher named under **1d** to include in this thesis portions of the publication named as included in **1c**.

2. **For multi-authored work, please give a statement of contribution covering all authors** (if single-author, please skip to section 4)

E.L., S.Q. and M.P. designed the study, E.L., R.K., F.N., G.W.C., L.D. and F.G. conducted experiments, E.L., R.K., F.N., L.D. and F.G. acquired data, E.L., R.K., F.N., analysed data, E.L. and M.P wrote the manuscript.

3. **In which chapter(s) of your thesis can this material be found?**

Chapter 2, 3 and 4

4. **e-Signatures confirming that the information above is accurate** (this form should be co-signed by the supervisor/ senior author unless this is not appropriate, e.g. if the paper was a single-author work)

Candidate

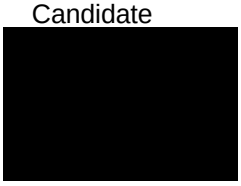

Date:

11th of July 2023

Supervisor/ Senior Author (where appropriate)

Date

11th of July 2023

I, Ernesto Lopez Cabrera, hereby confirm the work presented in this PhD thesis is my own. Where information has been derived from other sources, I confirm this was clearly indicated in the thesis.

Acknowledgments.

I think it is easy to convince ourselves that our victories are solely our own but reflecting on the (sometimes) Sisyphean task of doing public research, is easy to realize this PhD project could not have been done without the incredible support of family and friends. Not everyone can be thanked by name here, but I did my best.

This work is dedicated to my parents, Lilian and Pedro, and my stepdad, Miguel. Their unshakable tenacity is a constant inspiration and without their unconditional support from the beginning of my scientific path, I couldn't have developed the career I always dreamt of. Also, I must thank my long-suffering brother (Carlos) and sisters (Fernanda, Amparo and Ignacia). They had to hear me passionately talk about science for years now.

Thanks to my supervisors and mentors, Martin and Sergio, for their incredible commitment to research quality and the support to pursue my interests. All of this, together with the Pule and Quezada Lab members, with special mention to Raj, Ignacio, Dafne, Francesco, and Gordon. It is nice to meet new colleagues, but making friends along the way is even better.

I am lucky to have a great support network in at least two countries, an incredible group of friends who support me in ways that are hard to quantify scientifically. My high school and Uni friends have remained very close over the years, and they are a great group to bounce ideas and share stories. The Duckett family, I don't have many opportunities to rant about philosophy and politics in the lab, so I am glad I quickly found an incredible group of people to do so. Malika, growing as a scientist these last years has been incredibly rewarding, but growing as a person is incalculable.

Impact statement.

Chimeric antigen receptor (CAR) T cells have become the standard of care for patients with B-cell malignancies. However, most patients infused with CAR T cells relapse, highlighting the necessity of increasing their antitumoral efficacy by combination with other treatments.

My PhD aimed to improve CAR T cell therapies by exploiting metabolic vulnerabilities of cancer. This included testing changes in the antitumoral potential of CAR T cells in culture with small molecules blocking metabolic transporters, like monocarboxylate transporters (MCTs) and the Alanine, Serine, Cysteine Transporter 2 (ASCT-2), the main glutamine transporter in cancer and T cells.

From this research, we identify MCT-1 inhibition as an interesting target to improve the antitumoral potential of CD19-targeted CAR T cells; this could immediately impact the design of future clinical trials targeting MCT-1 positive tumours. Additionally, we have shown ASCT-2 blockade is deleterious in human CAR T cells by blocking glutamine consumption and identifying potential mechanisms to resist ASCT-2 inhibition.

This studentship greatly enhanced my knowledge and skill in several areas, including molecular biology, immunology, and protein engineering. With the support of my supervisors, I had excellent training and developed several skills, which helped me find a Postdoctoral training Fellow position after finishing the thesis at UCL.

Finally, most of this work has been recently published in the Journal of Immunotherapy of Cancer under the title “Inhibition of lactate transport by MCT-1 blockade improves chimeric antigen receptor T cell therapy against B cell malignancies.”

Abstract.

Chimeric antigen receptor (CAR) T cells have shown remarkable results against B cell malignancies, but only a minority of patients have long-term remission. The metabolic requirements of both tumour cells and activated T cells result in production of lactate and depletion of key nutrients fundamental for T cell function, like glucose and glutamine. Here, we studied the combination of CD19-specific CAR T cell therapy with pharmacological blockade of metabolic transporters against B cell lymphoma.

The export of lactate is facilitated by expression of monocarboxylate transporters (MCTs). CAR T cells express high levels of MCT-1 and MCT-4 upon activation, while certain tumours predominantly express MCT-1. MCT-1 inhibition with the small molecules AZD3965 or AR-C155858 induced CAR T cell metabolic rewiring, but their effector function and phenotype remained unchanged, suggesting CAR T cells are insensitive to MCT-1 inhibition. Moreover, improved cytotoxicity in vitro and antitumoral control on mouse models was found with the combination of CAR T cells and MCT-1 blockade.

Tumour and CAR T cells express high levels of the glutamine transporter ASCT-2 to sustain energy and biomass production. Pharmacological inhibition of ASCT-2 with V-9302 severely suppressed CAR T cell functions and expression of surrogate glutamine transporters like ATB^{0+}, partially restored CAR T cell proliferation. However, glutamine-neutralizing antibodies against ASCT-2 showed limited efficacy against tumour and CAR T cells.

This work highlights the potential of selective targeting metabolism via inhibition of metabolic transporters in combination with CAR T cells therapies against B cell malignancies.

List of abbreviations.

2-DG: 2-Deoxy-d-Glucose.

ACT: Adoptive cell therapy.

ADP: Adenosine diphosphate.

ALL: Acute lymphoblastic leukaemia.

ATCC: American Type Culture Collection.

ATP: Adenosine triphosphate.

BFP: Blue fluorescent protein

CAR: Chimeric antigen receptor.

CCR: C-C chemokine receptor.

CD: Cluster of differentiation.

CLL: Chronic lymphocytic leukaemia.

CTLA: Cytotoxic T-lymphocyte–associated antigen.

DMEM: Dulbecco's Modified Eagle Medium.

DMSO: Dimethyl sulfoxide.

DNA: Deoxyribonucleic acid.

DON: 6-Diazo-5-oxo-L-norleucine.

ECAR: Extracellular acidification rate.

FACS: Fluorescence-activated cell sorting.

FBS: Fetal bovine serum.

FDA: Food and Drug administration.

GFP: Green fluorescent protein

GM-CSF: Granulocyte macrophage colony-stimulating factor.

HLA: Human leukocyte antigen.

IL: Interleukin.

IMDM: Iscove's Modified Dulbecco's Medium.

IRES: Internal ribosome entry site.

IFN: Interferon.

LDH: Lactate dehydrogenase.

MCT: Monocarboxylate transporter.

MHC: Major histocompatibility complex.

mTOR: Mammalian target of rapamycin.

NAD: Nicotinamide adenine dinucleotide.

NHL: Non-Hodgkin lymphoma.

NK: Natural killer.

NSCLC: Non-small cell lung cancer.

NT: Non-transduced.

OCR: Oxygen consumption rate.

OXPHOS: Oxidative phosphorylation.

PD: Programmed cell death protein.

Rpm: Revolutions per minute.

RPMI: Roswell Park Memorial Institute.

SEM: Standard error of the mean.

SD: Standard deviation.

SLC: Human Solute Carrier

ScFv: Single-chain Fragment variable fragment.

TCA: Tricarboxylic acid.

TCR: T cell receptor.

TIL: Tumour infiltrating lymphocyte.

TIM: Transmembrane immunoglobulin and mucin domain

TME: Tumour microenvironment.

TNF: Tumour necrosis factor.

Table of Contents

List of Figures.

List of Tables.

1 Introduction.

1.1 Cancer Immunotherapy.

1.1.1 T cell immunology.

Immunotherapy has emerged as a promissory alternative for cancer treatment as it utilizes the capacity of the immune system, particularly cytotoxic T cells, to recognize and eliminate target cells. The antitumoral immune response is initiated by antigen-presenting cells (APCs), which can phagocyte malignant cells and load cancer antigens into their major histocompatibility complex (MHC) class I and II. cytotoxic T lymphocytes (T cells) can then recognize the peptide-MHC complex by engaging with a T cell receptor (TCR) expressed on the T cell surface and initiate T cell activation.

T cells are categorized by their function and interaction with MHC molecules as CD8 or CD4 T cells. CD8 T cells recognize antigens loaded to MHC-I and are the main drivers of tumour cell lysis while CD4 T cells recognize peptides loaded to MHC-II and sustain a pro-inflammatory by cytokine release and other stimulatory factors. Upon TCR engagement, multi-molecular signalosomes assemble to interact with the TCR-CD3 complex, recruiting Lck kinases to phosphorylate the TCR-CD3 complex and ZAP70. Distal signalling cascades are then initiated, including Ca^{2+} signalling, PI3K-mTOR-ERK activation, which in turn starts the activation of transcription factors to initiate gene upregulation [1,2]. This results in clonal expansion of T cells and differentiation into an effector program which includes the release of cytokines (such as IL-2 and IFN-γ), lytic molecules (such as Perforin and Granzyme B), expression of activation markers and chemokines receptors to guide T cell infiltration to specific tissues, all fundamental processes for T cell antitumoral immunity.

After activation, T cells can differentiate into distinct memory populations with specific metabolic requirements and functions. On IL-7 signalling helps naïve T cells to maintain their

homeostatic proliferation before antigen recognition, relying on fatty acid catabolism to sustain OXPHOS and ATP production instead of glucose [3]. After TCR engagement, the mTOR kinase pathway integrates activation and metabolic signals to induce T cell activation and is a global metabolic regulator as T cell activation profoundly rearrange their metabolic networks to meet the energetic demands of clonal expansion. In the initial minutes after MHC-TCR engagement, T cells show a rapid induction of aerobic glycolysis and mTOR activation, necessary steps for T cell activation [4]. mTOR deficient T cells failed to upregulate the glutamine transporter GLUT-1 and glycolytic enzymes [5] while having defects in lipid biosynthesis and oxidative phosphorylation [6].

Importantly, metabolites can also act as mTOR regulators and affect T signal transduction networks [7]. Mechanistically, activation of mTOR requires its translocation to the lysosome surface, a process mediated by Rag GTPases. In presence of amino acids, Rag GTPase remains in an active state, recruiting Rheb protein, a direct activator of mTORC1, finally inducing mTOR activity [8]. Glutamine availability directly acts as a signalling molecule for modulating mTOR activity and T cells cultured on reduced glutamine failed to engage mTOR and had reduced proliferation [9]. Additionally, leucine is sufficient to restore mTOR activity and impairing leucine uptake by blocking the transporter SLC7A5 reduces mTORC1 activity similar to pan-amino acid deprivation [10].

Similarly, the reduction of energy levels can be directly detected by the AMP-activated protein kinase (AMPK) network. AMPK binds to ATP, and the lower enzymatic products ADP and AMP, sensing their relative concentration. A reduction in ATP levels triggers AMPK kinase activity and activates different metabolic pathways promoting glycolysis, mitochondrial and lipid metabolism while suppressing mTOR activity [11].

After cognate antigen elimination, T cells develop immunological memory to quickly mount an immune response against repeated infections. T cells are categorized into different subsets of memory T cells with distinct functions and metabolic networks. Central memory T cells (T_{CM}) circulate between blood and secondary lymphoid organs, are long-lived and exhibit a metabolism more dependent on respiration, increased mitochondrial mass and utilize fatty acid oxidation to feed the TCA cycle rather than glucose. In contrast, effector memory T cells (T_{EM}) circulate between blood and non-lymphoid tissues, with quick proliferation after antigen engagement, relying more on glucose catabolism than respiration to sustain their energetic demands [12]. Moreover, cancer immunotherapies relying on naïve T cells or T_{CM} show superior antitumoral immunity in several mouse models and clinical trials [13].

1.1.2 Tumour infiltrating lymphocytes (TILs).

One of the first T cell immunotherapies was the ex vivo expansion of TILs from a biopsy of a tumour sample. T cells recovered from biopsies are cultured with high doses of IL-2 and with antibodies against CD3 to induce T cell activation. Patients are then lymphodepleted and the expanded TILs product is reinfused into the patients, followed by systemic administration of IL-2 to facilitate T cell expansion.

Patients with advanced cutaneous melanoma treated with TIL therapy between 1998 and 2016 had an objective response rate (OCR) of 41% and complete response rate of 12% [14,15]. A recent study recruiting metastatic melanoma showed 50% OCR with neoantigen-specific T cells detected for 3 years [15]. TILs treatment has found positive results against cervical cancers [16] and preliminary efficacy on colorectal, lung and breast cancer. To improve clinical responses, the identification of additional surface markers to select and expand tumour-reactive TILs instead of bulk T cells is a commonly used strategy. For example, expression of the programmed Cell Death Protein 1 (PD-1) or the tissue-resident markers CD103 or CD39 on CD8 T cells has been

associated with a better clinical response in patients with solid tumours, and selection of PD-1^{+} CD8 TILs or CD103^{+} CD39^{+} CD8 TILs showed improved antitumoral responses [17,18].

Cancer treatment has been revolutionized by the treatment with immune checkpoint blockade. Blocking PD-1, PD-L1 or CTLA-4 with monoclonal antibodies release the potential of the immune system to kill cancer cells. Immune checkpoint therapy had remarkable results in improving the response rate of patients with solid tumours and have been approved as 1st, 2nd and 3rd line treatment for melanoma, lung, breast, ovarian, and renal cancer, among others [19]. Therefore, the combination of TILs therapy with PD-1 antibodies has shown preliminary favourable results in melanoma and metastatic osteosarcoma, with more clinical trials ongoing for different metastatic solid tumours [20].

However, the main limitation of this treatment is the need for an accessible biopsy and enough tumour material to expand tumour-reactive T cells, which makes this treatment hard to access for most patients [21-23]. Additionally, a study with melanoma samples found only 67% of active, specific TILs identified in vitro were able to be expanded [24], making this therapy not accessible for most patients.

1.1.3 TCR-engineered T cell therapy.

To overcome these limitations, TCRs recognizing antitumoral antigens with high affinity can be identified within the TILs population. These antitumoral TCRs can be sequenced, and T cells can be genetically engineered to express these transgenic antitumoral TCRs. These "T cell receptor-engineered" T (TCR-T) cells are manufactured and injected into patients, eliciting a potent immune response and tumour regression.

Depending on the tumour antigen targeted, TCR therapy can be divided broadly in cancer germline antigens (CGAs) or neo-antigens. CGAs are proteins expressed in germline tissues while epigenetically silenced in somatic tissues. Due to genetic deregulation, cancer cells re-

express these proteins, making them ideal candidates for targeted therapies. Most clinical trials targeting CGAs are focused on the melanoma-associated antigen (MAGE-A) protein family and the New York oesophageal squamous cell carcinoma 1 (NY-ESO-1).

TCR-T cell targeting NY-ESO-1 showed an objective response rate between 20-67% percent in 107 patients with melanoma and synovial sarcoma from 5 different clinical trials, with 40 partial responses and 8 complete responses. Importantly, no significant toxicities were observed [25]. Meanwhile, a recent phase II clinical trial targeting MAGE-A4 in patients with synovial sarcoma showed an objective response rate of 39.4% and a disease control rate of 84.8% (NCT04044768). On the other hand, neo-antigens (NeoAgs) arise from somatic mutations, are only expressed in tumour cells, and can bind with high affinity to TCRs. TCR-T cell therapy targeting common cancer mutations in cancer driver genes, like TP53, KRAS, or PIK3CA are currently being tested in phase I clinical trials [26]. Recent advances have allowed the identification of multiple TCRs specific from each patient neo-antigen pool and inserting the new transgenic TCRs using CRISPR–Cas9 gene editing in 16 patients with refractory solid tumours (NCT03970382). Five patients infused had stable disease and the other 11 had disease progression as best response on therapy, with the neoTCR being detected in tumour samples at frequencies higher than the native TCRs [27].

However, some limitations exist with TCR-T cell therapy. HLA loss is an important resistance mechanism to TCR-based therapies, as it render tumour cells invisible to T cell recognition. Moreover, 80% of the clinical trials testing TCR-Ts are HLA-A*02 restricted. HLA-A*02 is the most common allele expressed in the Caucasian population, accounting for approximately 25%, of HLAs in the West [28], limiting the applicability of this therapy [29].

1.2 CAR T cell therapy.

1.2.1 CAR structure.

Chimeric antigen receptors are recombinant proteins with distinct domains: (a) an extracellular portion composed of a single-chain variable fragment (scFv) from a monoclonal antibody with high affinity to surface tumour antigens, (b) a hinge domain to confer flexibility to the construct, (c) a transmembrane domain and (d) signalling domains which mediates T cell activation (Figure 1.2).

CAR T cells recognize surface antitumoral antigens via the interaction of their antitumoral ScFv and the target protein independently of MHC-I/peptide interactions, triggering CAR dimerization and recruiting the components of the TCR-CD3z signalling pathways, activating T cells similar to TCR engagement. A first-generation CAR had only a CD3z intracellular domain, these CAR T cells showed efficient antigen engagement, tumour cell lysis and T cell activation; however, they failed to elicit significant tumour control in clinical trials due to poor T cell persistence after infusion [30]. To enhance CAR T cell efficacy, co-stimulation domains were added to the CAR structure to enhance T cell activation and proliferation. CD28 or 41BB co-stimulation domains are the most used in experimental settings and clinical trials. Human CD28-costimulated CAR T cells have shown exhibit rapid proliferation and IFN-γ production, providing an stronger effector response, while 41BB activation promotes persistence and increases the expression of anti-apoptotic proteins, favouring long-term proliferation [31].

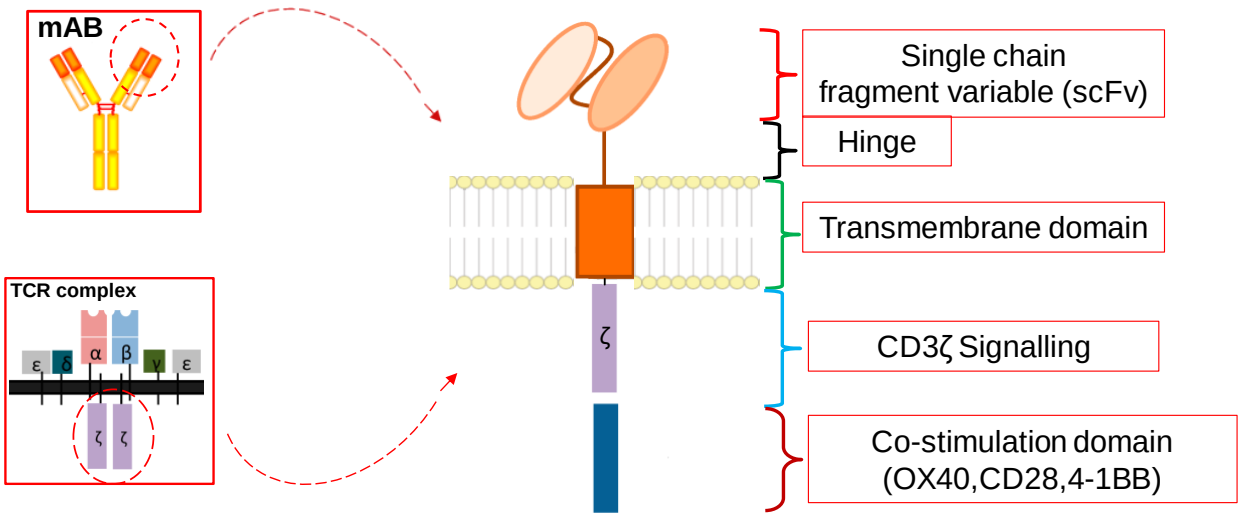

Figure 1.1: Structure of a second-generation chimeric antigen receptor.

1.2.2 CAR T cells against B cell malignancies.

Human CD19 antigen is a transmembrane protein part of the immunoglobulin superfamily. CD19 is highly expressed in mature B cells and in most B cell malignancies, including acute lymphoblastic leukaemia (ALL), chronic lymphocytic leukaemia (CLL) and B cell lymphomas [32].

Anti-CD19 CAR engineered T cells have proven highly effective in treating refractory lymphoid malignancies. Patients infused with CD19-directed CAR T-cells have shown complete response on 67%-85% for B-cell acute lymphoblastic leukaemia (B-ALL) and 50% for B-cell non-Hodgkin lymphoma (B-NHL) patients in numerous clinical trials [33-35]. Despite their success, CAR T cell therapies face important challenges. Despite long-term remissions in a proportion of patients with B-cell malignancies, however, most either subsequently relapse or do not respond [36,37]. B-ALL patient relapse could be as high as 50% after CAR T cell treatment and most recurrent tumours had no response to reinfusion of CD19-specific CAR T cells, even in the presence of cognate antigen [38]. Moreover, negative antigen expression relapse

accounts for 9–25% in B-ALL and has been described in other tumours, including B-NHL, diffuse B cell lymphoma, [39] among others.

Given the remarkable success and safety of CAR T cell therapy against B cell malignancies, CD19-CAR T cells were approved by the FDA in 2017 followed by clinical approval in the European Union, Canada, Australia, and Japan [40]. Meanwhile, phase III clinical trials have demonstrated significant improvement of CD19-CAR T cells as second-line therapy [41]. Additionally, a phase II trial with CAR T cells targeting B-cell maturation antigen (BCMA) showed complete response of 33% on patients with multiple myeloma [42], this treatment has also been approved by the FDA in 2021, with additional clinical trials targeting AML-restricted proteins, like CD123 and CD33 with CAR T cells [43].

1.2.3 CAR T cells against solid tumours.

Despite the remarkable success against haematological malignancies, CAR T cell therapy has had limited success in treating of non-lymphoid cancers. CAR T cells against carcinoembryonic antigen (CEA) showed some efficacy in a Phase I trial on metastatic colorectal cancer patients, with stable disease and reduced CEA serum levels on 7 out of 10 patients [44]. Similarly, 4 of 17 sarcoma patients had stable disease after infusion of CAR T cells against HER-2 [45], and 3 of 11 glioblastoma patients treated with GD2-CAR T cells achieved complete remission, but no response was observed in paediatric neuroblastoma patients [46,47]. CAR T cell against epidermal growth factor receptor variant III (EGFRvIII) showed partial response in one NSCLC cancer patient [48], while one patient with glioblastoma had stable disease [49]. Importantly, 5 patients analysed showed tumour CAR T cell infiltration, robust expression of inhibitory molecules and infiltration by regulatory T cells after CAR T cell infusion [49].

Multiple factors contribute to the lack of clinical response on CAR T cells. Pre-clinical cancer models have shown that increasing migration by expression of chemokines receptors, like CXCR2 or CCR2b [50,51], can enhance CAR T cell efficacy. Similarly, expression of heparinase on CAR T cells allowed efficient T cells infiltration into the tumour stroma, promoting antitumoral activity [52].

Upon infiltration, CAR T cells encounter a hostile tumour microenvironment, where several immune cells actively suppress T cell function. These cells support tumour development by expressing immunosuppressive molecules such as CTLA-4 or PD-1. Consequently, the combination of CAR-T cells and immune checkpoint blockade or strategies to reduce the expression or activation of PD-1 pathways increases CAR T cell persistence and reduced exhaustion in several pre-clinical models [53-55], and the combination of CAR T cells with PD-1/PDL1 blockade is actively being explored in clinical trials [53,56]. Additionally, CAR T cells targeting proteoglycans, like Glypican-3 (GPC3), have shown promising results in hepatocellular carcinoma patients, including complete responses [57,58]. Combination of GPC3 CAR T cells in combination with other treatments are currently being explored in clinical trials and are an example of the CAR T cell improvement on treating solid tumours.

1.3 Fundamentals of metabolism in cancer.

1.3.1 Cancer metabolism and the tumour microenvironment.

Among the key characteristics of all malignancies, a dysregulated metabolism has been identified as a hallmark of cancer development [59]. Glucose is the main sugar consumed by cells to obtain energy and metabolic intermediaries. Most cells uptake glucose and enzymatically break it down into pyruvate to obtain energy (Glycolysis). Under aerobic conditions, pyruvate is converted into Acetyl-Co-A and transported into the mitochondria to enter the tricarboxylic acid cycle (TCA), producing in total 38 ATP molecules per molecule of glucose. However, under low oxygen conditions (anaerobiosis), pyruvate is converted into lactic acid by lactate dehydrogenases (LDHs) instead of entering the TCA, producing only 2 ATP molecules per molecule of glucose (Figure 1.3). The discovery of metabolic dysregulation in cancer cells dates from the 1920s, Otto Warburg and his colleagues observed tumour cells uptake high amounts of glucose compared to non-malignant tissues, and glucose was fermented into lactate even in the presence of oxygen. The term "Warburg effect" was used to describe this metabolic dysregulation [60]. The reason cancer cells engage in aerobic lactate fermentation is not completely understood, as tumour cells quickly proliferate; they require ATP and intermediaries produced during the TCA. Lactate fermentation allows rapid ATP production, as energy production through lactate fermentation occurs 10-100 times faster than mitochondrial oxidation [61], while allowing the quick regeneration of key intermediaries to sustain a high glycolytic rate, like NAD^+ [62]. Importantly, highly proliferative immune cells engage in similar metabolic networks to tumour cells and due to the accelerated metabolism of tumour cells and poor stroma vascularization in the TME, two main consequences arise which severely compromise antitumoral T cell immunity: depletion of key nutrients fundamental for T cell antitumoral function and accumulation of immunosuppressive metabolic products.

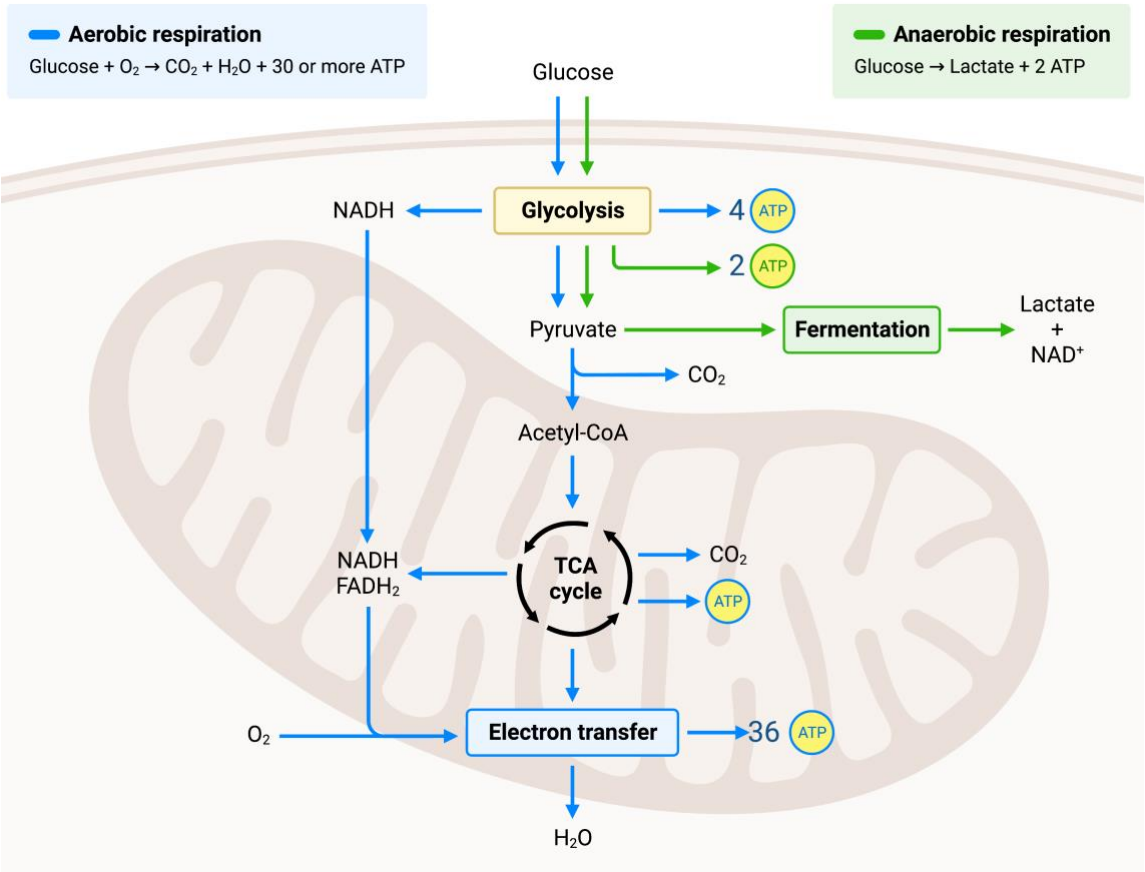

Figure 1.2: Fundamentals of cellular metabolism. Main intermediaries and ATP gain by glucose catabolism by aerobic (blue) and anaerobic respiration (green).

TILs from patients exhibit exhausted phenotypes and reduced glucose uptake [63,64]. In mouse sarcoma models, the reduction of glucose consumption of TILs dampened mTOR signalling, reducing glycolytic capacity and IFN-γ production [65]. Likewise, T cells require several amino acids to sustain their proliferation and effector functions, however, metabolic competition in the TME induces the depletion of key amino acids like glutamine [66], arginine [67], leucine [10], and others [68]. Additionally, several oncometabolites, metabolites which accumulate preferentially in the tumour microenvironment compared to healthy tissues, can directly suppress antitumor immunity. Highly glycolytic tumour accumulates high levels of lactic acid, increasing tumour extracellular acidosis, reducing glycolysis, and inhibiting T cell effector functions [69,70].

Moreover, mitochondria dysfunction and reduced metabolic fitness have been described in several solid tumours [71,72]. Melanoma samples obtained from mouse models and patients showed reduced mitochondrial mass and T cell respiration regardless of antigen specificity. Importantly, restoring mitochondrial fitness improved αPD-1 responses in mouse models [73,74]. NSCLC and melanoma patients overexpressing glycolytic enzymes had poorer T cell infiltration and was associated with T cell apoptosis. Moreover, increased tumour glycolytic activity was correlated with ACT resistance in melanoma patients [75]. Therefore, the tumour microenvironment is metabolically hostile to immune cells, with T cells unable to meet their energetic demands to sustain antitumoral functions.

1.3.2 CAR T cells and metabolic regulation.

As metabolic deregulation is a fundamental characteristic of tumour cells and T cells rely on similar metabolic pathways, several strategies have been developed to modify T cell metabolism and improve their antitumoral potential. Various studies have linked T cell function and phenotype to T cell metabolism; generally, inhibition of glycolysis and promoting OXPHOS increase T cell persistence and antitumoral potential.

The CAR structure can intrinsically imprint distinct metabolic and functional features into T cells with 41BB and CD28 as the most used in pre-clinical studies and clinical trials. Comparing both molecules, CAR T cells with a 41BB co-stimulation domain preferentially rely on respiration over glycolysis for energy production, they have increased mitochondrial biogenesis, central memory phenotype, and persistence. On the other hand, CD28 upregulates glycolytic pathways, promoting quick proliferation and an effector memory phenotype [76]. Moreover, single-cell transcriptional profiling of CAR T cells infused into patients revealed correlations between CAR T cell therapy efficacy and metabolism profile. Effector T cells and effector memory T cells exhibited extensive metabolic reprogramming by a shift to aerobic

glycolysis, characterized by increased expression of LDHA, GLUT1, and GAPDH but also increased in apoptosis genes, indicating persistence might be limited. In contrast, CAR T cells with a memory T cell signature expressing TCF7 and LEF1 were associated with long-term clinical CAR T-cell persistence [77]. Supporting this study, αCD19-CAR T cells had significantly higher expression of OXPHOS in responder patients with acute lymphoblastic leukaemia [78].

1.3.3 Glycolytic inhibition.

A common strategy to improve CAR T cell performance is to dimmish their dependence on glucose and the glycolytic pathway. 2-Deoxy-D-glucose (2DG) is a glucose analogue used since the 1950s. This molecule enters the cytoplasm via GLUT1 and is phosphorylated to form 2DG-6-phosphate. 2DG-6-phosphate cannot be metabolized, blocking the next steps on the glycolytic pathway. Activating T cells in presence of 2DG increase their central memory profile, persistence and antitumoral potential against B16 melanoma models [79]. Additionally, 2DG disrupts the expression of extracellular N-glycans on tumour cells, as high N-glycan expression can mask antigenic epitopes and hinder close cell-to-cell proximity. Therefore, the combination of CAR T cells and 2DG improved the tumour control against multiple solid tumours [80]. Additionally, to overcome the low glucose availability in the TME, the combination of PD-1 blocking antibodies or GD-2 CAR T cells with inosine improved supplementation of their antitumoral efficacy against several solid tumours [81].

1.3.4 Promoting mitochondria metabolism.

Within the tumour microenvironment, TILs are exposed to nutrient deprivation and are unable to sustain their effector function. TILs display reduced OXPHOS and mitochondria dysfunction regardless of antigen specificity [73,82] suggesting T cell dysfunction is mediated by energy requirements. Moreover, favouring respiration and fatty acid oxidation of T cells improves adoptive cell transfer (ACT) therapies against cancer by modifying mitochondria

dynamics which results in a memory-type phenotype and improved persistence of T cells [83]. Moreover, mitochondria remodelling in T cells by overexpressing the inner membrane fusion protein Opa1 or the transcription factor PGC1α [73] induced cristae remodelling, augmented oxidative phosphorylation and T cell tumour control. Interestingly, in patients infused with CD19-CAR T cells achieving complete responses, CAR T cells displayed increased mitochondrial mass correlated with CAR T cell expansion and persistence compared with non-responders [84].

Transient reduction on CAR T cell activation with a tyrosine kinase inhibitor (dasatinib) which reversibly inhibits proximal CAR signalling kinases, redirected T cell phenotype toward a memory-like state by transcriptional and epigenetic remodelling, improving CAR T cell efficacy in mouse models of B cell leukaemia and solid tumours [85]. Similarly, directly regulating pyruvate fate by culturing aCD19 CAR T cells with a mitochondrial pyruvate carrier inhibitor dramatically improves CAR T cells efficacy in pre-clinical models of B-cell leukaemia and solid tumours [86]. Generally, modifying CAR T cell metabolism to induce a central memory phenotype, with increased mitochondria metabolism, OXPHOS and reduced glycolytic dependency, increases CAR T cell persistence and antitumoral potential [87].

1.3.5 Cytokines.

A common strategy to modulate CAR T cells metabolism during manufacturing is the addition of different cytokines to polarize T cells into a more persistent phenotype. Cytokines are soluble proteins involved in multiple processes of immunity, including T cell activation, expansion, differentiation, and migration. IL-2 is the most common cytokine added during CAR T cell manufacturing as it promotes glycolysis and quick proliferation. However, excessive IL-2 signalling can induce T cell apoptosis while reduction of IL-2 increases CAR T cell expansion and superior antileukemic activity [88]. Moreover, co-administration of IL-2

promoted CAR T cell expansion in clinical trials, but significant toxicities were found in high doses [89]. In contrast, expansion of CAR T cells with IL-15 preserved a less-differentiated phenotype stem cell memory phenotype compared to IL-2 by decreasing mTORC1 activity, expression of glycolytic enzymes and improving mitochondrial fitness [90], while engineering CD19-CAR T cells to express IL-15 had superior antitumoral activity in vivo, improved proliferation and reduced PD-1 and apoptotic markers [91]. Similarly, culture CAR T cells with IL-15 and IL-7 during manufacturing enhances antitumoral responses and decreases the severity of cytokine release syndrome [92], while IL-7 producing CD19-CAR T cells had a distinct phenotypic and metabolic signature on CAR T cells, showing a less-differentiated phenotype and superior antitumor activity [93].

1.3.6 PI3K-AKT-mTOR axis.

PI3K-AKT-mTOR signalling is the central axis regulating T cell activation and metabolic requirements. Culture of CD19-CAR T cells with PI3K inhibitors enriches CD8 memory T cells, enhances in vitro cytotoxicity and antitumoral immunity in CLL and melanoma models [94,95]. Similarly, AKT inhibitors increased the expression of CD62L, a T cell lymphoid tissue marker, reduced gene expression associated with T cell activation, limited glycolytic metabolism and increased in vivo efficacy of CD19-CAR T cell against B cell leukaemia, EpCAM CAR T cells against colon cancer and CD33-CAR T cells against AML [96-99]. Rapamycin is an mTOR inhibitor first used to prevent acute renal allograft rejection and later used for treatment against renal cancer. However, as rapamycin does not bind to the catalytic domain of mTORC1 limiting its efficacy, several second-generation mTOR inhibitors have been developed to treat several malignancies and are currently being tested in clinical trials [100]. Treatment of EpCAM-CAR T cells with rapamycin allows bone-marrow infiltration and efficient elimination of AML cells in mouse models [101] and polarizes CD19-CAR T cells to a memory phenotype similar to culture with IL-15 [90] while transient mTOR inhibition reduced

tonic signalling on CAR-41BB Tregs, improving their in vivo function on graph-versus-host disease mouse models [102]

1.3.7 Reducing aminoacidic dependencies.

During T cell activation, several amino acids must be transported to be substrates for protein synthesis and act as metabolic mediators. Deprivation of glutamine, leucine, arginine or tryptophan during T cell activation severely impairs T cell activation, and amino acid depletion is a common immune checkpoint preventing T cell-mediated antitumoral function [103]. Therefore, strategies to identify amino acid vulnerabilities on CAR T cells is a powerful strategy to improve CAR T cell antitumoral function.

A knock-in CRISPR library on CD8 T cells identified overexpression of Proline Dehydrogenase 2 (PRODH2) as a metabolic checkpoint for T cell function. Expression of PRODH2 on CD22-specific CAR T cells increased mitochondria biomass, OXPHOS, and cytotoxic functions in vitro while increasing CAR-T in vivo efficacy in mouse models of B cell malignancies and solid tumours [104]. Similarly, an increase in arginine availability promoted CD8 T cell antitumoral control on models of solid cancer by supplementing mouse diets with arginine or culturing T cells in increased arginine [67]. Genetic engineering of GD2-specific CAR T cells to express arginine resynthesis enzymes, arginosuccinate synthase (ASS) and ornithine transcarbamylase (OTC) had increased proliferation and tumour clearance against solid and haematological tumours [105]. Moreover, overexpression of the amino acid transporters SLC7A5 or SLC7A11 in CAR T cells improves their proliferation under low tryptophan [106].

Collectively, metabolic regulation by modifying culture media or genetic engineering of CAR T cells to reduce their metabolic dependencies within the TME is a powerful strategy to improve CAR T cell function against haematological malignancies and solid tumours.

1.4 Lactic acid as an oncometabolite.

1.4.1 Immunosuppression by lactic acid.

Among the immunosuppressive oncometabolites, lactic acid is one of the most studied, as high lactate production is a hallmark of most cancers. Lactic acid can reach concentrations up to 40 mM in the tumour stroma due to quick lactate production and poor tumour vascularization [107,108]. This concentration directly shapes the TME by impeding the immune response: Lactic acid induces NK and T cell effector functions inhibition [109,110], polarization of macrophages into an M2 immunosuppressive phenotype [111,112], shaping the TME and favouring metastasis [113-115]. Accumulation of lactic acid in the tumour microenvironment was considered a waste product of cancer metabolism for decades; however, lactate instead of glucose has been described as a key carbon source of cancer and immune cells. In lung cancer samples, lactate contributed to a higher extend than glucose to fuel the TCA [116] and tumour-infiltrated Treg cells can consume lactate, increasing their anti-inflammatory potential and promoting tumorigenesis [117].

Lactic acid directly disrupts T cell function and phenotype. Activated T cells cultured with 20 mM of lactic acid showed reduced mobility, reduction of IFN-γ, impaired cytotoxicity by inhibition of granzyme B and perforin production [118-120]. Culture of T cells with lactic acid produced by tumour cells quickly induces T cell dysfunction, while reducing lactate acid production by LDH inhibition or genetic ablation restores T cell function in vitro and in vivo [121-123].

Additionally, metabolization of lactate drives T cells into a low energetic state by inhibition of LDH-A, reduction of NAD^+ into NADH which depletes post GAPDH-glycolytic intermediaries [124], the combine effect of lactate consumption is the reshaping of T cells into a suppressed state. Interestingly, lactic acid consumption on regulatory T (Treg) cells have

opposite effects. Treg cells rely less on glucose consumption for energy production and increase their respiration and lipids oxidation to feed the TCA cycle [125,126]. The transcription factor FOXP3 reprograms T cell metabolism by Myc inhibition and increasing NAD^+ production, therefore Treg can survive in low-glucose and high-lactate metabolism by continuing lactate metabolization and avoiding NAD^+ depletion [127]. Moreover, tumour infiltrating Tregs become more suppressive on highly glycolytic tumours by upregulation of PD-1 and dampening the efficacy of αPD-1 treatment [128].

1.4.2 Monocarboxylate transporters (MCT).

The main transporters of lactic acid are the monocarboxylate transporters (MCTs). MCTs are encoded by the solute carrier 16 gene (SLC16) and belong to a family of 14 transmembrane proteins which passively transport lactate, pyruvate, ketone bodies and short-chain fatty acids together with protons [129]. Comparing the most studied transporters in this family, MCT-1 and MCT-4, these 2 transporters have fundamental differences in expression and substrate dynamics. MCT-1 has a high affinity for lactate (3.5-10 mM) and is broadly expressed in healthy tissues, but its functions vary depending on the energetic demand on the organs [130]. MCT-1 is associated with lactate influx in heart, liver, and red skeletal muscle, as they use lactate for oxidative metabolism. In contrast, in highly glycolytic cells like skeletal muscle fibre, activated immune cells and tumour cells, MCT-1 mediates lactic acid efflux. MCT-4 has the lowest affinity to lactate and mostly facilitates lactic acid efflux from glycolytic cells, including astrocytes and immune cells [131] (Figure 1.4). Tumour cells without quick access to glucose upregulate MCT-4 [132] and oxidative cancer cells can uptake the lactic acid produced by highly glycolytic cells, augmenting glucose availability by not competing for the same carbon source [133] contributing to resistance to anti-cancer therapies [134] (metabolic symbiosis).

In cancer patients, upregulation MCT-1 and MCT-4 during the transition from normal to malignant tissue have been extensively reported [135] and their expression is associated with worse prognosis in patients with different cancers, including breast [136], lung [137], colorectal [138], brain [139], head and neck cancer [140,141] and acute myeloid leukaemia [142,143]. B- cell malignancies have the particularity of mainly expressing only MCT-1; an analysis of 120 DLBCLs patient samples found that 73% had high expression of MCT-1 were MCT-4 negative, and 10 BL samples were MCT-1^{+} $MCT4^{-}$ [144]. Additionally, 23% of NHL samples from 104 patient's samples expressed MCT-1 and was associated with highly aggressive tumours [145].

1.4.3 MCT-1 inhibition.

Several selective MCT-1 inhibitors have been developed and have been studied primarily on pre-clinical models of B cell malignancies. Two small molecules with the highest specificity and a Km in the nanomolar range, AZD3965 and AR-C155858 are the more commonly used.

Both AZD3965 and AR-C155858 are pyrrole pyrimidine derivatives with similar chemical composition and an IC_{50} against MCT-1 of 1.6 nM and 2.3 nM, respectively [146,147]. Mechanistically, small molecules reversely bind to the intracellular domains of MCT-1, blocking the movement of lactate and other ketones bodies by forcing the close conformation of the channel [148]. Moreover, incubation with MCT-1 inhibitors (iMCT-1) rapidly disables tumour proliferation by intracellular lactate accumulation, shutting down NAD^{+} regeneration, reducing glucose consumption and initiating apoptosis [149]. Metabolic rewiring is also induced on highly glycolytic cells treated with iMCT-1 by inhibition of the glycolytic pathway, accumulation of pyruvate [150] and increased mitochondrial respiration [151], indicating metabolic adaptations undergoes after lactate accumulation but sustained inhibition of lactate export induces cell death. Comparative studies using 4T-1 mouse breast cancer tumour cells found small differences between both small molecules. AR-C155858 behaves like an MCT-1

substrate with a trend toward higher uptake at lower pH [152] with higher affinity to MCT-1 and MCT-2 compared to AZD3965 [153] while the latter shows slightly higher liposolubility, which explains its oral availability and different saturation rates compare with AR-C155858.

Oral administration of AZD3965 at 50 mg/kg or 100 mg/kg on immunodeficient mouse models significantly reduced the tumour burden on subcutaneous models of non-Hodgkin's lymphoma [144,153], breast cancer [150,154], small cell lung cancer [146,155] and lung squamous carcinoma [8], while improving the antitumoral effects in combination with other therapies in models of head and neck squamous cell [156], colorectal [149] and renal cell carcinoma [157]. Moreover, AZD3965 has been recently tested in clinical trials (NCT01791595) and showed no significant toxicity, ongoing stable disease in one patient and an additional patient showing a complete response.

Similarly, tumour reduction was found on intraperitoneal injection of AR-C155858 in xenograft models of B cell malignancies, breast cancer [158], Ras-transformed fibroblasts [132] and gastric cancer [159]. Additionally, MCT-1 inhibition has been expanded to show less viability on in vitro treated prostate cancer [160], hepatocellular carcinoma [161], glioblastoma [162] and acute myeloid leukaemia cells [142] showing inhibition of lactate export is a general strategy for cancer treatment.

However, two important limitations exist in iMCT-1 research. Consistent in most studies, native high expression of MCT-4 or genetic manipulation of tumour cell lines to overexpress MCT-4 completely abrogates the effects of MCT-1 inhibition, limiting the therapeutic potential of this therapy [163]. Additionally, as most studies have been performed on immunodeficient mice, the effect of MCT inhibition on the immune compartment and cancer metabolic evolution is far less understood. iMCT-1 increases the Raji cell line tumour infiltration of NK cells and dendritic cells on mice transferred with human PBMCs [164] and iMCT-1 failed to exert

antitumoral control on a 4T1 mouse breast carcinoma model despite decreased lactate levels on blood and tumours after treatment [165].

Importantly, MCT-1 blockade was first identified as an immunosuppressant, particularly affecting T cells [166]. In vitro activated T cells quickly upregulate MCT-1 expression while the expression of MCT-4 increases after 2 days [167]. Human cytotoxic T cells activated with PMA/Ionomycin and cultured with non-specific MCT-1 blockers showed less glycolysis engagement, impaired proliferation, and reduced effector function [118,168]. In contrast, genetic ablation of MCT-1 on tumour-infiltrating Treg cells showed reduced proliferation and suppressive function on models of B16 melanoma, MC38 adenocarcinoma and MEER Head and neck squamous cell carcinoma [169].

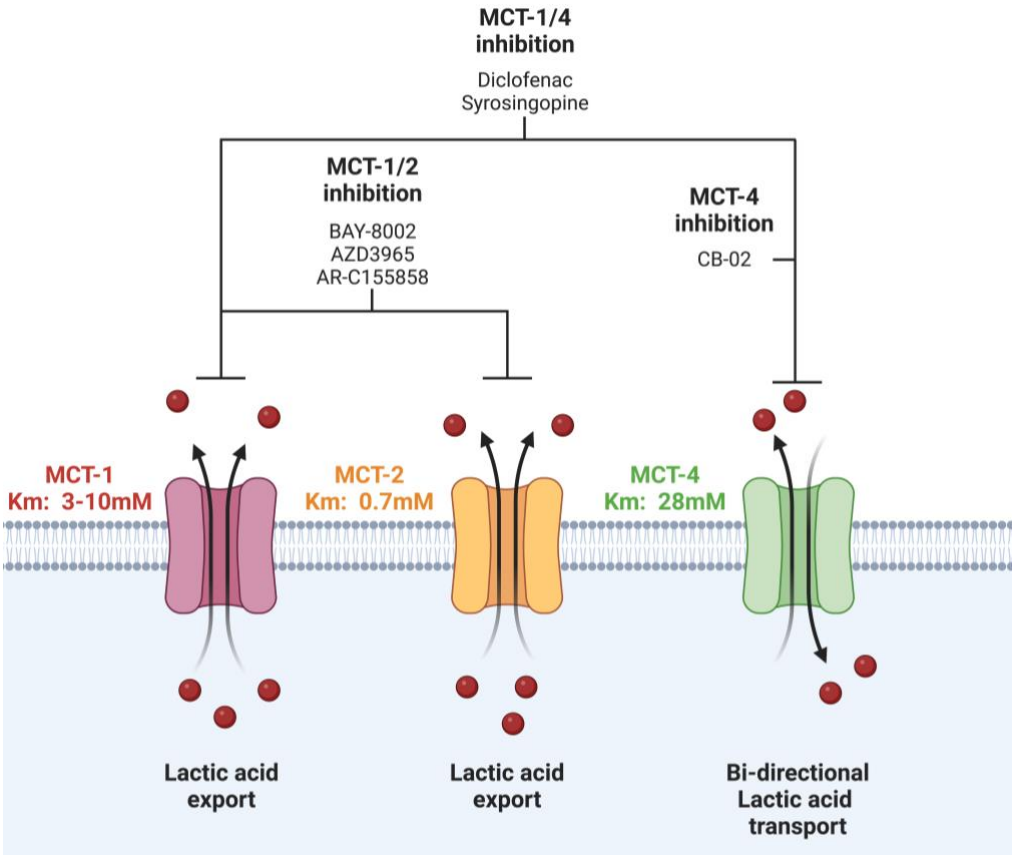

Figure 1.3: Monocarboxylate transporter in cancer and immunity. Km and transport direction for lactate transport on MCT-1/2/4. Also included the blocking small molecules used in pre-clinical models targeting each transporter.

1.4.4 Dual MCT-1/4 inhibition.

Given that most tumour cells overexpressing MCT-1 and MCT-4 are insensitive to iMCT-1 and the lack of therapies targeting MCT-4, a recent strategy has been to identify small molecules that target a broader range of monocarboxylate transporters.

Syrosingopine was developed in the 1960s as an anti-hypertension drug and has been recently researched for its anticancer properties [170]. Combination of metformin and syrosingopine shown high toxicity on leukemic patient samples and different tumour cell lines, including breast cancer, acute myeloid leukaemia, and colorectal cancer cells, among others [142,171,172]. Moreover, highly metastatic NSCLC patient samples carrying pathogenic mitochondrial NADH dehydrogenase (ND) gene mutations were shown to overexpress MCT-4 and be sensitive to syrosingopine [173]. Mechanistically, syrosingopine binds to MCT-1 and MCT-4 and prevents lactate efflux inducing the accumulation of high levels of lactic acid intracellularly. Combination with metformin or other NAD^+ producing pathways impairs respiration and key steps of NAD^+ regeneration leading to synthetic lethality of tumour cells [174].

Similarly, diclofenac has been explored recently for its anticancer properties. Diclofenac was developed as an anti-inflammatory drug by inhibiting cyclooxygenases (COX) and phospholipase A2 [175]. Diclofenac reduced the tumour burden on orthotopically inoculated pancreatic cancer cells [176], while dermal application on patients with precancerous skin lesions (actinic keratosis) showed reduced lactate and amino acid levels in responding lesions with an increase of dermal CD8 T cells [177]. Moreover, Diclofenac binds and block lactate export through MCT-1 and MCT-4 on melanoma and breast cancer cell lines without significantly impairing the T cell compartment. Additionally, the combination of αPD-1, αCTLA-4 and diclofenac significantly improved the antitumoral control against 4T1 cells [178], showing the potential combination of immunotherapies with lactate regulation.

1.5 Glutamine depletion as an immune checkpoint.

1.5.1 Glutamine metabolism on tumour and immune cells.

Glutamine is the most abundant amino acid in blood, accounting for more than 20% of the circulating free amino acid pool [179]. Glutamine is converted into glutamate by glutaminases (GLS) and metabolised into α-ketoglutarate (α-KG); α-KG enters the TCA, providing energy and metabolic intermediaries to synthesises macromolecules, a process named glutaminolysis. In cancer and immune cells, glutaminolysis is a fundamental metabolic process to sustain proliferation as glutamine is a versatile metabolite used for energy production, nitrogen source for nucleotide and aminoacidic production, and reduces oxidative stress by synthesis of glutathione and NADPH [180] (Figure 1.5). Genetic alterations in cancer, like Myc amplification and TP53 mutations, increased glutamine consumption by increasing the expression of glutamine transporters and GLSs [181,182]; meanwhile several immune cells consume glutamine at a higher rate than glucose to sustain their energy production [183]. Glutamine is essential for NK and T cell activation [184,185], CD4 T cells polarization into a pro-inflammatory Th1 phenotype [186], regulating macrophage differentiation and antigen presentation [187].

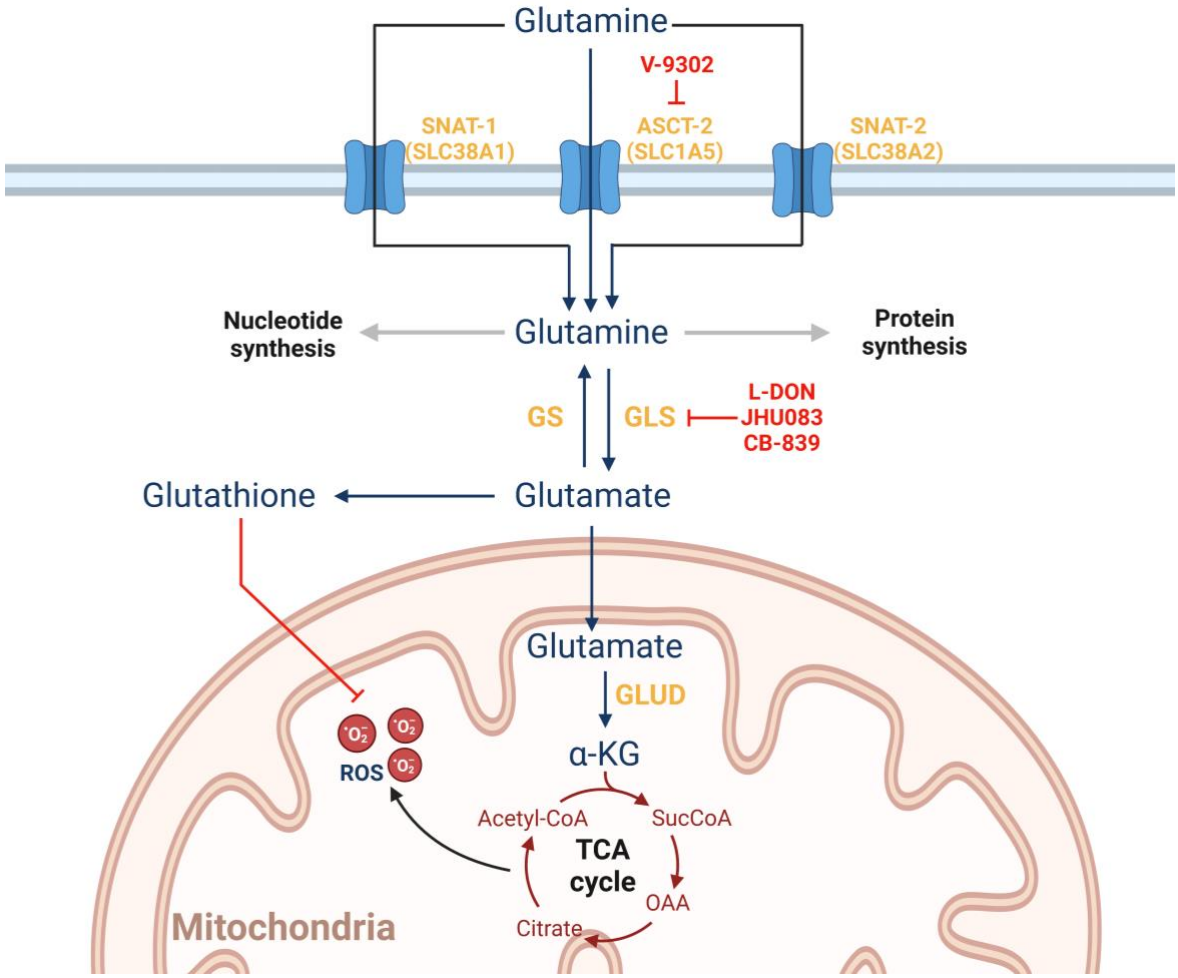

Figure 1.4: Glutamine metabolism. Glutamine is transported by amino acid transporters like SNAT-1, SNAT-2 or ASCT-2. Once in the cytoplasm, glutamine can be directed to amino acid synthesis, nucleotide production or energy production. For the later, glutamine is converted to glutamate by glutaminases (GLS), glutamate is then converted into α-ketoglutarate (α-KG) by glutamate dehydrogenase (GLUD), entering the TCA cycle. Mitochondria energy production produces reactive oxygen species (ROS) which can be neutralised by glutathione. To block glutamine metabolism, small molecules targeting amino acid transporters (V-9302) or GLS (L-DON and C-839) have been developed and some of them are being tested in clinical trials.

Glutamine competition is a hallmark of aggressive cancers, as several tumours show local depletion of glutamine, which contributes to an immunosuppressive TME [188]. Mouse tumour models of triple-negative breast cancer lacking GLS showed increased local glutamine levels and higher CD8 T cell cytotoxicity [189]. Tumour-infiltrating macrophages exposed to low glutamine are polarized into an immunosuppressive M2 phenotype and deletion of glutamine synthetases on macrophages promoted T cell accumulation and reduced tumour metastatic formation [190]. Additionally, low glutamine induces higher PD-L1 expression on bladder and colorectal cancer cell lines, directly contributing the tumour progression by increasing the immunosuppressive capabilities of cancer cells [191,192].

To sustain glutamine consumption, several amino acid transporters are upregulated in cancer and T cells to uptake glutamine. Several tumour models have shown upregulation of the Na^+ dependent neutral amino acid transporter SLC1A5 (ASCT-2) or the sodium-dependent cationic amino acid transporter SLC6A14 (ATB^{0+}) for glutamine uptake [193]. Similarly, TCR engagement induces the upregulation of ASCT-2 and other Na^+ dependent neutral amino acid transporters, SLC38A1 (SNAT1) and SLC38A2 (SNAT2) [68]. In mouse models, after ASCT-2 blockade, mouse T cells can also express ATB^{0+} to compensate for glutamine uptake and sustaining T cell effector functions [189]. In T cells glutamine uptake regulate several aspects of T cell functions, including feeding the TCA, synthesis of amino acids and nucleotides, reducing oxidative stress, regulating mTOR activity, TCR signalling, among others [103]. Therefore, T cells regulate the expression of several redundant amino acid transporters to ensure glutamine availability.

1.5.2 Glutamine as an immune checkpoint.

As glutamine consumption is a hallmark of tumour progression, different strategies have been developed to deprive cancer cells of glutamine. 6-Diazo-5-oxo-L-norleucine (L-DON) inhibits several glutamine-utilizing enzymes by competing binding to glutamine active sites [194], disrupting glutaminolysis and promoting a robust antitumoral effect. However, its use was associated with severe toxicities in patients, including acute nausea, vomiting and diarrhoea [195,196] abandoning its clinical use against cancer [197].

Regardless, glutamine restriction has been explored to improve cancer immunotherapies. Restricting glutamine during the 2 initial days of T cell activation or culture with L-DON improved the antitumoral capacity of mouse T cells. Mechanistically, transient glutamine deprivation induced lower PD-1 expression, improved metabolic fitness and higher expression of transcription factors associated with T cell survival [198]. Similarly, culture of CD19-CAR CD4 T cells with the GLS inhibitor CB-839 showed increased antitumoral control in vivo [186], while L-DON drives CD19-CAR T cells into a less differentiated phenotype, rewires their metabolism to rely more on OXPHOS and FAO, and enhancing antitumoral activity against leukaemia models [199]. However, in Lkb1-deficient lung adenocarcinoma mouse models, an increase in glutamine availability was linked to increased CD8 T cell infiltration and antitumoral response to PD-1 blocking therapy, while the combination with CB-839 inhibited CD8 T cell activation [200].

To solve some of the toxicities associated with systemic glutaminase inhibition, a version of inactive L-DON which is enzymatically activated on the TME was developed, potentially avoiding the side effects associated with systemic L-DON injection. JHU083 showed strong antitumoral potential against mouse models transferred with MC38 or B16 cell lines in vivo. Interestingly, JHU083 induced distinct metabolic rewiring in tumour and CD8 T cells. CD8 T

cells unregulated acetate consumption by expression of acetyl-CoA synthetase and pyruvate carboxylase enzymes, increasing T cell persistence and OXPHOS engagement, while JHU083 shutdown MC38 cancer cell metabolism and triggered cell death [201]. Similarly, a new L-DON derivate, DRP-104 showed high activity in colorectal cancer mouse models, with no gastrointestinal toxicity while systemic administration of DRP-104 enhanced PD-1 antibody therapy and polarize CD8 T cells to a stem-cell like phenotype [202].

1.5.3 ASCT-2: the main glutamine transporter in cancer.

Among the glutamine transporters in cancer, SLC1A5 (ASCT-2) is the most studied as it transports glutamine with high affinity and overexpression of ASCT2 is correlated with worse prognosis in patients with leukaemia, colorectal, melanoma, head and neck squamous cell carcinoma, and gastric cancer, among others [203].

Recently, a potent small molecule blocking ASCT-2 and impairing glutamine uptake was developed, V-9302. Pharmacological blockade of ASCT-2 with V-9302 preferentially neutralises glutamine uptake, with lower activity against other amino acids. Culture of V-9302 reduced the viability in vitro and significantly reduced tumour growth in vivo of glutamine-addicted tumour cell lines, while no changes in viability were found on activated CD8 T cells [204]. Moreover, ovarian cancer cell lines culture with V-9202 showed reduced mTOR activity and enhanced sensitivity to chemotherapy in vitro [205] and co-delivery of V-9302 with 2-DG reduced the tumour burden on mouse models of breast cancer [206].

Importantly, ASCT-2 inhibition could also synergise with immunotherapies. Culture of colorectal cell lines in low glutamine induces the expression of PD-L1 and the combination of V-9302 with αPD-L1 increases their antitumoral control in mouse models [191]. In TNBC mouse models, V-9302 increased effector T cell infiltration and reduced the number of intratumorally Tregs. Importantly, effector mouse T cells were insensitive to V-9302 and sustained

glutathione synthesis by expressing SLC16A14, a glutamine transporter not inhibited by V-9302 [189]. Additionally, monoclonal antibodies blocking glutamine entry through ASCT-2 has been developed. One of these antibodies was humanized and cloned under a human IgG1 format and showed glutamine neutralization in vitro against several human gastric cancer cell lines, inducing cell death by repressing glutathione synthesis and increasing intracellular ROS [207] while showing efficacy as a monotherapy against gastric cancer patient-derived xenograft on cells expressing low ASCT-2 [208].

Taken together, glutamine neutralization is an interesting approach to improve CAR T cell therapy against solid tumours and haematological malignancies.

1.6- Hypothesis and objectives.

Based on the information presented, we hypothesized the combination of metabolic regulation with CAR T cell therapy will synergise to improve their antitumoral control against B cell malignancies.

General objective 1.

To study the combination of human CD19-specific CAR T cells with blockade of the lactate transporter MCT-1 against B cell leukaemia in preclinical models.

Specific objectives.

1- Study the expression and functionality of MCTs transporters on human cancer cell lines and CAR T cells.

2- Metabolic and phenotypic characterisation of CAR T cells in culture with MCT-1 inhibitors.

3- Study killing potential and effector functions of CAR T cells against B cell lymphoma cell lines after MCT-1 blockade.

4- Stablish the antitumoral potential of CAR T cells and systemic MCT-1 inhibition on animal models of B cell malignancies.

General objective 2.

To study the combination of human CD19-specific CAR T cells with blockade of the glutamine transporter ASCT-2 against B cell leukaemia in preclinical models.

Specific objectives.

1- Study the combination of CAR T cells and pharmacological inhibition of ASCT-2 in vitro.

2- Expression of surrogate glutamine transporters to sustain CAR T cell functions after ASCT-2 inhibition.

3- Characterise glutamine-neutralizing ASCT-2 antibodies in combination with CAR T cells.

2. Materials and Methods.

2.1 Molecular Biology.

2.1.1 Cloning.

All DNA constructs used in this work are detailed in Table 2.1. DNA and protein sequences of human SLC38A1, SLC38A2, SLC6A14, and murine SLC1A5 were obtained from Uniprot. The DNA sequences of anti-ASCT2 antibodies were obtained from the patent US20120039904A1. 1000 ng of DNA were produced using gBlocks Gene fragments platform (Integrated DNA technologies). For cloning new plasmids, DNA fragments were amplified by standard PCR using Phusion® High-Fidelity DNA Polymerase (NEB # M0530L) with the primers in Table 2.2 and the protocol described in Table 2.3 for 35 cycles. The volumes per reaction are specified in Table 2.4.

The amplified fragments were cleaned using QIAquick PCR Purification Kit (Qiagen #28104) and cut using NEB High fidelity restriction nucleases: Nco-I (NEB #R3193), BamHI (NEB #R3136), AgeI (NEB # R3552) or Mlu-I (NEB #R3198) in Cutsmart buffer. The reaction mix is specified in Table 2.5.

DNA fragments were selected in a 1% agarose gel and purified using the QIAquick Gel Extraction Kit (Qiagen 28706X4) according to the manufacturer's instructions. The DNA was quantified with NanoDrop™ One (Thermo Scientific) by adding 1 µL of the sample. For ligation, 100 ng of vector were incubated in a 3:1 mass ratio of insert DNA using the NEBBioCalculator and ligated using the NEB Quick Ligase Kit according to the manufacturer's instructions (NEB # M220).

Plasmid	Description	Identifier number
SFGmR.RQR8-2A-aCD19fmc63-CD8STK-41BBZ	RQR8 co-expressed with anti-CD19 fmc63 CAR with CD8STK spacer and 41BBZ endodomain	MP12783
SFGmR.RQR8-2A-aCD19fmc63-CD8STK-CD28Z	RQR8 co-expressed with anti-CD19 fmc63 CAR with CD8STK spacer and CD28Z endodomain	MP18341
SFGmR.RQR8-2A-aHER2-CD8STK-41BBZ	RQR8 co-expressed with anti-HER2 CAR with a 41BBZ endodomain	MP30834
SFG.RQR8-2A-SNAT1	RQR8 co-expressed with human SLC38A1 transporter	MP38838
SFG.SNAT1.I2.eGFP	Human SLC38A1 transporter with an IRES and GFP	MP37827
SFG.RQR8-2A-SNAT2	RQR8 co-expressed with human SLC38A2 transporter	MP38839
SFG.SNAT2.I2.eGFP	Human SLC38A2 transporter with an IRES and GFP	MP37828
SFG.ATB0.I2.eGFP	Human SLC6A14 transporter with an IRES and GFP	MP37825
SFG.ASCT2m.I2.eGFP	Mouse SLC1A5 transporter with an IRES and GFP	MP37826
SFG.anti-FMC63_VH-muIgG2a.I2.eGFP	FMC63 scFv anti-idiotype 136.20.1 clone variable heavy chain with murine IgG2a constant domain and I2.eGFP	MP30148
SFG.anti-FMC63_VL-muIgKC.I2.eBFP2	FMC63 scFv anti-idiotype 136.20.1 clone variable light chain with murine kappa constant domain with I2.eBFP2	MP30150
SFG.anti-ASCT2_V08_VH-muIgG2a.I2.eGFP	Anti-human ASCT-2 V08 clone variable heavy chain with murine IgG2a constant domain in I2.eGFP vector.	MP32805
SFG.anti-ASCT1_V08_VL-muIgKC.I2.eBFP2	Anti-human ASCT-2 V12 clone variable light chain with murine kappa constant domain with I2.eBFP2	MP32809
SFG.anti-ASCT2_V12_VH-muIgG2a.I2.eGFP	Anti-human ASCT-2 V12 clone variable heavy chain with murine IgG2a constant domain in I2.eGFP vector.	MP32806
SFG.anti-ASCT1_V12_VL-muIgKC.I2.eBFP2	Anti-human ASCT-2 V12 clone variable light chain with murine kappa constant domain with I2.eBFP2	MP32811
SFG.anti-ASCT2_V18_VH-muIgG2a.I2.eGFP	Anti-human ASCT-2 V18 clone variable heavy chain with murine IgG2a constant domain in I2.eGFP vector.	MP32808
SFG.anti-ASCT1_V18_VL-muIgKC.I2.eBFP2	Anti-human ASCT-2 V18 clone variable light chain with murine kappa constant domain with I2.eBFP2	MP32812

Table 2.1: List of plasmids used in this work.

Insert DNA	Primers
Glutamine transporters	F:ggctgcaggtccgatccaccggtcgccaccatggctctcccagtgactg R:tcgagtcgacgactccggaacgaattctgattagcgagggggcagggc
Heavy Chain aASCT2 antibodies	F: CTGTGGGTCGACGGCAGCACC R: GCGCCTGTACATGTCTCGAGCT
Light Chain aASCT2 antibodies	F: CTGTGGGTGATGCATCCCGGCA R: CGTGTCGAGCGGGATCAAT

Table 2.2: PCR inserts used for new plasmids.

Reagent	Concentration	Volume
DNA template	100 ng	1 µL
Forward primer	10 µM	5 µL
Reverse primer	10 µM	5 µL
Buffer	5X	10 µL
dNTP	10 mM	1 µL
Polymerase	100 units/µl	0.5 µL
Nuclease Free Water	N/A	22.5 µL

Table 2.3: Standard PCR reaction reagents and concentrations.

Step	Description	Temperature	Time
1	Initial Denaturation	98°C	30 seconds
2	Denaturation	98°C	10 seconds
3	Annealing	55-65°C	20 seconds
4	Extending	72°C	1 minute
5	Final extension	72°C	10 minutes
6	Hold	4°C	-

Table 2.4: Standard PCR reaction protocol.

Reagent	Concentration	Volume
DNA	1000 ng/mL	1 µL
Restriction Enzyme 1	20,000 units/ml	0.5 µL
Restriction Enzyme 1	20,000 units/ml	0.5 µL
Cutsmart buffer	10X	5 µL
Nuclease Free Water	N/A	43 µL

Table 2.5: Standard digestion reaction protocol.

2.1.2 Bacteria transformation.

The Quick ligase DNA reactions were transformed into NEB® 5-alpha Competent E. coli (High Efficiency) (NEB # C2987H). An aliquot of competent cells was thawed on ice, and 25 uL of bacteria was transferred to an Eppendorf tube. 2 uL of quick ligation reaction was placed into the middle of the thawed competent cells, incubated on ice for 30 minutes and heat-shocked for 35 seconds at 42°C. The mixture was put on 250 uL of SOC medium and grown in a shaker incubator at 37°C for 30 min at 220 RPM. Bacteria were then plated on Lysogeny broth (LB) agar plates containing ampicillin (100 µg/mL) and incubated for 16 hours at 37°C.

2.1.3 Plasmid preparation and sanger sequencing.

Ampicillin-resistant colonies were picked and transferred to 5 mL of LB medium and grown in a shaker incubator at 37°C for 16 hours at 220 RPM. After that, 1 mL of bacteria was centrifugated at 6000 g for 15 min, and plasmid DNA was extracted using QIAGEN Plasmid Mini Kit (Qiagen 12125) according to the manufacturer's instructions. DNA concentration was measured with NanoDrop™ One (Thermo Scientific) sent for Sanger sequencing (Genewiz). Sanger sequences were compared to reference plasmid maps using SnapGene Insightful Science. When a larger quantity of DNA was needed, 500 µL of bacteria were cultured on 100 mL of Terrific Broth media and grown in a shaker incubator at 37°C for 16 hours at 220 RPM. Bacteria were centrifugated at 6000 g for 30 min at 4°C, and plasmid DNA was extracted using QIAGEN® Plasmid Plus Midi Kit (Qiagen 12145) according to the manufacturer's instructions. 100 ng of DNA were digested as specified in Table 2.5, and the plasmid was sent to Sanger sequencing after verifying the correct digestion pattern.

2.2 Cell culture.

2.2.1 Cell lines and reagents.

Iscove's Modified Dulbecco's Medium (IMDM), Dulbecco's Modified Eagle Medium (DMEM), and Roswell Park Memorial Institute 1640 (RPMI Gibco - Life Technologies) were supplemented with 10% Fetal Bovine Serum (FBS, Gibco - Life Technologies) and 200 µM glutamine-alanine dipeptide (Glutamax, Gibco – Life Technologies). HEK-293T, HepG2, Raji NALM-6, Jurkat, and SupT1 cell lines were obtained from ATCC. Raji cell lines knockout of CD19 and NALM-6 expressing red luciferase were previously produced and validated [209]. AZD3965 and AR-C155858 (MedChemexpres) were resuspended on DMSO at 50 mg/mL and stored at -80°C. Syrosingopine and V-9302 (MedChemexpres) were resuspended on DMSO at 50 mg/mL and stored at -80°C.

2.2.2 Viral supernatant production by Transient Transfection.

Retroviral particles were produced by transfecting with 3.125 ug of RD114 expression plasmid, 4.687 ug of Peqpam-env and bicistronic plasmids containing RQR8 separated by 2A peptide and 4.687 ug of antigen-specific second-generation CARs as specified on Table 2.1. Transfection of HEK 293T was performed by seeding $1.8x10^6$ cells in 10 cm tissue culture plates over 24 hours on DMEM. Antibodies were produced by transfecting with 6 ug of the heavy chain and by transfecting with 6 ug of the light chain (Table 2.1) on HEK 293T cells in DMEM media without phenol red.

GeneJuice (Merck) was added to plain RPMI (30µl to 470µl of media) and incubated at room temperature for 5 minutes, followed by incubation with the DNA mixture for further 15 minutes. The DNA-GeneJuice mixture was added dropwise to the HEK293T cells and gently agitated to disperse the material evenly. Supernatants were harvested and pooled at 48- and 72-hours post-transfection. Supernatants were stored at -80°C after snap freezing until further use.

2.2.3 Isolation of Peripheral blood mononuclear cells.

Peripheral blood mononuclear cells (PBMCs) containing the lymphocyte fraction were isolated by Ficoll-Paque^{TM} PLUS (GE Healthcare) separation. Blood from healthy donors was diluted to a 1:1 ratio with plain RPMI. 10 ml of Ficoll-Paque^{TM} was added to a 50 ml centrifuge tube, and 30 ml of the diluted blood was carefully layered onto the Ficoll-Paque^{TM} solution. Each centrifuge tube was centrifuged at 750G for 40 minutes at 20°C with minimal acceleration and no brake. The buffy layer was harvested and washed twice with plain RPMI. Natural killer (NK) cell depletion was performed by positive selection using CD56 MACS Microbeads (Miltenyi Biotec) kit according to the manufacturer's instructions. The magnetic Microbeads mixed with the cells were passed through an LD column used for the negative selection of CD56-expressing cells. The eluted CD56 negative cell population was used for the transduction procedures. PBMC were counted, resuspended at $2x10^6$ cells/ml of complete RPMI, and activated using CD3 (clone OKT3 - 0.5ug/ml) and CD28 (clone 28.2 - 0.5ug/ml each) antibodies (Miltenyi Biotec) and 100IU/ml of IL-2 (Proleukin, Chiron) for 48 hours.

2.2.4 PBMC Transduction.

Non-tissue treated 6 well plates were coated with 2 mL of PBS containing RetroNectin (40 µg/mL – Takara) and incubated at 4°C overnight. PBS was aspirated from the plates, and 3 mL per well of retroviral supernatant was added, incubated for 20 minutes at room temperature, followed by seeding of $2x10^6$ PBMC on RPMI supplemented with 400 IU/ml of IL-2. T cells were harvested 48 hours post-transduction and resuspended in fresh RPMI supplemented with 100 UI/mL of IL-2. CAR transduction efficiency was determined by staining RQR8 with Fluorescence-activated cell sorting (FACS).

2.3 Flow cytometry.

2.3.1 Protein expression staining.

Cells were counted and pelleted by centrifugation at 400G for 5 minutes in 96-well round bottom tissue culture plates, washed with 200 µL of PBS, resuspended in 100 µl of PBS containing fluorescent-conjugated antibodies, and incubated for 30 minutes at 4°C in the dark. After incubation, the samples were washed once and resuspended in 200 µl for analysis. For intracellular staining, cells were incubated with 100 µL of Citofix/Cytoperm (BD biosciences) for 20 minutes at room temperature and washed twice with Perm/Wash, and stained according to the manufacturer's instructions. Cells were resuspended on 200 µL of PBS for analysis.

Color	Antibody	Clone	Company	Dilution
FITC	CD19	SJ25C1	Biolegend	1/100
	TIM3	F38-2E2	Biolegend	1/100
	RQR8	SIT-01	Biolegend	1/50
	CD3	HIT1a	Biolegend	1/100
Alexa Fluor 488	TNF-a	MAb11	Biolegend	1/100
	CD147	MEM-M6/1	Abcam	1/100
PerCP/Cyanine5.5	CD197	G043H7	Biolegend	1/100
	PD1	EH12.2H7	Biolegend	1/100
	Perforin	D69	Biolegend	1/100
	CCR7	BVD2-21C11	Biolegend	1/100
PE	IFN-y	4S.B3	Biolegend	1/100
	CD27	O323	Biolegend	1/100
	CD137	4B4-1	Biolegend	1/100
	RQR8	SIT-01	Biolegend	1/50
	CD3	HIT1a	Biolegend	1/100
PE-Dazzle 594	CD137	4B4-1	Biolegend	1/100
	CD8	RPA-T8	Biolegend	1/100
PE/Cy7	ICOS	C398.4A	Biolegend	1/100
APC	CD3	HIT1a	Biolegend	1/100
	GLUT-1	202915	R&D Systems	1/50
	MCT-1	882616	R&D Systems	1/50
	CD19	SJ25C1	Biolegend	1/100
	CD45RA	HI100	Biolegend	1/100
	Annexin V	-	Biolegend	1/50
Alexa Fluor 647	Granzyme B	GB11	Biolegend	1/100
Alexa Fluor 700	Granzyme B	QA16A02	Biolegend	1/100
Pacific Blue	Granzyme B	GB11	Biolegend	1/100
	CD3	HIT1a	Biolegend	1/100
	Annexin V	-	Biolegend	1/50
Brilliant Violet 421	CD45RO	UCHL1	Biolegend	1/100
	TIM3	F38-2E2	Biolegend	1/100
	CD28	CD28.2	Biolegend	1/100
	FOXP3	206D	Biolegend	1/100
Brilliant Violet 510	CD25	M-A251	Biolegend	1/100
	CD2	RPA-2.10	Biolegend	1/100
Brilliant Violet 605	PD-1	EH12.2H7	Biolegend	1/100
	CD69	FN50	Biolegend	1/100
Brilliant Violet 650	IL-2	MQ1-17H12	Biolegend	1/100
	CD8a	RPA-T8	Biolegend	1/100
	LAG3	11C3C65	Biolegend	1/100
Brilliant Violet 711	LAMP-1	H4A3	Biolegend	1/100
	CD134	Ber-ACT35 (ACT35)	Biolegend	1/100
Brilliant Violet 784	CD4	OKT4	Biolegend	1/100
Unconjugated	MCT-4	Polyclonal	Proteintech	1/50
BUV395	KI67	B56	BD	1/100
BUV496	CD8	RPA-T8	BD	1/100
BUV563	CD45RA	HI100	BD	1/100
BUV661	CD45m	SK11	BD	1/100
BUV737	CD28	CD28.2	BD	1/100
BUV805	CD3	SK7	BD	1/100

Table 2.6: List of monoclonal antibodies used for FACS.

2.3.2 Metabolic analysis staining.

MitoTracker Deep Red FM and Mitotracker Green FM (Thermofisher) staining were performed by incubating 50 nM of dyes on 100 µL of RPMI without serum at 37°C for 30 minutes. 2-NBDG (Thermofisher) labeling was performed by starving the cells for 30 minutes on 5% BSA-PBS, followed by incubating 50 µM of dye on 100 µL of RPMI without serum at 37°C for 30 minutes.

2.3.3 Absolute number cell counting.

The absolute number of cells was calculated by adding 2 µL/well (2160 beads) of CountBrightTM Absolute Counting Beads (Invitrogen) to 200 µL of PBS with target cells. The absolute number of cells was analysed with the formula:

$$\text{Absolute cell count} = \frac{\text{Target cell count}}{\text{Bead count}} * 2160$$

2.3.4 Flow cytometry data collection and analysis.

BD LSRFortessa™ Cell Analyzer (BD Biosciences) or CytoFLEX Flow Cytometer (Beckman Coulter) were used for data collection. Raw FACS data was analysed using FlowjoTM V10 (TreeStar).

2.4 Antibody production.

2.4.1 Antibody production by Transient Transfection.

An antibody against the variable region of the αCD19 FMC63 present on the CAR was produced by transfection of ExpiCHO-S™ (Thermo Fisher Scientific) using plasmids coding for the heavy chain anti-FMC63-muIgG2a and the light chain anti-FMC63-muIgk (Clone 136.20.1) using the ExpiCHO expression kit (Thermo A29133) according to the manufacturer instructions. Briefly, CHO cells were cultured to $1x10^6$ cells/ml 2 days before transfection in 30 mL of ExpiCHO media (Thermo A291000). When ExpiCHO cells reached a density of 4-6x106 cells/mL, 30 µg of sterile plasmid (1µg/ml culture) and 82 µl of Expifectamine (Thermo) were added and incubated for 5 minutes at room temperature. The mix was added to 1.5 ml of serum-free Optipro media (Thermo) and incubated for 10 minutes at room temperature. The DNA mix was added dropwise to the ExpiCHO culture and returned to incubation conditions (37°C, 125 RPM, 8% CO2, 85% humidity). After 20 hours of incubation, Enhancer 1 (150 µl) and Enhancer 2 (6 ml) were added. The supernatant was harvested after 5 days by centrifugation at 600g for 15 minutes at 4° C and filtered through a 0.22µm filter.

2.4.2 Antibody Purification.

ÄKTA start was used for protein purification with a HiTrap Protein G HP column according to the manufacturer's instructions (GE Healthcare). The HiTrap Protein G HP column was plugged into the AKTA Start and visually inspected for fluid leaking. The supernatant containing the antibodies was diluted in a 1:1 ratio with citrate buffer at pH 3.5 and 0.15 M NaCl buffer (citrate buffer) and loaded into the machine. UNICORN 1.1 software was used using the System pump Affinity Step 1 mL HiTrap protocol with Sodium phosphate (250 mM and pH 7.5) as a binding buffer and Citrate buffer (100 mM and pH 3.0) for Elution buffer.

The sample was collected on 10 fractions of 500 µL each on tubes containing 250 µL of 1 M Tris-HCl, pH 9.0 (Thermo Fisher Scientific). The protein was dialysed with Slide-A-Lyzer™ Dialysis Cassettes (Thermo Fisher Scientific) in PBS at 4°C overnight. Protein Quantification was performed using Pierce™ BCA Protein Assay Kit (Thermo Fisher Scientific) according to the manufacturer's instructions.

2.5 CAR T cell functional assay.

2.5.1 CAR T cell activation and Cytotoxicity Assay.

Activation assay was performed by culturing $5x10^4$ target cells and $5x10^4$ CAR T cells in 200 µL of RPMI media with small molecules or vehicle as a negative control. Cells were incubated for 24-48 hours and stained for flow cytometry. Cytotoxicity assay was performed by culturing $2.5x10^4$ target cells in 200 µL of RPMI media with CAR T cells at different Target: Effector (E:T) ratios in the presence of small molecules or vehicle as a negative control. Cells were incubated for 48 hours and stained for RQR8, CD19, CD3 and viability dye (eFlour 780) to distinguish target cells from T cells by flow cytometry.

2.5.2 Proliferation assay.

Raji cells were incubated with 4µg/ml mitomycin C for 2 hours at 37°C. After incubation, cells were washed 5 times with sterile PBS, and $1x10^4$ target cells were cultured with $5x10^4$ CAR T cells (1:5 ratio) for 16 hours. For the initial absolute number of T cells (Input), $5x10^4$ CAR T cells were counted by adding CountBrightTM Absolute Counting Beads (Invitrogen) cells. Small molecules or vehicle were added to the culture and counted after 4-7 days, fold expansion was calculated by dividing the absolute number of CAR T cells by the input.

2.5.3 Measuring Cytokine production by ELISA.

Human IL-2 and IFN-γ were quantified using the ELISA MAX™ kits (Biolegend) according to the manufacturer's instructions. IL-2 and IFN-γ production were determined from clarified supernatant harvested from $2.5x10^4$ CAR T cells cultured with $2.5x10^4$ target cell lines for 48 hours. Absorbance was measured at 450 nm and 570 nm within 15 minutes in a Varioskan™ LUX multimode microplate reader (Thermofisher).

2.5.4 Measurement of intracellular lactate.

CAR T cells were activated by incubation with Raji cell lines at a 1:10 ratio (E: T) for 24 hours. Afterwards, CAR T cells were purified by positive selection using the CD34 magnetic separation (Miltenyi) kit according to the manufacturer's protocol. CAR T cell purity was verified by staining with CD3, RQR8, and CD19 and analysed by FACS. Intracellular lactate was measured by culturing $5x10^4$ CAR T cells or Raji cells with small molecules or vehicle as a control for 6 hours and measure of luminescence by Lactate-Glo assay (Promega). Cells were spined at 400g for 5 minutes, washed twice with 200 µL of PBS, and resuspended on 75 µL of 0.2N HCl diluted on PBS. The cells were mixed by shaking for 10 minutes, 25 µL of 1M Tris base (Trizma®) was added and shacked for 60 seconds. 50 µL of Lactate Detection Reagent was prepared as described by the manufacturer's instructions and incubated for 60 minutes. Relative Luminesce Intensity (RLU) was read on Varioskan™ LUX multimode microplate reader (Thermofisher). Lactate accumulation was calculated as follows:

$$\text{Intracellular lactate accumulation} = \left(\frac{\text{RLU treated cells}}{\text{RLU untreated cells}}\right) \text{ x } \left(\frac{1}{\text{Number of cells}}\right).$$

2.5.5 Intracellular pH measurement.

$5x10^4$ CAR T cells were activated by culture with Raji cell lines at a 1:1 ratio (E:T) for 48 hours in 200 µL of RPMI media with small molecules or vehicle as a negative control. Intracellular pH was measured using the Intracellular pH Calibration Buffer Kit (Invitrogen) according to the manufacturer's instructions. Tumour and T cells were stained for RQR8, CD3 and viability dye to identify the CAR T cell population. Cells were then washed with HEPES-based pH 7.4 buffer, labelled with pHrodo™ Green AM and PowerLoad™ concentrate and incubated at 37°C for 30 minutes. Cells were washed once with HEPES buffer, suspended in 100 µL of pH Calibration Buffer pH 6.5 with Valinomycin/Nigericin at 10 µM and incubated for 10 minutes. Changes in pH were determined by pHrodo™ Green A mean fluorescence intensity measured by flow cytometry.

2.5.6 In vitro memory CAR T cells formation.

$5x10^5$ CAR T cells were activated by culture with $5x10^4$ Mitomycin C treated Raji cells in presence of 100 IU/mL of IL-2 RPMI media in presence of small molecules or DMSO as a negative control. Cells were counted and expanded after 4 days of culture by spinning at 400g for 5 minutes, discarding the supernatant and adding fresh RPMI supplemented with 100 UI/mL of IL-2 and small molecules. At day 7, CAR T cells were counted re-cultured with a new batch of 5x104 Mitomycin C treated Raji cells. This cycle was repeated at day 14 and 21 from the initial activation. Memory profile was assessed by staining of CD3, RQR8, CCR7, CD45RA and CD45RO and analysed by flow cytometry.

2.6 Metabolic assays.

2.6.1 Activation of CAR T cells with αCD19 anti-idiotype antibody.

12-well non-treated culture plates were incubated with 500 µL of coating buffer (Biolegend) containing 5 µg/mL of αCD19 FMC63 antibody and stored overnight at 4°C. The media was carefully removed, and 1 mL of 5% BSA-PBS blocking solution was added. After 20 minutes of incubation at room temperature, the blocking solution was removed, and $4x10^6$ CAR T cells on 4 mL of RPMI supplemented with 100 UI/mL were added. CAR T cells were incubated for 24 hours at 37°C for subsequent experiments.

2.6.2 Extracellular acidification rate and Oxygen consumption rate measurement.

CAR T cell Extracellular acidification rate (ECAR) and Oxygen consumption rate (OCR) were measured as previously described [210]. XF cell culture microplate was coated with poly-D-lysine at 50 µg/mL (Sigma-Aldrich) for 24 hours at 4°C. The solution was then removed, washed twice with sterile water, and $2x10^5$ cells per well were seeded on XF media supplemented with glucose, glutamine, and pyruvate (Gibco) for 1 hour in a non-CO_2 incubator. For OCR interrogation, 1 µM of oligomycin, 1.5 µM of FCCP, and 1µM of Antimycin A were used (Agilent). ECAR interrogation was performed by adding 10 mM of glucose (Gibco), 1 µM of oligomycin (Agilent), and 50 mM of 2-DG (Sigma-Aldrich). Metabolic parameters were measured using Seahorse XF Analyzer (Agilent) using Seahorse Wave Controller Software. OCR was measured with the XF Cell Mito Stress Test, and ECAR was measured with XF Glycolysis Stress test according to the manufacturer's instructions.

2.7 Animal B cell leukaemia Xenograft animal models.

2.7.1 B cell leukaemia mouse tumour challenge.

NOD.CB17-Prkdcscid/J (NOD/SCID) mice were bred and kept at the Kathleen Lonsdale Building animal facility of UCL. Same-sex mice were allocated randomly in the different experimental procedures. NALM-6 expressing luciferase (NALM6-Fluc) cells were inoculated by intravenous injection of $5x10^5$ cells. 6 days after tumour inoculation, $5x10^5$ αCD19 FMC63 CAR or αHER2 CAR T cells were transferred intravenously on 200 µL of sterile PBS. AR-C155858 was administered by daily intraperitoneal injections of 5 mg/kg on 10% DMSO-PBS solution or vehicle as control. Tumour growth was monitored by injecting 200 µL of luciferase at 200 µg/mL (BioScience) intraperitoneally and measuring luminescence (Photons/s/cm2/sr) on the IVIS® Spectrum In Vivo Imaging System (PerkinElmer).

2.7.2 In vivo T cell phenotyping on B cell leukaemia challenged mouse.

In vivo T cell phenotype was performed by obtaining femur and spleen from mice after 7 days of treatment with CAR T cells and small molecules. Spleen was mechanically dissociated and filtered through a cell strainer (70 µm – Falcon) into complete RPMI media. Cells were washed twice with sterile PBS, resuspended on ACK Lysing buffer (Gibco) for 5 minutes at room temperature, and washed three times with RPMI for staining. Bone marrow cells were obtained by chopping the tissue with scissors and incubating it on 5 mL of plain RPMI with 0.35 µg/mL Liberase (Roche) and 0.25 µg/mL DNAse (Sigma) for 30 minutes at 37°C. After incubation, 5 mL of RPMI with 5 µM of EDTA (Sigma) was added, filtered through a cell strainer (70 µm – Falcon), and washed twice with plain RPMI. Staining was performed by incubating the samples on 25µL of Human Fc block (Life-Technologies) solution for 10 min at 4°C. The samples were washed and stained to FACS as previously described. For intranuclear staining,

eBioscienceTM Fixation/Perm diluent and Fixation/Permeabilization concentrate (Invitrogen) was used according to the manufacturer's instructions. The compensation matrix was obtained using Ultracomp ebeads and ArC reactive beads (Invitrogen) according to the manufacturer's instructions. BD FACSymphony™ Cell Analyzer (BD Biosciences) was used for data collection. Raw FACS data was analysed using FlowjoTM V10 (TreeStar). The absolute number of cells per gram was calculated by adding CountBrightTM Absolute Counting Beads (Invitrogen) and dividing it by organ weight. T cells were defined as human $CD45^+$, Mouse $CD45^-$, $CD3^+$ $CD19^-$. Tregs were defined from T cells population as $CD4^+$, $CD8^-$, $CD25^+$, $FOXP3^+$.

2.8 Statistical analysis.

Statistical analysis was performed using Graphpad Prism software (Graphpad Software Inc.). Data from healthy donors was compared using paired t-tests between relevant groups; when comparing more than two groups in the same dataset, a Friedman One-Way ANOVA with Dunn's multiple comparison was performed instead. Tumour burden in mouse experiments was compared using a two-way ANOVA with a Sidak's multiple comparison test between groups at each time point. In vivo phenotyping was analysed using a parametric unpaired t-test between relevant groups. Data normal distribution was checked using a Kolmogorov-Smirnov test. Error bars in the figures indicate the mean plus SD or SEM. P value < 0.05 was considered statistically significant; *$P \leq 0.05$, **$P \leq 0.01$, ***$P \leq 0.001$ and ****$P \leq 0.0001$.

3. Results: Characterisation of MCT-1 pharmacological inhibition on αCD19-CAR T cells.

3.1 Introduction.

Pharmacological MCT-1 blockade has shown promising results for cancer treatment, particularly against B cell malignancies [33,34,144]. However, a limited number of studies explore the combination of MCTs inhibition and cancer immunotherapies. Several pre-clinical studies using Raji cells, a model of human B cell lymphoma, showed inhibition of MCT-1 with small molecules induced tumour cell apoptosis in vitro [158] and reduced the proliferation of Raji cells in vivo [211]. However, expression of MCT-4 has been described as sufficient to avoid the antitumoral capabilities of MCT-1 pharmacological inhibition in tumour models [132,212]. Moreover, B cell lymphomas from patients show high expression of MCT-1 and low levels of MCT-4, which makes them ideal target for MCT-1 inhibitors.

As T cells express MCT-4 upon activation, we hypothesised systemic MCT-1 inhibition is compatible with T cell ACT therapies and would exploit metabolic vulnerabilities on tumour cells without impairing T cell antitumoral potential (Figure 3.1-1). Therefore, we aimed to study MCT-1 inhibition in combination with a commonly used treatment against B cell malignancies: CD19-specific CAR T cells with a 4-1BB endo-domain (αCD19-CAR). Given the lack of highly specific antibodies against MCT-1 blocking lactate transport, we used small molecules which specifically block MCT-1/2 mediated lactic acid transport: AZD3965 or AR-C155858.

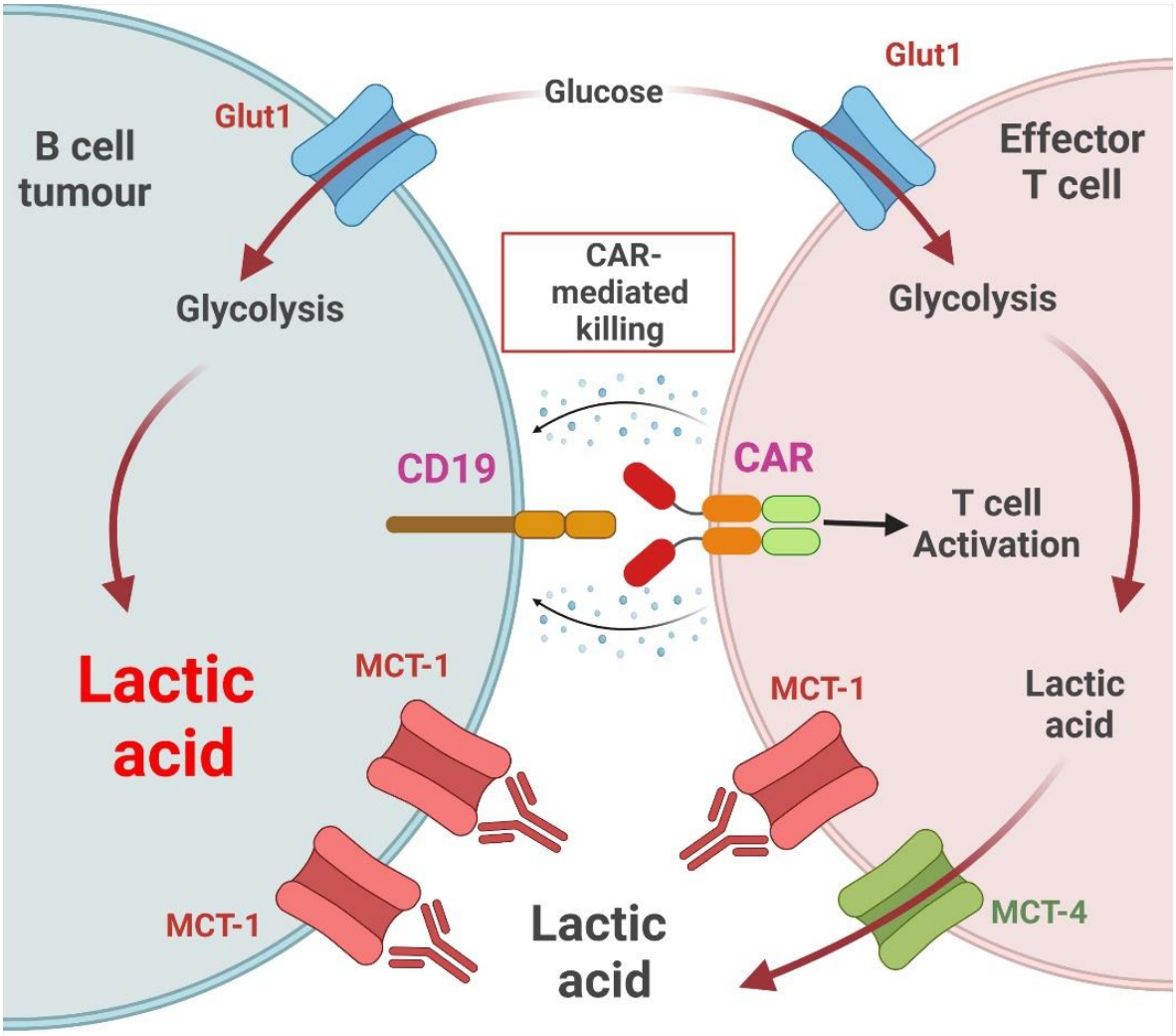

Figure 3.1-1: Inhibition of lactate export through MCT-1 on tumour and CAR T cells. Lactic acid is produced by glycolysis and exported by tumour cells and CAR T through MCTs. Inhibition of MCT-1 on tumour cells induced intracellular accumulation of lactic acid, while CAR T cells can continue their lactic acid export by the expression of MCT-4. Therefore, CAR T cells avoid lactic acid function suppression and exert their antitumoral function.

3.2 Expression and function of MCT on CAR T cells.

We transduced T cells with a CAR specific for the CD19 antigen (αCD19-CAR) using the ScFv of the FMC63 clone, as this format has been used extensively in clinical trials and has shown remarkable efficacy against B cell malignancies [213]. Activated T cells were genetically modified with retroviral particles to express the CAR in the cell surface; transduced cells were identified by expression of the marker gene RQR8 in the construct using antibodies against CD34 and detected by flow cytometry (Figure 3.2-1A-B) [214].

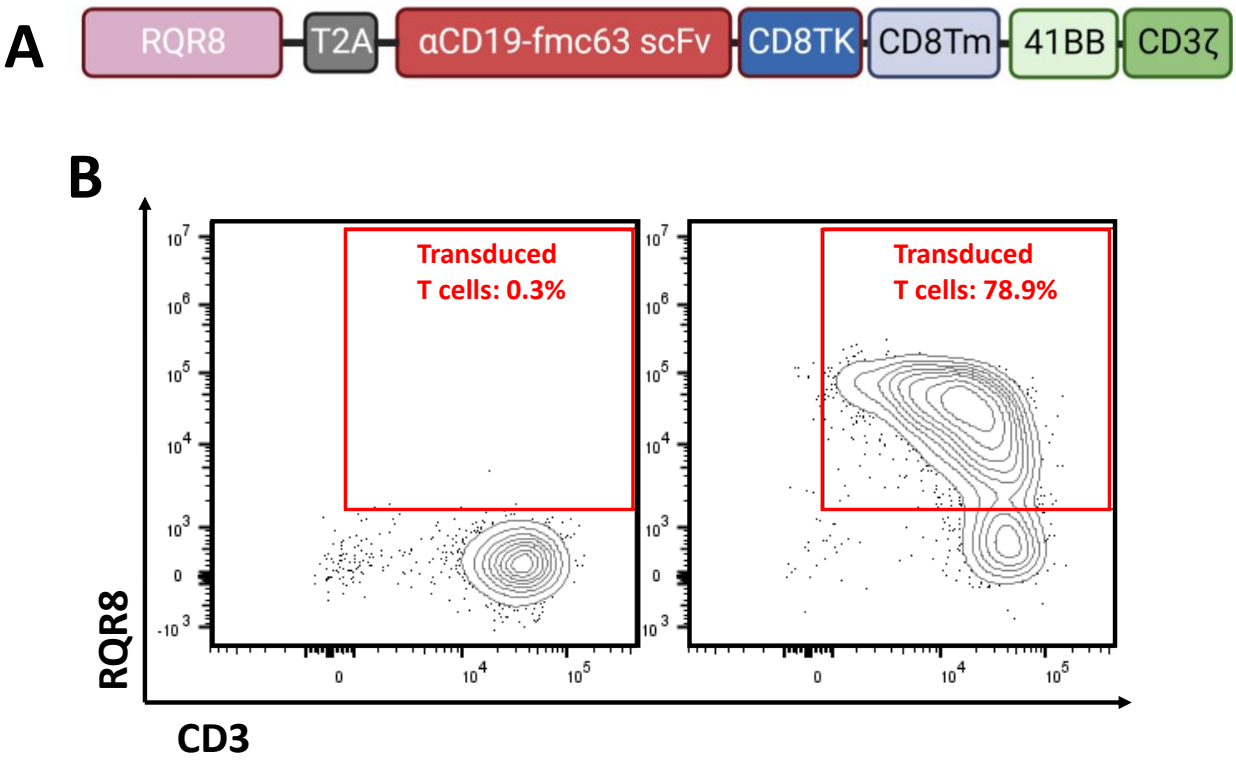

Figure 3.2-1: FMC63 αCD19-CAR T cell transduction. (A) Schematic representation of the retroviral construct used to transduce T cells. **(B)** Contour plot of representative transductions identified by RQR8 staining on Non transduced (left) and transduced (right) T cells.

Non-transduced (NT) or αCD19-CAR T cells were activated for 48 hours by co-culture with Raji cells, a $CD19^+$ human B cell lymphoma cell line. To discard background activation of CAR T cells induced by tonic signalling [215,216], we used a Raji cell line lacking CD19 by knockout by Crips/Cas9 as a negative control for CAR T cell activation (Raji-$CD19^{KO}$). Three different co-cultures conditions were analysed; Non-transduced T cells with Raji cells (NT T cells), αCD19-CAR T cells with Raji-$CD19^{KO}$ cells (Resting CAR T cells) and αCD19-CAR T cells with Raji cells (Activated CAR T cells) (Figure 3.2-2A).

We measured the expression of MCT transporters on CAR T cells by flow cytometry and analysed the changes in expression after activation. A small percentage of MCT-1 expression was found on resting CAR T cells and CD19-mediated activation induced upregulation of MCT-1 expression (Figure 3.2-2B). The same upregulation was observed in the expression of CD147, an ancillary protein necessary for MCT-1 expression and function (Figure 3.2-2C) [217].

To validate the staining of MCT-4, we analysed its expression on Raji cells (MCT-4 negative), αCD19-CAR T cells (MCT-4 positive) and HEP-G2 cells (MCT-4 positive) (Figure 3.2-2D). HEP-G2 is a human hepatocellular carcinoma model previously described to express high MCT-4 [218]. MCT-4 had a similar high expression on NT, resting and activated αCD19-CAR T cells (Figure 3.2-2E), indicating CAR T cells do not increase the expression of MCT-4 after activation. Consistent with publications measuring MCTs in tumour cells, no expression of MCT-4 and high levels of MCT-1 and CD147 were detected in Raji and NALM-6 cell lines, two models of B cell malignancies (Figure 3.2-3A-B). These results indicate that CAR T cells express both MCT-1 and MCT-4 upon antigen stimulation while B cell lymphomas cell lines only express MCT-1.

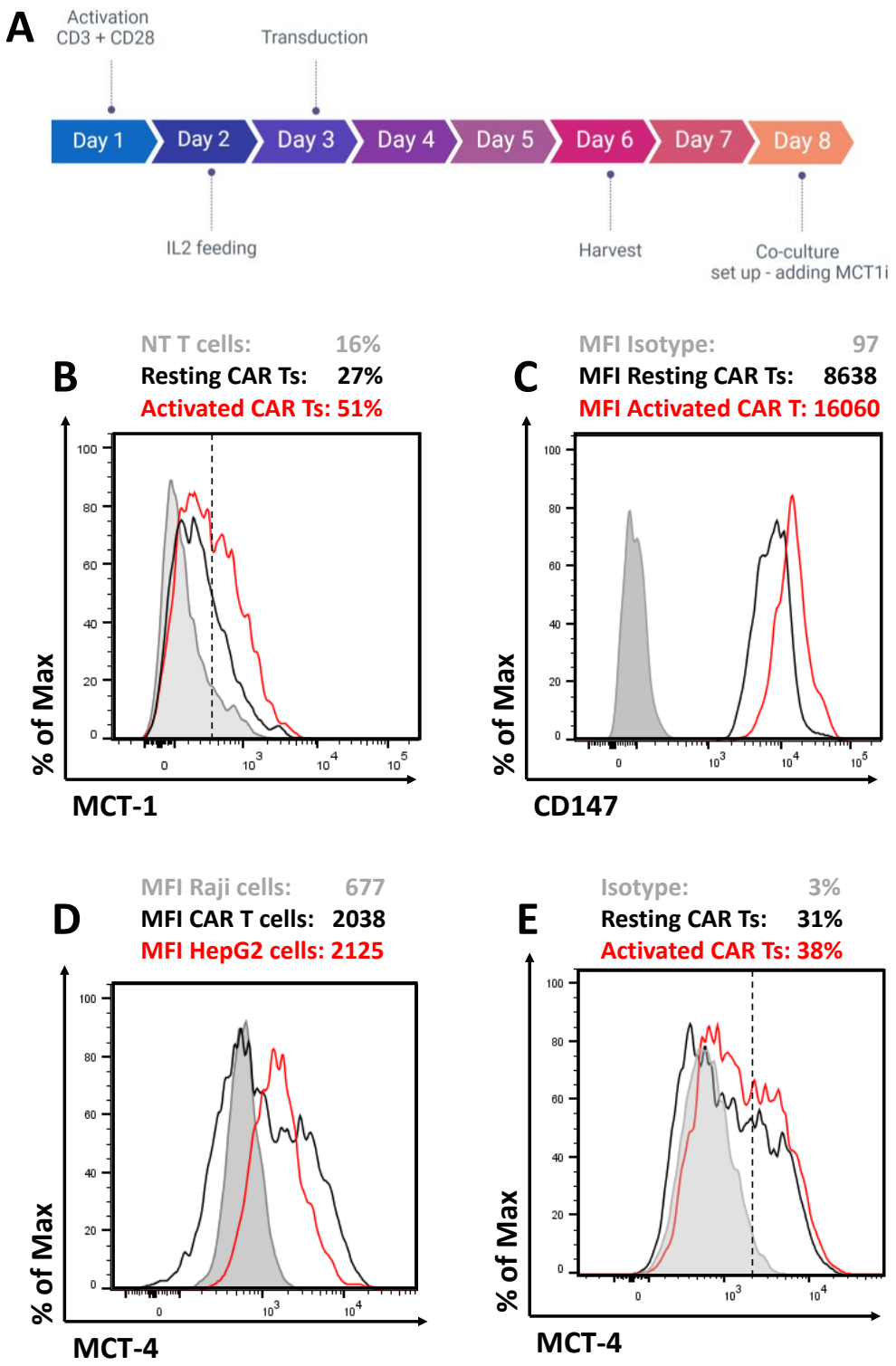

Figure 3.2-2: Expression of MCTs on CAR T cells. (A) Non-transduced or αCD19-CAR T cells were cultured with Raji or Raji-CD19^{KO} cells for 48 hours. Representative histogram of **(B)** MCT-1 and **(C)** CD147 expression on CAR T cells. Representative histogram of MCT-4 expression on **(D)** tumour cell lines and **(E)** CAR T cells measured by flow cytometry. Data representative of 3 independent experiments, n = 5-6 healthy donors per group.

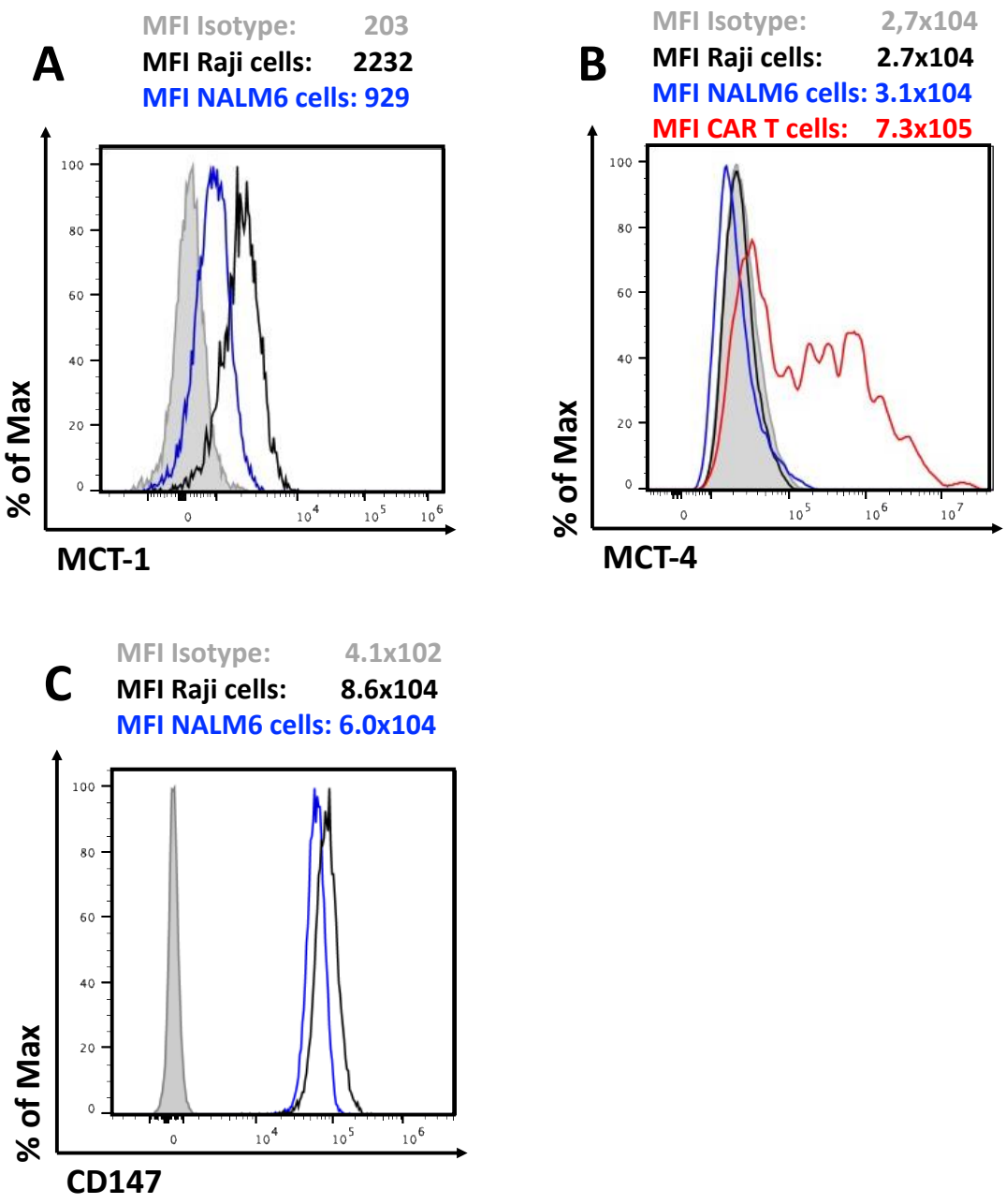

Figure 3.2-3: Expression of MCTs on B cell lymphoma cell lines. Representative histogram of **(A)** MCT-1, **(B)** MCT-4 and **(C)** CD147 expression on Raji and Nalm-6 cells measured by flow cytometry. Data representative of 2 independent experiments.

We next evaluated if exposure to MCT inhibitors (MCTi) impacts the function or expression of MCT-1 on CAR T cells. αCD19-CAR T cells were cultured for 48 hours with 100 nM of AZD3965 and AR-C155858, and MCTs expression was measured by flow cytometry. Importantly, MCT-1 inhibition did not impact the expression of MCT-1 (Figure 3.2-4A), MCT-4 (Figure 3.2-4B) or CD147 (Figure 3.2-4C) on activated αCD19-CAR T cells. MCT-1 functionality was assessed by measuring the intracellular accumulation of lactic acid. αCD19-CAR T cells were activated with Raji cells for 24 hours and purified by magnetic separation. Activated αCD19-CAR T cells were counted and cultured with different concentrations of MCT-1i for 6 hours. As a positive control of MCT-1 inhibition, Raji cells were cultured in the same conditions. Raji cells quickly accumulated intracellular lactate upon MCT-1 blockade with AZD3965 (Figure 3.2-4D) or AR-C155858 (Figure 3.2-4E). In contrast, αCD19-CAR T cells did not significantly accumulate lactic acid intracellularly upon activation at any of the concentrations measured.

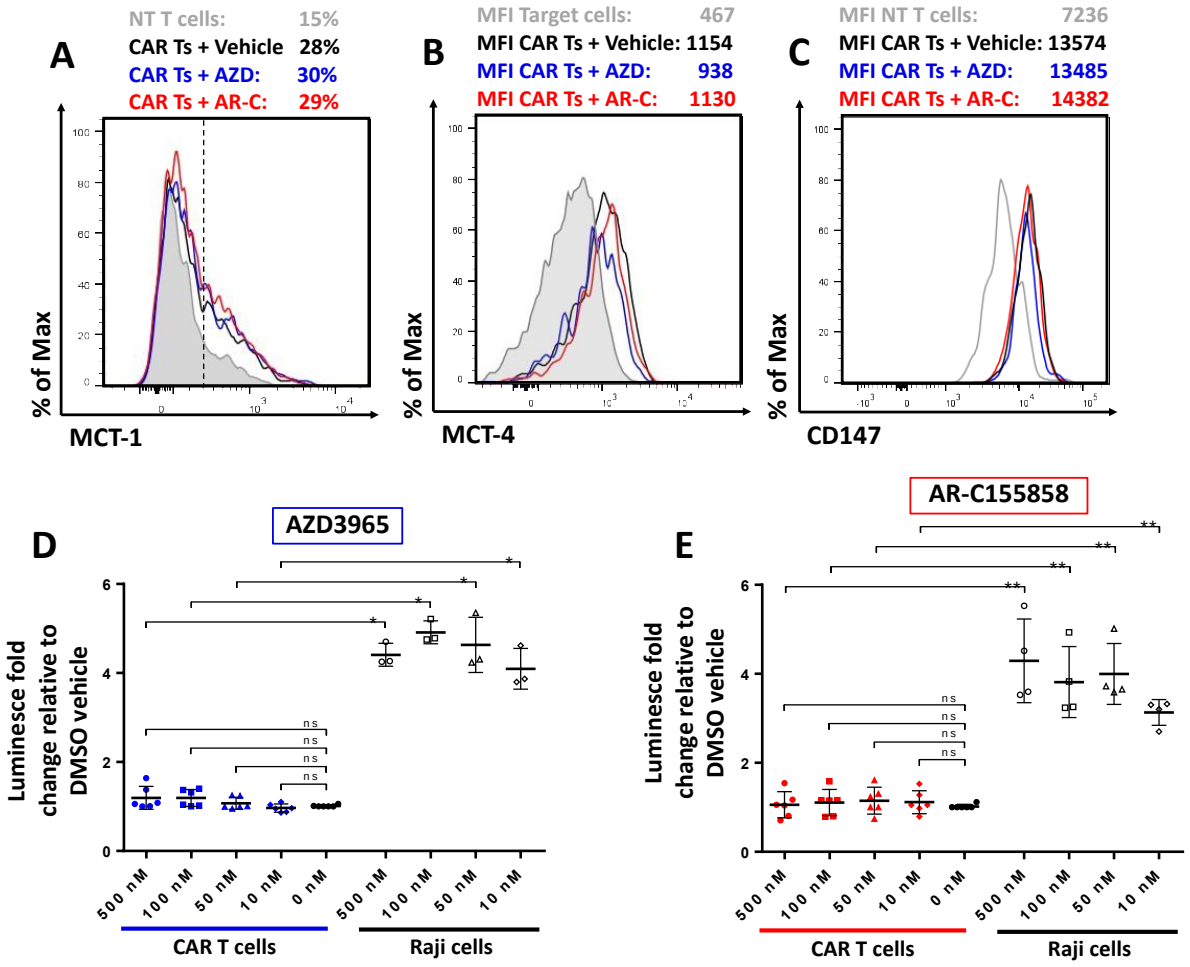

Figure 3.2-4: MCTs expression and functionality on CAR T cells after MCT-1 pharmacological blockade. Non-transduced or αCD19-CAR T cells were cultured with Raji or Raji-CD19^{KO} cells and 100 nM of MCT-1i for 48 hours. Representative histogram of **(A)** MCT-1, **(B)** MCT-4 and **(C)** CD147 expression on CAR T cells measured by flow cytometry. Intracellular lactate relative to the vehicle on purified cells cultured with **(D)** AZD3965 or **(E)** AR-C155858 for 6 hours. Data representative of 2 independent experiments, n = 5-6 healthy donors per group. Bars are the mean ± SD. *p < 0.05, **p < 0.01, ns = non-significant by Friedman One-Way ANOVA.

The immunosuppressive effects of lactic acid accumulation are partially mediated by increasing extracellular and intracellular pH [219]. We tested if MCT-1 inhibition induces changes in intracellular pH on Raji cells and activated CAR T cells using a dye which allows measuring increases in intracellular pH: pH Rodo Green AM (pH-Green). Incubation of Raji cells with MCT-1 inhibitors significantly increased the pH-Green MFI, indicating an decrease in intracellular pH. In contrast, no changes were found in activated αCD19-CAR T cells (Figure 3.2-5A-B).

MCT-1 blockade quickly induces apoptosis and diminishes the proliferation of tumour cells [158]. We tested if long exposure to MCT-1i could have similar effects on activated CAR T cells. No differences in CAR T cell expansion were found by counting the number of effector cells after 4- or 7- days of exposure to MCT-1 blockers (Figure 3.2-6A). Similarly, no significant increase was found in early apoptotic cells measured by annexin V staining on CAR T cells (Figure 3.2-6B). These results suggest CAR T cells increase the expression of MCT-1 and MCT-4 upon activation, and pharmacology blockade of MCT-1 is insufficient to significantly impair lactic acid export.

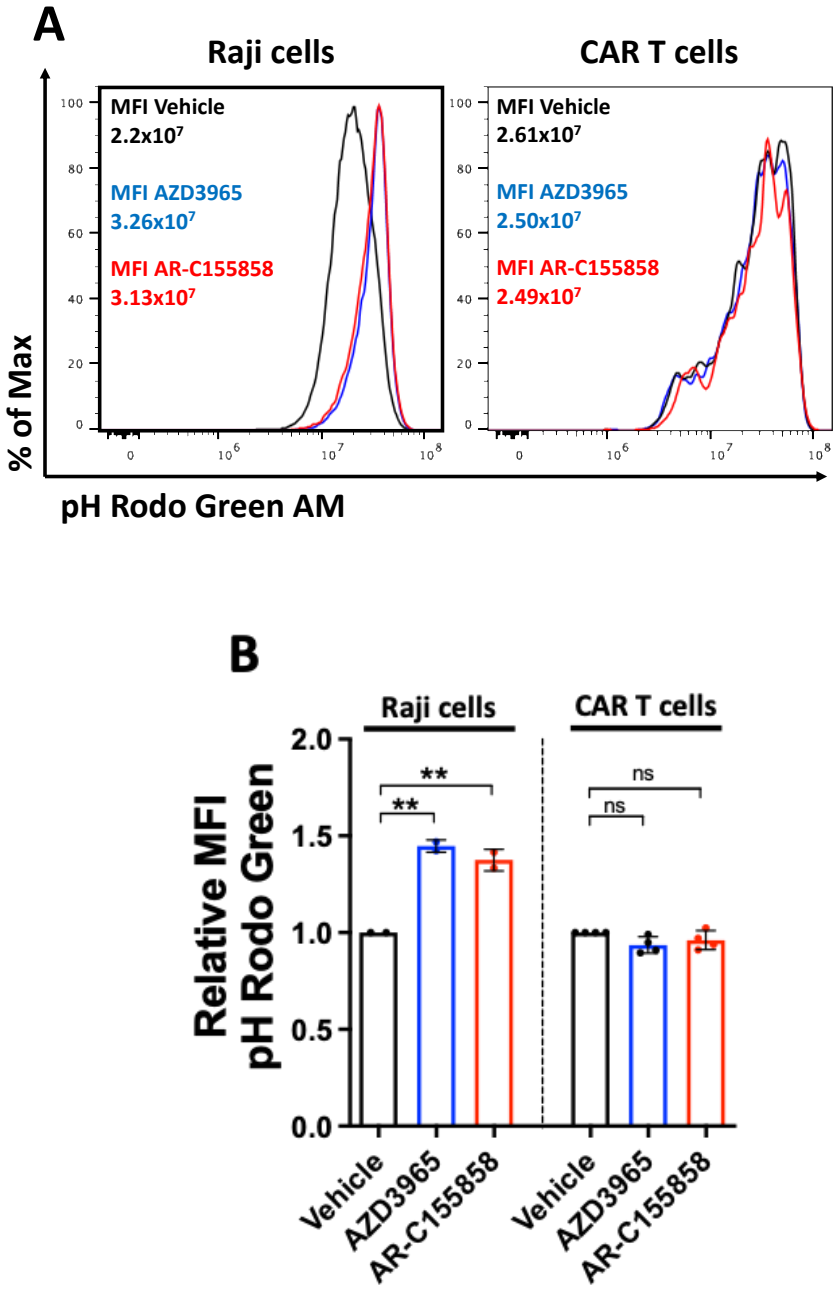

Figure 3.2-5: Changes in intracellular pH in CAR T cells after MCT-1 pharmacological blockade. Activated αCD19-CAR T cells with Raji cells and Raji cells only were cultured with 100 nM of MCT-1i for 48 hours and intracellular pH was measured by staining with pH Rodo Green AM. **(A)** Representative histogram and **(B)** Relative MFI of pH Rodo Green AM in Raji cells and activated CAR T cells. Data representative of 2 independent experiments, n = 3 healthy donors per group. Bars are the mean ± SEM. **p < 0.01, ns = non-significant by Friedman One-Way ANOVA.

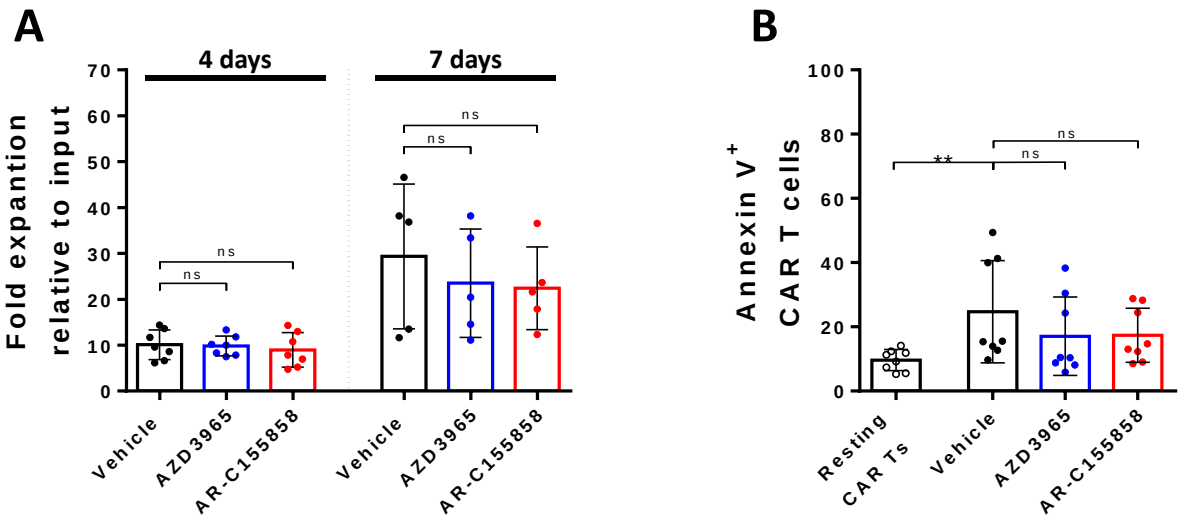

Figure 3.2-6: CAR T cell expansion after MCT-1 inhibition. (A) Fold expansion of CAR T cells after four and seven days of culture with 100 nM of MCT-1 inhibitors. **(B)** Expression of annexin V on CAR T cells after 48 hours of activation measured by flow cytometry. Pooled data of two or three independent experiments, n = 5-7 healthy donors per group. Bars are the mean ± SD. **p < 0.01, ns = non-significant by Friedman One-Way ANOVA.

3.3 MCT-1 blockade induces metabolic rewiring on CAR T cells.

On tumour cells, MCT-1 inhibition quickly reduces glycolytic flux and increases mitochondrial metabolism [151]. As T cell phenotype and metabolic networks are linked, we studied if MCT-1 inhibition could rewire the metabolic network of CAR T cells similarly as observed in tumour models. We analysed glucose uptake by culturing αCD19-CAR T cells with 2-NBDG, a fluorescent analogue of glucose, and measuring the uptake of 2-NBDG by flow cytometry. Consistent with other publications, αCD19-CAR T cells increased their glucose uptake after activation (Figure 3.3-1A), and incubation with AZD3965 or AR-C155858 did not impact glucose consumption on αCD19-CAR T cells (Figure 3.3-1B).

We tested if MCT-1 blockade impacted mitochondrial status by staining with dyes which specifically bind to the mitochondria. An increase in Mitotracker Green staining indicates an increase in mitochondrial mass, while Mitotracker Deep Red staining is proportional to mitochondrial potential. Both AZD3965 and AR-C155858 increased mitochondrial mass by 20% on activated αCD19-CAR T cells, but mitochondrial potential marginally increased (Figure 3.3-1 C-E), suggesting MCT-1 inhibition could induce metabolic reprogramming by increasing mitochondrial metabolism.

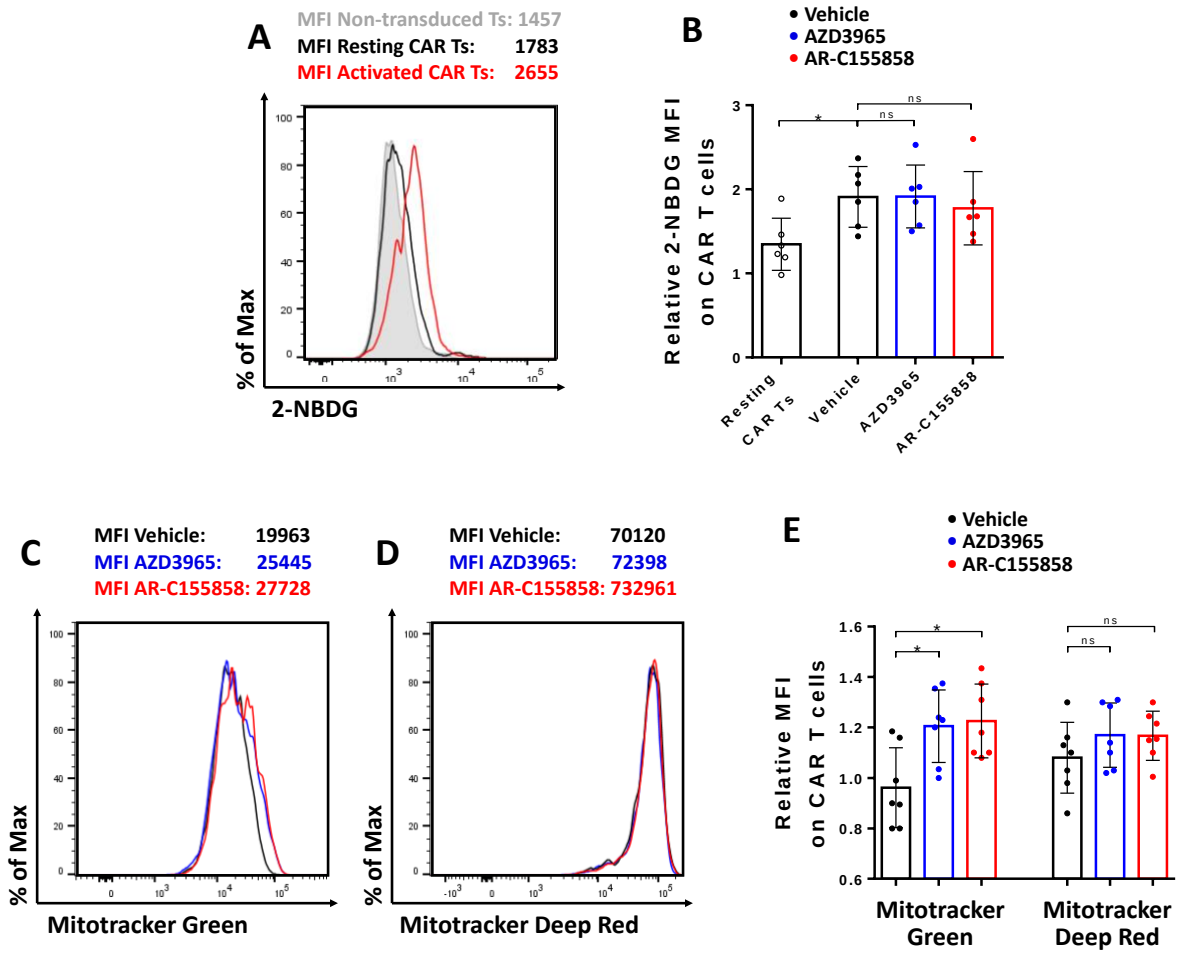

Figure 3.3-1: Metabolic characterisation by flow cytometry on CAR T cells upon MCT-1 blockade. Non-transduced or αCD19-CAR T cells were cultured with Raji or Raji-CD19^{KO} and 100 nM of MCT-1 inhibitors for 48 hours. **(A)** Representative histogram and **(B)** pooled data of 2-NBDG uptake. **(C)** Mitochondrial mass and **(D)** potential were measured with Mitotracker Green and Mitotracker Deep Red staining. **(E)** Pooled data of Mitotracker expression. Pooled data of two to three independent experiments, n=6-7 healthy donors per group. Bars are the mean ± SD. *p < 0.05, ns = non-significant Friedman One-Way ANOVA.

To further validate if MCT-1 inhibition induces metabolic rewiring, we performed a CAR T cell metabolic profiling by real-time measurement of oxygen consumption rate (OCR) and extracellular acidification rate (ECAR) with a Seahorse XFe96 Analyzer. To avoid background measurement from Raji contamination after co-culture with CAR T cells, we aimed to activate αCD19-CAR T cells with plate-bound antibodies. An-idiotype antibodies bind to the variable region of another antibody and have been used to activate CAR T cells. The anti-idiotype antibody against the αCD19-FMC63 portion of the CAR (αFMC63) [76] was validated by comparing RQR8 expression with αFMC63 binding by flow cytometry on CAR T cells (Figure 3.3-2A). Plate-bound αFMC63 antibody activated αCD19-CAR T cells similar to culture with Raji cells as measured by IFN-γ (Figure 3.3-2B) and IL-2 (Figure 3.3-2C) production. Moreover, Plate-bound αFMC63 antibody increased the OCR (Figure 3.3-3A) and ECAR (Figure 3.3-3B) of CAR T cells, indicating metabolic activation of cells.

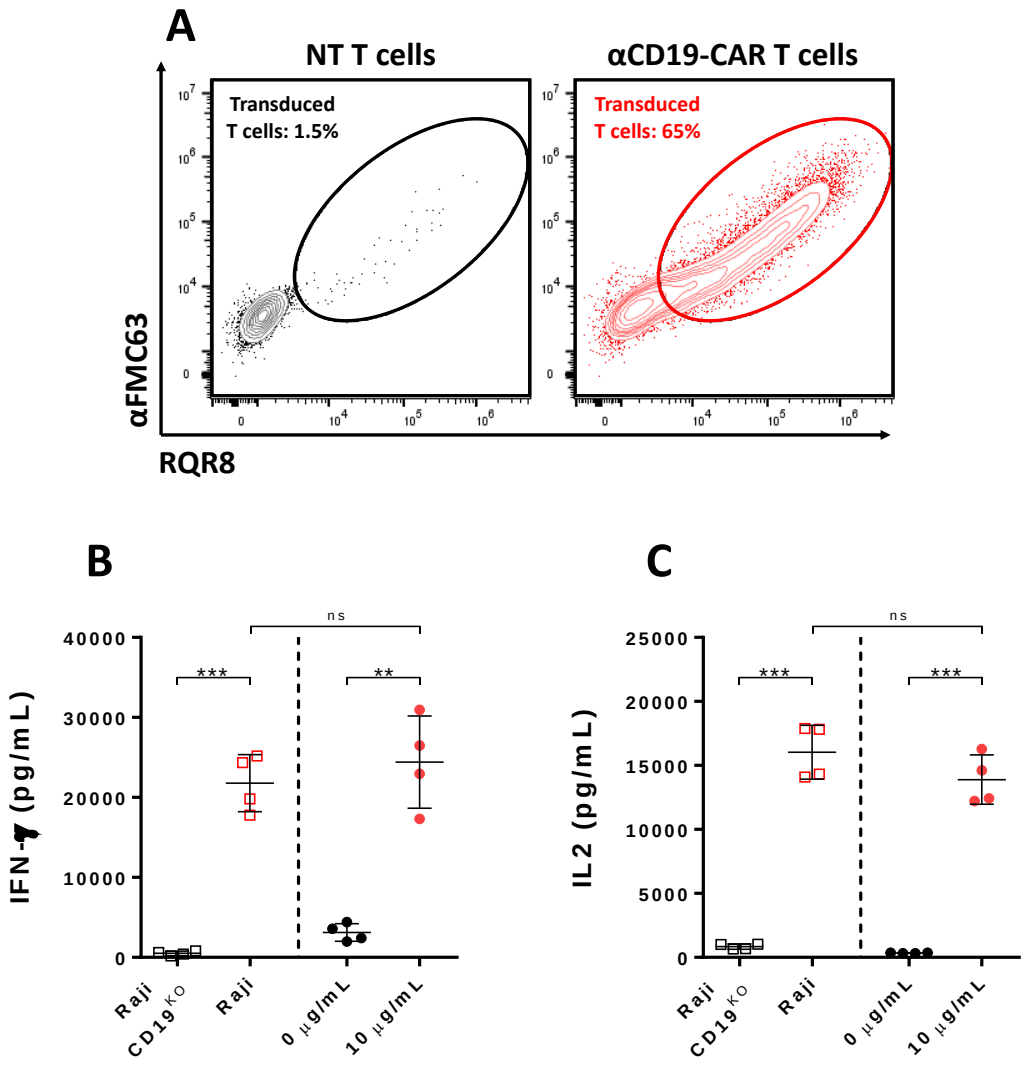

Figure 3.3-2: Activation of CAR T cells with plate-bound anti-idiotype antibody. (A) Representative histogram of αFMC63 antibody staining on non-transduced or αCD19-CAR T cells. **(B)** IFN-γ and **(C)** IL-2 production on CAR T cells activated with plate-bound αFMC63 or Raji cells for 24 hours. Pooled data of two independent experiments, n = 4 healthy donors per group. Bars are the mean ± SD. **p < 0.01, ***p < 0.001, ns = non-significant by Paired t-test.

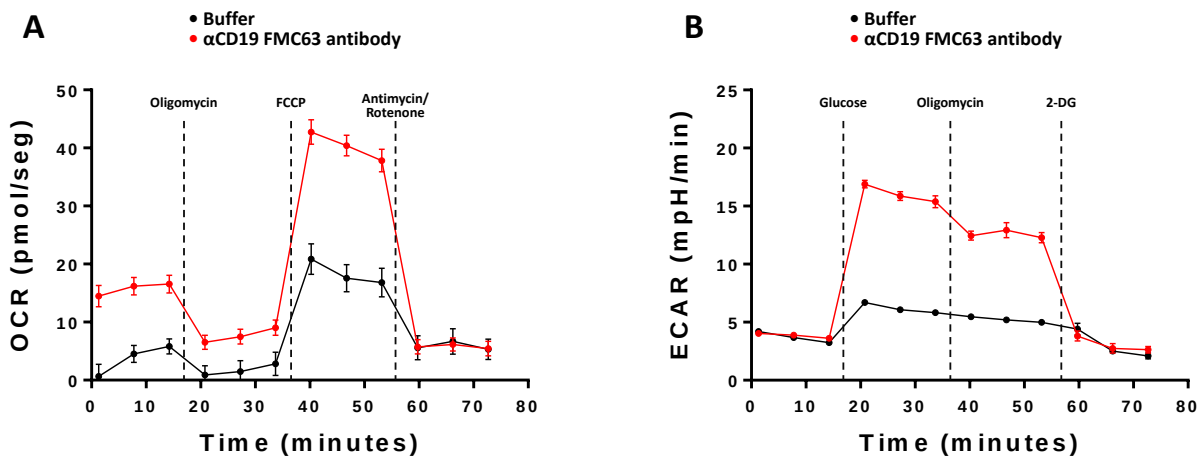

Figure 3.3-3: Seahorse profile of CAR T cells activated with plate-bound anti-idiotype antibody. CAR T cells were activated with plate-bound αFMC63 for 24 hours and collected for metabolic assays. Representative plot of **(A)** oxygen consumption rate (OCR) and **(B)** extracellular acidification rate (ECAR) on CAR T cells activated for 24 hours with plate-bound αFMC63 antibody, n=7 replicates. Bars are the mean ± SEM. Data representative of 3 donors.

With the stimulation of CAR T cells using antibodies validated, OCR and ECAR were measured on αCD19-CAR T cells activated overnight with plate-bound αFMC63 antibodies in the presence of MCT-1 blockers (Figure 3.3-4 A-B). MCT-1 inhibition with AZD3965 did not significantly increase basal, ATP-linked or maximal respiration on CAR T cells, while AR-C155858 significantly increased maximal respiration on CAR T cells (Figure 3.3-4C). Moreover, MCT-1 inhibition with both small molecules induced a reduction of glycolysis and glycolytic capacity, while only AR-C155858 induced a significant increase in the glycolytic reserve of CAR T cells (Figure 3.3-4D). In contrast, incubation of Raji cells with MCT-1 inhibitors severely reduced their ECAR, reducing glycolysis, glycolytic capacity and reserve of Raji cells (Figure 3.3-4 E-F). Taken together, our results suggest MCT-1 blockade induced partial metabolic rewiring on CAR T cells by reducing glucose flux into glycolytic pathways and increasing mitochondrial mass and respiration, particularly AR-C155858.

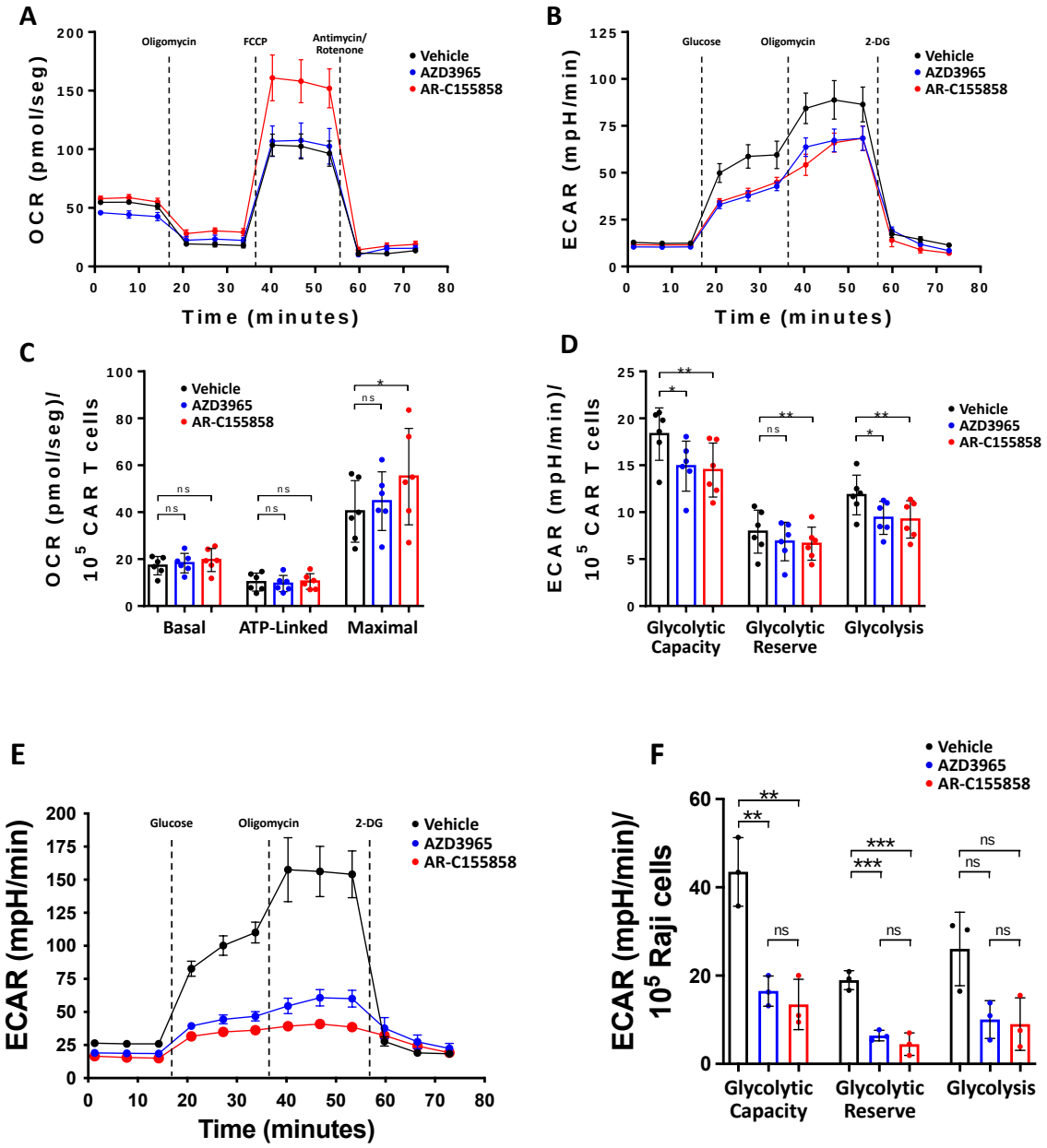

Figure 3.3-4: Real-time metabolic characterisation on Raji and CAR T cells upon MCT-1 blockade. Representative plot of **(A)** oxygen consumption rate (OCR) and **(B)** extracellular acidification rate (ECAR) on CAR T cells activated for 24 hours with plate-bound αFMC63 antibody, n=7 replicates. Bars are the mean ± SEM. **(C)** Basal, ATP-linked respiration and maximal respiration. **(D)** Glycolytic capacity, glycolytic reserve and glycolysis. Data from two independent experiments, n = 6 healthy donors per group. Bars are the mean ± SD. **(E)** Representative plot of extracellular acidification rate (ECAR) on Raji cells cultured for 24 hours with MCT-1 inhibitors, n=5 replicates. Bars are the mean ± SD. **(F)** Glycolytic capacity, glycolytic reserve and glycolysis. Data from three independent experiments. Bars are the mean ± SD. *p < 0.05, **p < 0.01, **p < 0.001, ns = non-significant by Friedman One-Way ANOVA.

3.4 MCT-1 inhibition improved CAR T cells mediated cytotoxicity against B cell lymphoma cell lines without impacting T cell phenotype.

Previous publications have shown that decreased T cell glycolytic metabolism could partially impact T cell killing potential, particularly in vitro [90]. Moreover, as both CAR T cells and MCT-1 inhibition have shown potent cytotoxicity against B cell lymphoma models, the antitumoral potential of combining CAR T cell therapies with MCT-1 blockade was tested by killing assays against Raji cell lines. αCD19-CAR T cells were co-culture with Raji ($CD19^{+}$) and Raji $CD19^{KO}$ cells on media with 100 nM of AZD3965 or AR-C155858 and counted the absolute number of tumour cells after 48 hours (Figure 3.4-1A). Both inhibitors showed a 40% reduction of live tumour cells compared to vehicle control, while at 1:16 effector/target ratio (E: T), αCD19-CAR alone showed a 55% reduction of live tumour cells. The combination of MCT-1i with CAR T cells increased the tumour cell killing compared with either treatment alone to 74% with AZD3965 and 71% with AR-C155858. Increasing the number of αCD19-CAR T cells to 1:8 E: T showed the killing of 85% of Raji cells, while the combination with MCT-1i increased tumour cell killing to 93% and 90% with AZD3965 and AR-C155858, respectively. At 1:4 E: T, 98% of Raji cells were killed with CAR T cells alone, while the combination with MCT-1i increased tumour cell killing to 100%. Generally, incubation with MCT-1i increased the killing of Raji cells by 50% at different concentrations of αCD19-CAR T cells.

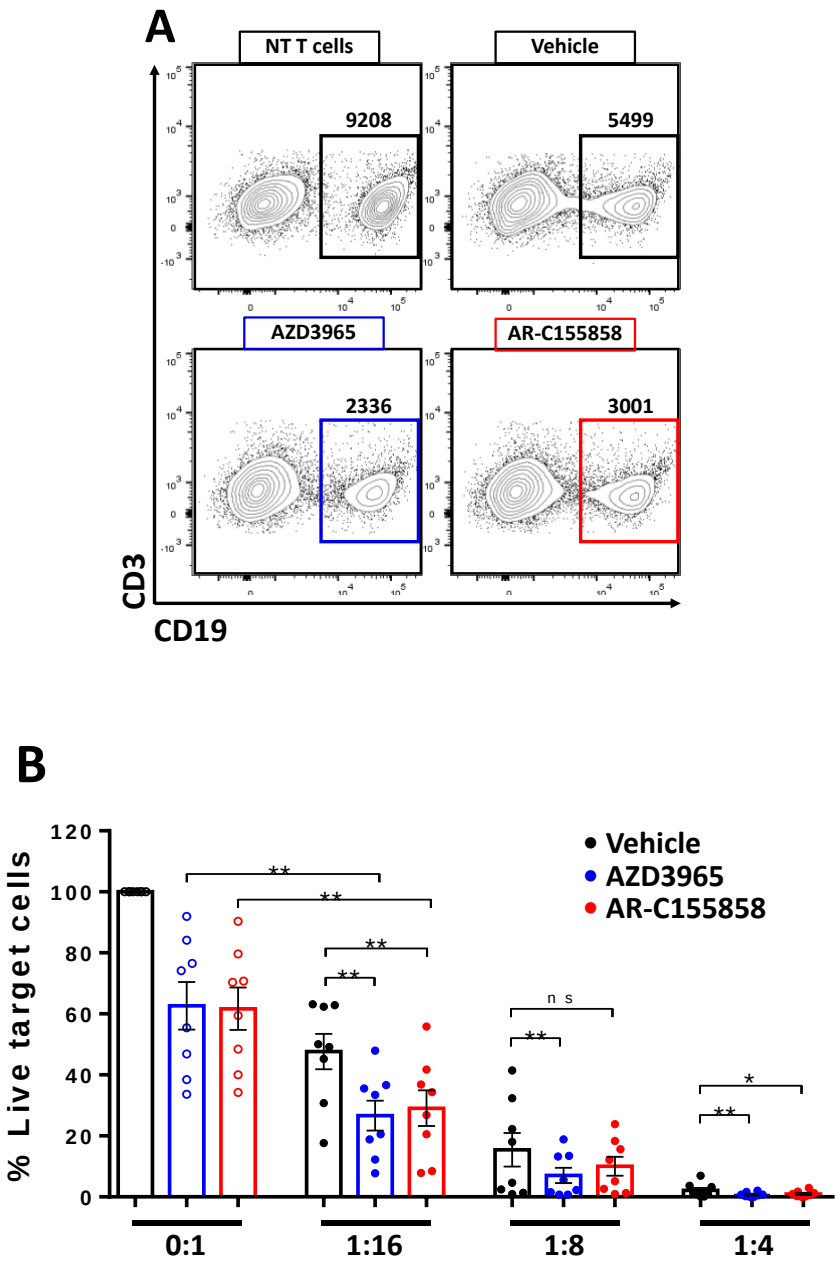

Figure 3.4-1: MCT-1 inhibition improved CAR T cells mediated cytotoxicity against B cell lymphoma cell lines. MCT-1 inhibitors were added to non-transduced or αCD19-CAR T cells in culture with target cells for 48 hours. **(A)** Representative contour plot and total number of Raji cells. **(B)** Percentage of live Raji cells cultured with CAR T cells at different effector: target ratios (E: T) ratios. Pooled data of three independent experiments, n=8 healthy donors per group. Bars are the mean ± SEM. *p < 0.05, **p < 0.01, ***p < 0.001, ****p < 0.0001, ns = non-significant by Friedman One-Way ANOVA.

The improved killing of CAR T cells against B cell malignancies was confirmed not to be limited to one tumour model by a cytotoxicity assay against NALM-6 cells, a B cell acute lymphoblastic leukaemia cell line (Figure 3.4-2A). Both AZD3965 and AR-C155858 showed a 30% reduction of live tumour cells compared to the vehicle. At a 1:32 (E: T) ratio, αCD19-CAR alone showed a 23% reduction of live tumour cells, while the combination improved the killing of tumour cells to 54% with both small molecules. Increasing the number of αCD19-CAR T cells to 1:16 E: T showed killing of 85% of NALM6 cells, while the combination with MCT-1i increased tumour cell killing to 92%. At 1:8 E: T, 96% of NALM6 cells were killed with CAR T cells alone, while the combination with MCT-1i increased tumour cell killing to 99% (Figure 3.4-1B). Together, incubation with MCT-1i increased the killing of B cell malignant cells by 50% compared to αCD19-CAR T cells alone.

Metabolic networks are closely linked with T cell memory formation and phenotype [220]. To confirm if the increase in tumour cell killing was due to an increase in CAR T cells effector phenotype, we measured activation markers on activated αCD19-CAR T cells by flow cytometry. CD147 (4-1BB) and CD134 (OX40) are members of the tumour necrosis factor receptor (TNFR) family, which are upregulated upon T cell activation, while CD69 is a commonly used early activation marker [221]. Expression of the 4-1BB (Figure 3.4-3A), OX40 (Figure 3.4-3B) and CD69 (Figure 3.4-3C) were upregulated on CAR T cells upon CD19-mediated activation with Raji cell lines and were not significantly altered after MCT-1 blockade with either AZD3965 or AR-C155858.

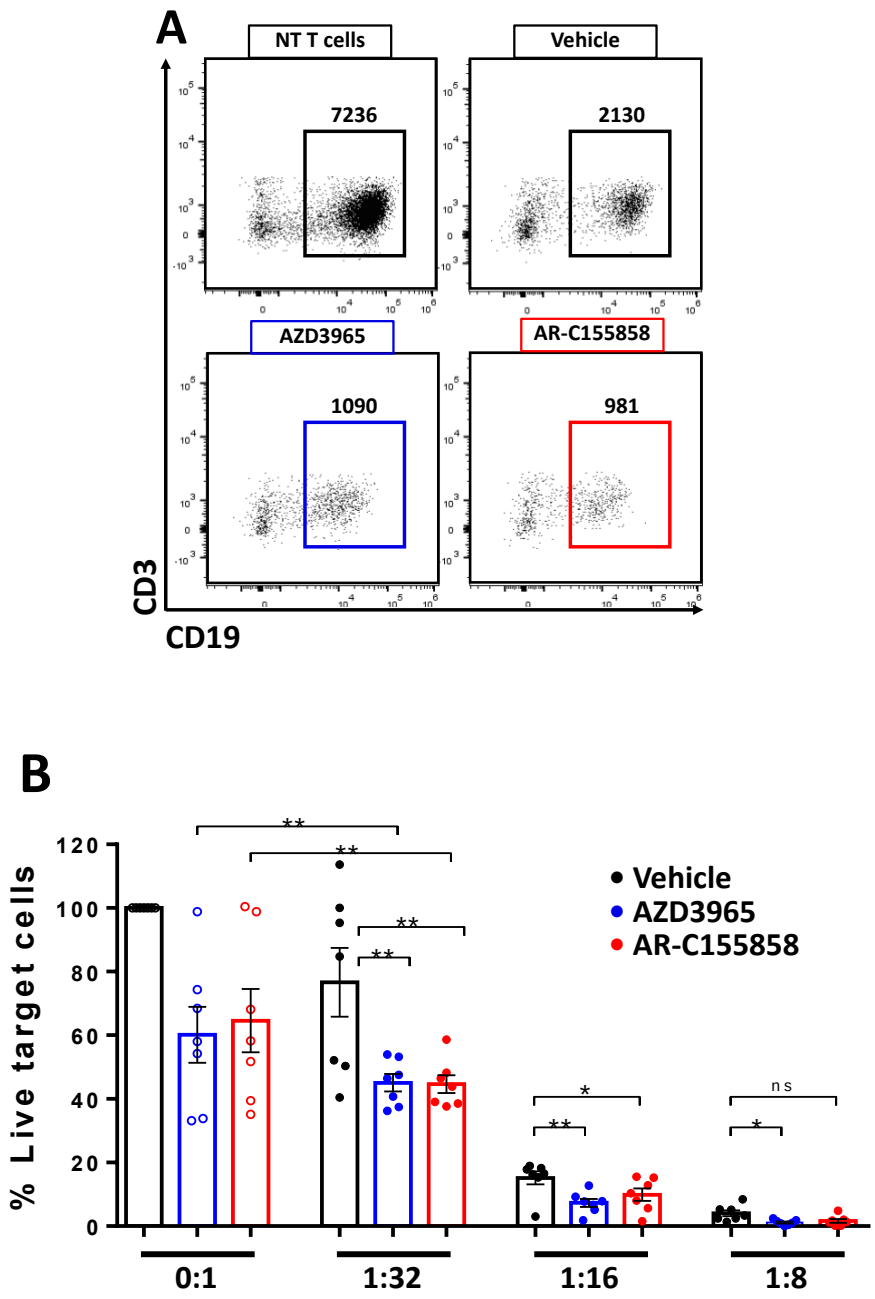

Figure 3.4-2: MCT-1 inhibition improved CAR T cells mediated cytotoxicity against B cell leukaemia cell lines. MCT-1 inhibitors were added to non-transduced or αCD19-CAR T cells in culture with target cells for 48 hours. **(A)** Representative contour plot and total number of NALM-6 cells. **(B)** Percentage of live NALM-6 cells cultured with CAR T cells at different E: T ratios. Pooled data of three independent experiments, n=7 healthy donors per group. Bars are the mean ± SEM. *p < 0.05, **p < 0.01, ***p < 0.001, ****p < 0.0001, ns = non-significant by Friedman One-Way ANOVA.

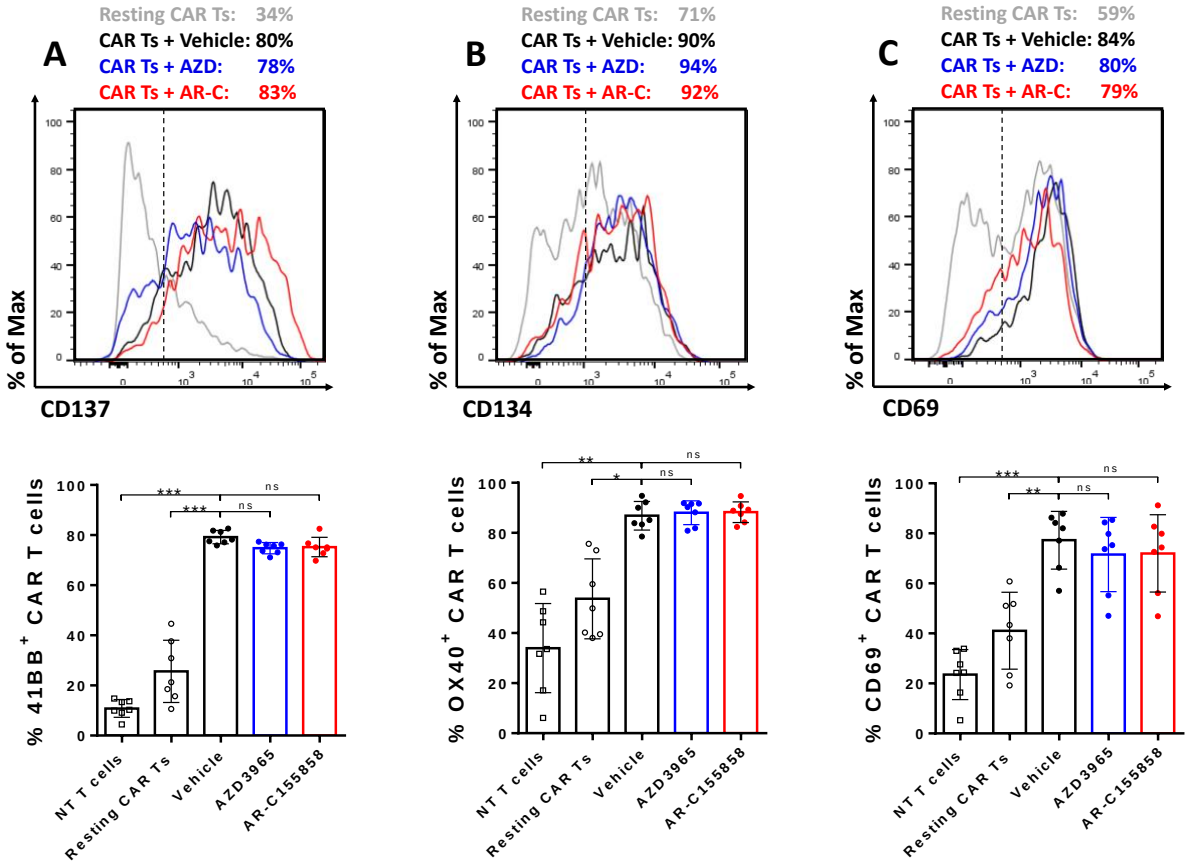

Figure 3.4-3: MCT-1 inhibition did not impact CAR T cells activation phenotype. Expression of activation markers (**A)** 4-1BB, **(B)** OX40 and **(C)** CD69 on activated CAR T cells with Raji cells or Raji-CD19^{KO} for 24 hours. Pooled data of three independent experiments, n = 7 healthy donors per group. Bars are the mean ± SD. *p < 0.05, **p < 0.01, ***p < 0.001, ns = non-significant by Friedman One-Way ANOVA.

We continued the phenotyping by analysing the expression of functional proteins directly involved in antitumoral T cell response. Granzyme B production is critical to T cell cytolytic functions [222]; likewise, the release of inflammatory cytokines like IFN-γ activates the immune system and increases MHC-I expression on cancer cells [223], while IL-2 increases the proliferation and effector functions of antitumoral T cells [224]. Activated αCD19-CAR CD8 T cells had high expression of Granzyme B, which did not significantly change after MCT-1 blockade (Figure 3.4-4A). Similarly, activated CAR T cells expressed high amounts of IFN-γ (Figure 3.4-4B) and IL-2 (Figure 3.4-4C), while MCT-1 inhibition did not alter IFN-γ production, and IL-2 was slightly reduced. Likewise, no differences in exhaustion markers PD-1 (Figure 3.4-4A) or TIM-3 (Figure 3.4-5B-C) expression were found on activated CAR T cells. Taken together, this suggests metabolic rewiring mediated by MCT-1 inhibition is insufficient to induce changes in the phenotype of CAR T cells. Moreover, the combination of CAR T cells with MCT-1 blockade significantly improved tumour cell killing suggesting MCT-1 inhibition selectively affects B cell leukaemia cells and is compatible with T cell immunotherapies.

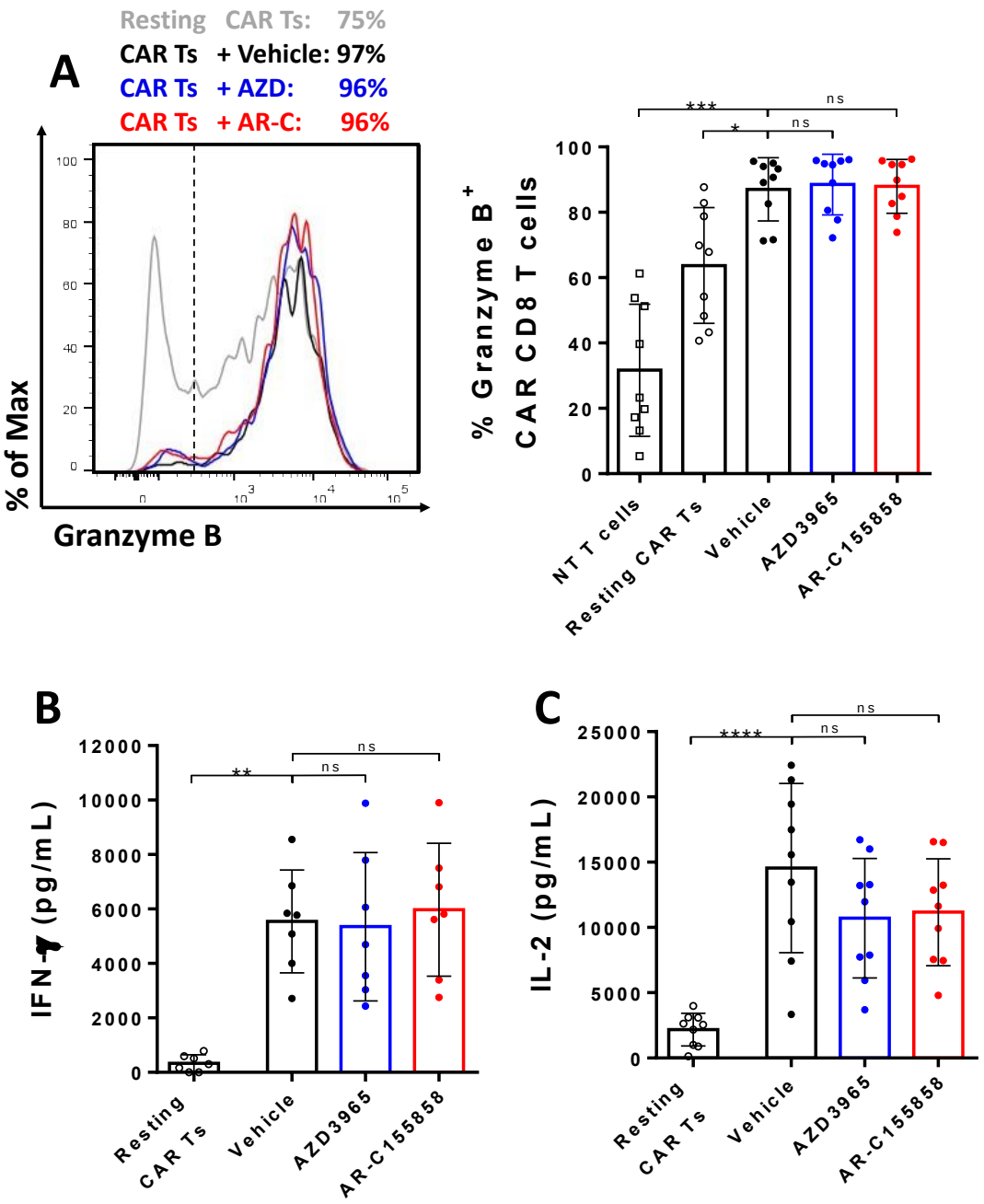

Figure 3.4-4: MCT-1 inhibition did not impact CAR T cells effector functions. (A) Expression of Granzyme B on activated CD8 CAR T cells with Raji cells or Raji-CD19^{KO} for 24 hours. (**B)** IFN-γ and **(C)** IL-2 production were measured by ELISA after 48 hours. Pooled data of three independent experiments, n = 7 healthy donors per group. Bars are the mean ± SD. *p < 0.05, **p < 0.01, ***p < 0.001, ****p < 0.0001, ns = non-significant by Friedman One-Way ANOVA.

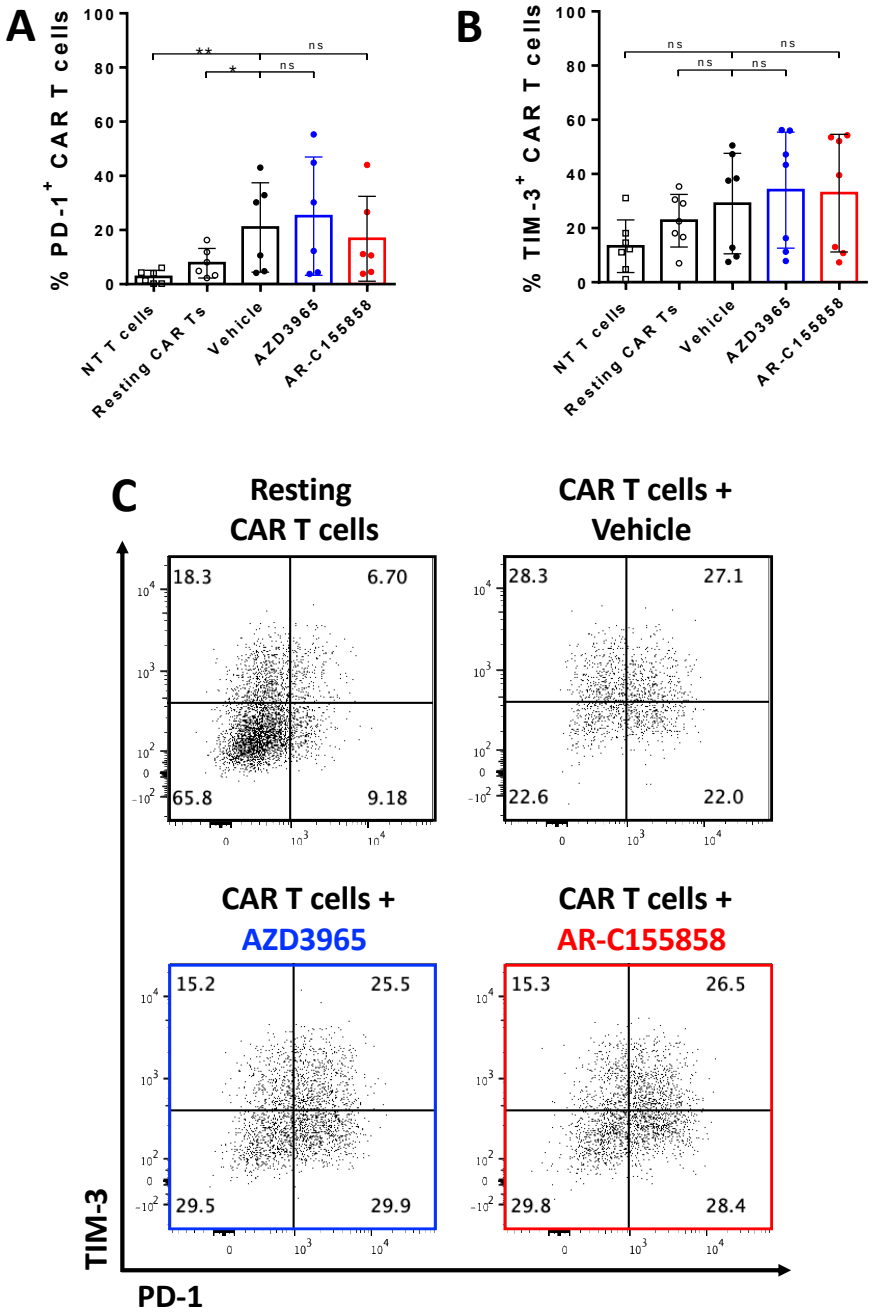

Figure 3.4-5: MCT-1 inhibition did not impact CAR T cells exhaustion profile. Expression of exhaustion markers (**A)** PD-1, **(B)** TIM-3 and **(C)** PD-1/TIM-3 on activated CAR T cells with Raji cells or Raji-CD19^{KO} for 24 hours Pooled data of three independent experiments, n = 7 healthy donors per group. Bars are the mean ± SD. *p < 0.05, **p < 0.01, ***p < 0.001, ****p < 0.0001, ns = non-significant by Friedman One-Way ANOVA.

3.5 CAR T cells memory phenotype remains unchanged after long-term MCT-1 inhibition.

T cells memory formation is an integrating node for metabolism and phenotype as different memory T cells engage in distinct metabolic networks, including CAR T cells [225]. To further explore if metabolic rewiring induced by long-term MCT-1 blockade translates into phenotype changes, we analysed the ex vivo T cell memory phenotype. αCD19-CAR T cells were cultured for 21 days by weekly restimulation with Raji cells in the presence of MCT-1 blocking molecules. Different CAR T cell memory populations were defined by the expression of CD45RA, CD45RO and CCR7 (Figure 3.5-1A) [226]. No significant differences were observed in the percentage of Naïve T cells, effector memory T cells CD45RA (TEMRA), effector memory T cells (T_{EM}) or central memory T cells (T_{CM}) (Figure 3.5-1 B-E) after 7-, 14- and 21-days confirming MCT-1 inhibition does not impact CAR T cell memory formation.

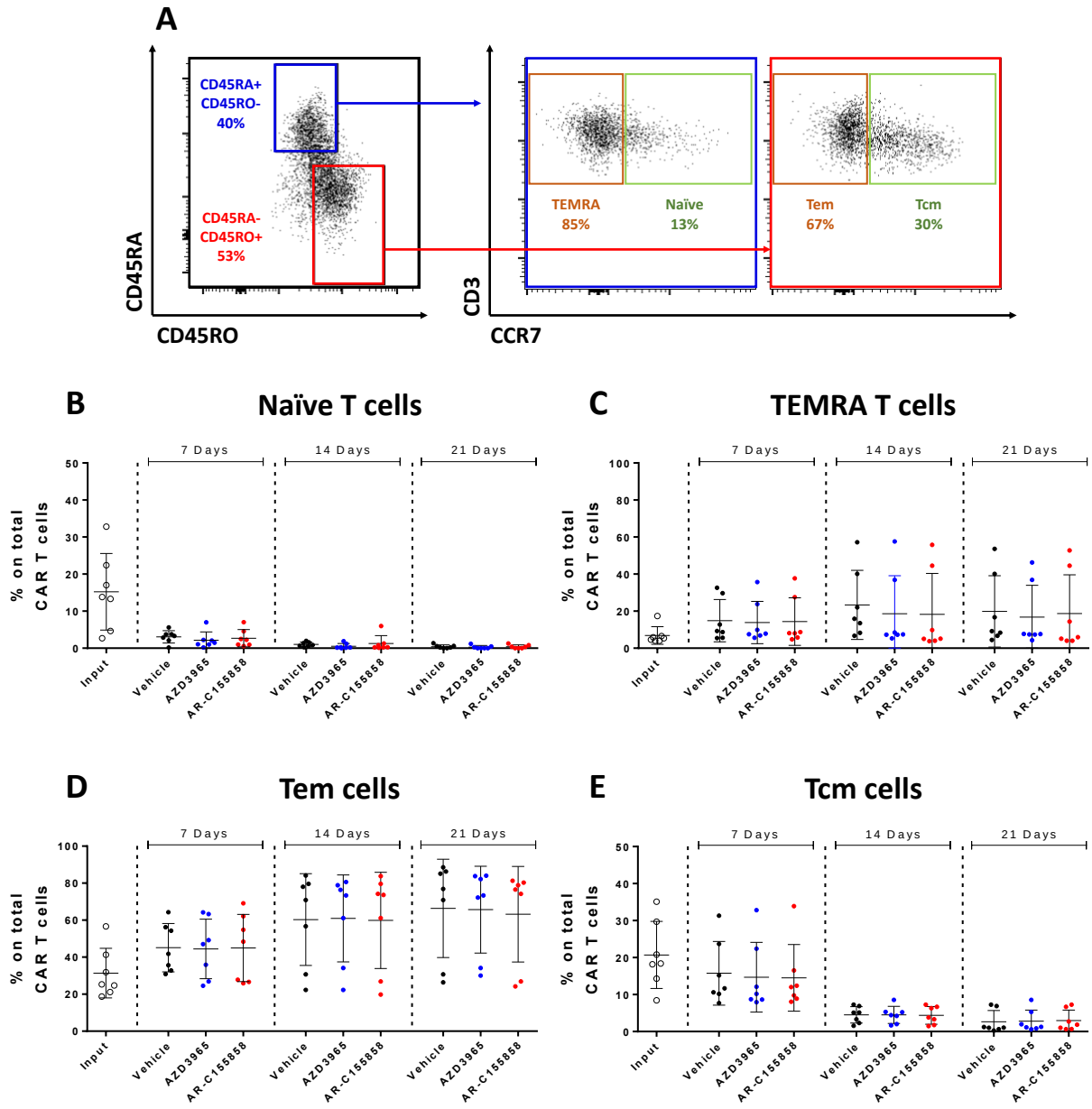

Figure 3.5-1: Memory phenotype of CAR T cells after long exposure with MCT-1 blockers. αCD19-CAR T cells were re-stimulated with Raji cells every 7 days. (**A)** Representative expression of CD45RA, CD45RO and CCR7 on CAR T cells. (**B)** Percentage of naïve T cells, (**C)** TEMRA T cells, (**D)** effector memory T (Tem) cells and (**E)** central memory T (Tcm) cells measured by flow cytometry every 7 days. Pooled data of three independent experiments, n = 7 healthy donors per group. Bars are the mean ± SD. Ns = non-significant by Friedman One-Way ANOVA.

3.6 CD28 co-stimulation on αCD19-CAR T cells does not impact MCT-1 blockade profile.

All our experiments were performed using a CAR with a 4-1BB co-stimulation domain, as is the structure commonly used in clinical trials. However, different co-stimulatory domains within the CAR structure confer different metabolic programs, particularly 41BB stimulation favours oxidative metabolism, while CD28 imprints a more glycolytic phenotype on T cells. A more glycolytic CAR could render T cells susceptible to MCT-1 inhibition by increasing intracellular lactic. To discard this possibility, we performed similar experiments on the same αCD19-CAR with a CD28 signalling domain instead of 4-1BB (CAR-CD28). Importantly, no difference in glucose uptake was found on activated CAR-CD28 T cells measured by 2-NBDG uptake (Figure 3.6-1A). Similarly, expression of the activation markers 4-1BB (Figure 3.6-1B) or CD69 (Figure 3.6-1C) was not affected by MCT-1i on CAR-CD28 T cells.

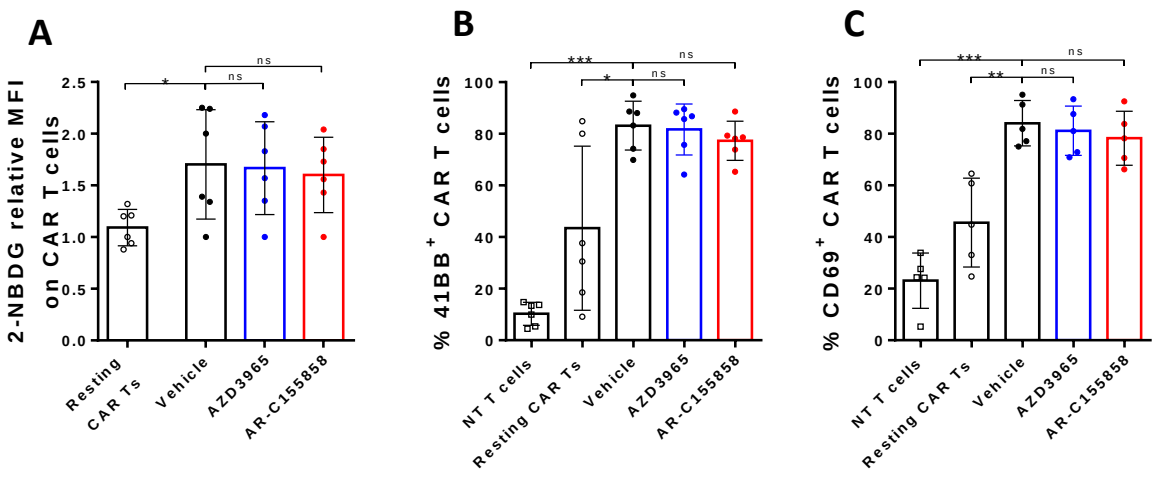

Figure 3.6-1: Activation markers after MCT-1 inhibition on CD19-CD28 CAR T cells. MCT-1 inhibitors were added to non-transduced or αCD19-CAR T cells with a CD28 co-stimulatory domain. (**A)** 2-NBDG uptake and expression of (**B)** 4-1BB and **(C)** CD69 in re-stimulated CAR T cells with Raji cells or Raji-CD19^{KO} (Resting CAR T cells) for 24 hours. Pooled data of two independent experiments, n = 5-6 healthy donors per group. Bars are the mean ± SD. *p < 0.05, **p < 0.01, ***p < 0.001, ns = non-significant by Friedman One-Way ANOVA.

We next evaluated if the expression of inflammatory cytokines or CAR T cells cytotoxicity was compromised on CAR-CD28 T cells after MCT-1 blockade. No differences in IFN-y (Figure 3.6-2A) or IL-2 (Figure 3.6-2B) production after 48 hours of co-culture of CAR-CD28 T cells with Raji cells. Similarly, at 1:16 CAR-CD28 alone showed a 38% reduction of Raji cells. The combination of MCT-1i with CAR T cells increased the tumour cell killing to 64%.

Increasing the number of CAR-CD28 T cells to 1:8 E: T showed killing of 61% of Raji cells while the combination with MCT-1i increased tumour cell killing to 81%. At 1:4 E: T, 93% of Raji cells were killed with CAR T cells alone while the combination with MCT-1i increased tumour cell killing to 99% (Figure 3.6-2C). Taken together, MCT-1 blockade on CD28 signalling CARs did not significantly impact CAR T cell phenotype or killing potential; moreover, we observed similar results comparing CD28 with 4-1BB signalling.

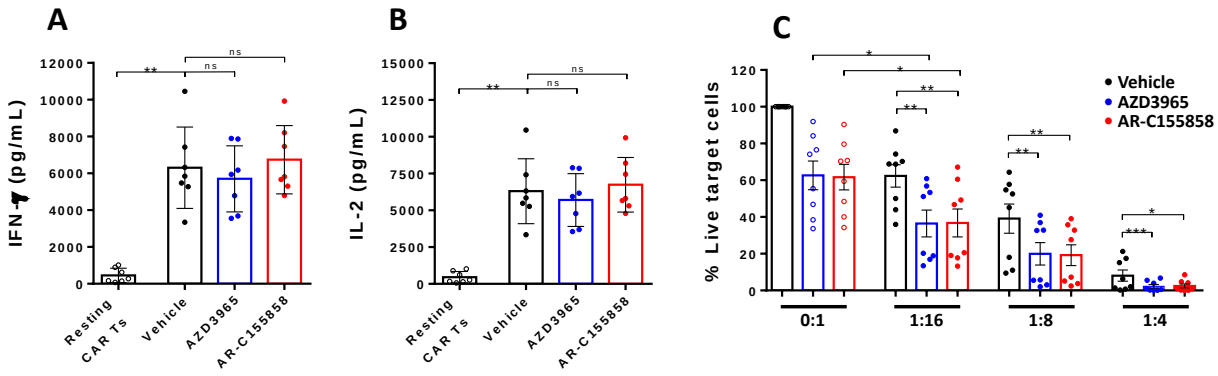

Figure 3.6-2: Antitumoral potential of CD19-CD28 CAR T cells after MCT-1 inhibition. MCT-1 inhibitors were added to non-transduced or αCD19-CAR T cells with a CD28 co-stimulatory domain. (**A)** IFN-γ and **(B)** IL-2 production measured by ELISA after 48 hours. **(C)** Percentage of live Raji cells cultured with CAR T cells at different effector: target ratios (E: T) ratios. Bars are the mean ± SEM. Pooled data of three independent experiments, n = 7-8 healthy donors per group. Bars are the mean ± SD. *p < 0.05, **p < 0.01, ***p < 0.001, ns = non-significant by Friedman One-Way ANOVA.

3.7 Dual blockade on MCT-1 and MCT-4 severely impairs CAR T cell effector functions.

Studies using MCT-1 inhibitors have found the expression of MCT-4 as a key mechanism of resistance to MCT-1 blockade on tumour cells. Therefore, we hypothesised that MCT-4 expression on CAR T cells is sufficient to exert lactate export in the absence of functional MCT-1, and dual inhibition of MCT-1 and MCT-4 could significantly impair T cell survival.

Raji and CAR T cells were cultured with syrosingopine, an anti-hypertensive drug which blocks lactate export through MCT-1 and MCT-4 [171] at concentrations between 20 µM and 0.65 µM. Titration of syrosingopine showed sensitivity on Raji cells at the micromolar range (Figure 3.7-1A), similar to previous works with other cell lines [174]. In addition, the culture of activated αCD19-CAR T cells with Raji cells in the presence of syrosingopine significantly reduced CAR T cell expansion (Figure 3.7-1B) and IFN-γ production (Figure 3.7-1C) in a dose-dependent manner, with 20 µM reducing by at least 90% the αCD19-CAR T cells numbers and IFN-γ production, while not non-statistically significant difference was found at 2.5 µM.

We confirmed syrosingopine induced lactate accumulation by measuring intracellular lactate on Raji or αCD19-CAR T cells cultured with 100 nM of AR-C155858 or different concentrations of syrosingopine. Both small molecules induced 20-fold lactate accumulation on Raji cells, while significant lactate accumulation was found on syrosingopine-treated CAR T cells compared to MCT-1 inhibition with AR-C155858 (Figure 3.7-1D). Moreover, culture with syrosingopine did not change the expression of MCT-1 (Figure 3.7-1E) or MCT-4 (Figure 3.7-1F) on activated CAR T cells.

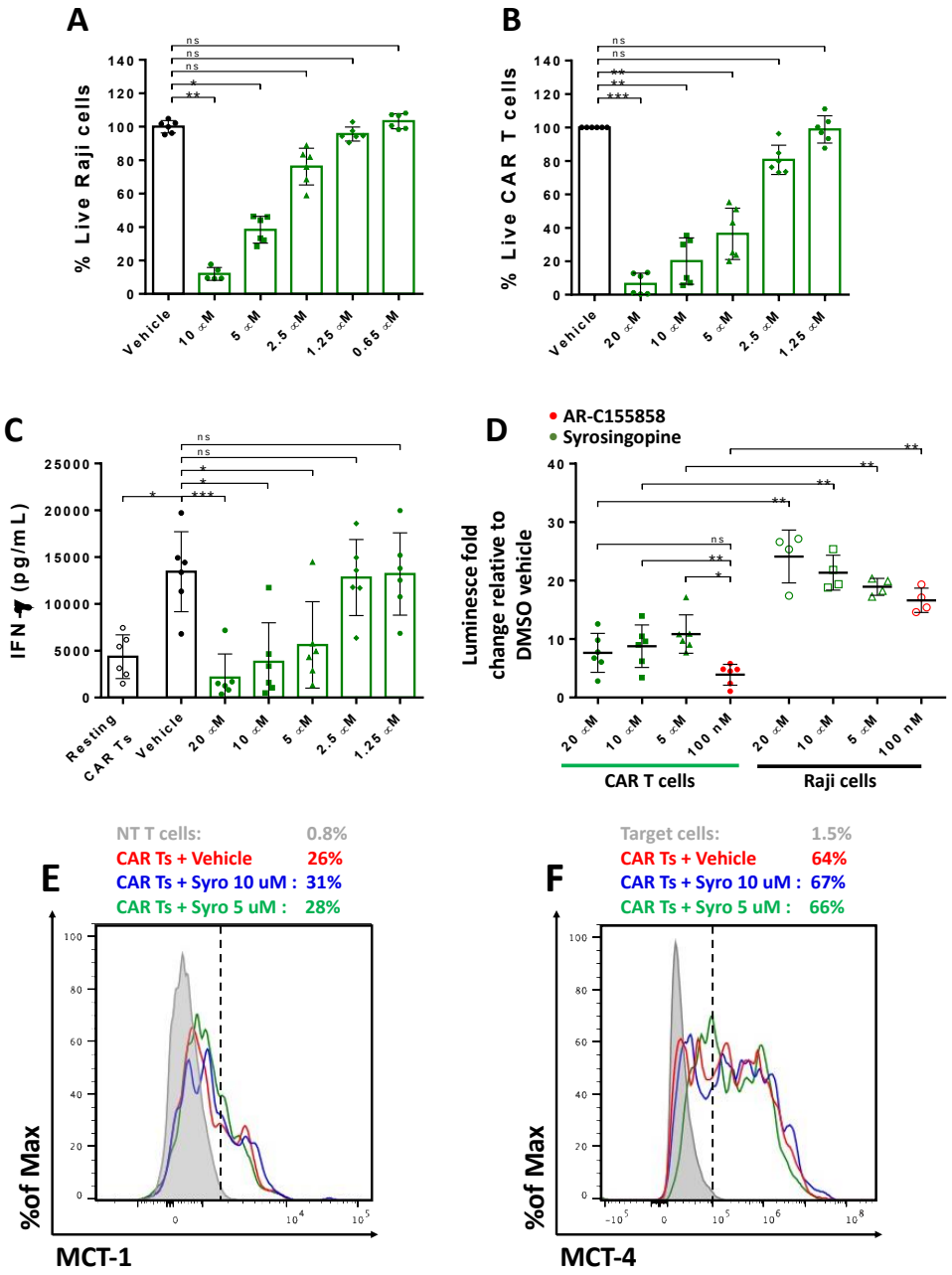

Figure 3.7-1: Dual blockade of MCT-1/4 impairs CAR T cell activation phenotype. Raji, non-transduced or αCD19-CAR T cells were cultured with different concentrations of Syrosingopine or vehicle as control. **(A)** Percentage of live Raji cells or **(B)** αCD19-CAR T cells measured by flow cytometry. **(C)** IFN-γ production of activated CAR T cells measured by ELISA after 48 hours. **(D)** Intracellular lactate relative to vehicle control on cells cultured with Syrosingopine. Expression of **(E)** MCT-1 and **(F)** MCT-4 on αCD19-CAR T cells cultured with target tumour cells and syrosingopine for 24 hours. Bars are the mean ± SD. Pooled data of two independent experiments, n = 6 healthy donors per group. *p < 0.05, **p < 0.01, ***p < 0.001, ns = non-significant by Friedman One-Way ANOVA.

Previously we found cooperation in tumour cell killing between αCD19-CAR T cells and MCT-1 inhibitors (Figure 3.4-1). To confirm if dual MCT-1/4 is compatible with CAR T cell therapy, we performed a cytotoxicity against Raji cells on media with syrosingopine by flow cytometry (Figure 3.7-2A).

Syrosingopine alone significantly reduced the percentage of live Raji cells by 82% and 64% with 20 µM and 10 µM, respectively (Figure 3.7-2B). At low E: T ratios (1:16), no statistical difference in tumour killing was found comparing CAR mediating killing with syrosingopine alone. When a higher number of CAR T cells were used, no significant difference was observed comparing CAR T cells alone and adding syrosingopine (Figure 3.7-2C), indicating dual MCT-1/4 blockade did not induce cooperation in killing tumour cells as observed with MCT-1 blockade. The substantial toxicity on CAR T cells and tumour cells after MCT1/4 inhibition suggests CAR T cell function requires MCT-1 and MCT-4 for lactate export and dual inhibition severely impairs CAR T cell antitumoral potential.

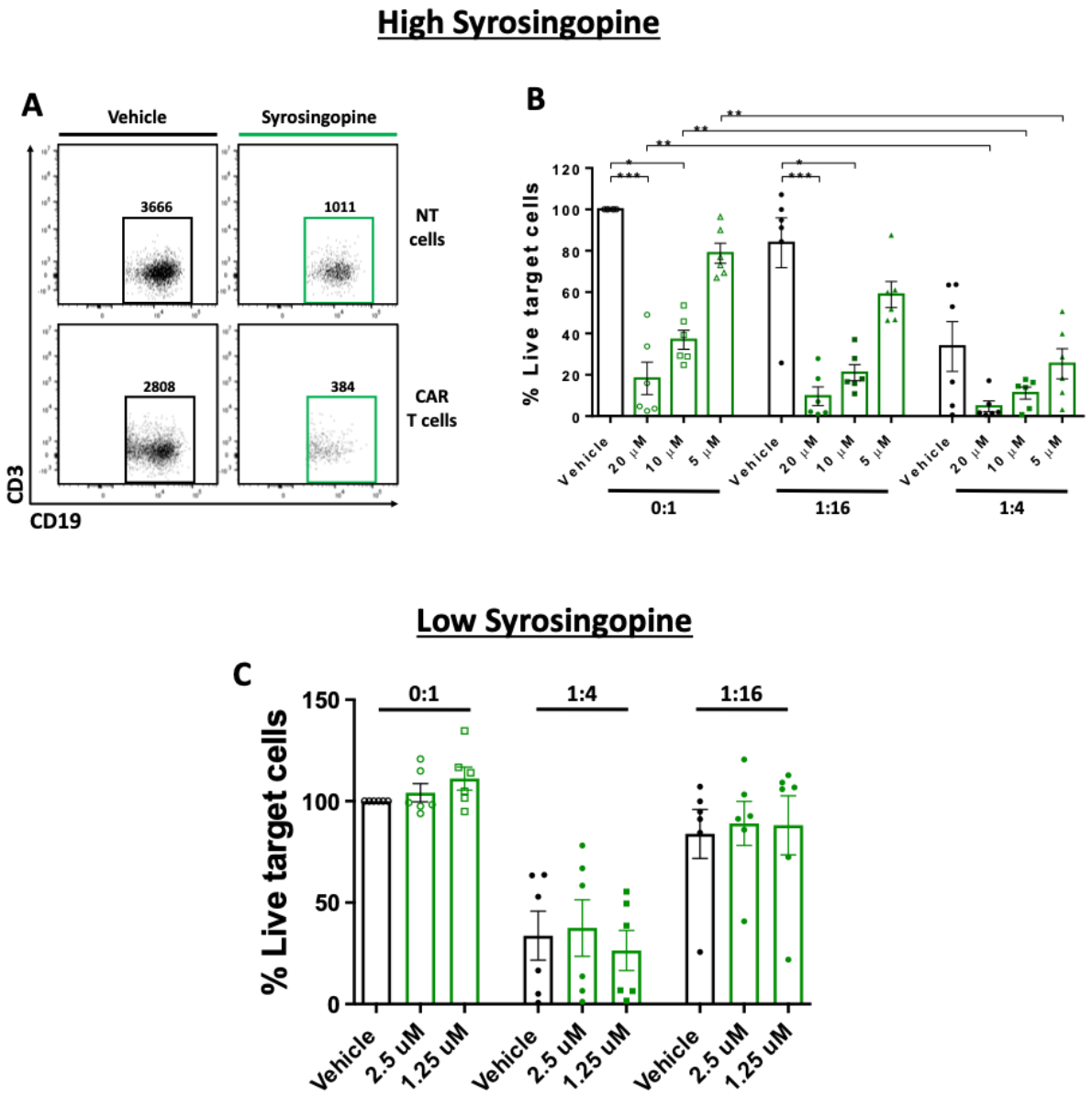

Figure 3.7-2: Dual blockade of MCT-1/4 does not synergise with CAR T cell killing. Raji, non-transduced or αCD19-CAR T cells were cultured with different concentrations of Syrosingopine or vehicle as control. **(A)** Representative contour plot and total number of Raji cells. Percentage of live Raji cells cultured with CAR T cells at different effector: target ratios (E: T) ratios in **(B)** 10-5 µM (high) or **(C)** 2.5-1 µM (low) syrosingopine. Bars are the mean ± SEM. Pooled data of two independent experiments, n = 6 healthy donors per group. *p < 0.05, **p < 0.01, ***p < 0.001, ns = non-significant by Friedman One-Way ANOVA.

3.8 Summary.

In this work, he showed CD19-specific CAR T express high levels of the lactate transporters MCT-1 and MCT-4 upon activation with tumour cells expressing CD19 and pharmacological inhibition of MCT-1 did not impact the expression of lactate transporters on T cells. Additionally, CAR T cells did not accumulate lactic acid intracellularly after incubation with MCT-1i, which supports the hypothesis that CAR T cells and MCT-1 blockade could cooperate against B cell malignancies.

MCT-1 inhibition induced metabolic re-arrangement on activated CAR T cells by diminishing glycolytic pathways engagement, increasing respiration, and slightly increasing mitochondrial potential. However, no differences in T cell phenotype were observed measured by expression of activation markers 4-1BB, OX40, CD69 and Granzyme B. Release of inflammatory molecules IFN-γ or IL-2 and in vitro memory phenotype profile was unaffected by MCT-1 blockade. Furthermore, the combination of CAR T cells with MCT-1 inhibition increased the killing of tumour cells by 50% compared to CAR T cells alone. Importantly, dual inhibition with syrosingopine severely impairs CAR T cell activation, suggesting MCT-1 and MCT-4 are utilised to lactate export on CAR T cells.

4. Results: The combination of MCT-1 blockade with CAR T cells improved the antitumoral control in animal models.

4.1 Introduction

Our results highlight the potential combination of MCT-1 inhibition with CAR T cells as an antitumoral therapy; however, a significant limitation should be considered when interpreting this data. All these experiments were performed in standard culture conditions with an abundance of glutamine, glucose and O_2, which did not recapitulate the tumour microenvironment and the complex and dynamic metabolic requirements of T cells engaging with tumour cells. Research with tumour cells has shown that the metabolic network of cancer cells changes depending on the culture conditions; tumour cells in vitro rely heavily on glucose consumption instead of glutamine to sustain their energetic demands, while the same cells forming a solid tumour in mice reverse these requirements and rely preferentially on glutamine over glucose [227,228].

To address some of these limitations, we tested the antitumoral potential of MCT-1 inhibition and αCD19 CAR T cells using an orthotopic model of B cell leukaemia on a model of immunodeficient mice commonly used in pre-clinical studies. We opted to use NALM-6 cells, a model of acute lymphoblastic leukaemia, as no studies have been published with this cell line, while Raji has been extensively studied on mice models using AZD3965 and AR-C155858.

4.2 Titration of AR-C155858 efficacy in a xenograft NALM-6 model.

We tested the antitumoral potential of MCT-1 inhibition in vivo by transferring NALM-6 cells expressing luciferase (NALM6-Fluc) intravenously into NSG immunodeficient mice [209]. After 6 days of tumour inoculation, a daily dose of AR-C155858 was intraperitoneal injected. AR-C155858 was used instead of AZD3965 as more significant differences in CAR T cell metabolic phenotype were found (Results section 3.1). The treatment was stopped after 9 days and tumour growth was monitored for additional 6 days (Figure 4.2-1A). Tumour burden was assessed by intraperitoneal injections of luciferin and measuring Photons/s/cm2/sr on an IVIS Spectrum Fluorescence. We confirmed that daily injections of AR-C155858 did not negatively impact mice health as instructed in the guidelines for animal care by measuring body weight 3 times a week. No significant reduction in mouse weight was observed during these experiments (Figure 4.2-1B).

NALM6-Fluc cells were significantly reduced 6 days after treatment with both 5 mg/kg and 10 mg/kg doses. Interestingly, stopping AR-C155858 injections increased the tumour burden on treated groups and the statistical significance of these groups was lost loss quickly, indicating daily injections are necessary for future experiments (Figure 4.2-1C). As daily injections of 5 mg/kg and 10 mg/kg of AR-C155858 have similar antitumoral effects, we opted to use 5 mg/kg per mouse in subsequent experiments.

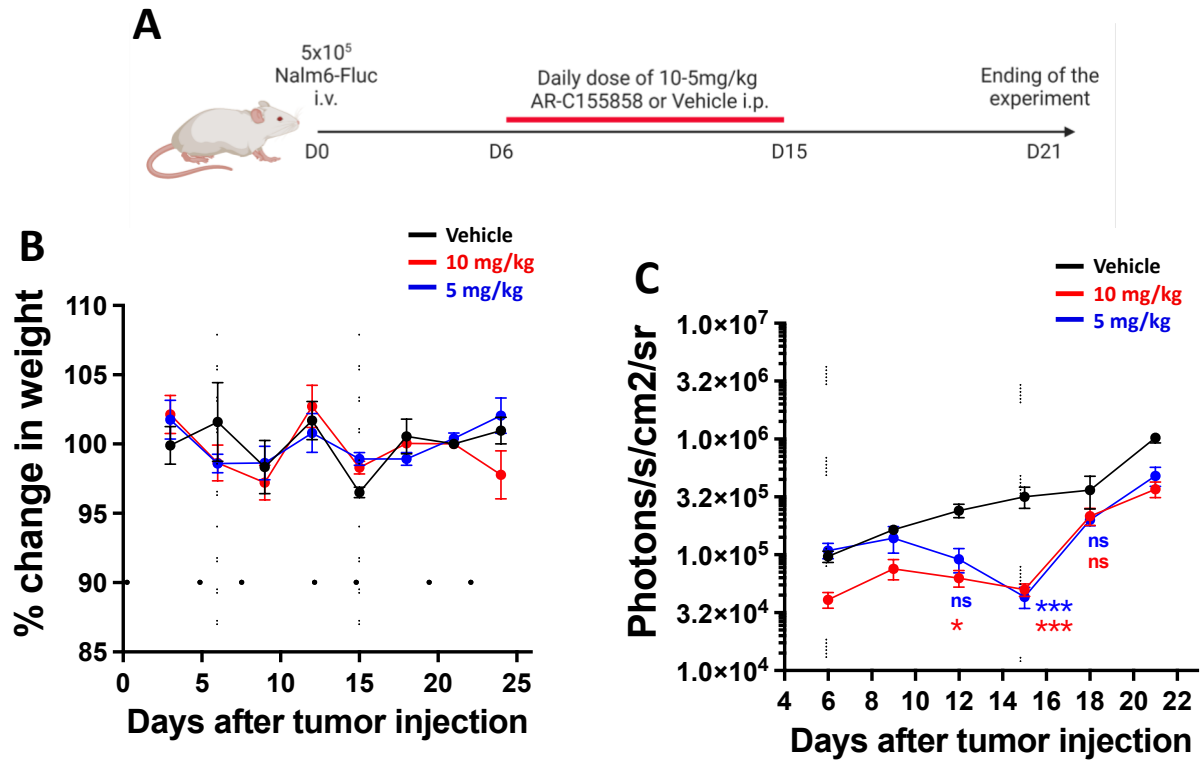

Figure 4.2-1: Titration of AR-C155858 on a B cell leukaemia xenograft animal model. $5x10^5$ NALM-6 cells expressing luciferase were intravenously inoculated on NOD/SCID mice. After 6 days, intraperitoneal injections of AR-C155858 at 5mg/kg or 10mg/kg were administered daily. **(A)** Overview of in vivo experiment. **(B)** Percentage of change of body weight. **(C)** Geometric mean of bioluminescence radiance (photons/s/cm2/sr) of NALM-6 tumours in NOD/SCID mice. Statistical analysis through two-way ANOVA with multiple comparisons between groups at each time point. Bars are mean ± SEM. *p < 0.05, ****p < 0.001 ns = non-significant. Data of one experiments, n =5.

4.3 Combining CAR T cells with MCT-1 blockade improved T cell antitumoral control against a B cell leukaemia xenograft animal model.

We next seek to study the combination of αCD19-CAR T cells with MCT-1 inhibition on immune-deficient mice bearing NALM-6 tumours. After 6 days of tumour inoculation, αCD19-CAR T cells were transferred intravenously together with daily intraperitoneal injections of the MCT-1 inhibitor (Figure 4.3-1A). As a negative control, a CAR with the same structure but specific for the human epidermal growth factor receptor 2 (HER2) was used to transduced T cells as an αHER-CAR better recapitulates the effects of CAR expression on T cells compared to non-transduced T cells.

MCT-1 blockade quickly reduced tumour burden 4 days after treatment and reduced the tumour burden by 60% during the duration of the treatment. Similarly, αCD19-CAR T cells efficiently controlled tumour burden 4 days post transference. The combination of MCT-1 and αCD19-CAR T cells significantly decreased tumour burden by around 60% compared to αCD19-CAR T cells (Figure 4.3-1B-C). Importantly, after 12 days of treatment, the combination significantly reduced the engraftment of NALM-6 compared to either treatment alone, confirming that both therapies work in cooperation to eliminate B cell tumour cells (Figure 4.3-1D).

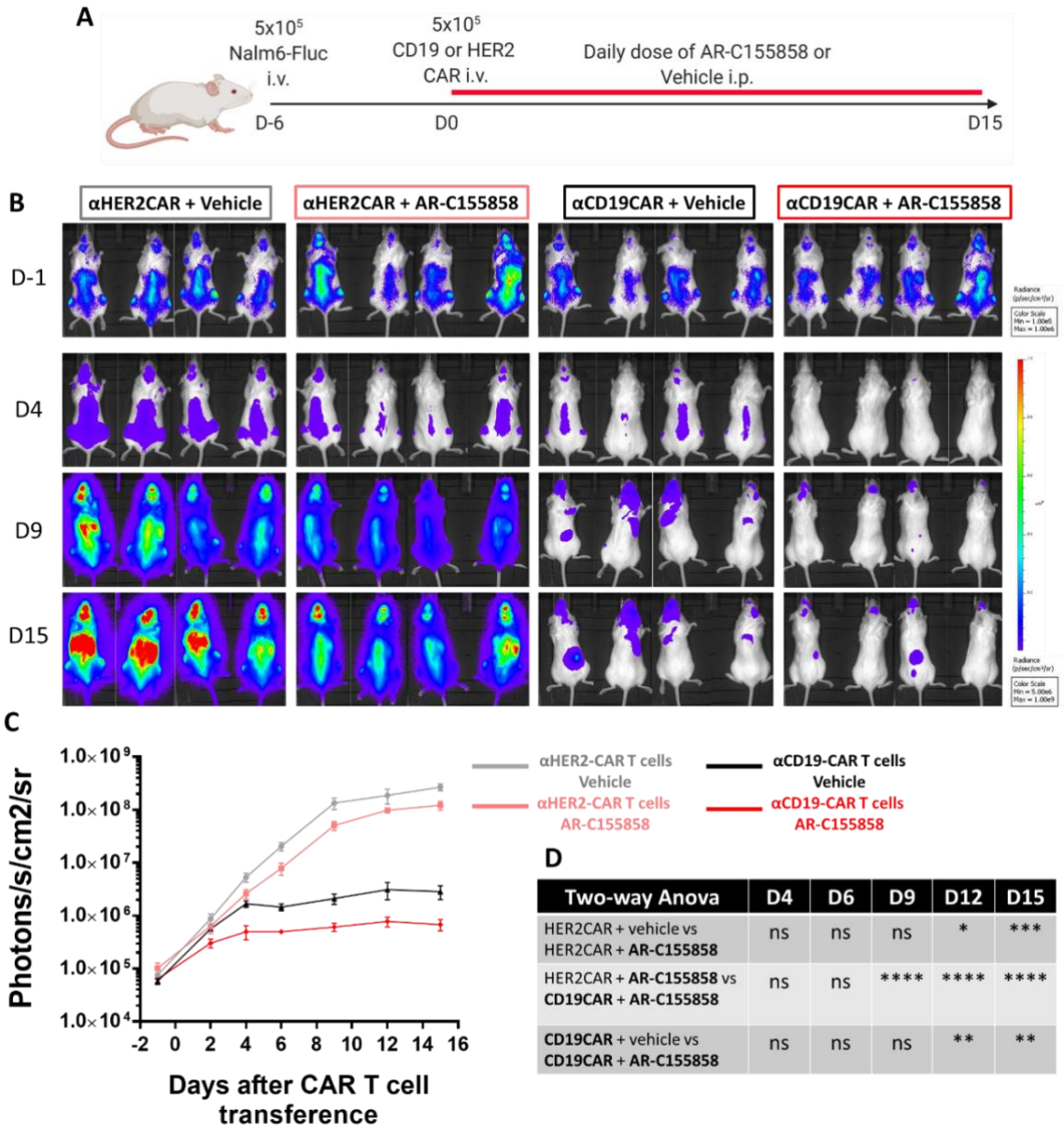

Two-way Anova	D4	D6	D9	D12	D15
HER2CAR + vehicle vs HER2CAR + **AR-C155858**	ns	ns	ns	*	***
HER2CAR + **AR-C155858** vs **CD19CAR** + **AR-C155858**	ns	ns	****	****	****
CD19CAR + vehicle vs **CD19CAR** + **AR-C155858**	ns	ns	ns	**	**

Figure 4.3-1: Combining CAR T cells with MCT-1 blockade improved T cell antitumoral control against a B cell leukaemia xenograft animal model. $5x10^5$ NALM-6 cells expressing luciferase were intravenously inoculated on NOD/SCID mice. After 6 days, $5x10^5$ αCD19-CAR or αHER-CAR T cells were transferred intravenously, and intraperitoneal injections of AR-C155858 at 5mg/kg were administered daily. **(A)** Overview of in vivo experiment. **(B)** Bioluminescence radiance (photons/s/cm2/sr) of NALM-6 tumours in NOD/SCID mice. **(C)** Geometric mean radiance of NALM-6 cells in all groups. **(D)** Table with statistical analysis through two-way ANOVA with multiple comparisons between groups at each time point. Bars are mean ± SEM. *p < 0.05, **p < 0.01, ****p < 0.001 ns = non-significant. Pooled data of two independent experiments, n =7-8.

4.4 CAR T cells phenotype is unaffected after MCT-1 inhibition on a B cell leukaemia xenograft model.

Given the different metabolic requirements between tumour cells and T cells cultured ex vivo and in vivo [229], we tested if long-term exposure to MCT-1 inhibitors impacts CAR T cell phenotype in tumour-bearing mice. Phenotyping of bone marrow and splenic T cells was performed after 7 days of treatment with AR-C1585585 (Figure 4.4-1A) in NALM-6 bearing mice transferred with αCD19-CAR T cells. The combination of αCD19-CAR T cells with MCT-1 significantly reduced the tumour burden after 7 days of treatment (Figure 4.4-1B). We gated CD8 T cells defined as Live/CD45m$^-$/CD3$^+$/CD19$^-$/CD8$^+$/CD4$^-$, CD4 T cells as Live/CD45m$^-$/CD3$^+$/CD19$^-$/CD8$^-$/CD4$^+$ and regulatory T cells (Tregs) as CD4 T cells FOXP3$^+$/CD25$^+$ (Figure 4.4-2A).

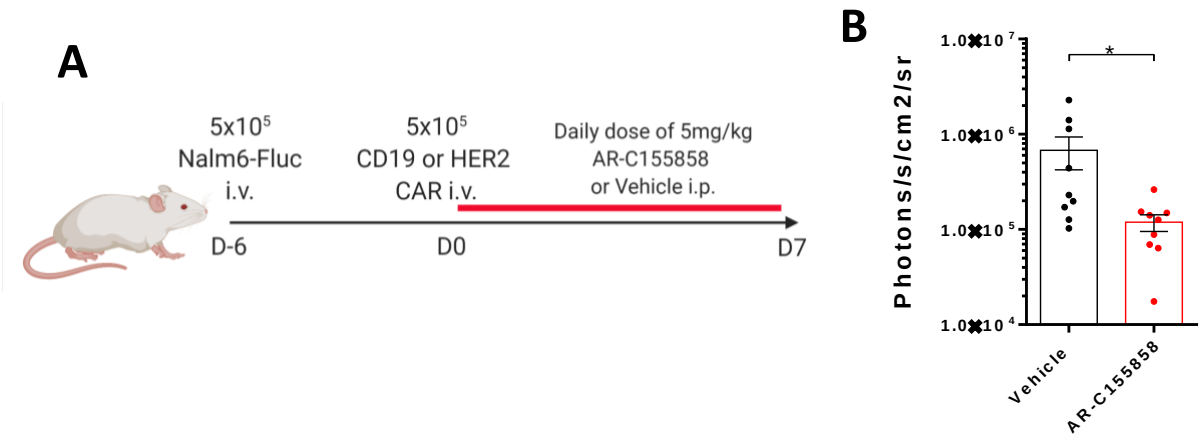

Figure 4.4-1: Overview of in vivo phenotyping experiments. 5x10^5 NALM-6 cells expressing luciferase were intravenously inoculated on NOD/SCID mice. After 6 days, 5x10^5 αCD19-CAR were transferred intravenously and intraperitoneal injections of AR-C155858 were administered daily. After 7 days of treatment, bone marrow and spleen were analysed by flow cytometry. **(A)** Overview of experiment. **(B)** Bioluminescence radiance (photons/s/cm2/sr) of NALM-6 tumours. Pooled data from two independent experiments, n=8-9 per group. Bars are mean ± SEM. *p < 0.05, ns = non-significant by Unpaired t test with Welch correction.

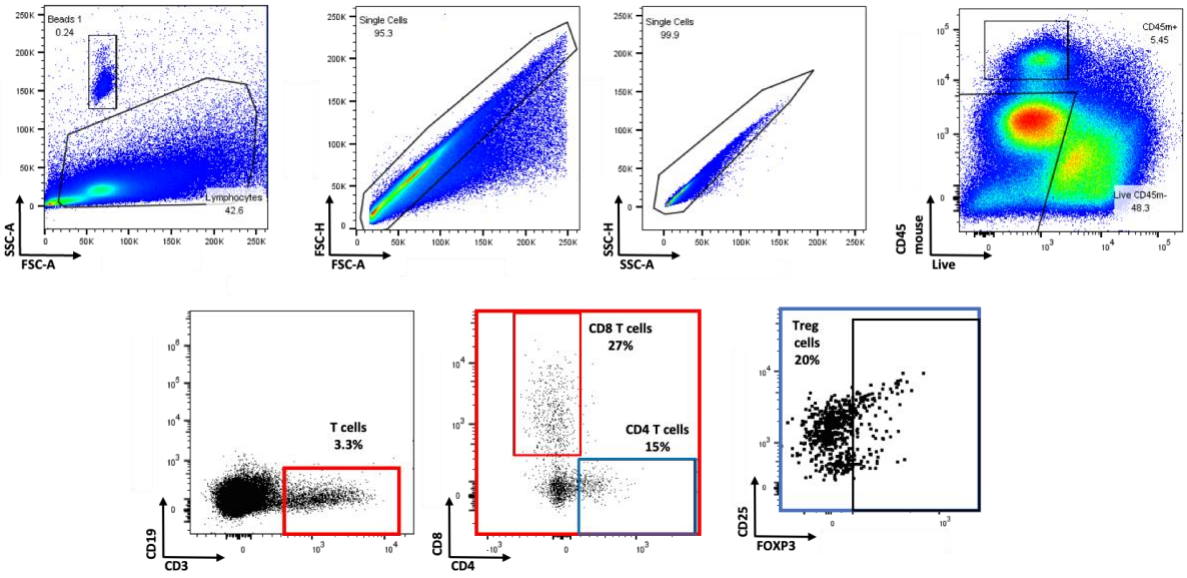

Figure 4.4-2: Gating strategy for T cells phenotype on a B cell leukaemia xenograft model. NOD/SCID mice bearing $5x10^5$ NALM-6 cells were injected with αCD19-CAR and AR-C155858 as previously described (Figure 4.3-1). **(A)** Gating strategy to identify CD8 T cells, CD4 T cells and Treg cells.

No differences were found in the number of CD8 T cells, CD4 T cells or regulatory CD4 T cells in bone marrow or spleen after MCT-1 inhibition (Figure 4.4-3A). Furthermore, analysing bone-marrow infiltrated T cells, no differences in the expression of activation markers 4-1BB (Figure 4.4-3B) and ICOS (Figure 4.4-3C), the exhaustion marker PD-1 (Figure 4.4-3D) or proliferation marker Ki67 (Figure 4.4-3E) were found on CD8 or CD4 T cells treated with AR-C155858. Similarly, IFN-γ and IL-2 production were not affected in both compartments (Figure 4.4-3F-G) and no differences in LAMP-1 expression on bone marrow CD8 T cells (Figure 4.4-3H). Consistent with our in vitro results, no differences in memory formation evaluated by CD45RO and CCR7 expression was found after MCT-1 blockade (Figure 4.4-3 I-J). Similar results were found on all markers analysed on splenic T cells (Figure 4.4-4A-G), confirming that MCT-1 inhibition does not impact T cell phenotype or functionality in vivo.

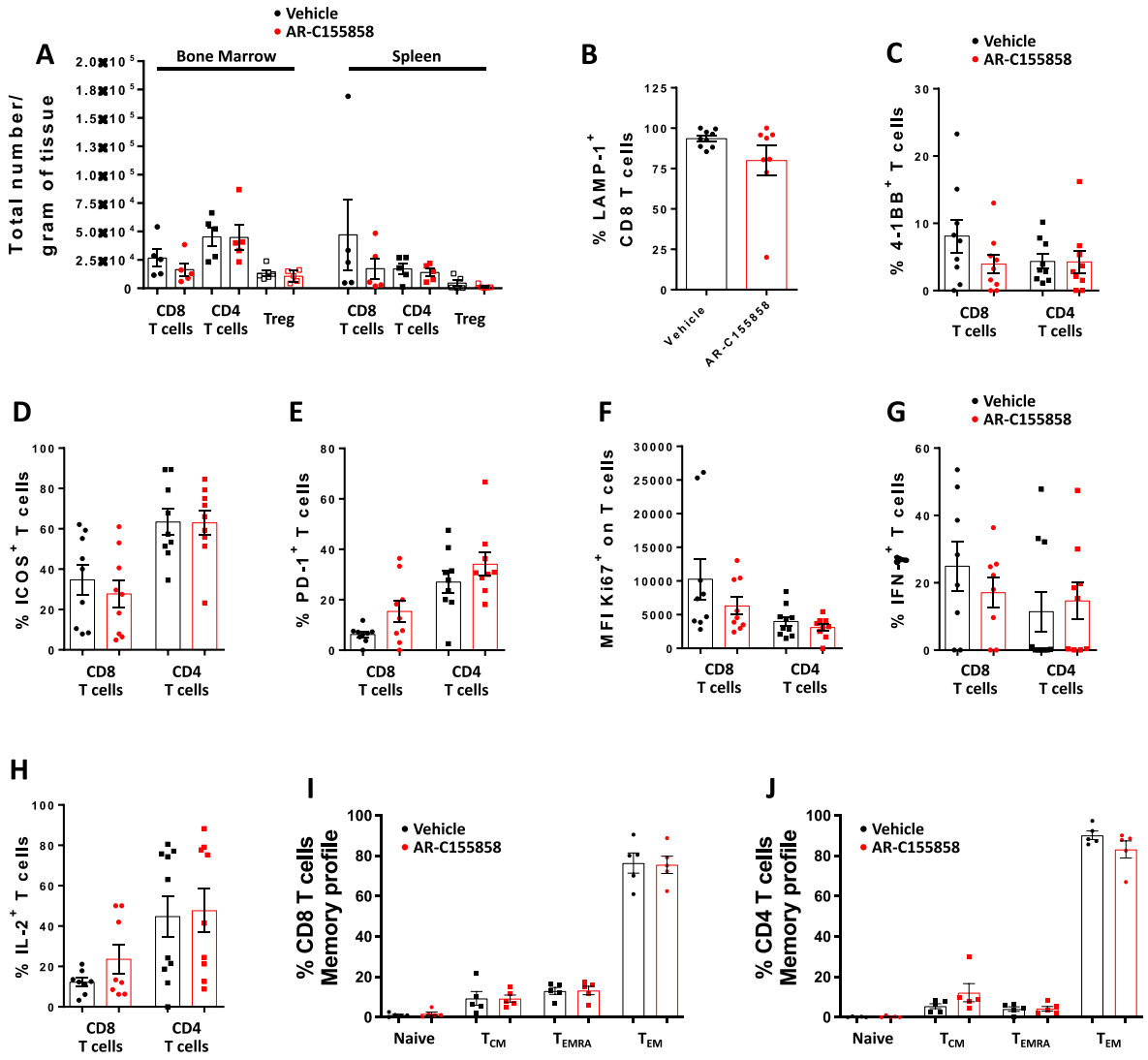

Figure 4.4-3: Bone-marrow infiltrated CAR T cells phenotype is unaffected by MCT-1 inhibition. NOD/SCID mice bearing 5x10^5 NALM-6 cells were injected with αCD19-CAR and AR-C155858 as previously described (Figure 4.3-1). **(A)** Total number of lymphoid cells on bone marrow and spleen. Representative data of two independent experiments, n =5 mice per group. Expression of **(B)** 41BB, **(C)** ICOS, **(D)** PD-1, **(E)** Ki-67, **(F)** IFN and **(G)** IL-2 and **(D)** LAMP-1 on bone marrow-infiltrated T cells. Pooled data from two independent experiments, n=8-9 per group. Characterisation of **(I)** CD8 T cells and **(J)** CD4 T cells based on the expression of CD45RO and CCR7. Data from one experiment, n=5. Bars are mean ± SEM. *p < 0.05, ns = non-significant by Unpaired t test with Welch correction.

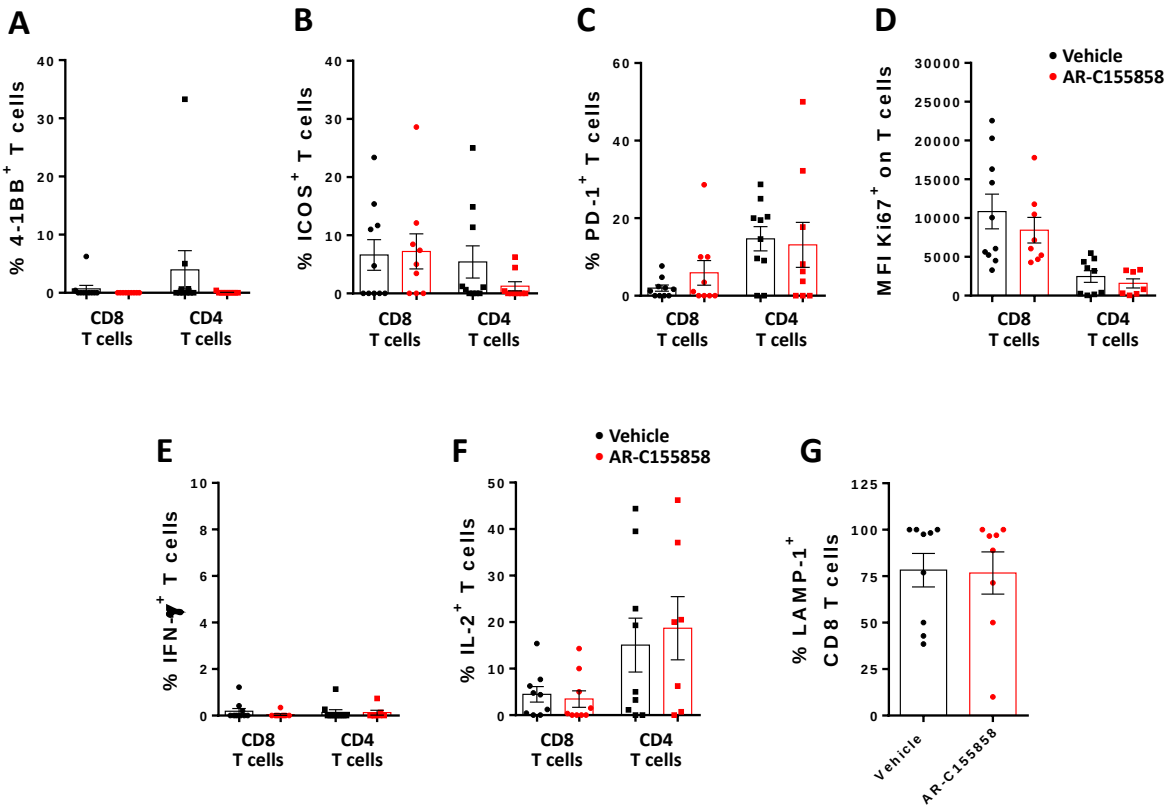

Figure 4.4-4: Splenic CAR T cells phenotype is unaffected by MCT-1 inhibition. NOD/SCID mice bearing $5x10^5$ NALM-6 cells were injected with αCD19-CAR and AR-C155858 as previously described (Figure 4.3-1). Expression of **(A)** 41BB, **(B)** ICOS, **(C)** PD-1, **(D)** Ki-67, **(E)** IFN and **(F)** IL-2 and **(G)** LAMP-1 on bone marrow-infiltrated T cells. Pooled data from two independent experiments, n=8-9 per group. Bars are mean ± SEM. *$p < 0.05$, ns = non-significant by Unpaired t test with Welch correction.

4.4 Summary

We confirmed that daily injection of 5 mg/kg AR-C155858 efficiently controls the tumour growth on a model of B cell leukaemia NALM-6 without any apparent side effect.

Moreover, the combination of αCD19-CAR T cells with MCT-1 blockade significantly improved the killing of tumour cells and increased CAR T cell antitumoral control in mouse models compared to each treatment alone, confirming the conclusions on the in vitro cytotoxicity experiments (Results 3.4).

Additionally, αCD19-CAR T cell phenotype measured by expression of 4-1BB, ICOS, PD-1, Ki67, IFN-γ, IL-2 and LAMP-1 remained the same on T cells transferred on tumour-bearing mice injected for 7 days with AR-C155858, corroborating MCT-1 inhibition did not impact CAR T cell phenotype in vivo or in vitro.

In summary, the pharmacological blockade of MCT-1 selectively impairs B cell tumour growth without hindering CD19-specific CAR T cell antitumoral potential, making combining both treatments an interesting approach against B cell malignancies.

5. Results: Systemic inhibition of glutamine uptake via ASCT-2 on CAR T cells against C cell malignancies.

5.1 Introduction.

Highly proliferative cells, like tumour cells and activated immune cells completely rewire their metabolism to sustain their energetic demands. Glutamine is the most abundant amino acid in blood, and several studies have shown it is crucial in sustaining both tumour development and T cell responses. However, glutamine depletion has been observed on several tumour models, hindering T cell antitumoral potential [191,200]. Moreover, several strategies have been developed to avoid glutamine-addictive T cells. One common strategy is restricting glutamine in the initial stages of T cell activation, which moves T cell metabolism to rely more on oxidative respiration, increasing their persistence and tumour clearing [198], including in CAR T cells against B cell malignancies [199]. More recently, small molecules which block glutamine conversion into glutamate selectively in the TME have been developed, suppressing oxidative and glycolytic metabolism of cancer cells, but effector T cells responded by up-regulating oxidative metabolism and adopting a long-lived, highly activated phenotype [201].

A key adaptation of proliferative cells is the upregulation of the glutamine transporter SLC1A5 (ASCT-2). ASCT-2 upregulation is a hallmark of aggressiveness on many tumours and is fundamental for effector T cell function [230,231]. Among the tools developed for ASCT-2 inhibition, a small molecule which specifically blocks ASCT-2 (V-9302) has been shown efficacy as a treatment in colorectal, breast and lung cancer on immunodeficient animal models [204] and the combination of V-9302 with αPD-1 showed complete tumour clearance in triple-negative breast cancer on immunocompetent animal models [232,233].

Additionally, glutamine-neutralising monoclonal antibodies binding to ASCT-2 have shown efficacy on gastric cancer models [234] and open an opportunity to genetically manipulate T cells to produce antibodies and avoid the high toxicities associated with glutamine inhibition. Therefore, we aimed to study the combination of αCD19-CAR T cells with glutamine inhibition and develop a resistant mechanism via T cell genetic engineering to glutamine addiction in CAR T cells.

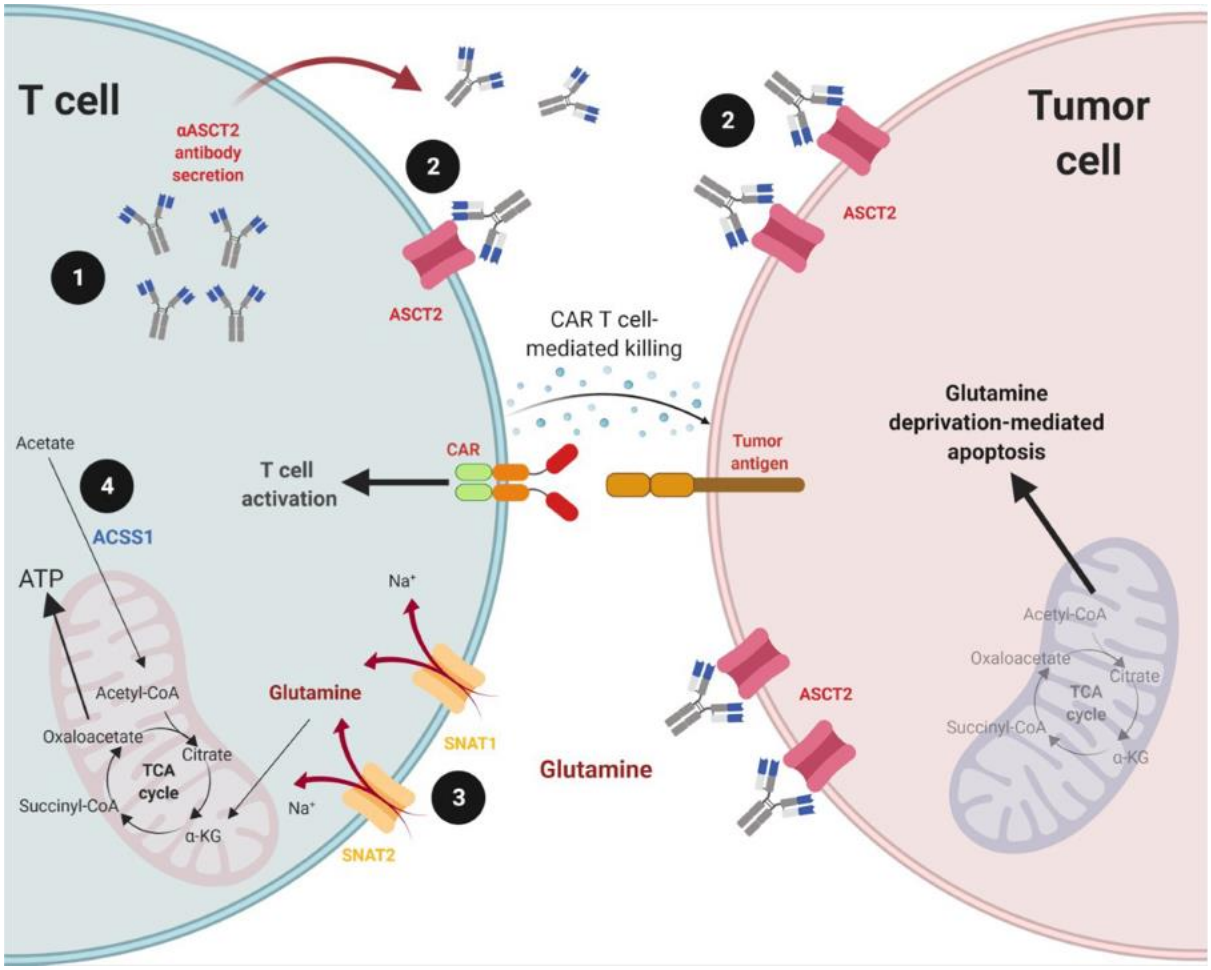

Figure 5.1-1: Inhibition of glutamine uptake through ASCT-2 on tumour and CAR T cells. Proposed development of glutamine-resistant CAR T cells. **(1)** Production of αASCT-2 antibodies from CAR T cells or **(2)** adding exogenous blocking antibodies or V-9302 to block glutamine uptake of tumour and CAR T cells. Glutamine-depravation cell death would be induced, but genetically engineered CAR T cells to express **(3)** alternative glutamine transporters or **(4)** enzymes to bypass glutamine addiction like Acyl-CoA Synthetase Short Chain Family Member 1 (ACSS1) should be resistant to ASCT-2 blockade.

5.2 Pharmacological blockade of ASCT-2 on CAR T cells impairs their antitumoral potential.

A recent publication studying the effects of V-9302 on mouse T cells found that upon ASCT-2 blockade, T cells overexpress SLC6A14 (ATB^{0+}), resisting ASCT-2 inhibition and increasing the killing of triple-negative breast cancer cells on immuno-competent mouse models [189]. We aimed to study the effect of V-9302 on human CAR T cells and test if ASCT-2 blockade impairs their antitumoral potential. Non-transduced (NT) T cells or activated αCD19-CAR T cells were cultured with different concentrations of V-9302 and with Raji cells or Raji $CD19^{ko}$. Notably, 25 μM of V-9302 reduced IFN-γ production to resting CAR T cell levels. At 18-10 μM, IFN-γ was diminished by approximately 50%, while no significant reduction was found at lower concentrations (Figure 5.2-1A). Similarly, IL-2 production by activated CAR T cells was reduced by 50% after incubation with V-9302 at 10 μM or higher concentrations, while no significant reduction was found at 5-2.5 μM (Figure 5.2-1B). However, no differences were found in the expression of activation markers 4-1BB and CD69 in activated CAR T cells incubated with 10 μM of V-9302 (Figure 5.2-1C-D). Together, these results suggest that pharmacological inhibition of ASCT-2 severely impacts CAR T cells, reducing their cell number and, therefore, the production of antitumoral cytokines but without impacting T cell phenotype.

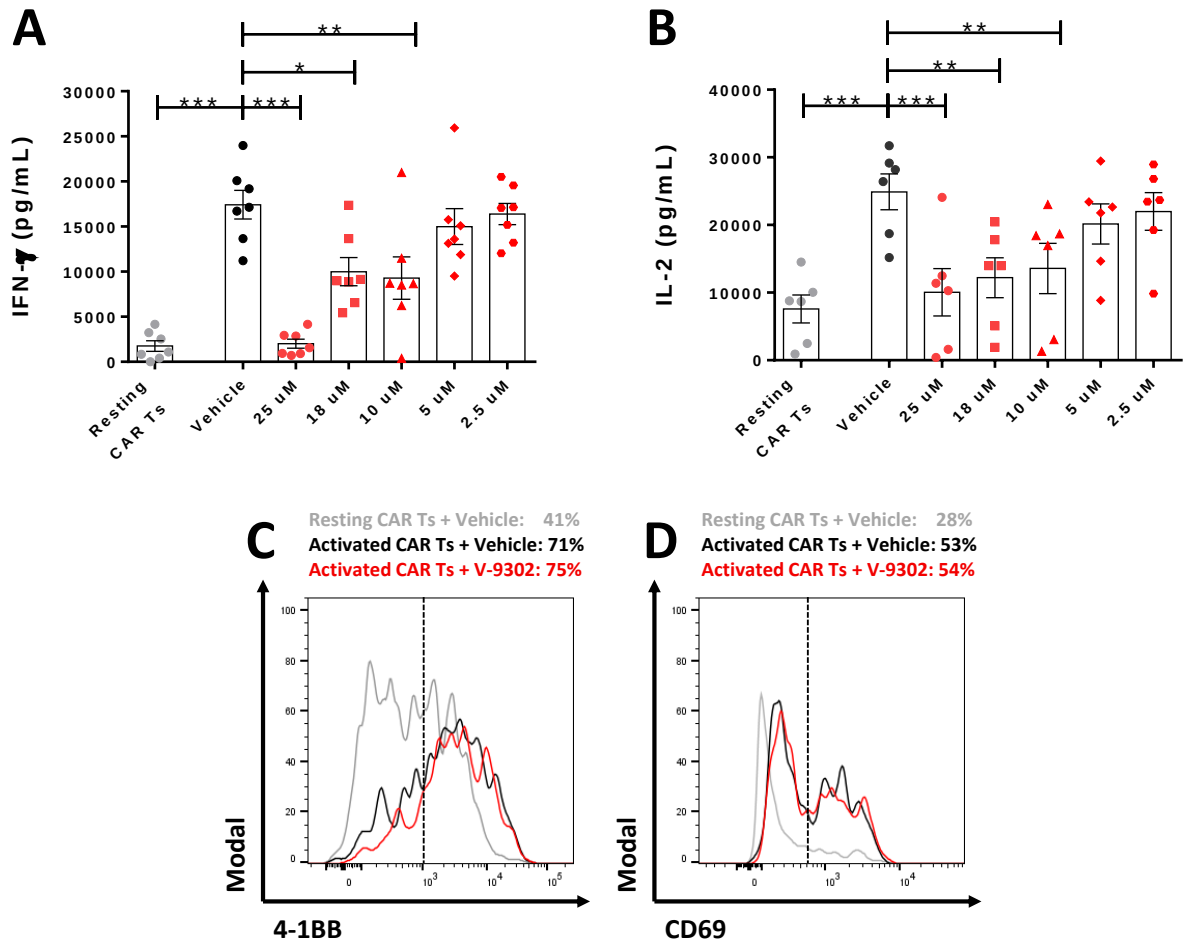

Figure 5.2-1: ASCT-2 inhibition reduced CAR T cells cytokine production but not activation markers. V-9302 at different concentrations were added to non-transduced or αCD19-CAR T cells in culture with target cells for 48 hours. (**A)** IFN-γ and **(B)** IL-2 production measured by ELISA after 48 hours. Pooled data of three independent experiments, n = 7 healthy donors per group. Bars are the mean ± SD. *p < 0.05, **p < 0.01, ***p < 0.001, ns = non-significant by Friedman One-Way ANOVA. Representative histogram of expression of activation markers (**C)** 4-1BB and **(D)** CD69 on activated CAR T cells with Raji cells or Raji-CD19^{KO} for 24 hours.

To test if CAR T cell antitumoral control against B cell malignancies could be improved by adding ASCT-2 inhibitors, αCD19-CAR T cells were co-culture with Raji ($CD19^{+}$) on media with different concentrations of V-9302 and counted the absolute number of tumour cells after 48 hours at different effector/target ratio (E: T). V-9302 showed a reduction of 50% of live Raji cells compared to the vehicle, showing similar toxicity compared to activated CAR T cells. At high ratios (1:4), the CAR T cell reduced by 90% the number of live tumour cells, and no differences were observed with the addition of V-9302 (Figure 5.2-2A). Similarly, no statistically significant differences between the killing of tumour cells by CAR T cells alone or in combination with V-9302 were observed at 1:8 E: T. At 1:16 (E: T), and no differences were observed between comparing the vehicle with V-9302 (Figure 5.2-2B). Notably, at 25 μM, no CAR T cells or Raji cells were detected, suggesting this concentration induced severe cell death in both cell types. These results suggest ASCT-2 blockade severely reduced CAR T cell antitumoral potential, and the combination of both treatments interferes rather than cooperates in killing tumour cells.

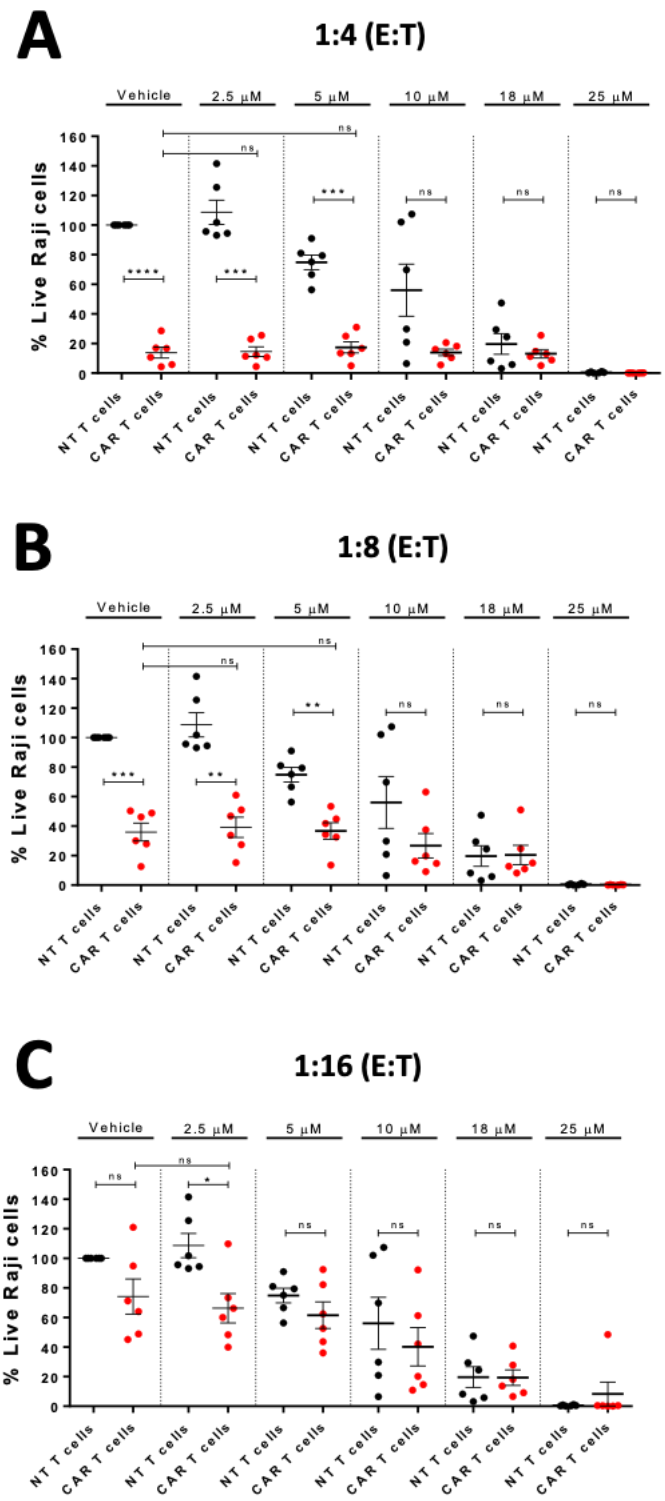

Figure 5.2-2: ASCT-2 inhibition does not cooperate with CAR T cells mediated cytotoxicity against B cell lymphoma cell lines. V-9302 at different concentrations were added to non-transduced or αCD19-CAR T cells in culture with target cells for 48 hours. Percentage of live Raji cells cultured with CAR T cells at **(A)** 1:4, **(B)** 1:8 or **(C)** 1:16 effector: target ratios (E: T) ratios. Pooled data of two independent experiments, n=6 healthy donors per group. Bars are the mean ± SEM. *p < 0.05, **p < 0.01, ***p < 0.001, ****p < 0.0001, ns = non-significant by Friedman One-Way ANOVA.

A common strategy to avoid glutamine addiction in T cells is decreasing glutamine concentration at the initial stages of activation. Studies on primary mouse T cells and human CAR T cells have shown that incubating T cells with low glutamine increased their respiratory metabolism, persistence and T cell antitumoral potential. We designed to test if culture with low glutamine at the initial activation phase could render CAR T cells insensitive to ASCT-2 inhibition. We culture CAR T cells with 0 mM, 0.2 mM, 1 mM and 2 mM (standard media concentration) of glutamine for 7 days, followed by a co-culture with Raji cells in standard media (2 mM of glutamine) and different concentrations of V-9302 (Figure 5.2-3A), simulating the conditions CAR T cell would encounter interacting with tumour cells. We kept the co-culture for 48 hours and measured IFN-γ release by ELISA as an indicator of T cell activation. Changing glutamine concentrations for 7 days did not impact IFN-γ production on αCD19-CAR T cells cultured with the vehicle. Adding 5 μM or 10 μM of V-9302 reduced IFN-γ production; however, culturing T cells with no glutamine doubled the production compared to standard media concentration (2 mM) (Figure 5.2-3B). Importantly, increasing V-9302 concentration significantly reduced IFN-γ production on αCD19-CAR T cells in all conditions, with some increase in CAR T cells cultured with no glutamine (Figure 5.2-3C).

Taken together, our results suggest ASCT-2 inhibition impairs αCD19-CAR T cells antitumoral potential. While CAR T cells have some plasticity to resist V-9302 by reducing glutamine concentrations at the initial stages of activation, this is insufficient to render CAR T cells insensitive to ASCT-2 inhibition, and alternative strategies will be explored.

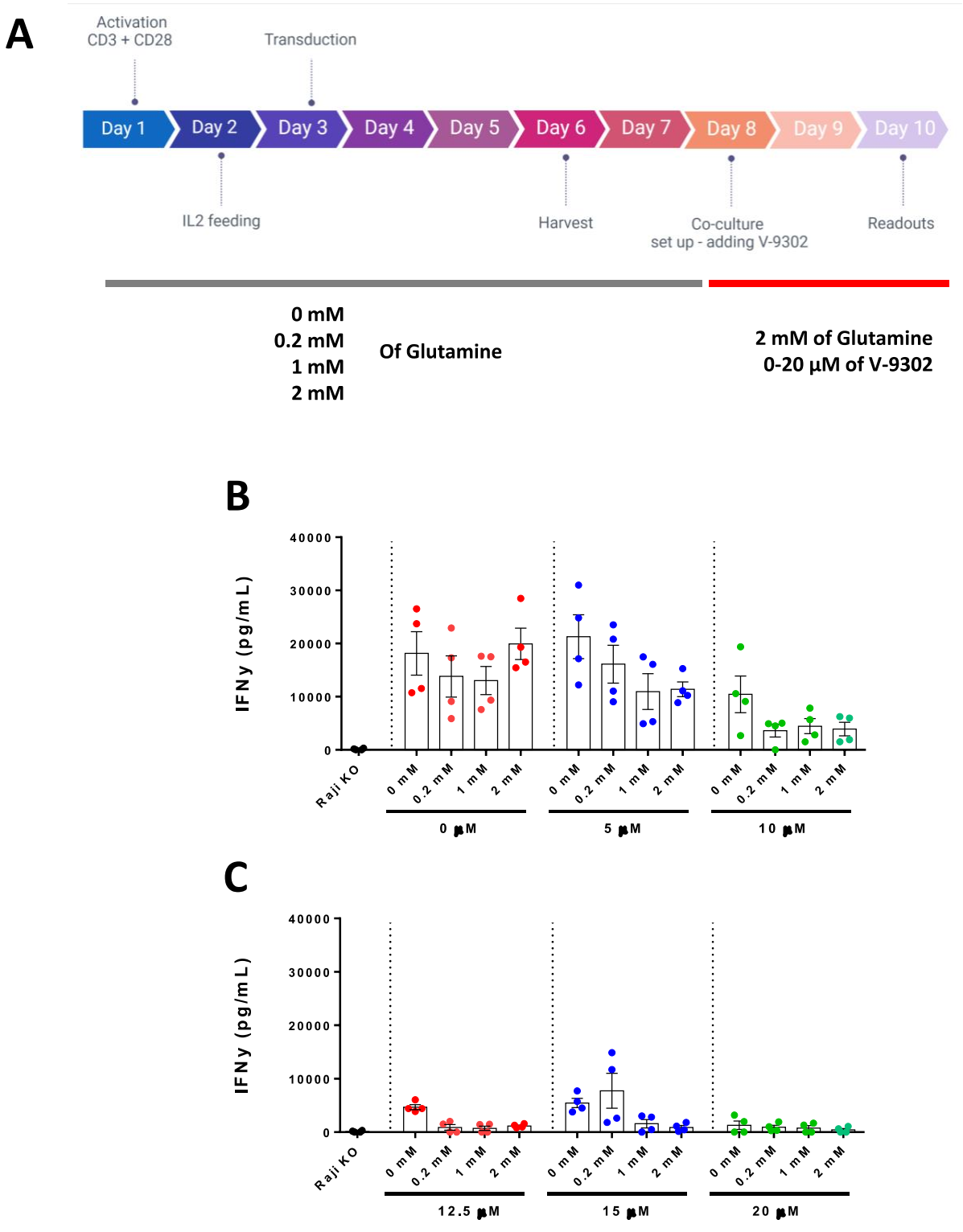

Figure 5.2-3: Culture of CAR T cells on low glutamine media partially reduced ASCT-2 inhibition. (A) V-9302 at different concentrations were added αCD19-CAR T cells in culture with target cells for 48 hours. (**B)** IFN-γ and production were measured by ELISA after 48 hours. Pooled data of two independent experiments, n = 4 healthy donors per group. Bars are the mean ± SEM. *p < 0.05, **p < 0.01, ***p < 0.001, ****p < 0.0001, ns = non-significant by Friedman One-Way ANOVA.

5.3 Expression of surrogate glutamine transporters attenuated ASCT-2 blockade on CAR T cells.

Glutamine has been found critical to regulating T cell activation and differentiation into inflammatory phenotypes. Therefore, T cells express different amino acid transporters at different stages of their activation to supply the high demand for glutamine [186,235]. ASCT-2 co-transports glutamine and Na^+ at a 1:1 ratio, and other amino acid transporters have similar functions. SLC38A1 (SNAT-1) and SLC38A2 (SNAT-2) are sodium-coupled neutral amino acid transporter expressed in the initial stages of T cell activation and are critical for glutamine uptake [9]. Therefore, we hypothesised that genetic engineering of T cells to induce expression of alternative glutamine transporters with similar functions to ASCT-2 could render CAR T cells insensitive to V-9302 inhibition (Figure 5.3-1).

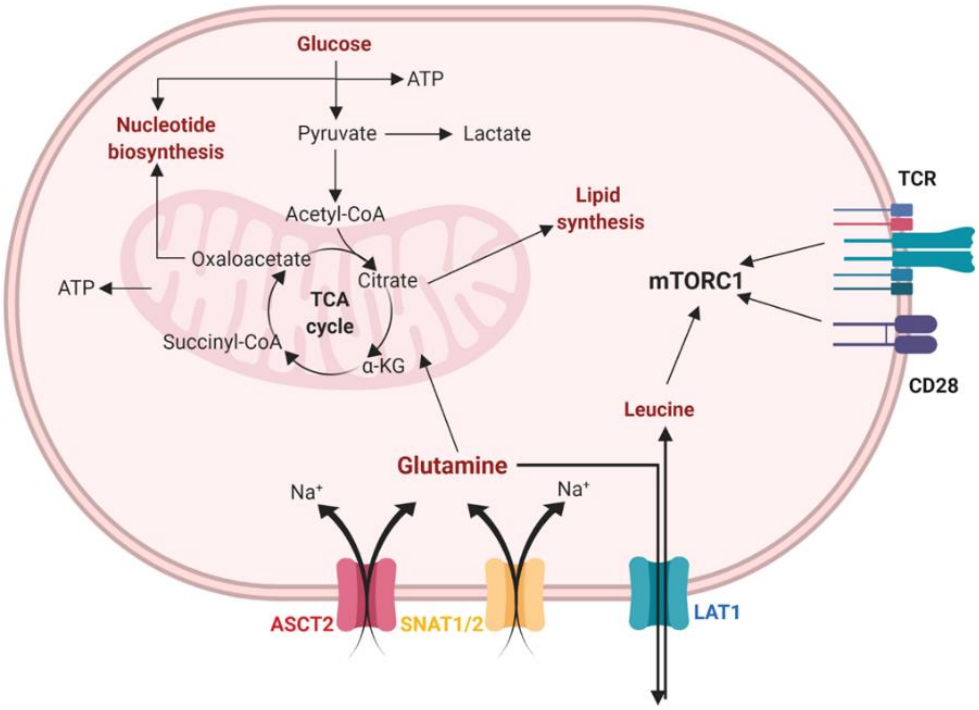

Figure 5.3-1: Glutamine fate on activated T cells. T cells regulate glutamine uptake upon activation by expressing different amino acid transporters like ASCT-2, SNAT-1 or SNAT-2. Glutamine is then converted into α-ketoglutarate to enter the TCA cycle for energy production or antiport transport coupled with leucine, which directly regulates mTOR activity and T cell activation.

Jurkat cells are an immortalised CD4 T lymphocyte cell line commonly used as a model for T cell activation [236]. We tested Jurkat cell sensitivity to ASCT-2 inhibition by culturing these cell lines with different concentrations of V-9302 for 48 hours. High concentrations of V-9302 (between 25-10 μM) reduced by >90% the number of live Jurkat cells while reducing the concentration of V-9302 (5-2.5 μM) significantly reduced the number of live cells by 20%, indicating Jurkat cells are susceptible to V-9302 (Figure 5.3-2A).

Jurkat cells were transduced to overexpress SNAT-1 or SNAT-2 using plasmids containing an RQR8 marker separated by a 2A (Figure 5.3-2B). RQR8 contains the epitopes for CD34 and CD20, and cells expressing this construct can be detected by flow cytometry by CD34 staining. After transduction, Jurkat cells were purified by positive selection using magnetic separation of CD34 cells, producing a stable cell line expressing SNAT-1 or SNAT-2 (Figure 5.3-2C). We cultured non-transduced Jurkat cells (WT), Jurkat cells transduced with RQR8-SNAT1 construct (SNAT-1) or RQR8-SNAT2 construct (SNAT-2) for 48 hours in the presence of different concentrations of V-9302. However, no difference in the number of live cells was observed comparing Jurkat cells transduced with SNAT-1, SNAT-2 or WT at different concentrations of V-9302 (Figure 5.3-2D).

Jurkat cells are metabolically active and highly homogeneous [237]. To study if overexpression of SNAT transporters could revert ASCT-2 dependence in other T cell types, activated T cells from healthy donors were transduced with RQR8-SNAT1 and RQR8-SNAT2 (Figure 5.3-3A) and cultured them for 48 hours in the presence of different concentrations of V-9302. Interestingly, activated T cells showed lower toxicities associated with ASCT-2 inhibition, with no significant difference in the percentage of live cells cultured with 10 μM of V-9302. However, similar to the results with Jurkat cells, no differences were observed comparing the percentage of live T cells expressing SNAT-1 or SNAT-2 (Figure 5.3-3B). These results suggest that expression SNAT transporters cannot revert ASCT-2 blockade on T cells.

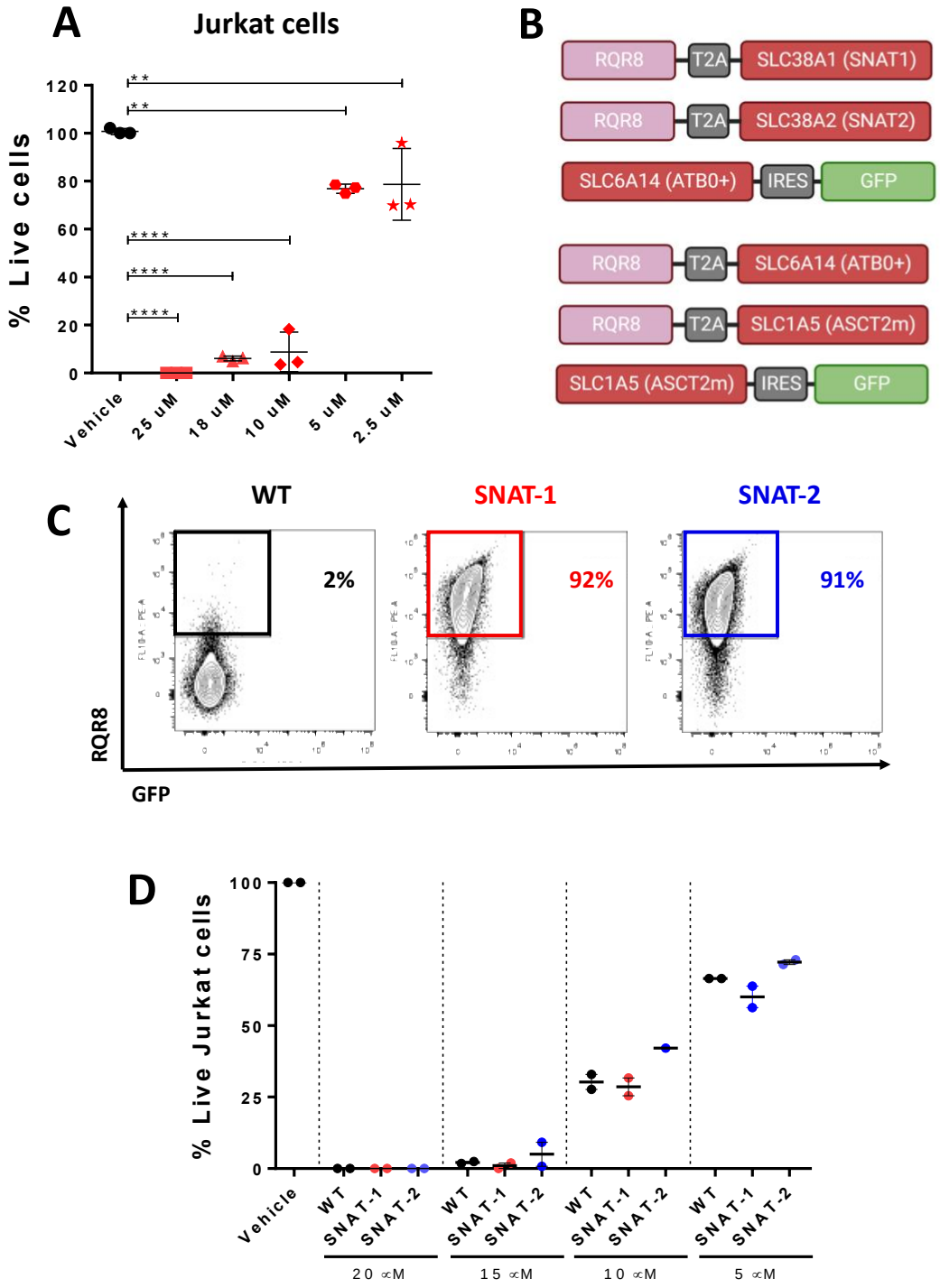

Figure 5.3-2: ASCT-2 inhibition impairs Jurkat cell viability. Non-transduced (WT), RQR8-SNAT1 (SNAT-1) or RQR8-SNAT2 (SNAT-2) transduced Jurkat cells were cultured with different concentrations of V-9302 or DMSO as the vehicle. **(A)** Percentage of live Jurkat cells measured by flow cytometry. **(B)** Schematic representation of the retroviral construct used to transduce Jurkat cells. **(C)** Representative contour plot of transduced Jurkat cells. **(D)** Percentage of live transduced Jurkat cells measured by flow cytometry. Bars are the mean ± SD. Pooled data of two independent experiments, n = 2-3 per group. **p < 0.01 and ****p < 0.001, by One-Way ANOVA.

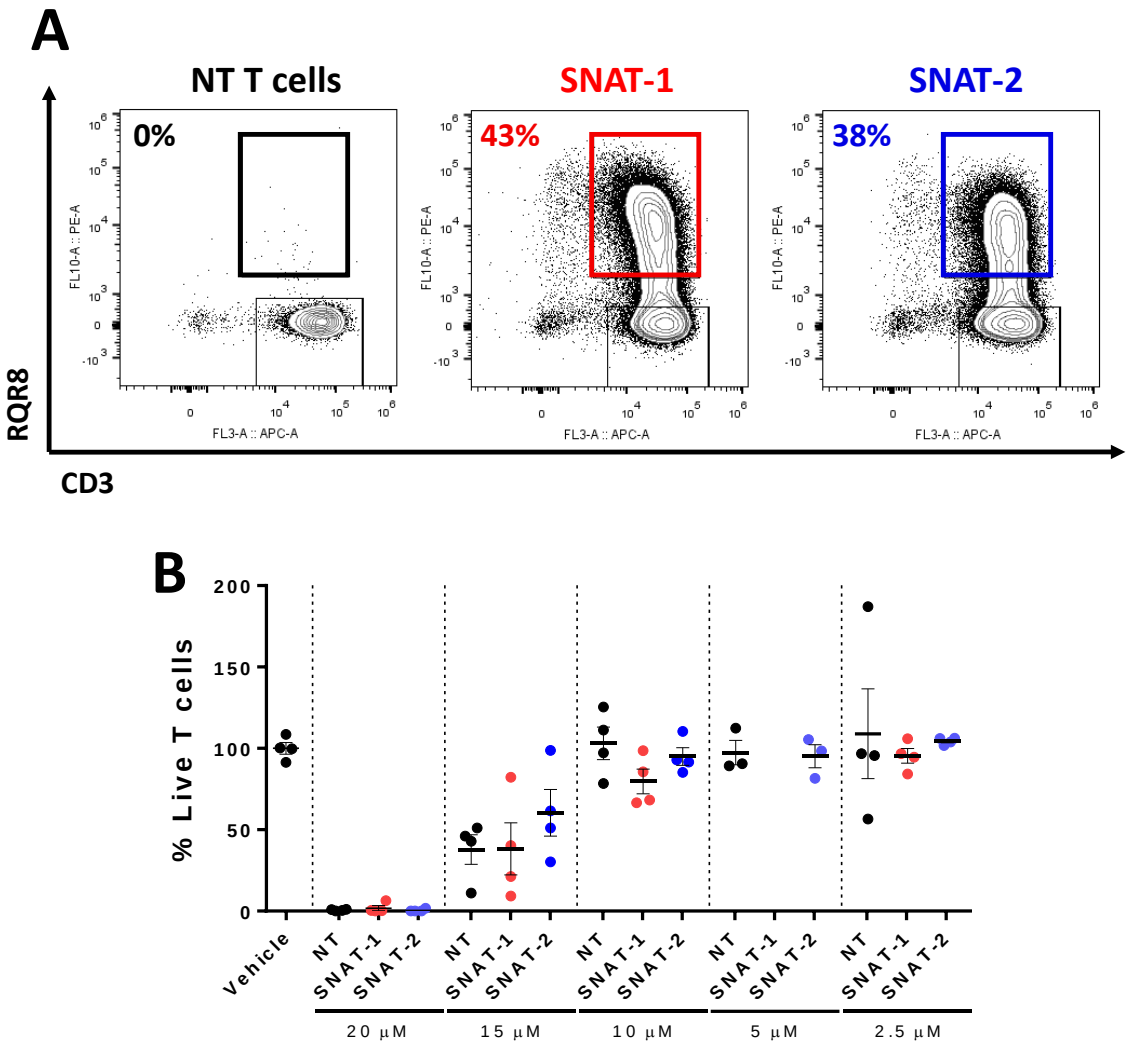

Figure 5.3-3: ASCT-2 inhibition impairs T cell viability. Non-transduced (WT), RQR8-SNAT1 (SNAT-1), or RQR8-SNAT2 (SNAT-2) transduced T cells were cultured with different concentrations of V-9302 or DMSO as the vehicle. **(A)** Representative contour plot of transduced T cells. **(B)** Percentage of live transduced T cells measured by flow cytometry. Bars are the mean ± SD. Pooled data of two independent experiments, n=4 healthy donors per group. Ns = not significant by One-Way ANOVA.

To study if the expression of different glutamine transporters could reverse T cell death after ASCT-2 blockade, we expanded the strategy to include two additional transporters: SLC6A14 (ATB^{0+}) is a neutral and cationic amino acids transporter dependant of Na^+ and Cl^-. Previous publications have shown that mouse T cells overexpress ATB^{0+} after ASCT-2 inhibition [189], so we aimed to replicate the effect of ATB^{0+} expression on human CAR T cells. Additionally, we cloned ASCT-2 gene from a mouse (ASCT-2m) as it has significant structural differences compared to ASCT-2 gene from humans. Comparing ASCT-2 amino acid sequences from mice and humans, they share 80% of sequence homology; moreover, the structural differences of both transporters have been used to identify binding regions for human or mouse-specific antibodies against ASCT-2 [234].

Additionally, to discard the lack of effect observed on SNAT transduced T cells is due to an artefact of the 2A peptide included to separate RQR8 and the transporters, ATB^{0+} and ASCT-2m were cloned to co-express GFP separated with an internal ribosome entry site (IRES). T cells from healthy donors were activated with CD3 and CD28 antibodies as described previously and transduced with retroviral particles containing: RQR8-2A-SLC38A1 (SNAT-1), RQR8-2A-SLC38A2 (SNAT-2), RQR8-2A-SLC6A14 (ATB^{0+}), RQR8-2A-SLC1A5m (ASCT-2m), SLC6A14-IRES-GFP (ATB^{0+}) or SLC1A5m-IRES-GFP (ASCT-2m) (Figure 5.3-4A).

Transduction efficiency was detected on T cells by expression of RQR8 or GFP. All constructs efficiently transduced T cells: however, constructs with IRES-GFP had higher transduction efficiency than RQR8-2A (Figure 5.3-4B). Transduced T cells were cultured with different concentrations of V-9302 for 48 hours, and the percentage of live transduced cells was counted by flow cytometry relative to the vehicle. Raji cells were used as a positive control for V-9302 as this cell line is susceptible to ASCT-2 inhibition. Incubation with 5 µM of V-9302 reduced the number of live Raji cells and transduced T cells by 28%. Only activated T cells transduced with ATB^{0+} -GFP or ASCT2m- GFP showed increased viability (Figure 5.3-4C). Similarly, increasing the concentration of V-9302 to 10 µM decreased by 50% the number of live Raji cells. All constructs increased the number of live T cells, except RQR8-ASCT2m and RQR8-SNAT2, with a higher increase in T cells transduced with ATB^{0+} -GFP (Figure 5.3-4D). Taken together, genetically engineering T cells to express glutamine transporters co-transduced with GFP partially restored the inhibitory effects of ASCT-2 blockade on transduced T cells.

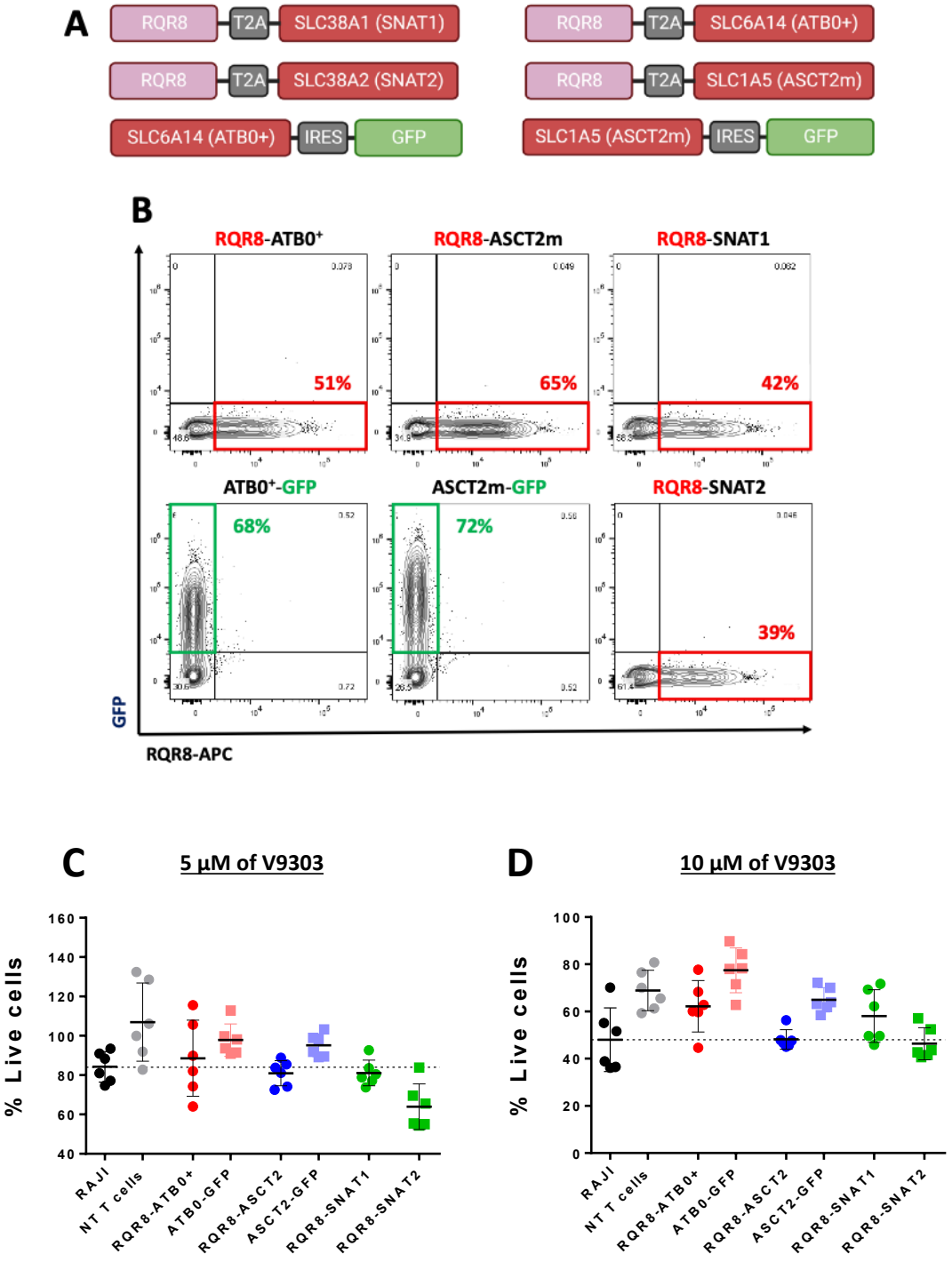

Figure 5.3-4: Transduction of activated T cells to express glutamine transporters. T cells were transduced with different retroviral constructs expressing glutamine transporters. **(A)** Schematic representation of the retroviral construct used to transduce T cells. **(B)** Representative contour plot of transduced T cells with RQR8 or GFP constructs. Transduced T cells were cultured with different concentrations of V-9302 or DMSO as vehicle. Percentage of live transduced T cells cultured with **(C)** 5 µM or **(D)** 10 µM of V-9302 for 48 hours. Bars are the mean ± SD. Pooled data of three independent experiments, n=5 healthy donors per group. Ns = not significant by One-Way ANOVA.

As re-stimulated CAR T cells have higher metabolic requirements compared to resting transduced T cells, we hypothesised activated CAR T cells should rely more on ASCT-2 for glutamine uptake and be more sensitive to incubation with V-9302. To study if overexpression of different glutamine transporters could surrogate for ASCT-2 inhibition on CAR T cells, T cells were co-transduced with plasmids expressing RQR8-αCD19CAR and glutamine transporter-IRES-GFP (Figure 5.3-5A). Transductions were analysed by flow cytometry with GPF expression and staining RQR8. Co-transductions efficiency varied between 40%-80% (Figure 5.3-5B) and was used for subsequent experiments.

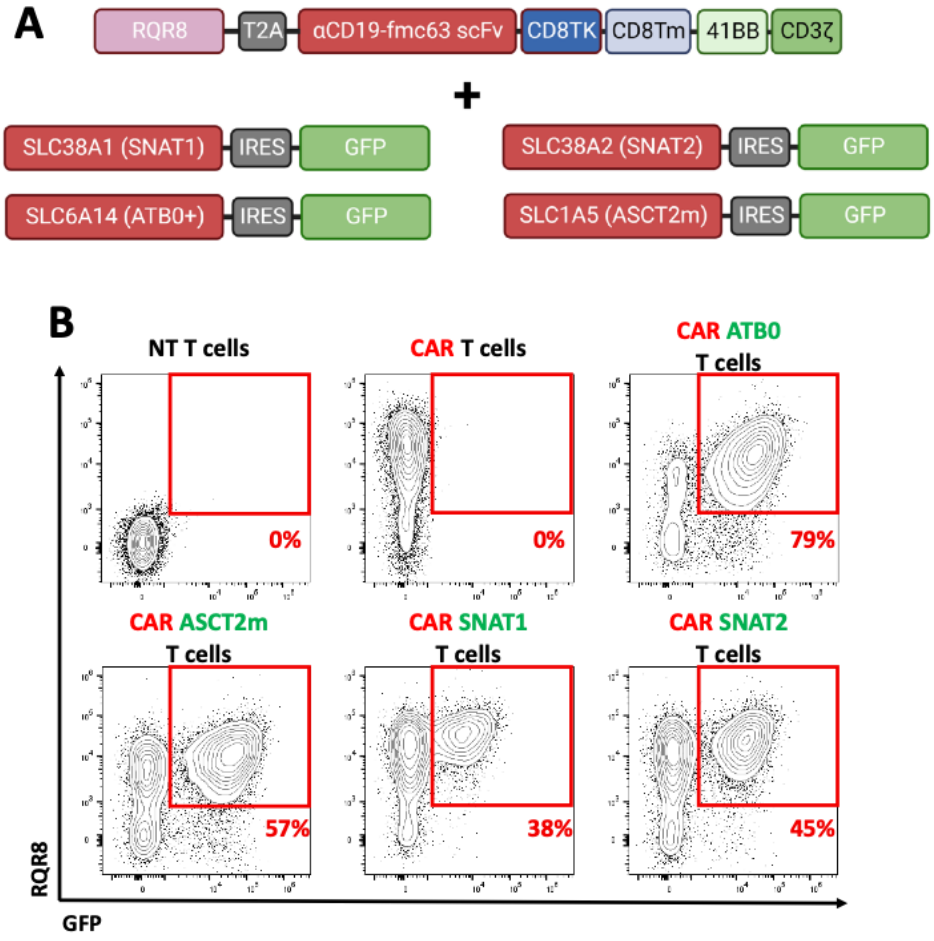

Figure 5.3-5: Transduction of activated T cells to co-express αCD19 CAR and glutamine transporters. T cells were co-transduced with two retroviral particles expressing the FMC63 αCD19 CAR with RQR8 and glutamine transporters with a GFP. **(A)** Schematic representation of the retroviral constructs used to transduce T cells. **(B)** Representative contour plot of transduced T cells with RQR8-CAR and Glutamine transporters-GFP constructs.

Co-transduced CAR T cells were cultured with Raji cells for 48 hours in media containing 5 µM or 10 µM of V-9302. Incubation with 10-5 µM of V-9302 reduced the number of live Raji cells and transduced T cells by 50% and 28% respectively. Only activated CAR T cells transduced with ATB^{0+} -GFP or SNAT2- GFP showed increased viability at both V-9302 concentrations (Figure 5.3-6A-B). However, no differences in production of IFN-γ was observed among all the groups (Figure 5.3-6C). Taken together, genetically engineering of T cells to express the glutamine transporter ATB^{0+} partially restored the inhibitory effects of ASCT-2 blockade on transduced CAR T cells.

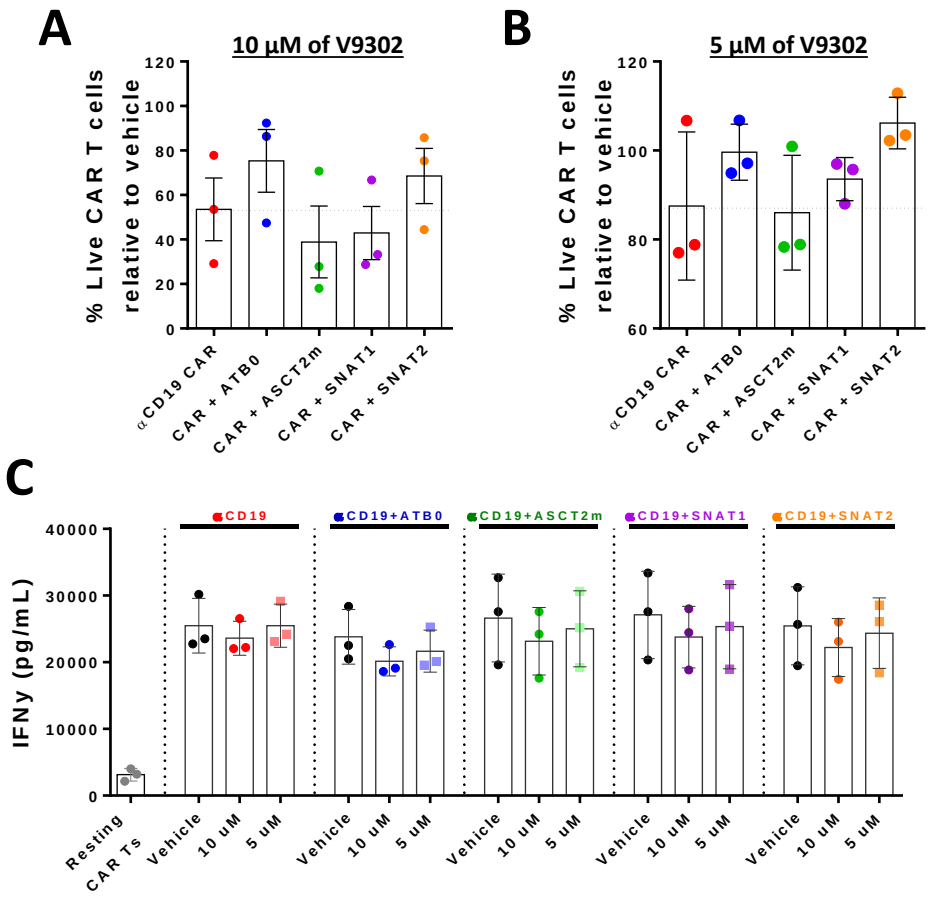

Figure 5.3-6: ASCT-2 blockade inhibition was reduced by the expression of glutamine transporters on αCD19 CAR T cells. Transduced T cells were cultured with different concentrations of V-9302 or DMSO as vehicle for 48 hours. Percentage of live transduced T cells cultured with **(A)** 5 µM or **(B)** 10 µM of V-9302. **(C)** IFN-γ production measured by ELISA. Bars are the mean ± SEM. Pooled data of three independent experiments, n=3 healthy donors per group. Ns = not significant by One-Way ANOVA.

5.4 Production and validation of glutamine neutralizing αASCT-2 antibodies.

Small molecules for blocking metabolic transporters have been extensively researched for cancer treatments. However, small molecules usually have problems with the selectivity of the target transporters, and unintentional side effects can arise. To overcome this limitation, antibodies blocking the movement of metabolites or reducing the expression of target transporters have been developed, allowing to specifically target surface proteins and reducing the risk of side effects [238]. Kyowa Hakko Kirin Co., Ltd developed 3 antibodies to neutralize glutamine uptake through ASCT-2. KM4008 and KM4012 were obtained from mouse hybridomas, while KM4018 was obtained from rat hybridomas. These αASCT-2 antibodies had similar neutralization kinetics, showing blockade of glutamine uptake and cell growth inhibition at 10-1 μg/mL on gastric cancer cell lines cultured in vitro.[234].

We obtained the sequences of KM4008, KM4012 and KM4018 from the US20100196392A1 patent and cloned these sequences under IgG2a and Igk constant domains. To identify transfected cells, an IRES domain was included separating a BFP or GFP protein (Figure 5.4-1A). Antibodies were produced transient transfection of HEK293T and verified the transfection by expression of BFP and GFP (Figure 5.4-1B).

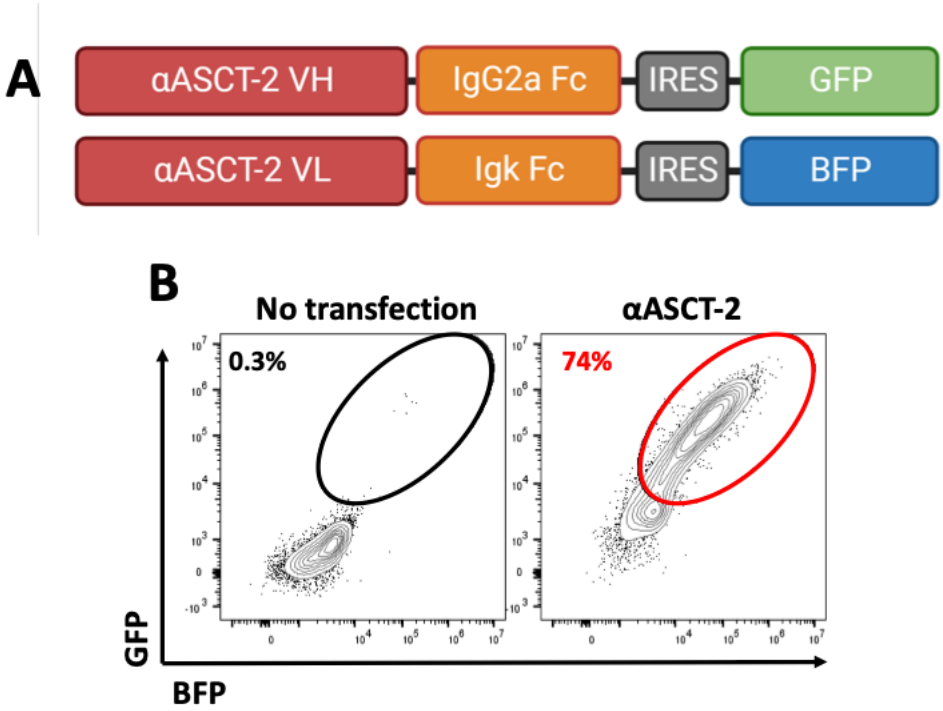

Figure 5.4-1: Transfection of HEK293T cells with αASCT-2 antibodies. HEK293 cells were co-transfected to express αASCT-2 antibodies. **(A)** Schematic representation of the constructs used to transfect HEK293T cells. **(B)** Representative histogram transfected cells.

As a pilot study of the efficacy of αASCT-2 antibodies, KM4008 (V08), KM4012 (V12), and KM4018 (V18) antibodies produced from HEK293T transfected supernatant were purified using the AKTA machine and used to stain Raji cells (ASCT-2+). Secondary staining with a mouse αIgG2a conjugated to APC was used to detect the αASCT-2-aIgG2a antibodies. As a negative control, the anti-idiotype antibody against FMC63 previously described was used, as it does not bind to Raji cells. All αASCT-2 antibodies stained Raji cells compared to the negative controls at 1 μg/mL (Figure 5.4-2A). Next, 10-5 μg/mL of αASCT-2 antibodies were added with Raji cells, and the number of tumour cells was counted by flow cytometry after 48 hours. V-9302 was used as a positive control for ASCT-2 inhibition. αASCT-2 antibodies reduced by 40% the percentage of Raji cells at 10 μg/mL and 5 μg/mL, and no significant differences were observed comparing V08, V12 and V18 αASCT-2 antibodies (Figure 5.4-2B). Importantly, V-9302 reduced the number of Raji cells by >90%, indicating Raji cells are sensible to glutamine depletion by ASCT-2 blockade. These results suggest that αASCT-2 antibodies are sufficient to impact Raji cells survival.

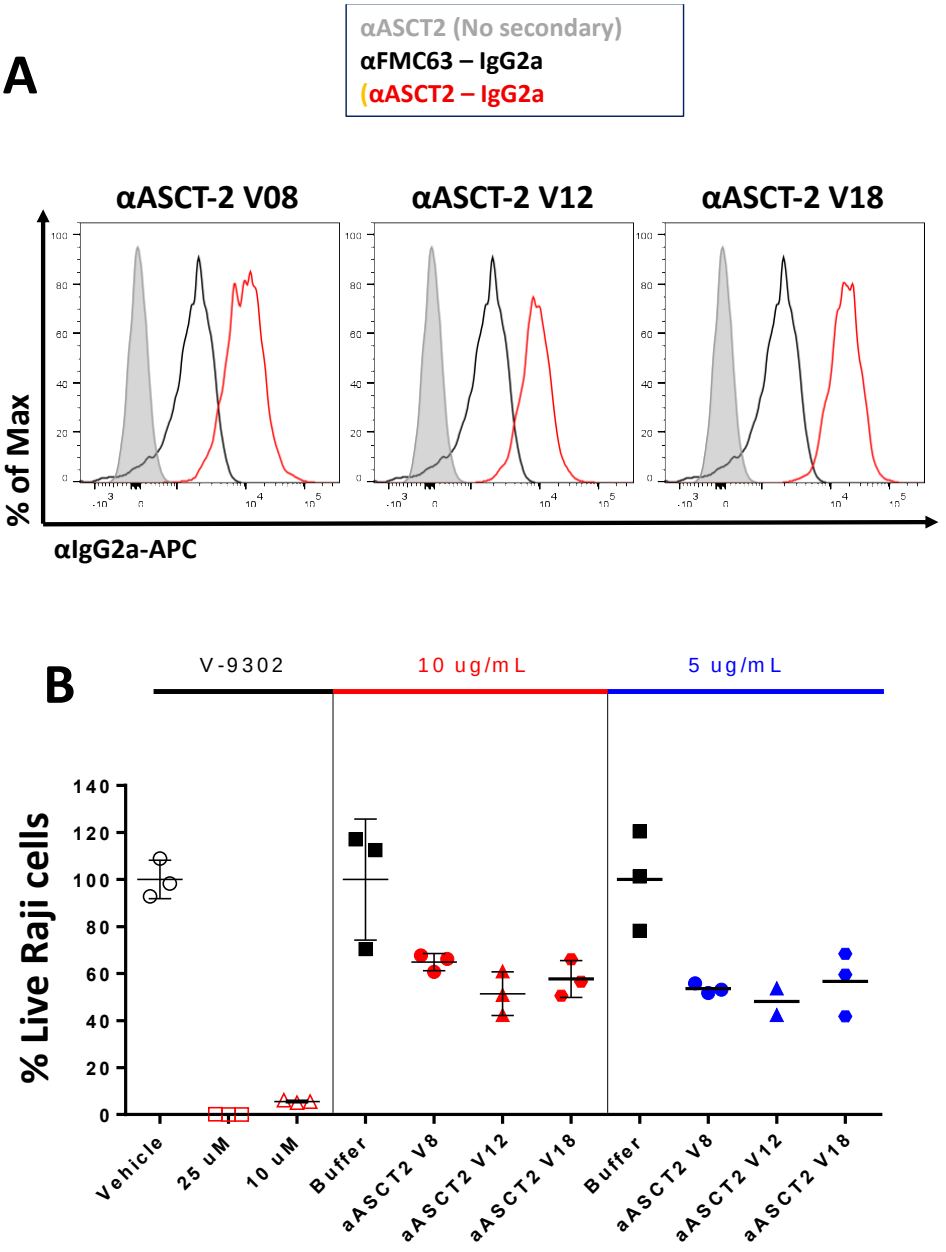

Figure 5.4-2: Validation of αASCT-2 antibodies on Raji cells. Raji cells were incubated with different αASCT-2 antibodies and analysed by flow cytometry. **(A)** Representative histogram of staining of Raji cells with 1µg/mL of antibodies and a secondary staining with an αIgG2a-APC. **(B)** Percentage of live Raji cells cultured with 5-10 µg/mL αASCT-2 antibodies for 48 hours. Bars are the mean ± SD. Pooled data of three independent experiments, n=4-6 healthy donors per group. Ns = not significant by One-Way ANOVA.

The antibody sequences were sent to GenScript for protein production to increase the conditions tested. A monoclonal antibody against hen egg lysozyme (αHEL) was used as a negative control. Binding to ASCT-2 was tested by staining Raji cells with a mouse αIgG2a conjugated to APC. Similar to previous experiments, all αASCT-2 antibodies stained Raji cells compared to the negative controls (Figure 5.4-3A).

20-1 μg/mL of αASCT-2 antibodies were cultured with Raji cells, and the number of tumour cells was counted by flow cytometry after 48 hours. αASCT-2 V12 antibody significantly reduced by 40% the percentage of live Raji cells at 20 μg/mL and 10 μg/mL, while a similar reduction was observed using the antibody at 1 μg/mL. αASCT-2 V08 and V18 reduced by 20% the number of Raji cells, but no statistical significance was observed (Figure 5.4-3B). Taken together, the culture of Raji cells with αASCT-2 antibodies reduced the number of Raji cells by 20-40%, with the αASCT-2 V12 antibody achieving the stronger effect of the three antibodies tested.

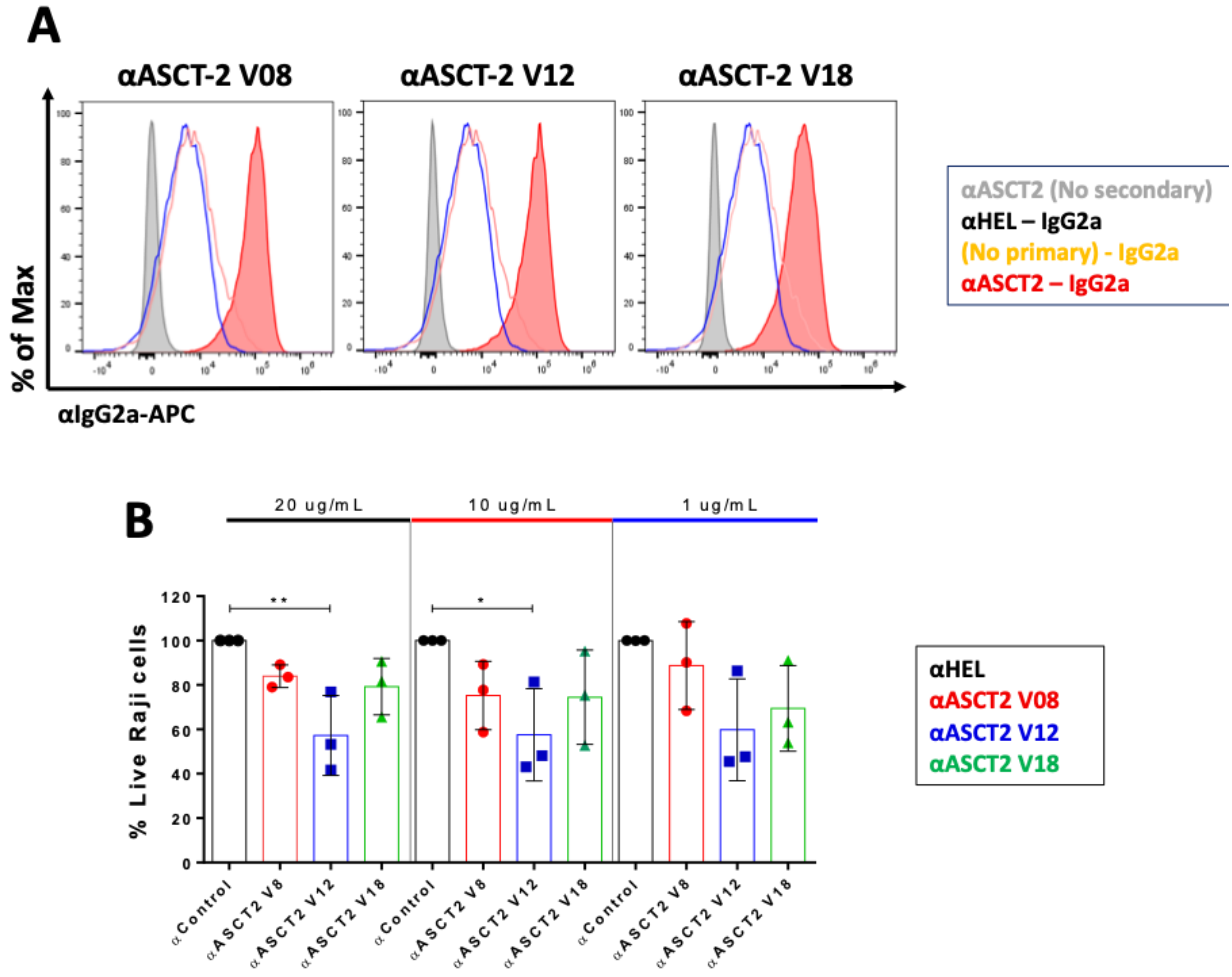

Figure 5.4-3: Purified αASCT-2 antibodies reduced the viability of Raji cells. Raji cells were incubated with different αASCT-2 antibodies and analysed by flow cytometry. **(A)** Representative histogram of staining of Raji cells with 1μg/mL of antibodies and a secondary staining with an αIgG2a-APC. **(B)** Percentage of live Raji cells cultured with 5-10 μg/mL αASCT-2 antibodies for 48 hours. Bars are the mean ± SD. Pooled data of three independent experiments, n=4-6 healthy donors per group. Ns = not significant by One-Way ANOVA.

Finally, we tested if ASCT-2 blockade with monoclonal antibodies impacts activated αCD19-CAR T cells proliferation and IFN-γ production, similar as observed after culture with V-9302. CAR T cells were co-transduced with surrogate glutamine transporters ATB^{0+}, ASCT-2m, SNAT-1 or SNAT-2, as previously described in this work (Figure 5.3-5). αCD19-CAR T were co-cultured with Raji cells and incubated with 10 or 5 μg/mL of αASCT-2 antibodies for 48 hours.

No differences were observed in CAR T cell expansion after using 5 μg/mL of any αASCT-2 antibodies tested (Figure 5.4-4A). Increasing the concentration to 10 μg/mL showed a 25% reduction of CAR T cell number only with V08 αASCT-2; however, no statistical significance was found (Figure 5.4-4B). Similarly, no differences were observed in IFN-γ production after culture with 5 μg/mL (Figure 5.4-4C) or 10 μg/mL (Figure 5.4-4D).

Taken together, ASCT-2 blocking antibodies were produced and validated. These antibodies were able to reduce the proliferation of Raji cells, but no effect was observed on activated CAR T cells, indicating they are not sufficient to impact CAR T cell function.

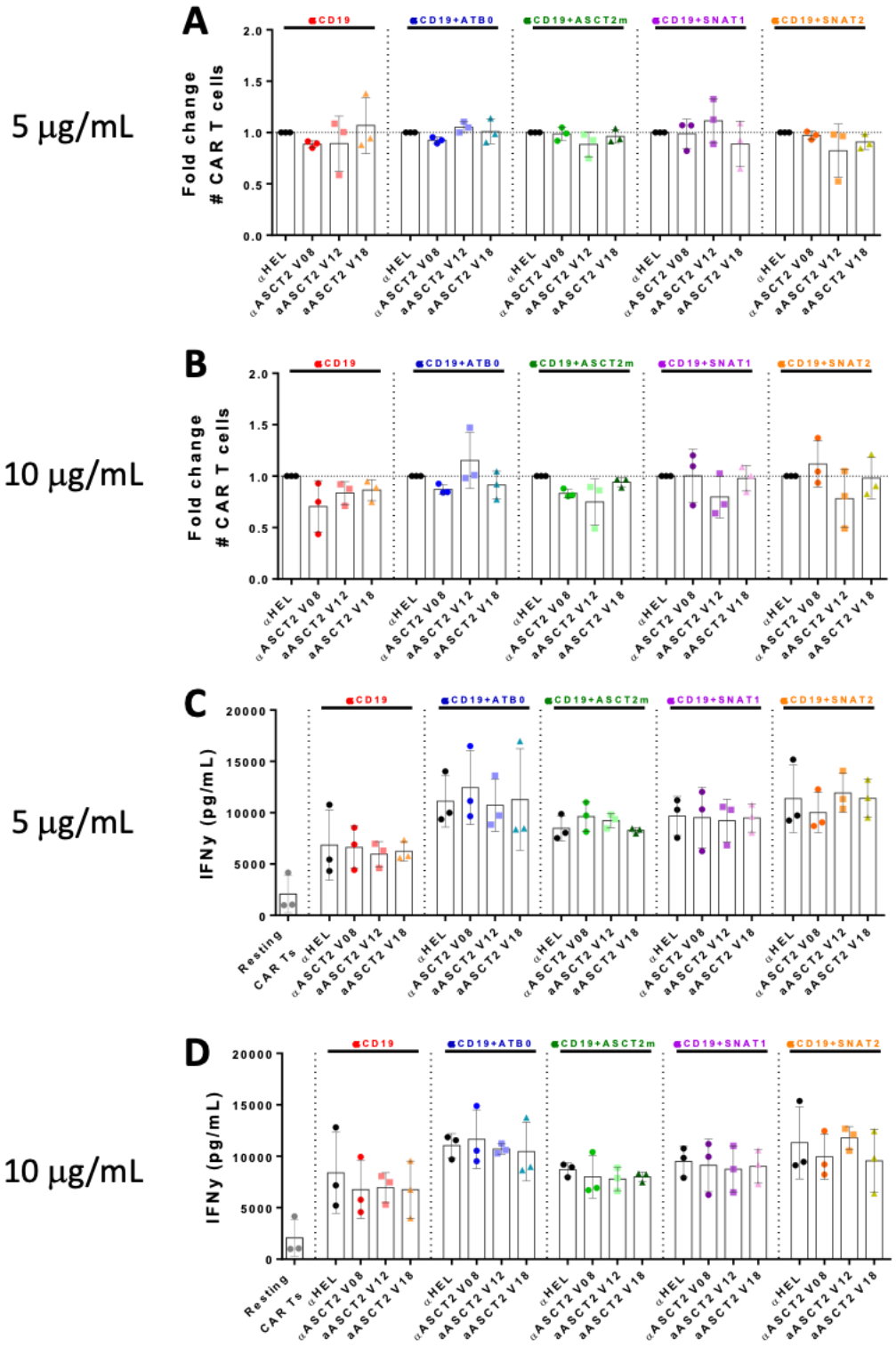

Figure 5.4-4: Combination of αASCT-2 antibodies and αCD19-CAR T cells. αASCT-2 antibodies were added to αCD19-CAR T cells in culture with Raji cells for 48 hours. Fold change of absolute number of cells cultured with **(A)** 10 µg/mL or **(B)** 5 µg/mL of αASCT-2. IFN-γ production from CAR T cells in culture with **(C)** 10 µg/mL or **(D)** 5 µg/mL of αASCT-2. Bars are the mean ± SD. Pooled data of two independent experiments, n=3 healthy donors per group. Ns = not significant by One-Way ANOVA.

5.5 Summary

We found that inhibiting glutamine uptake through ASCT-2 on αCD19-CAR T cells using a small molecule V-9302 impacted CAR T cell effector functions. At 10 μM, IFN-γ and IL-2 production was reduced by 50% while not cooperating in killing Raji cells, indicating inhibition of glutamine uptake though ASCT-2 is detrimental to CAR T cell antitumoral function. These results contrast with similar studies using mouse T cells, as they are insensitive to the V-9302 blockade.

We tested if overexpression of amino acid transporters SNAT-1, SNAT-2, ASCT-2 mouse or ATB^{0+} could surrogate glutamine uptake after ASCT-2 inhibition. Increased viability on resting T cells and activated CAR T cells expressing ATB^{0+} -IRES-GFP as found, indicating this construct is the best candidate for a combination of ASCT-2 inhibition with CAR T cell therapy.

To address the limitations of using small molecules to block metabolic transporters in clinical settings, we tested 3 different glutamine-neutralizing aASCT-2 antibodies on Raji cells and CAR T cells. V12 aASCT-2 antibody consistently reduced the viability of Raji cells by 40% at 1 μg/mL and was, therefore, the best antibody candidate. However, any of the antibodies tested reduced CAR T cell viability or IFN-γ production, indicating that at the conditions and concentrations tested, αASCT-2 did not neutralize enough glutamine to impact CAR T cell survival.

6. Discussion.

6.1 CAR T cells and metabolic regulation.

CAR T cell therapy directed at B-lineage antigens is becoming increasingly established in treating relapsed/refractory B-cell malignancies. However, while these therapies can induce sustained complete responses, most patients either do not enter remission or relapse. A proportion of CAR T cell failure is caused by antigen escape, but most failure occurs due to antigen loss. Comparatively, clinical responses against solid cancers have been modest. Infusion of TILs or transgenic TCR therapies results in clinical responses against melanoma, NSCLC, among other solid tumours [22,239], but their efficacy is still limited, partially due to a hostile tumour microenvironment [240]. The TME comprises an intricately integrated network of immunosuppressive elements, which render T-cell-based therapies ineffective in solid tumours by limiting T cell infiltration and activation. Moreover, initial strategies to overcome tumour immunosuppression included combining CAR T cells with immune checkpoint blockers or pro-inflammatory cytokines. In recent years, the role of immune metabolism to shape T cell responses have been exploited to increase OXPHOS and reduce glycolytic dependency, increasing CAR T cell efficacy in pre-clinical models, as increasing T cell persistence by genetic engineering improves T cell antitumoral potential [241,7].

The CAR can imprint distinct metabolic characteristics into T cells, as different signalling domains polarize T cells to engage into different metabolic networks, increasing CAR T cell persistence and antitumoral potential; therefore, modulating T cell or tumour/microenvironmental metabolism opens up a range of possibilities for enhancing CAR T cell efficacy. For instance, increasing mitochondrial metabolism to produce a less-differentiated phenotype by manipulating the cultured media or adding IL-15 and IL-7 is a commonly used strategy [242]. Additionally, the combination of CAR T cells with metabolic

regulators reducing glycolytic engagement, like AKT [97] and mTOR [90] has shown increasing antitumoral efficacy in pre-clinical models of B cell leukaemia and solid tumours.

More recently, the identification of crucial amino acids depleted in the TME and genetic manipulation of CAR T cells to bypass nutrient scarcity has shown promising results in reshaping T cell metabolism and improving their antitumoral potential [104,105]. However, strategies which selectively affect tumour cells without hindering T cell immunity have been challenging to develop, as tumour cells and proliferating T cells share many metabolic requirements. Moreover, two studies combining metformin with CAR T cells reached opposite conclusions; an αCD19-CAR against B cell lymphoma cell lines had reduced cytotoxicity and antitumoral effects [243], while αHER2-CAR against lung carcinoma had enhanced antitumoral activity [244]. Different in media composition, the concentration of IL-2 used to expand T cells or the CAR structure, which can induce different levels of tonic signalling [245] could explain these differences. Regardless, this highlights the necessity of studying metabolic regulation in each CAR T cell therapy context.

Taken together, an increasing understanding of T cell metabolic requirements and their interaction with the TME will lead to more sophisticated and efficient antitumoral therapies.

6.2 Pharmacological inhibition MCT-1 on αCD19-CAR T cells.

Pharmacological blockade of lactate transporters like MCT-1 has shown promising results against B cell malignancies, as these cancer cells rely exclusively on this transport for lactic acid export and B cell lymphomas patient samples show high expression of MCT-1 and low levels of MCT-4, which makes them an ideal target for MCT-1 inhibitors, as activated T cells express high levels of MCT-4 and should be insensitive to MCT-1 blockade. Therefore, we aimed to study MCT-1 inhibition in combination with αCD19-CAR T cells to exploit B cell malignancy metabolic vulnerabilities.

6.2.1 Expression of MCT transporters on tumour and CAR T cells.

Small molecules have been developed to exploit the Warburg effect. For instance, monocarboxylate transporters are highly expressed across several cancers [135] and small molecules which block lactate transporters such as MCT-1 and MCT-4 have been developed. These small molecules induce quick accumulation of lactic acid intracellularly, arresting proliferation and inducing cell death of tumour cells [158]. Combining small molecules which exploit the Warburg effect with ACT is not straightforward however, since activated T cells increased glucose uptake and fermentation of glucose to lactate. Even so, as DLBCL patient samples and cell lines predominately express MCT-1 for lactate export, with little or no expression of MCT-4 [144,145] while T express both MCT-1 and MCT-4 upon activation [178], we hypothesized that differential use of lactate transporters by tumour and T cells might allow selective metabolic disruption of tumour cells. More specifically, we sought to explore the use of selective MCT-1 inhibitors for this strategy.

We found high MCT-1, MCT-4 and CD147 expression on resting CAR T cells and an increase of MCT-1 and CD147 levels after CAR T cell activation. Other studies have shown MCT-1 expression peaks on activated T cells after 12 hours, while MCT-4 expression is found after 48 hours post T cell activation. As the transduction of T cells with pseudo-retroviral particles requires an activation step with αCD3 and αCD28 monoclonal antibodies, it is possible non-transduced and resting CAR T cells maintained some expression of MCT1/4 after activation, while T cells restimulated via the CAR induces higher expression of MCT-1 and CD147. Notably, both B-cell tumour cell lines used in this work, Raji and NALM6, had high CD147 and MCT-1 levels, with no expression of MCT-4 detected. Expression of metabolic transporters on Raji cells has been extensively studied, as it is the main cell line used in studies regarding pharmacological MCT-1 inhibition [211], while no studies using NALM-6 cells have been reported. Therefore, in most experiments, we decided to use Raji cells as a positive control

for MCT-1 inhibition as a lot of data has been published with this cell line. Moreover, Raji cells are highly glycolytic, even compared to other DLBCL cell lines [246], making them more susceptible to glycolytic manipulation.

For MCT-1 inhibition, we studied the 2 main small molecules used in pre-clinical studies; AR-C155858 and its derivative, AZD3965. Both drugs are potent inhibitors of MCT-1 but they also target with lower affinity MCT-2. Limited information exists regarding functional differences between both MCT-1 inhibitors to account for the differences between AZD3965 and AR-C155858. Studies using mouse 4T-1 breast tumour cells found minor differences comparing both small molecules. AR-C155858 behaves like an MCT-1 substrate with a trend toward higher uptake at lower pH and with higher affinity to MCT-1 and MCT-2 compared to AZD3965, while the latter shows higher liposolubility, which explains its oral availability and different saturation rates compare with AR-C155858 [152]. Despite these differences, both small molecules are used interchangeably for MCT-1/2 blockade, so we decided to use both in most experiments to minimize the possibility the effects observed in our experiments were due to off-target effects or limited to one MCT-1 inhibitor.

6.2.2 Metabolic rewiring of CAR T cells after MCT-1 inhibition.

After the blockade of lactate export, the first effect on tumour cells is a quick intracellular lactate build-up. Lactate accumulation triggers profound biochemical changes, including metabolic rewiring [164] and lactate dehydrogenases (LDH) conversion of lactate to pyruvate, depleting ATP and NAD^+. Over time, this reaction induces the accumulation of lactic acid, increasing intracellular acidosis and T cells dysfunction [158]. Both accumulation of lactate and increase in intracellular acidosis contribute to impair proliferation and an increase cell death in tumour and T cells after MCTs inhibition [70].

Importantly, short MCT-1/2 inhibition did not increase the intracellular lactate of αCD19-CAR T cells while a 4x fold increase of intracellular lactate was found on Raji cells. We also measured increases in intracellular acidosis using a pH-sensitive dye; pH Rodo Green. MCT-1 inhibition for 48 hours induced a 50% decrease on intracellular pH in Raji cells, but no differences were found in αCD19-CAR T cells. Similarly, no differences in the percentage of apoptotic CAR T cells measured by annexin V or differences in proliferation of CAR T cells after 4 and 7 days of culture with MCT-1 inhibitors were found. Our results suggest αCD19-CAR T cells are insensitive to MCT-1 inhibition, as we could not find the early signs of lactate accumulation (a quick lactate build-up) or late effects of metabolic shutdown after severe intracellular lactic acid (increase in acidosis, apoptosis induction and reduced proliferation).

Moreover, in breast cancer cell lines, MCT-1 inhibition can induce changes in the expression of MCT-1/2/4 [154]. We measured the expression of MCT-1, MCT-4 and CD147 on activated CAR T cells to confirm if MCT-1/2 blockade insensitivity in our CAR T cells was explained by an increase in MCT-4 expression or a loss of MCT-1. However, no differences on MCT-1, CD147 or CD147 expression were found, suggesting differences found in CAR T cells after MCT-1 inhibition are not explained by the downregulation of their main lactate transporters.

As changes in metabolism can profoundly impact T cells development, and MCT-1 inhibition causes metabolic rewiring in cancer cells by increasing OXPHOS and reducing glycolysis, we next explored the metabolic status of CAR T cells by analysing metabolic parameters by flow cytometry and Seahorse assays. For the glycolytic analysis, we measured the extracellular acidification rate (ECAR) of activated αCD19-CAR T cells in culture with MCT-1 inhibitors. Interestingly, extracellular acidification rate was reduced by 20% in CAR T cells cultured with either AZD3965 or AR-C155858, impacting their glycolytic reserve and glycolysis values. The Seahorse assay measures ECAR by directly sensing changes in proton release in the media, mainly by lactic acid release. It is possible the reduction in ECAR in CAR T cells is due to

blocking lactic acid release by MCT-1 inhibition rather than a general reduction in glycolysis. However, 2-NBDG uptake, a measure of glucose consumption, was unaffected in αCD19-CAR T cells treated with MCT-1 inhibitors and we did not observe a quick lactate accumulation in previous experiments, suggesting the reduction in ECAR is due to a general metabolic rewiring.

Supporting this hypothesis, we found that activated αCD19-CAR T cells showed a shift towards a respiratory metabolism after MCT-1 blockade. Measuring CAR T cells oxygen consumption rate showed a 20% increase in maximal respiration after AR-C155858 incubation and a 25% increase in mitochondrial mass was found by staining with Mitotracker Green. These results suggest αCD19-CAR T cells increase their mitochondrial biogenesis after long exposure to MCT-1 inhibitors, similar results were obtained in Raji and non-cancerous cells, where intracellular lactate activated AMPK, increasing MCT-1 expression and mitochondrial biogenesis [151,247]. However, we did not perform an extensive mitochondrial profile, as not only mitochondria mass but also cristae remodelling, and mitochondrial fusion status profoundly shape T cells metabolism [83].

Changes in lactate levels could induce metabolic rearrangement of CAR T cells by inhibition of lactate dehydrogenases (LDH) and stabilization of hypoxia-inducible factor 1 alpha (HIF-1α). LDH inhibition would explain the reduction of ECAR without shutting down glycolysis while increasing the influx of metabolites towards the TCA cycle and mitochondrial biogenesis, as observed in tumour models [248], while local accumulation of lactate is a known trigger of HIF-1α, promoting a metabolic shift to OXPHOS [249]. Directly measuring HIF-1α and LDH protein expression and activity, together with an electronic microscopy of T cells mitochondria could partially answer if our CAR T cells rewire their metabolism after MCT-1 inhibition. Similarly, single-cell metabolic dynamics of CAR T cells infused on DLBCL patients have identified a metabolic profile of early-activated CAR T cells [250]. Comparing CAR

T cells treated with different MCT inhibitors and metabolic profiling by stable isotope tracing could answer more broadly the potential functional consequences of MCT regulation on T cell-based therapies [251].

6.2.3 Activation profile of CAR T cells after MCT-1 inhibition.

As T cell metabolism directly regulates T cells activation and functions, we performed an extensive analysis of CAR T cell activation and phenotype to address if MCT-1 inhibition impacted CAR T cell due to their increase in mitochondrial metabolism. We measured the classic activation markers 41BB, OX40, CD69 and Granzyme B by flow cytometry and found no differences in their expression comparing activated αCD19-CAR T cells with MCT-1 inhibitors and vehicle control. Similarly, initial studies culturing T cells with high levels of lactic acid did not impact their expression of CD69 [118], and blocking lactate export of T cells with diclofenac did not change their 4-1BB expression, suggesting the activation profile of T cells is resilient to the inhibitory effects of lactic acid accumulation. Comparably, the reduction of IFN-γ and IL-2 production is a well-described consequence of lactic acid accumulation [109,118,121]; however, IFN-γ and IL-2 production was unaffected by MCT-1 blockade in our CAR T cells. Continuous lactic acid exposure in the TME induces T cell anergia and increases their expression of exhaustion markers, like PD-1, LAG-3 and TIM-3 [252], while increasing acidosis or lactic acid concentration in vitro also increases T cell expression of exhaustion markers. In contrast, our activated αCD19-CAR T cells did not increase the percentage of apoptotic T cells nor increased PD-1 or TIM-3 expression after 48 of MCT-1 inhibitors exposure. Our results suggest that the increase in CAR T cell OXPHOS after MCT-1 blockade did not meaningfully impact CAR T cell effector functions.

Previous publications have shown MCT-1 inhibitors stop the proliferation of Raji cells. As Raji and NALM6 cells only express MCT-1, we tested if combining αCD19-CAR T cells with

MCT-1 inhibitors could enhance tumour cell killing. We cultured αCD19-CAR T cells with $CD19^+$ tumour cell lines at different Effector:Target ratios and consistently found the drugs alone and in combination with CAR T cells reduced the percentage of live tumour cells by 50%, indicating that, in vitro, there is a cooperative effect on tumour cell killing, rather than synergy between treatments. As we did not find any meaningful differences in MCT1-blocked CAR T cell phenotype, we believe these drugs selectively impact tumour cells, leaving CAR T cells unaffected.

An important consideration in these experiments is our CAR design. All these experiments were performed with a CAR with a CD3z and a 4-1BB signalling domain. In T cells, agonistic antibodies against 4-1BB induce profound metabolic reprogramming by raising mitochondrial membrane potential, increasing OPA-1 expression, mitochondria fusion and improving T cell respiratory capacity [253]. Similarly, 4-1BB signalling in CAR T cells increased their respiratory capacity and resistance to activation-induced cell dead by increasing antiapoptotic Bcl-2 family members Bcl-xL and Bfl-1 [254]. Therefore, it is possible MCT-1 inhibition did not impact CAR T cell function, as the 4-1BB signalling polarise them to a phenotype less reliant on glycolysis and less lactate-dependant. We repeated a set of experiments but changing the 4-1BB signalling domain with a CD28 intracellular domain, as CD28 engagement polarize T cells into a more glycolytic network [255].

We obtained similar results comparing 4-1BB and CD28 domains. αCD19-CAR-CD28 T cells had similar expression of 4-1BB and CD69 after activation. IFN-y and IL-2 production did not decrease after culture with MCT-1 inhibitors, nor was glucose consumption affected. Co-culture of Raji cells and αCD19-CAR-CD28 T cells in presence of MCT-1 inhibitors also increased T cell killing by 50% at different target:effector ratios. In general, we did not find any meaningful differences in αCD19-CAR-CD28 T cells after MCT-1 blockade, suggesting the cooperation between treatments is not limited to 4-1BB CAR T cells. However, we did not

test a CD28 CAR T cell in vivo or analyse its long-term activation. CD28 imprints a more glycolytic phenotype, with higher expression of GLUT-1 and higher acidification rates after 7 days activation [76], so it is possible different co-stimulation domains have different sensitivity to MCT-1 inhibition not addressed in this work. Optimising CAR signalling and their interaction with metabolic regulators could become a powerful tool for CAR T cell therapy. Most studies comparing CAR T cell signalling domains focuses on 4-1BB and CD28, but other members of the TNF family members have been shown to improve CAR T cell persistence and reduce exhaustion [256,257], particularly in CD4 T cells, which are a fundamental component of the antitumoral cytotoxic response [258].

6.2.4 CAR T cell Memory formation after MCT-1 inhibition.

A key factor for CAR T cell clinical responses is T cell engraftment; moreover, different T cells memory subsets have shown different kinetics in clearing tumour cells. Effector memory T cells rely more preferentially on glycolytic pathways to sustain their energy, quickly inducing T cell expansion and tumour clearance. On the other hand, central memory T cells persist over time, allowing a slower but continuous tumour killing, relying on fatty acid oxidation and respiration [259]. Metabolic networks shape T cell memory formation, several studies have shown increasing OXPHOS in T cells increases the formation of long-lived memory populations, like central memory T cells [7]. As culture with MCT-1 inhibitors induced an increase in OXPHOS but no differences in CAR T cell phenotype or effector functions were found, we performed a T cell memory analysis by weekly stimulation of αCD19-CAR T cells with Raji cells in presence of IL-2 to simulate the conditions CAR T cells encounter after patient infusion. With our protocol, we found a significant reduction of CAR T cells with a Naïve and central memory phenotype over time due to loss of expression of CCR7, a marker used to identify these populations. Meanwhile, we found an increasing percentage of effector T cells and T_{EMRA} cells, indicating this protocol simulates chronic antigen stimulation, reducing the percentage of long-

lived memory T cells over time while increasing the number of exhausted CAR T cells. Importantly, no differences in the memory T cell profile were found with either MCT-1 inhibitor, indicating long-term culture with MCT-1 inhibitors did not impact CAR T cell metabolic networks enough to induce changes in memory development, further supporting the hypothesis CAR T cells are insensitive to MCT-1/2 blockade. Importantly, weekly CAR T cells stimulation in presence of IL-2 should polarise T cells to engage in a glycolytic metabolism, which would make them susceptible to MCT-1 inhibition, we did not test if the same phenotype would be obtained by culture with other cytokines, like IL-15 or IL-7. No studies have been published systematically studying T cell memory formation after MCT-1/2 blockade so the effects of MCT-1 inhibition in memory T cell development and their impact on antitumoral immunity remains to be studied.

6.3 Dual blockade of MCT-1/4 on αCD19-CAR T cells.

6.3.1 Syrosingopine and diclofenac.

Our results suggest CAR T cells do not rely exclusively on MCT-1 for lactate export. Other transporters could substitute this function, particularly MCT-4 expressed on activated T cells, including in our CAR T cells as MCT-4 expression is the most common resistance mechanism to MCT-1 inhibition [163]. Therefore, we hypothesised MCT-4 expression was sufficient to render CAR T cells insensitive to MCT-1 inhibition. As there are no small molecules targeting specifically MCT-4, we tested this hypothesis by culturing CAR T cells with syrosingopine, a dual blocker of MCT-1 and MCT-4 [174]. Culture with syrosingopine severely impaired T cell expansion, IFN-γ production and did not synergise with CAR T cell killing of target cancer cells. Moreover, CAR T cells cultured with syrosingopine quickly accumulated intracellular lactic acid, indicating CAR T cells rely at least on functional MCT-1 and MCT-4 for lactate export and T cell functionality.

However, our results need to be contrasted with publications using diclofenac, a non-steroidal anti-inflammatory drug which also blocks MCT-1/4. Renner et al., found dual blocking of MCT-1 and MCT-4 with diclofenac showed minimal impact on human T cells IFN-γ production and activation profile, while a two-fold reduction in proliferation and lactate release was found [178]. Additionally, blocking MCT-1/2/4 on mouse T cells showed minimal impact on IFN-γ production, and combination of diclofenac with immune checkpoint blockers against PD-1 and CTLA-4 showed a strong protection in a breast cancer mouse model. Interpreting the differences observed between syrosingopine and diclofenac is challenging, as no studies comparing both drugs have been published. On tumour models, diclofenac has shown direct metabolic regulation by inhibition of lactate dehydrogenase activity and impaired glucose metabolism by inhibiting MYC [260]; diclofenac also directly modulates T cell activity by inhibition of the potassium transporter Kv1.3 [261] and high doses causes the activation of T cells in a popliteal lymph node assay by the accumulation of mouse memory T cells [262].

On the other hand, the potential off-target effects on T cells are less understood. Syrosingopine has shown antitumoral effects in combination with mitochondrial inhibitors, particularly metformin, by depleting NADH and inducing tumour cell dead [174].

6.3.2 Enolase expression in tumour and T cells.

Additionally, syrosingopine has been shown to bind to α-enolase (ENO1). α-enolase is part of the glycolytic pathway, as it catalyses the conversion of 2-phosphoglycerate to phosphoenolpyruvate, but no drop in α-enolase activity was found in HL60 cells cultured with syrosingopine. However, in tumour cells models which rely only on glycolysis for energy production, these models were sensitive to α-enolase inhibition by syrosingopine. Moreover, expression of γ-enolase was a marker of resistance to the combination of syrosingopine-metformin, and overexpression of γ-enolase conferred resistance to syrosingopine in vitro [171].

In T cells, α-enolase is expressed on activated CD4 and CD8 T cells and is critical for T cell function in diseases like diabetes and multiple sclerosis [263,264]. Murine melanoma-infiltrating CD8 T cells showed reduced glycolytic activity by downregulating α-enolase activity and adding pyruvate, a downstream product of α-enolase, reversed the metabolic inhibition on sorted TILs. Importantly, these TILs expressed similar levels of α-enolase but with significantly reduced activity, suggesting the regulation of this pathway is post-transcriptionally regulated [265]. Our results showed a quick accumulation of intracellular lactate in Raji and CAR T cells after exposure to syrosingopine, suggesting the inhibitory effect observed in activated αCD19-CAR T cells cultured with syrosingopine is mediated by lactate accumulation rather than α--enolase activity.

To definitively answer the role of α-enolase on syrosingopine T cell inhibition, activated αCD19-CAR T cells in the presence of syrosingopine could be cultured in media supplemented with pyruvate or with molecules blocking enolase activity, like NaF, POMHEX [266] or ENOblock, an inhibitor of the non-glycolytic functions of enolase [267]. Additionally, CAR T cells could be transduced with γ-enolase to confer resistance to syrosingopine; these strategies could answer if the immunosuppressive effects of syrosingopine are due to lactate accumulation or α-enolase inhibition.

Additional factors can contribute to MCT-1/4 inhibition differences with different small molecules. Acute myeloid leukaemia cells expressing only MCT-1 engage in different cell-death pathways depending on which MCT blocker is used. AR-C155858 caused necrosis while dual MCT-1/4 with syrosingopine induced autophagy [142], even if both drugs induced similar levels of lactate accumulation, suggesting an off-target effect on one or both small molecules.

6.3.3 Expression of surrogate lactate transporters.

A significant limitation of our experiments is the expression of surrogate lactate transporters on T cells after activation. For example, T cells can express MCT-2 [268], although MCT-1 is expressed faster than other monocarboxylate transporters [178]. MCT-2 can transport lactate with lower affinity than MCT-1, and the former has been described to be key on sustaining tumour growth in certain cancer models. In mouse models of lung cancer, genetic deletion of MCT-2 improved tumour control and MCT-2 deletion on macrophages induced a distinct TME, with increased T-cell differentiation and response to oxidative stress [269]. Considering this, in all our in vitro experiments, we used a dose of 100 nM, which should be sufficient to block both MCT-1 and MCT-2, as AZD3965 and AR-C155858 block MCT-2 with an affinity of 10 nM. Therefore, we do not expect a contribution of MCT-2 on T cell lactate export in the conditions analysed in this thesis.

Regardless, in this thesis we did not directly explore the functionality of other lactate transporters. Genetic deletion of MCT-1/2/4 using CRISPR/Cas electroporation of T cells could answer questions regarding the functionality of these transporters on CAR T cell biology. However, as our objective was to explore the possible combination of metabolic regulators with CAR T cells to improve their antitumoral potential, and as we did not find any meaningful impact on CAR T cell function, we did not pursue loss-of-function experiments to answer these questions.

Additionally, activated CD4 T cells can express the sodium-dependant lactate transporter SLC5A12, which mediates lactate uptake in mouse models of inflammation, promoting fatty acid oxidation and Th17 polarization. Moreover, the blockade of SLC5A12 with monoclonal antibodies improved the disease score of murine models of arthritis [270]. However, this

transporter primary function is lactate import, as it was first discovered as the main transporter for lactate absorption in kidney [271] and its role in T cell dysfunction remains to be addressed.

More recently, another member of the MCT family has been described in T cells. MCT-11 is highly expressed in the thyroid, liver, and salivary gland [131] but limited information is available regarding functional expression in other tissues, including immune populations. However, early reports from Delgoffe team have shown MCT-11 is expressed on exhausted CD8 T cells in mouse melanoma models, contributing to lactate import and accelerating T cell exhaustion. Conversely, genetic deletion of MCT-11 on CD8 T cells or blocking MCT-11 with monoclonal antibodies reduced tumour burden, suggesting targeting MCT-11 could be an interesting approach to combine with T cells immunotherapies against solid tumours [272].

6.4 Combination of MCT-1 blockade and αCD19-CAR T cells on mouse models of B cell leukaemia.

6.4.1 Efficacy of MCT-1 blockade and αCD19-CAR T cells against a NALM6 model.

NAML6 and Raji only expressed MCT-1 and both cell lines showed similar sensitivity to MCT-1 inhibition, implying the differential expression of MCTs on T cells and tumour cells offers a therapeutic opportunity. However, studies on human breast cancer cell lines showed MDA-MB-231 sensitivity to MCT-1/4 inhibition with syrosingopine in vitro, but not as tumour xenografts in immunodeficient mice [170]. Important metabolic differences between in vitro and in vivo models, with cells cultured in vitro preferentially using glucose as a carbon source, while in vivo explants rely more on glutamine, changing the sensitivity to metabolic regulators [228]. Therefore, we developed a xenograft mouse model of B cell leukaemia by injecting NALM6 cells intravenously, allowing systemic engraftment of tumour cells in the animals.

We found a high tumour burden after 6 days of NALM6 injection, measured by the luciferase signal in the NALM6 cells. A single low dose of $5x10^5$ αCD19-CAR T cells efficiently reduced the tumour burden of NALM6 cells after 4 days post-infusion. This dose of CAR T cells was used for all experiments as higher doses of intravenously transferred αCD19-CAR T cells, like $1x10^6$ CAR T cells, completely eradicated the NALM6 tumour cells and did not allow us to compare the effect of the combination. Meanwhile, daily injections of 5mg/kg of AR-C155858 intraperitoneally reduced tumour engraftment by around 50%, but only reaching statistical significance after 12 days of treatment.

The combination of αCD19-CAR T cells with daily intraperitoneal injections of AR-C155858 significantly improved tumour control in vitro against NALM6 cells compared with each treatment alone, reaching significance after 12 days of treatment. Comparing the tumour burden of mouse transferred with αCD19-CAR T cells with vehicle or control, injecting AR-C155858 also reduced the tumour burden by 50%. We obtained similar results on 2 additional independent experiments analysing CAR T cell phenotype in vivo, where after 7 days of treatment with AR-C155858, a reduction of 50% of tumour burden comparing the vehicle with MCT-1 inhibitors was observed in mice treated with αCD19-CAR T cells. Similar results were seen in our in vitro killing assays, which further support the hypothesis that both treatments act as having an additive rather than a synergistic effect in treating B-cell malignancies.

6.4.2 In vivo phenotyping of αCD19-CAR T cells.

We also performed a detailed phenotype analysis of the infused CAR T cells to test if the lack of differences after MCT-1 blockade in T cell phenotype seen in vitro were replicated in vivo. For this, T cell phenotype was analysed in bone marrow and spleen, as they are 2 of the main organs for CAR T cell trafficking after a NALM6 tumour challenge [104,273]. First, no differences were observed in the number of T cells infiltrating either spleen or bone marrow, analysed by

dissecting the percentage of Treg, CD8 and CD4 T cells, indicating MCT-1 inhibition did not impact expansion of the main T cell subsets. Lactate build-up can polarise CD4 T cells into specific phenotypes, inducing Th17 responses and decreasing the percentage of Th1 CD4 T cells in mouse models of prostate carcinoma and rheumatism [270,274]. No differences were observed in the production of Il-2 and IFN-γ on CD8 or CD4 T cells, suggesting the Th1 phenotype was not reduced in vivo. However, a more details analysis of T cell phenotype is lacking in these experiments, and if MCT-1 inhibition induces different types of inflammatory CD4 T cells, like Th9 and Th21, remains to be solved.

In our model, bone marrow αCD19-CAR T cells were more abundant than splenic CAR T cells and expressed higher levels of activation markers, like 4-1BB, IFN-y and IL-2, indicating they have a more activated phenotype. Single-cell imaging of mouse αCD19-CAR T cells on transgenic mice that spontaneously develop Burkitt-like B cell lymphoma revealed CAR T cells preferentially kill tumour cells in the bone marrow [275], explaining the differences in the activation profile in our experiments. Importantly, we did not find meaningful differences in splenic or bone-marrow infiltrated αCD19-CAR T cells activation markers (4-1BB, ICOS and Ki67), expression of effector molecules (IFN-γ, IL-2 and LAMP-1) or exhaustion markers (PD-1) comparing prolonged MCT-1 inhibition with their negative control on neither CD8 nor CD4 T cells. We analysed similar activation markers in vitro (4-1BB, OX40, CD69, PD-1, IFN-γ, and IL-2 release) and found no differences in their expression, suggesting the metabolic niche found in vivo or in vitro did not significantly change the sensitivity of αCD19-CAR T cells to MCT-1 inhibition.

Finally, we analysed the αCD19-CAR T cell memory profile in the bone marrow. More than 80% of the infused T cells were effector memory T cells in both CD8 and CD4 compartments, similar to our results with in vitro chronic stimulation of CAR T cells, suggesting CAR T cells engaged in repeated antigen stimulation after intravenous infusion. Taken together, our results

indicate MCT-1 blockade did not meaningful impact αCD19-CAR T cells phenotype and shows the potential of targeting metabolic susceptibilities of tumour cells by the cooperation of targeting lactate metabolism via MCT-1 in combination with a CAR T cells therapy against B cell lymphoma.

To strengthen this conclusion, additional tumour models should be used, like a systemic injection of Raji cells. Raji cells seem to be particularly sensitive to MCT-1 inhibition, as they have a quicker metabolism compared with other malignant B-cell cell lines [246] and they have been extensively used to test the efficacy of MCT-1 inhibition in preclinical models. [211]. The comparison of different B-cell cancer cell lines, susceptibility to metabolic regulation and its translational implications remains to be elucidated.

In summary, the pharmacological blockade of MCT-1 selectively impairs B cell tumour growth without hindering CD19-specific CAR T cell antitumoral potential, making combining both treatments an interesting approach against B cell malignancies.

6.4.3 Hypoxia and T cell dysfunction.

The combination of CAR T cells and MCT-1 inhibition may be broadened by the exploration of MCTs expression of different tumours, particularly sub-categories of solid tumours expressing MCT-1 and negative for MCT-4, like melanoma, breast cancer, gliomas and others [276,277]. Subcutaneous injection of NALM6 or Raji cell lines could recapitulate immunosuppressive elements of the TME, which are not present in systemic models. MCT-1 inhibition have been shown to reduce the lactate accumulation in solid tumours [164]; even if blockade of MCT-1 did not directly impact CAR T cells functions, the reduction of tumour acidity could improve the antitumoral efficacy of CAR T cells, as seen in other solid tumours models, where genetic engineering of anti-glycan CAR T cells to reduce their intracellular acidity improved the antitumoral efficacy in mouse models of hepatocellular carcinoma [278].

Another common feature of the tumour microenvironment is the reduction of oxygen availability. During homeostasis, T cells encounter a wide range of oxygen concentrations, between 3 and 19% oxygen [279], while tumour hypoxic tissue have an oxygen concentration below 2% [280]. HIF-1α is the main regulator of oxygen homeostasis in T cells. Upon infiltrating low oxygen tissues or during T cell activation, HIF-1α can dimerize with HIF-1β and translocate into the nucleus, activating HIF target genes. HIF signalling reshapes T cell metabolism, augmenting their reliance on glycolysis while reducing oxidative phosphorylation [281,282]. On CD8 T cells, HIF signalling contributes to maintaining cytotoxic activity by increasing the expression of effector molecules like Granzyme B and Perforin [5], and genetic engineering to sustain HIF-1 activity leads to an increase of accumulation of resident memory T cells, improved response to αPD-1 therapy and antitumoral control [283]. However, persistent antigen stimulation and low oxygen exposure contribute to T cell exhaustion within the TME. In vitro, the combination of hypoxia and VEGF-A promoted the differentiation of terminally exhausted-like CD8 T cells expressing PD-1, TIM-3 and CXCR3 without affecting Granzyme B, TNF-α and interferon IFN-γ production [284]. T cell dysfunction in hypoxia is partially mediated by additional factors, tumour-infiltrating T cells express a transcriptional feature similar to Tregs, increasing the expression of CD39 and reducing extracellular ATP concentrations by conversion into the immune-suppressive oncometabolite adenosine. CD39 deletion in endogenous CD8 T cells resulted in slowed tumour progression and reinforced the efficacy of αPD-1/ αCTLA-4 against melanoma mouse models [285]. Moreover, analysis in melanoma TILs in mouse models found continuous T cell activation during hypoxia drives T cell exhaustion by reducing mitochondrial activity and mTOR signalling, accumulating terminally-differentiated T cells [73], while pharmacological prevention of HIF-1α/β dimerization increases the efficacy of vaccine treatment or αPD-1 blockade on melanoma model [286].

6.4.4 Lactic acid impact on other immune compartments.

A key limitation of this study is the use of immune-deficient mice. NOD/SCID mice lack lymphoid cells and functional NK cells and have defective macrophages and dendritic cells; all these cells are fundamental components for antitumoral responses. Moreover, potential synergies between CAR T cells and MCT-1 blockade are lost in this model as high levels of lactic acid shape many immune cell compartments [287]. Interestingly, the correlation of metabolic networks and inhibitory mechanisms on tumour infiltrating immune cells are actively being explored. Tumour infiltrating regulatory T (Treg) cells which preferentially use lactate as a carbon source, have been found to overexpress inhibitory molecules and increase their suppressive potential. Both tumour-infiltrating effector T cells and Treg cells can metabolise lactate, but only Treg cells have mechanisms to regenerate NAD^+ and avoid metabolic shutdown [124,127]. Furthermore, pharmacological inhibition of MCT-1 or genetically editing this transporter on Treg cells increases the efficacy of αPD-1 treatment in mouse models [128,169].

High lactic acid impairs NK cells similarly to T cells by reducing IFN-γ release and cytotoxicity against tumour cell lines, diminishing their antitumoral potential [109]. In mouse breast cancer models, inhibition of lactate influx through MCT-4 using the small molecule 7ACC1 or MCT-4 silencing strengthens intratumorally NK functions by increasing perforin and NKG2D expression, suggesting MCT-4 is the main transporter for lactate uptake on tumour infiltrating NK cells.

Lactic acid modulates the phenotype of other immune compartments, like macrophages and dendritic cells. Culture of myeloid cells with lactic acid induces a tolerogenic phenotype on myeloid cells [111]. Increasing acidosis directly impairs monocyte differentiation into DCs in culture with IL-4, TNF-a and GM-CSF by regulating mTOR activity [288]. Additionally, the

culture of dendritic in high densities produces high levels of IL-10 and reduced capacity to induce Th1 responses, which is mediated by accumulation of lactic acid in the culture media [289]. Macrophage culture with lactic acid induced cell death and increased production of cytokines like IL-1β, IL-6, TNF-α, and CXCL8, while also increasing the production of pro-tumoral chemokine CCL2, CCL13, and CXCL5, indicating culture with lactic acid produced macrophages with a non–Th1-promoting inflammatory phenotype [290]. Macrophages express MCT-1 after 16 hours of activation with LPS and TNF-a [291], and their polarisation into an immunosuppressive phenotype is mediated by lactic acid uptake through MCT-1 [290]. Moreover, expression of MCT-1 on suppressive tumour-infiltrated macrophages correlates with decreased recurrence-free survival in breast cancer patients [292], and blocking of MCT-1 with AZD3965 reduces the expression of PD-L1 on macrophages cultured with lactic acid [293].

Furthermore, other compartments of the tumour microenvironment, like cancer-associated fibroblasts (CAFs), can shape the tumour evolution after metabolic regulation. CAFs are a key component of the cancer stroma, as they can secrete several growth factors to modify the extracellular matrix and preventing the infiltration of drugs and immune cells into the tumour niche [294]. Metabolically, CAFs sustain tumour acidosis by secreting lactic acid and providing cancer cells with additional ATP [295]. High levels of lactic acid polarise other stromal cells into CAFs [296] while simultaneously mediating CAF activation by downregulation of p62 and reduction of NAD^+ levels [297]. In models of pancreatic cancer, it was shown CAFs can upregulate MCT-1 to uptake lactate from cancer cells, enhancing CAFs proliferation, secretion of IL-6 and suppression of cytotoxic immune cell activity [298].

Taken together, the reduction of lactic acid production by MCT-1 inhibition could wider antitumoral immune benefits by reducing the TME acidity, polarising myeloid cells into a pro-inflammatory phenotype, starving Treg from an important metabolite from their function, and augmenting the cytotoxicity activity of NK and T cells.

6.4.5 Potential side effects of MCT-1 inhibition.

As MCT-1 is expressed in most tissues [299], an important concern for antitumoral therapeutic targeting is the potential side effects of blocking this transporter. Mice administrated AZD3965 by oral gavage showed reduced blood leukocyte count and spleen size [144,300]. Other groups have reported AZD3965 had minimal impact in mice at doses as high as 100 mg/kg with only transient perturbed orientation [154]. A monoclonal antibody blocking MCT-1 showed no significant side effects after weekly exposure of 50 mg/kg for 4 weeks. However, a tamoxifen-inducible MCT-1 knockout mouse had smaller testis and partial spermatid degeneration (patent WO2019136300A2).

Importantly, the data from a phase I clinical trial using AZD3965 on 51 patients had recently been published. This study found high doses of AZD3965 were well tolerated by patients, with extreme fatigue and temporary changes to the retina (catalogued as severe) as the main side effects (NCT01791595) and a rare case of one patient with hyperlactaemic acidosis after treatment, possibly due to the large tumour burden [301]. Retinal degradation was particularly important to address, as MCT-1 is the main lactate transporter in the retina serving as a lactate exporter and succinate exporter [302,303].

On the other hand, several mouse models have been developed to study CAR T cell biology and toxicities observed in patients. Infusion of αCD19-CAR T cells in patients has several adverse effects, including cytokine-release syndrome (CRS), immune effector cell-associated neurotoxicity syndrome, and B cell aplasia [304,305]. CRS is the most common acute side effect with an incidence of 42%-100% in treated patients and consists of the increase of several proinflammatory cytokines, such as IL-1, IL-6, IFN-γ and GM-CSF produced by T cells and macrophages, causing fever, nausea, vomiting, among others [306]. Meanwhile, B-cell aplasia is the most common long-term side effect of αCD19-CAR T cell therapy, present in 25–38% of

patients and persisting for several years, even after the loss of detectable CAR T cells in blood [307]. It is hard to speculate how the combination of αCD19-CAR T cell therapy and MCT-1 inhibition could interact in terms of toxicities. MCT-1 inhibition promotes cell death by apoptosis of tumour cells rather than pyroptotic cell death [151]. As pyroptotic cell death has been linked to the initial stages of CRS in patients, is possible the combination will reduce the severity of the side effects by decreasing the release of proinflammatory factors. Furthermore, MCT-1 blockade can inhibit the initial stages of T cell function, possibly further reducing the general inflammatory landscape.

Syngenetic and transgenic mouse models have been developed to recapitulate CAR T cell interactions with different immune system compartments and clinical toxicities [308]. In a transgenic mouse model expressing B-cell restricted human CD19, transference of a mouse lymphoma cell line (TBL12) and treated with αCD19 CAR T cells recapitulate the CAR T cell toxicities. These mice had dose-dependent CRS and neurotoxicity which was neutralized by blocking IFN-γ or IL-6 with monoclonal antibodies [309]. Additionally, syngenetic models, like the A20 mouse lymphoma cell line, have been used to test the efficacy of αCD19 CAR T cells. This model has been used to study the importance of immunodepletion for CAR T cell engraftment, and the recruitment of immune cells to clear cancer cells in combination with IL-12 producing CAR T cells [310].

Metabolic profile, tumour aggressiveness and immune cell phenotype are fundamentally linked, as further demonstrated by the metabolic shift in T cells after immune checkpoint therapy and the improvement of αPD-1 therapy after metabolic regulation [311]. Detailed studies on immunocompetent mouse models infused with CAR T cells interrogating how changes in the tumour metabolic landscape after MCT inhibition will lead to a deeper understanding of immune metabolism and better therapies against cancer.

6.4.6 Challenging the concept of lactate as an oncometabolite.

The view of lactic acid as a waste product and its role in modulating T cell immunity has changed dramatically in recent years. Accumulation of lactate on inflamed tissue reduces CD4 T cell mobility and allows T cell retention during injuries [119], while also as a carbon source by lung cells and Tregs [312].

The culture of CD8 T cells on modified media also gives some clues of the contribution of lactate to T cell function. Activating CD8 T cells on media with physiological carbon sources, meaning adjusting glucose, glutamine and lactate concentrations to 5, 0.5 and 2 mM respectively, shows CD8 T cells preferentially use lactate to feed the TCA cycle, with glucose being utilized for the pentose phosphate pathway instead [313]. Similarly, culture with 40 mM of lactate promoted CD8 T cells differentiation by increasing the expression of Granzyme B, Perforin, 4-1BB, ICOS and other activation molecules. Culture with lactate also suppressed glycolysis and promoted oxidative metabolism in activated CD8 T cells, profoundly altering their metabolism and expression of transcription factors, particularly HIF-1 [314]. Importantly, these effects were lactate specific, as culture with lactic acid severely suppressed CD8 T cell activation instead.

In cancer mouse models, subcutaneous injection of lactate improved the efficacy of αPD-1 treatment in melanoma and breast cancer by increasing the infiltration of CD8 T cells and their memory T cell gene signature. Culture of OT-1 T cells with lactate increased the expression of TCF1 and modulated T cell epigenetic regulation to increase stemness and reduced apoptosis, which translates into a superior antitumoral control [315]. Additionally, tumour infiltrating CD8 T cells can metabolise lactate instead of glucose and modulation of the mitochondrial pyruvate carrier 1 (MPC1) severely impaired T cell effector function in tumours but not in the spleen. During high lactate and low glucose conditions, pyruvate is preferentially produced from

lactate oxidation, therefore blocking MPC1 deprives the mitochondria of this crucial metabolite to sustain the TCA cycle. Importantly, blocking MPC1 during the later stages of PBMC activation (5 days post-culture with αCD3/αCD28 antibodies) dramatically improved human αCD19-CAR T cell therapy in B cell leukaemia animal models [86].

Blocking MCT-1 during the initial stages of T cell activation has been consistently demonstrated to be detrimental to T cell proliferation and activation; however, depending on the experimental conditions and cancer model, modulating lactate metabolism can have a plethora of unexpected effects in T cell biology. For example, MCT-1 deficiency in mouse CD8 T cells showed impaired proliferation and cytokine production, a shift to respiratory metabolism and reduced infiltration in epididymal visceral adipose tissue, reducing adipogenesis [316]. MCT-1 can also transport succinate, and tumour-derived succinate uptake by MCT-1impaired CD4 T cell effector function by inhibiting succinyl-CoA synthetase activity [317].

Local nutrient availability changes dramatically for an antitumoral T cell, with distinct local concentrations of carbon sources, amino acids and co-factors in circulation, lymph nodes, tumour stroma and during inflammation, the pharmacological blockade of MCT-1 represents an interesting strategy to target tumour cells in combination with CAR T cell, and a better understanding of the metabolic interactions between cancer cells and T cells can only lead to improved and safer cancer therapies.

6.5 ASCT-2 inhibition on CAR T cells.

Following the results obtained with MCT-1 inhibition, we explored if this strategy could be expanded to other metabolites. Inhibition of glutamine uptake on tumour cells has shown promising results on preclinical models of breast, colorectal and lung cancers [204], but initial clinical trials found unacceptable toxicities in patients. Moreover, the role of glutamine uptake and the antitumoral potential of T cells is less understood, precluding the development of combinatory treatments targeting glutamine and T cell-based immunotherapies. As ASCT-2 is the main glutamine transporter in both tumour and T cells, we explored if the combination of CAR T cells with ASCT-2 inhibitors could cooperate in treating B cell malignancies.

6.5.1 Modulating glutamine metabolism in combination with T cell immunotherapies.

To reduce some of the toxicities observed in patients treated with glutaminase inhibitors, Leone et al., developed a modified version of the glutaminase antagonist 6-diazo-5-oxo-l-norleucine (DON), which is only active on the TME. In mouse models, glutamine inhibition led to nutrient depletion in cancer cells by suppressing oxidative and glycolytic metabolism of cancer cells; meanwhile, effector T cells had increased oxidative metabolism and a long-lived, activated phenotype [201]. Additionally, V-9302 selectively blocked glutamine uptake by triple-negative breast cancer cells but not mouse OT-1 CD8 T cells. Moreover, CD8 T cells increased the expression of ATB^{0+} and glutathione synthesis, improving CD8 T cell effector function [189], suggesting the combination of glutamine inhibition and adoptive T cell therapy could synergise in cancer treatments.

In contrast with the results published by Edwards et al., culture of human CAR T cells with 20-5 uM of V-9302 severely reduced T cell viability, IFN-γ and IL-2 production in a dose-dependent manner, indicating that ASCT-2 inhibition is toxic at the concentrations commonly used on other publications. Similarly, the combination of V-9302 with αCD19-CAR T cells

did not significantly increase Raji cell killing, suggesting both treatments interfere with their antitumoral capacity. At high concentrations, V-9302 induce cell death of both tumour cells and CAR T cells, so toxicity against Raji cells in those conditions is driven primarily by ASCT-2 inhibition. In contrast, with lower concentrations of V-9302, the effect of CAR T cell killing was dominant. This T cell suppression led us to explore strategies to render αCD19 CAR T cells insensitive to ASCT-2 blockade.

Metabolic networks on mouse and human T cells are likely conserved; generally, conclusions obtained from mice data are assumed to closely resemble their human counterparts. However, few comparative studies exist directly comparing human and mouse T cell metabolic networks. For example, aerobic glycolysis has a different role in human and mouse Treg differentiation. After TCR engagement, human Treg induction and suppressive function is dependent on increasing glycolysis, which is controlled by FOXP3 and α–enolase [318]. Meanwhile, glycolysis has a pivotal role in determining Th17 and Treg fate in mice, where blocking glycolysis did not impact Treg differentiation but is critical for generating Th17 cells in HIF-1α dependant manner [319]. Key differences in glutamine utilisation have also been found between human and mouse myeloid cells. In human monocytes cultured in vitro, the differentiation of monocytes to dendritic cells or macrophages was independent of extracellular glutamine supply as they can produce endogenous glutamine by glutamine synthetase [320]. In contrast, glutamine synthetase was undetectable in murine macrophages, explaining previous reports that glutamine uptake is essential for cytokine production and phagocytic functions [321].

As strong CAR T cell inhibition was found after V-9302 blockade, we tested the plasticity of glutamine depletion on activated CAR T cells to test if T cell metabolism could be modified to render our CAR T cell resistant to αASCT-2 blockade. Glutamine was reduced after T cell transduction instead of during the initial of the culture, as reducing glutamine during the initial stages of T cell activation could reduce T cell proliferation and impair retroviral transductions,

as this viral particles can only insert their genetic package on active proliferating cells [322]. Culture of CAR T cells with no glutamine provided some resistance to V-9302 inhibition. At 10 μM of the small molecule, a 45% IFN-γ production reduction was observed after culturing CAR T cells with no glutamine compared to a 70-80% reduction in cultures with 0.2 – 2 mM of glutamine, suggesting CAR T cells have some plasticity to resist glutamine depravation. However, increasing the concentrations of V-9302 eliminated this protection, and by 20 μM no live cells were detected. With these results, we decided to genetically engineer CAR T cells to express surrogate glutamine transporters instead of further modifying T cells media.

6.5.2 Expression of surrogate glutamine transporters.

Among the transporters analysed for ASCT-2 substitution, expression of ATB^{0+} showed a better viability increase on transduced T cells and activated CAR T cells compared to expression of SNAT-1 or SNAT-2. It is possible forcing the expression of ATB^{0+} on human T cells recapitulates the results obtained in mouse OT-I T cells [189], suggesting ATB^{0+} is a suitable candidate to replace ASCT-2 function on human T cells. ATB^{0+} is overexpressed in several cancers, as it transports all neutral and basic amino acids [323], while SNAT-1 and SNAT-2 transport mainly neutral amino acids [68]. Experiments on glutamine-deprived tumour cells showed proliferation and mTOR activity can be sustained by expressing arginine transporters SLC7A3 or asparagine supplementation [180,324]. ATB^{0+} expression could not only allow normal flux of glutamine but also increases in the availability of additional amino acids, like asparagine and arginine, sustaining the TCA cycle in absence of glutamine.

Interestingly, we found the constructs expressing the transporters followed by an IRES sequence and GFP had better results than vectors expressing RQR8 followed by a 2A cleavage peptide and the transporters. Research comparing bi- and tri-cistronic vectors has shown the cleavage efficiency of 2A peptides varies depending on the cell line and gene being expressed

[325]. A western blot comparing the protein expression of both constructs could elucidate if the differences observed are explained by differences in expression. The combination of V-9302 and CAR T cells transduced to express ATB^{0+} offers a therapeutic opportunity to generate non-glutamine addicted T cells. A better characterisation of the biological and metabolic impact of ATB^{0+} forced expression and experiments in animal models to test the synergy between V-9302 and CAR T cells are necessary to explore their therapeutic potential.

6.5.3 ASCT-2 blocking antibodies.

To reduce the potential toxicities of ASCT-2 inhibition, we sought to expand this strategy by studying ASCT-2 blocking monoclonal antibodies. Systemic glutamine-neutralisation by glutaminase inhibitors had unacceptable gastrointestinal toxicities [326] and off-target toxicity is a common feature of small molecules developed for cancer research [327,328] Therefore, T cells producing monoclonal antibodies could provide local administration of targeted drugs without the limitations of small molecules.

We tested 3 monoclonal antibodies against ASCT-2 from Kyowa Hakko Kirin Co., Ltd. We found these αASCT-2 antibodies can stain Raji cells and reduce their proliferation by 40% at a concentration of 10 μg/mL, comparable to using 10 μM of V-9302, suggesting the antibodies can neutralise glutamine in these conditions. However, no significant differences in activated αCD19-CAR T cells proliferation or IFN-γ release were found, indicating the blocking ASCT-2 with antibodies is insufficient to impact CAR T cell effector functions. The reduction in viability of CAR T cells with V-9302 but not with antibodies has several explanations. For instance, ASCT-2 can be expressed on the mitochondria and other organelles to facilitate glutamine uptake, so V-9302 could target ASCT-2 expressed in intracellular organelles that neutralising antibodies do not have access to [329].

Suzuki et al. and Osanai-Sasakawa. et al. used gastric cancer cell lines cultured in media with reduced glutamine (0.2 mM) while the standard culture media have 2 mM of glutamine. At 10 μg/mL, the antibodies reduced the viability of ASCT-2^{high} tumour cell lines by 50% [207]. We tested the antibodies with Raji cells at standard glutamine conditions and using 5-10 ug/mL of the antibodies, finding a similar reduction in viability. Raji cells have increased metabolism compared to other cell lines and they are heavily glutamine-reliant in vitro [246], so we hypothesised this cancer cells would be more sensitive to a partial reduction of glutamine availability compared to activated CAR T cells.

The sensitivity of Raji and CAR T cells to V-9302 but not to monoclonal antibodies could have other explanations. SLC1A5-knockdown in HNSCC cell lines treated with V-9302 had reduced glutamine metabolism in vivo and in vitro, suggesting this small molecule targets other glutamine transporters [330], like SLC38A2 (SNAT-2) and SLC7A5 (LAT-1) expressed in cancer cells [331]. Therefore, V-9302 can exerts a broader glutamine transport disruption compared to αASCT-2 antibodies, explaining their potent immunosuppressive effects of V-9302 on CAR T cells cultured in vitro.

Additionally, under hypoxia, cancer cells can express an alternative variant of ASCT-2 which localise in the mitochondria. This enhances glutamine uptake in the mitochondria, feeding the TCA cycle and promoting the production of glutathione (GSH) [329]. GSH is a tripeptide composed of glutamate, glycine, and cysteine with potent antioxidant capacities. Several glutamine-addictive tumour cells use glutamine for GSH synthesis, protecting tumour cells from cell dead triggered by reactive oxygen species (ROS) DNA damage [332]. V-9302 can permeate the plasma membrane and could access ASCT-2 expressed in the mitochondria, further impeding glutamine catabolism in ways αASCT-2 antibodies do not have access to.

6.5.4 Glutamine inhibition in the TME.

Several clinical trials are ongoing testing modulating glutamine metabolism against solid tumours. For example, the combination of the glutaminase inhibitor CB-839 has been tested in combination with Nivolumab as a treatment for melanoma, renal cell carcinoma (RCC), and NSCLC (NCT02771626), and various animal models have shown the benefit of combining glutamine inhibitors with immune checkpoint blockade therapy.

However, glutamine inhibition has some contradictory evidence in animal models. In the triple-negative breast cancer model E0771, systemic ASCT-2 inhibition with V-9302 suppressed tumour growth and increased T lymphocyte activation [189]. However, in a murine colorectal cancer model, injection of V-9302 induced increased PD-L1 expression in cancer cells. V-9302 or αPD-L1 antibody did not control the growth of CT26 tumour cells in immunocompetent mice, but the combination significantly reduced tumour growth by inducing cancer cells death and increasing the influx of CD8 T cells [191]. Glutaminase inhibition with JHU083 induced tumour regression in the colorectal cancer mouse model MC38 by shutting down tumour metabolism and rewiring CD8 T cell metabolism to replenish TCA intermediaries with other metabolites, like acetate [201]. Meanwhile, Kras mutated adenocarcinoma models had increased glutamine uptake and glutaminase inhibition with CB-839 reduced the number of effector CD8 T cells and their clonal expansion [200].

Glutamine inhibition has a plethora of effects on several immune compartments that could explain the differences in these tumour models. ASCT-2 deficient models have shown this transporter is critical for the development of Th1 and Th17 CD4 T cells but not for Th2 or Tregs, as glutamine-derived α-ketoglutarate decreases IFN-y production and Tbet expression [66]. In contrast, NK cells are less glutamine-dependant, as in vitro culture in glutamine-free media does not impact NK cells OXPHOS, but glutamine export by SLC7A5 (LAT1) is critical

for sustaining c-Myc and mTOR activity, suggesting maintaining glutamine homeostasis regulates NK activation signals [184]. Glutamine availability can also regulate myeloid fate in tumour-infiltrated macrophages. Glutamine deprivation decreased M2 polarization and production of chemokine CCL22, while M1 macrophages express an active variant of the aspartate-arginosuccinate shunt and can compensate for the lack of glutamine in the environment [333]. In a breast cancer mouse model, blocking glutamine metabolism with JHU-083 induced primary tumour regression and reduced lung metastasis by reducing the infiltration of myeloid-derived suppressor cells, reprogramming macrophages into an inflammatory phenotype and increasing cross-presentation to T cells [187]. Meanwhile, glutamine-deprivation promotes CAFs migration [334] and they can sustain cancer cells proliferation by providing exogenous glutamine [335]. Metabolomics analysis has shown that cancer and immune cells engage in metabolic partitioning, with cancer cells preferentially consuming glutamine, while myeloid cells uptake an important percentage of glucose. Modifying glutamine availability would severely hinder cancer cell metabolism and reshape the TME [336], developing a favourable niche for T cells antitumoral functions.

6.5.5 Production of glutamine-resistant CAR T cells.

Additional strategies to render glutamine-resistant CAR T cells could involve the development of single-domain antibodies (nanobodies). Nanobodies are becoming a powerful tool to target metabolic transporters; nanobodies are smaller (12–15 kDa and 2.5 nm × 4 nm), and the generally more convex binding site allows them to target epitopes less accessible to conventional antibodies. Therefore, nanobodies have the potential to produce molecules against cell membrane transporters, with higher affinities and stability suitable for clinical use [337]. The smaller size allows them to infiltrate tissues otherwise inaccessible for regular antibodies. For example, a nanobody targeting the ATP-binding cassette sub-family C member 3 (ABCC3) was recently developed for glioblastoma treatment [338]. ABCC3 transport organic

anions, like glutathione and glucuronide, but it has also been associated with tumour chemoresistance, as the expression of ABCC transporters reduced the intracellular retention of anti-cancer agents in several malignancies [339,340]. Nanobodies against ABCC3 were able to cross the blood–brain barrier, normally inaccessible for most therapeutic antibodies, and infiltrate orthotopically implanted glioblastoma tumours [338]. Nanobodies have also been used to modulate the enzymatic activity of CD38 [341], a NAD^+-hydrolyzing ecto-enzyme present in B cells and NK cells. CD38 hydrolyses NAD^+ as part of the pathway to adenosine, a known immunosuppressive onco-metabolite [342]. Therefore, nanobodies targeting metabolic transporters hold substantial potential for the next generation of metabolic-regulating immunotherapies.

Metabolic plasticity after glutamine inhibition is a common feature of tumour cells. A frequent mechanism to resist glutamine addiction in tumour cells and T cells is overexpressing enzymes involved in pyruvate metabolism, like pyruvate carboxylate (PC) [201,343,344]. These enzymes can fuel the TCA and compensate for the lack of glutamine by producing oxalacetate, expressing PC at the beginning of T cell activation, before T cells have the chance to become glutamine-addicted, could imprint them a phenotype resistant to glutamine inhibition. Additionally, pancreatic ductal adenocarcinoma treated with the glutaminase inhibitor CB-839 adapted their metabolism in vivo by engaging in fatty acid and lipid metabolism to overcome glutamine inhibition [345]. Tumour cells can also uptake alternative amino acid transporters after glutamine depletion, like the aspartate/glutamate transporter SLC1A3, which can feed the TCA cycle and maintain nucleotide synthesis under glutamine deprivation by metabolising aspartate [346]. Learning about the metabolic adaptability of cancer cells could allow exploiting this resistance mechanism for targeted therapies, and the genetic engineering of T to overcome glutamine addiction could be interesting approaches to apply for CAR T cell therapies.

7. Conclusions.

In this work, he showed CD19-specific CAR T express high levels of the lactate transporters MCT-1 and MCT-4 upon activation with tumour cells expressing CD19 and pharmacological inhibition of MCT-1 did not impact the expression of lactate transporters on T cells. Additionally, CAR T cells did not accumulate lactic acid intracellularly after incubation with MCT-1i, which supports the hypothesis that CAR T cells and MCT-1 blockade could cooperate against B cell malignancies.

MCT-1 inhibition induced metabolic re-arrangement on activated CAR T cells by diminishing glycolytic pathways engagement, increasing respiration, and slightly increasing mitochondrial potential. However, no differences in T cell phenotype were observed measured by expression of activation markers 4-1BB, OX40, CD69 and Granzyme B. Release of inflammatory molecules IFN-γ or IL-2 and in vitro memory phenotype profile was unaffected by MCT-1 blockade. Furthermore, the combination of CAR T cells with MCT-1 inhibition increased the killing of tumour cells by 50% compared to CAR T cells alone. Importantly, dual inhibition with syrosingopine severely impairs CAR T cell activation, suggesting MCT-1 and MCT-4 are utilised to lactate export on CAR T cells.

We confirm that daily injection of 5 mg/kg AR-C155858 efficiently controls the tumour growth on a model of B cell leukaemia NALM-6 without any apparent side effects. Moreover, the combination of αCD19-CAR T cells with MCT-1 blockade significantly improved the killing of tumour cells and increased CAR T cell antitumoral control in mouse models compared to each treatment alone, confirming the conclusions on the in vitro cytotoxicity experiments. Additionally, αCD19-CAR T cell phenotype measured by expression of 4-1BB, ICOS, PD-1, Ki67, IFN-γ, IL-2 and LAMP-1 remained the same on T cells transferred on tumour-bearing

mice injected for 7 days with AR-C155858, corroborating MCT-1 inhibition did not impact CAR T cell phenotype in vivo or in vitro.

In summary, the pharmacological blockade of MCT-1 selectively impairs B cell tumour growth without hindering CD19-specific CAR T cell antitumoral potential, making combining both treatments an interesting approach against B cell malignancies.

We found that inhibiting glutamine uptake through ASCT-2 on αCD19-CAR T cells using a small molecule V-9302 impacted CAR T cell effector functions. At 10 μM, IFN-γ and IL-2 production was reduced by 50% while not cooperating in killing Raji cells, indicating inhibition of glutamine uptake though ASCT-2 is detrimental to CAR T cell antitumoral function. These results contrast with similar studies using mouse T cells, as they are insensitive to V-9302 blockade. We tested if overexpression of amino acid transporters SNAT-1, SNAT-2, ASCT-2 mouse or ATB^{0+} could surrogate glutamine uptake after ASCT-2 inhibition. Increased viability on resting T cells and activated CAR T cells expressing ATB^{0+} was found, indicating this construct is the best candidate for a combination of ASCT-2 inhibition with CAR T cell therapy.

To address the limitations of using small molecules to block metabolic transporters in clinical settings, we tested 3 different glutamine-neutralizing αASCT-2 antibodies on Raji cells and CAR T cells. αASCT-2 V12 antibody reduced the viability of Raji cells by 40% at 1 μg/mL and was, therefore, the best antibody candidate. However, any of the antibodies tested reduced CAR T cell viability or IFN-γ production, indicating that at the conditions and concentrations tested, αASCT-2 did not neutralize enough glutamine uptake to impact CAR T cell survival.

Taken together, this work highlights the potential of selective targeting cancer metabolism via blockade of metabolic transporters in combination with CAR T cells therapies.

8. Future perspectives.

Given the limited efficacy against solid tumours, the first strategies to improve CAR T cell efficacy focused on modifying the tumour microenvironment by directly disrupting inhibitory signals. However, T cell metabolism, a fundamental component of T cell immunity, was comparatively neglected.

Recent studies have demonstrated the intersection between tumour and T cell phenotype and metabolic networks, and several articles have shown modifying T cell metabolism can increase antitumoral potential. Additionally, recent advances in single-cell genomics and metabolomics allow categorizing tumours according to their metabolic characteristics, coming one step closer to developing personalized therapies.

In the context of this work, as metabolic transporters can be targeted by small molecules or antibodies, innovative and safe treatments have been recently tested in pre-clinical models and clinical trials. The clinical trial blocking MCT-1 showed good tolerability in patients with solid tumours; unfortunately, MCT expression was not assessed in all patients, and no patients with B cell malignancies were treated, limiting the efficacy of this drug. Future clinical trials targeting MCT-1 restricted tumours and the combination with CAR T cells hold great potential for cancer treatment.

Additionally, T cell tolerability to glutamine restriction seems to vary according to tumour type and species. This work suggests human T cells cannot adapt to ASCT-2 inhibition with the same mechanisms as mouse T cells. Understanding T cell dependency on different amino acids within the TME and designing strategies to overcome T cell metabolic restrictions while targeting tumour cells is an exciting and growing research field with exceptional translational possibilities.

9. References.

1 Shah, K., Al-Haidari, A., Sun, J. & Kazi, J. U. T cell receptor (TCR) signaling in health and disease. *Signal Transduct Target Ther* **6**, 412 (2021). https://doi.org:10.1038/s41392-021-00823-w

2 Courtney, A. H., Lo, W. L. & Weiss, A. TCR Signaling: Mechanisms of Initiation and Propagation. *Trends Biochem Sci* **43**, 108-123 (2018). https://doi.org:10.1016/j.tibs.2017.11.008

3 Jacobs, S. R., Michalek, R. D. & Rathmell, J. C. IL-7 is essential for homeostatic control of T cell metabolism in vivo. *J Immunol* **184**, 3461-3469 (2010). https://doi.org:10.4049/jimmunol.0902593

4 Menk, A. V. *et al.* Early TCR Signaling Induces Rapid Aerobic Glycolysis Enabling Distinct Acute T Cell Effector Functions. *Cell Rep* **22**, 1509-1521 (2018). https://doi.org:10.1016/j.celrep.2018.01.040

5 Finlay, D. K. *et al.* PDK1 regulation of mTOR and hypoxia-inducible factor 1 integrate metabolism and migration of CD8+ T cells. *J Exp Med* **209**, 2441-2453 (2012). https://doi.org:10.1084/jem.20112607

6 Angela, M. *et al.* Fatty acid metabolic reprogramming via mTOR-mediated inductions of PPARgamma directs early activation of T cells. *Nat Commun* **7**, 13683 (2016). https://doi.org:10.1038/ncomms13683

7 Shyer, J. A., Flavell, R. A. & Bailis, W. Metabolic signaling in T cells. *Cell Res* **30**, 649-659 (2020). https://doi.org:10.1038/s41422-020-0379-5

8 Apicella, M. *et al.* Increased Lactate Secretion by Cancer Cells Sustains Non-cell-autonomous Adaptive Resistance to MET and EGFR Targeted Therapies. *Cell Metab* **28**, 848-865 e846 (2018). https://doi.org:10.1016/j.cmet.2018.08.006

9 Sinclair, L. V. *et al.* Control of amino-acid transport by antigen receptors coordinates the metabolic reprogramming essential for T cell differentiation. *Nat Immunol* **14**, 500-508 (2013). https://doi.org:10.1038/ni.2556

10 Ananieva, E. A., Powell, J. D. & Hutson, S. M. Leucine Metabolism in T Cell Activation: mTOR Signaling and Beyond. *Adv Nutr* **7**, 798S-805S (2016). https://doi.org:10.3945/an.115.011221

11 Herzig, S. & Shaw, R. J. AMPK: guardian of metabolism and mitochondrial homeostasis. *Nat Rev Mol Cell Biol* **19**, 121-135 (2018). https://doi.org:10.1038/nrm.2017.95

12 O'Sullivan, D. The metabolic spectrum of memory T cells. *Immunol Cell Biol* **97**, 636-646 (2019). https://doi.org:10.1111/imcb.12274

13 Liu, Q., Sun, Z. & Chen, L. Memory T cells: strategies for optimizing tumor immunotherapy. *Protein Cell* **11**, 549-564 (2020). https://doi.org:10.1007/s13238-020-00707-9

14 Dafni, U. *et al.* Efficacy of adoptive therapy with tumor-infiltrating lymphocytes and recombinant interleukin-2 in advanced cutaneous melanoma: a systematic review and meta-analysis. *Ann Oncol* **30**, 1902-1913 (2019). https://doi.org:10.1093/annonc/mdz398

15 van den Berg, J. H. *et al.* Tumor infiltrating lymphocytes (TIL) therapy in metastatic melanoma: boosting of neoantigen-specific T cell reactivity and long-term follow-up. *J Immunother Cancer* **8** (2020). https://doi.org:10.1136/jitc-2020-000848

16 Guo, J. *et al.* Eradicating tumor in a recurrent cervical cancer patient with autologous tumor-infiltrating lymphocytes and a modified lymphodepleting regimen. *J Immunother Cancer* **10** (2022). https://doi.org:10.1136/jitc-2021-003887

17 Duhen, T. *et al.* Co-expression of CD39 and CD103 identifies tumor-reactive CD8 T cells in human solid tumors. *Nat Commun* **9**, 2724 (2018). https://doi.org:10.1038/s41467-018-05072-0

18 Fernandez-Poma, S. M. *et al.* Expansion of Tumor-Infiltrating CD8(+) T cells Expressing PD-1 Improves the Efficacy of Adoptive T-cell Therapy. *Cancer Res* **77**, 3672-3684 (2017). https://doi.org:10.1158/0008-5472.CAN-17-0236
19 Morad, G., Helmink, B. A., Sharma, P. & Wargo, J. A. Hallmarks of response, resistance, and toxicity to immune checkpoint blockade. *Cell* **184**, 5309-5337 (2021). https://doi.org:10.1016/j.cell.2021.09.020
20 Zhao, Y. *et al.* Tumor Infiltrating Lymphocyte (TIL) Therapy for Solid Tumor Treatment: Progressions and Challenges. *Cancers (Basel)* **14** (2022). https://doi.org:10.3390/cancers14174160
21 Zacharakis, N. *et al.* Immune recognition of somatic mutations leading to complete durable regression in metastatic breast cancer. *Nat Med* **24**, 724-730 (2018). https://doi.org:10.1038/s41591-018-0040-8
22 Creelan, B. C. *et al.* Tumor-infiltrating lymphocyte treatment for anti-PD-1-resistant metastatic lung cancer: a phase 1 trial. *Nat Med* **27**, 1410-1418 (2021). https://doi.org:10.1038/s41591-021-01462-y
23 Tran, E. *et al.* T-Cell Transfer Therapy Targeting Mutant KRAS in Cancer. *N Engl J Med* **375**, 2255-2262 (2016). https://doi.org:10.1056/NEJMoa1609279
24 Goff, S. L. *et al.* Tumor infiltrating lymphocyte therapy for metastatic melanoma: analysis of tumors resected for TIL. *J Immunother* **33**, 840-847 (2010). https://doi.org:10.1097/CJI.0b013e3181f05b91
25 Baulu, E., Gardet, C., Chuvin, N. & Depil, S. TCR-engineered T cell therapy in solid tumors: State of the art and perspectives. *Sci Adv* **9**, eadf3700 (2023). https://doi.org:10.1126/sciadv.adf3700
26 Zhu, Y., Qian, Y., Li, Z., Li, Y. & Li, B. Neoantigen-reactive T cell: An emerging role in adoptive cellular immunotherapy. *MedComm (2020)* **2**, 207-220 (2021). https://doi.org:10.1002/mco2.41
27 Foy, S. P. *et al.* Non-viral precision T cell receptor replacement for personalized cell therapy. *Nature* **615**, 687-696 (2023). https://doi.org:10.1038/s41586-022-05531-1
28 Middleton, D., Menchaca, L., Rood, H. & Komerofsky, R. New allele frequency database: http://www.allelefrequencies.net. *Tissue Antigens* **61**, 403-407 (2003). https://doi.org:10.1034/j.1399-0039.2003.00062.x
29 Shafer, P., Kelly, L. M. & Hoyos, V. Cancer Therapy With TCR-Engineered T Cells: Current Strategies, Challenges, and Prospects. *Front Immunol* **13**, 835762 (2022). https://doi.org:10.3389/fimmu.2022.835762
30 Brocker, T. & Karjalainen, K. Signals through T cell receptor-zeta chain alone are insufficient to prime resting T lymphocytes. *J Exp Med* **181**, 1653-1659 (1995). https://doi.org:10.1084/jem.181.5.1653
31 Weinkove, R., George, P., Dasyam, N. & McLellan, A. D. Selecting costimulatory domains for chimeric antigen receptors: functional and clinical considerations. *Clin Transl Immunology* **8**, e1049 (2019). https://doi.org:10.1002/cti2.1049
32 Cooper, L. J. *et al.* Development and application of CD19-specific T cells for adoptive immunotherapy of B cell malignancies. *Blood Cells Mol Dis* **33**, 83-89 (2004). https://doi.org:10.1016/j.bcmd.2004.03.003
33 Chavez, J. C., Bachmeier, C. & Kharfan-Dabaja, M. A. CAR T-cell therapy for B-cell lymphomas: clinical trial results of available products. *Ther Adv Hematol* **10**, 2040620719841581 (2019). https://doi.org:10.1177/2040620719841581
34 Nie, Y. *et al.* Mechanisms underlying CD19-positive ALL relapse after anti-CD19 CAR T cell therapy and associated strategies. *Biomark Res* **8**, 18 (2020). https://doi.org:10.1186/s40364-020-00197-1

35 Zhang, X. *et al.* Efficacy and safety of anti-CD19 CAR T-cell therapy in 110 patients with B-cell acute lymphoblastic leukemia with high-risk features. *Blood Adv* **4**, 2325-2338 (2020). https://doi.org:10.1182/bloodadvances.2020001466
36 Schuster, S. J. *et al.* Tisagenlecleucel in Adult Relapsed or Refractory Diffuse Large B-Cell Lymphoma. *N Engl J Med* **380**, 45-56 (2019). https://doi.org:10.1056/NEJMoa1804980
37 Neelapu, S. S. *et al.* Axicabtagene Ciloleucel CAR T-Cell Therapy in Refractory Large B-Cell Lymphoma. *N Engl J Med* **377**, 2531-2544 (2017). https://doi.org:10.1056/NEJMoa1707447
38 Xu, X. *et al.* Mechanisms of Relapse After CD19 CAR T-Cell Therapy for Acute Lymphoblastic Leukemia and Its Prevention and Treatment Strategies. *Front Immunol* **10**, 2664 (2019). https://doi.org:10.3389/fimmu.2019.02664
39 Cheng, J. *et al.* Understanding the Mechanisms of Resistance to CAR T-Cell Therapy in Malignancies. *Front Oncol* **9**, 1237 (2019). https://doi.org:10.3389/fonc.2019.01237
40 Braendstrup, P., Levine, B. L. & Ruella, M. The long road to the first FDA-approved gene therapy: chimeric antigen receptor T cells targeting CD19. *Cytotherapy* **22**, 57-69 (2020). https://doi.org:10.1016/j.jcyt.2019.12.004
41 Perales, M. A. *et al.* Role of CD19 Chimeric Antigen Receptor T Cells in Second-Line Large B Cell Lymphoma: Lessons from Phase 3 Trials. An Expert Panel Opinion from the American Society for Transplantation and Cellular Therapy. *Transplant Cell Ther* **28**, 546-559 (2022). https://doi.org:10.1016/j.jtct.2022.06.019
42 Munshi, N. C. *et al.* Idecabtagene Vicleucel in Relapsed and Refractory Multiple Myeloma. *N Engl J Med* **384**, 705-716 (2021). https://doi.org:10.1056/NEJMoa2024850
43 Mardiana, S. & Gill, S. CAR T Cells for Acute Myeloid Leukemia: State of the Art and Future Directions. *Front Oncol* **10**, 697 (2020). https://doi.org:10.3389/fonc.2020.00697
44 Zhang, C. *et al.* Phase I Escalating-Dose Trial of CAR-T Therapy Targeting CEA(+) Metastatic Colorectal Cancers. *Mol Ther* **25**, 1248-1258 (2017). https://doi.org:10.1016/j.ymthe.2017.03.010
45 Ahmed, N. *et al.* Human Epidermal Growth Factor Receptor 2 (HER2) -Specific Chimeric Antigen Receptor-Modified T Cells for the Immunotherapy of HER2-Positive Sarcoma. *J Clin Oncol* **33**, 1688-1696 (2015). https://doi.org:10.1200/JCO.2014.58.0225
46 Straathof, K. *et al.* Antitumor activity without on-target off-tumor toxicity of GD2-chimeric antigen receptor T cells in patients with neuroblastoma. *Sci Transl Med* **12** (2020). https://doi.org:10.1126/scitranslmed.abd6169
47 Louis, C. U. *et al.* Antitumor activity and long-term fate of chimeric antigen receptor-positive T cells in patients with neuroblastoma. *Blood* **118**, 6050-6056 (2011). https://doi.org:10.1182/blood-2011-05-354449
48 Feng, K. *et al.* Chimeric antigen receptor-modified T cells for the immunotherapy of patients with EGFR-expressing advanced relapsed/refractory non-small cell lung cancer. *Sci China Life Sci* **59**, 468-479 (2016). https://doi.org:10.1007/s11427-016-5023-8
49 O'Rourke, D. M. *et al.* A single dose of peripherally infused EGFRvIII-directed CAR T cells mediates antigen loss and induces adaptive resistance in patients with recurrent glioblastoma. *Sci Transl Med* **9** (2017). https://doi.org:10.1126/scitranslmed.aaa0984
50 Whilding, L. M. *et al.* CAR T-Cells Targeting the Integrin alphavbeta6 and Co-Expressing the Chemokine Receptor CXCR2 Demonstrate Enhanced Homing and Efficacy against Several Solid Malignancies. *Cancers (Basel)* **11** (2019). https://doi.org:10.3390/cancers11050674
51 Craddock, J. A. *et al.* Enhanced tumor trafficking of GD2 chimeric antigen receptor T cells by expression of the chemokine receptor CCR2b. *J Immunother* **33**, 780-788 (2010). https://doi.org:10.1097/CJI.0b013e3181ee6675
52 Caruana, I. *et al.* Heparanase promotes tumor infiltration and antitumor activity of CAR-redirected T lymphocytes. *Nat Med* **21**, 524-529 (2015). https://doi.org:10.1038/nm.3833

53 Liu, H. *et al.* CD19-specific CAR T Cells that Express a PD-1/CD28 Chimeric Switch-Receptor are Effective in Patients with PD-L1-positive B-Cell Lymphoma. *Clin Cancer Res* **27**, 473-484 (2021). https://doi.org:10.1158/1078-0432.CCR-20-1457
54 Choi, B. D. *et al.* CRISPR-Cas9 disruption of PD-1 enhances activity of universal EGFRvIII CAR T cells in a preclinical model of human glioblastoma. *J Immunother Cancer* **7**, 304 (2019). https://doi.org:10.1186/s40425-019-0806-7
55 Hosseinkhani, N. *et al.* Immune Checkpoints and CAR-T Cells: The Pioneers in Future Cancer Therapies? *Int J Mol Sci* **21** (2020). https://doi.org:10.3390/ijms21218305
56 Barros, L. R. C. *et al.* Systematic Review of Available CAR-T Cell Trials around the World. *Cancers (Basel)* **14** (2022). https://doi.org:10.3390/cancers14112667
57 Shi, D. *et al.* Chimeric Antigen Receptor-Glypican-3 T-Cell Therapy for Advanced Hepatocellular Carcinoma: Results of Phase I Trials. *Clin Cancer Res* **26**, 3979-3989 (2020). https://doi.org:10.1158/1078-0432.CCR-19-3259
58 Sun, H. *et al.* Long term complete response of advanced hepatocellular carcinoma to glypican-3 specific chimeric antigen receptor T-Cells plus sorafenib, a case report. *Front Immunol* **13**, 963031 (2022). https://doi.org:10.3389/fimmu.2022.963031
59 Hanahan, D. & Weinberg, R. A. Hallmarks of cancer: the next generation. *Cell* **144**, 646-674 (2011). https://doi.org:10.1016/j.cell.2011.02.013
60 Warburg, O., Wind, F. & Negelein, E. The Metabolism of Tumors in the Body. *J Gen Physiol* **8**, 519-530 (1927). https://doi.org:10.1085/jgp.8.6.519
61 Shestov, A. A. *et al.* Quantitative determinants of aerobic glycolysis identify flux through the enzyme GAPDH as a limiting step. *Elife* **3** (2014). https://doi.org:10.7554/eLife.03342
62 Vander Heiden, M. G., Cantley, L. C. & Thompson, C. B. Understanding the Warburg effect: the metabolic requirements of cell proliferation. *Science* **324**, 1029-1033 (2009). https://doi.org:10.1126/science.1160809
63 Siska, P. J. *et al.* Mitochondrial dysregulation and glycolytic insufficiency functionally impair CD8 T cells infiltrating human renal cell carcinoma. *JCI Insight* **2** (2017). https://doi.org:10.1172/jci.insight.93411
64 Lim, A. R., Rathmell, W. K. & Rathmell, J. C. The tumor microenvironment as a metabolic barrier to effector T cells and immunotherapy. *Elife* **9** (2020). https://doi.org:10.7554/eLife.55185
65 Chang, C. H. *et al.* Metabolic Competition in the Tumor Microenvironment Is a Driver of Cancer Progression. *Cell* **162**, 1229-1241 (2015). https://doi.org:10.1016/j.cell.2015.08.016
66 Nakaya, M. *et al.* Inflammatory T cell responses rely on amino acid transporter ASCT2 facilitation of glutamine uptake and mTORC1 kinase activation. *Immunity* **40**, 692-705 (2014). https://doi.org:10.1016/j.immuni.2014.04.007
67 Geiger, R. *et al.* L-Arginine Modulates T Cell Metabolism and Enhances Survival and Anti-tumor Activity. *Cell* **167**, 829-842 e813 (2016). https://doi.org:10.1016/j.cell.2016.09.031
68 Wang, W. & Zou, W. Amino Acids and Their Transporters in T Cell Immunity and Cancer Therapy. *Mol Cell* **80**, 384-395 (2020). https://doi.org:10.1016/j.molcel.2020.09.006
69 Wu, H. *et al.* T-cells produce acidic niches in lymph nodes to suppress their own effector functions. *Nat Commun* **11**, 4113 (2020). https://doi.org:10.1038/s41467-020-17756-7
70 Apostolova, P. & Pearce, E. L. Lactic acid and lactate: revisiting the physiological roles in the tumor microenvironment. *Trends Immunol* **43**, 969-977 (2022). https://doi.org:10.1016/j.it.2022.10.005
71 Zhang, L. *et al.* Mitochondria dysfunction in CD8+ T cells as an important contributing factor for cancer development and a potential target for cancer treatment: a review. *J Exp Clin Cancer Res* **41**, 227 (2022). https://doi.org:10.1186/s13046-022-02439-6
72 Li, W. & Zhang, L. Rewiring Mitochondrial Metabolism for CD8(+) T Cell Memory Formation and Effective Cancer Immunotherapy. *Front Immunol* **11**, 1834 (2020). https://doi.org:10.3389/fimmu.2020.01834

73 Scharping, N. E. *et al.* The Tumor Microenvironment Represses T Cell Mitochondrial Biogenesis to Drive Intratumoral T Cell Metabolic Insufficiency and Dysfunction. *Immunity* **45**, 374-388 (2016). https://doi.org:10.1016/j.immuni.2016.07.009
74 Yu, Y. R. *et al.* Disturbed mitochondrial dynamics in CD8(+) TILs reinforce T cell exhaustion. *Nat Immunol* **21**, 1540-1551 (2020). https://doi.org:10.1038/s41590-020-0793-3
75 Cascone, T. *et al.* Increased Tumor Glycolysis Characterizes Immune Resistance to Adoptive T Cell Therapy. *Cell Metab* **27**, 977-987 e974 (2018). https://doi.org:10.1016/j.cmet.2018.02.024
76 Kawalekar, O. U. *et al.* Distinct Signaling of Coreceptors Regulates Specific Metabolism Pathways and Impacts Memory Development in CAR T Cells. *Immunity* **44**, 380-390 (2016). https://doi.org:10.1016/j.immuni.2016.01.021
77 Chen, G. M. *et al.* Integrative Bulk and Single-Cell Profiling of Premanufacture T-cell Populations Reveals Factors Mediating Long-Term Persistence of CAR T-cell Therapy. *Cancer Discov* **11**, 2186-2199 (2021). https://doi.org:10.1158/2159-8290.CD-20-1677
78 Bai, Z. *et al.* Single-cell multiomics dissection of basal and antigen-specific activation states of CD19-targeted CAR T cells. *J Immunother Cancer* **9** (2021). https://doi.org:10.1136/jitc-2020-002328
79 Sukumar, M. *et al.* Inhibiting glycolytic metabolism enhances CD8+ T cell memory and antitumor function. *J Clin Invest* **123**, 4479-4488 (2013). https://doi.org:10.1172/JCI69589
80 Greco, B. *et al.* Disrupting N-glycan expression on tumor cells boosts chimeric antigen receptor T cell efficacy against solid malignancies. *Sci Transl Med* **14**, eabg3072 (2022). https://doi.org:10.1126/scitranslmed.abg3072
81 Wang, T. *et al.* Inosine is an alternative carbon source for CD8(+)-T-cell function under glucose restriction. *Nat Metab* **2**, 635-647 (2020). https://doi.org:10.1038/s42255-020-0219-4
82 Song, M. *et al.* IRE1alpha-XBP1 controls T cell function in ovarian cancer by regulating mitochondrial activity. *Nature* **562**, 423-428 (2018). https://doi.org:10.1038/s41586-018-0597-x
83 Buck, M. D. *et al.* Mitochondrial Dynamics Controls T Cell Fate through Metabolic Programming. *Cell* **166**, 63-76 (2016). https://doi.org:10.1016/j.cell.2016.05.035
84 van Bruggen, J. A. C. *et al.* Chronic lymphocytic leukemia cells impair mitochondrial fitness in CD8(+) T cells and impede CAR T-cell efficacy. *Blood* **134**, 44-58 (2019). https://doi.org:10.1182/blood.2018885863
85 Weber, E. W. *et al.* Transient rest restores functionality in exhausted CAR-T cells through epigenetic remodeling. *Science* **372** (2021). https://doi.org:10.1126/science.aba1786
86 Wenes, M. *et al.* The mitochondrial pyruvate carrier regulates memory T cell differentiation and antitumor function. *Cell Metab* **34**, 731-746 e739 (2022). https://doi.org:10.1016/j.cmet.2022.03.013
87 Huang, Y. *et al.* Rewiring mitochondrial metabolism to counteract exhaustion of CAR-T cells. *J Hematol Oncol* **15**, 38 (2022). https://doi.org:10.1186/s13045-022-01255-x
88 Kaartinen, T. *et al.* Low interleukin-2 concentration favors generation of early memory T cells over effector phenotypes during chimeric antigen receptor T-cell expansion. *Cytotherapy* **19**, 1130 (2017). https://doi.org:10.1016/j.jcyt.2017.06.003
89 Charych, D. *et al.* Modeling the receptor pharmacology, pharmacokinetics, and pharmacodynamics of NKTR-214, a kinetically-controlled interleukin-2 (IL2) receptor agonist for cancer immunotherapy. *PLoS One* **12**, e0179431 (2017). https://doi.org:10.1371/journal.pone.0179431
90 Alizadeh, D. *et al.* IL15 Enhances CAR-T Cell Antitumor Activity by Reducing mTORC1 Activity and Preserving Their Stem Cell Memory Phenotype. *Cancer Immunol Res* **7**, 759-772 (2019). https://doi.org:10.1158/2326-6066.CIR-18-0466

91 Hoyos, V. *et al.* Engineering CD19-specific T lymphocytes with interleukin-15 and a suicide gene to enhance their anti-lymphoma/leukemia effects and safety. *Leukemia* **24**, 1160-1170 (2010). https://doi.org:10.1038/leu.2010.75
92 Arcangeli, S. *et al.* CAR T cell manufacturing from naive/stem memory T lymphocytes enhances antitumor responses while curtailing cytokine release syndrome. *J Clin Invest* **132** (2022). https://doi.org:10.1172/JCI150807
93 Li, L. *et al.* Transgenic expression of IL-7 regulates CAR-T cell metabolism and enhances in vivo persistence against tumor cells. *Sci Rep* **12**, 12506 (2022). https://doi.org:10.1038/s41598-022-16616-2
94 Funk, C. R. *et al.* PI3Kdelta/gamma inhibition promotes human CART cell epigenetic and metabolic reprogramming to enhance antitumor cytotoxicity. *Blood* **139**, 523-537 (2022). https://doi.org:10.1182/blood.2021011597
95 Dwyer, C. J. *et al.* Ex vivo blockade of PI3K gamma or delta signaling enhances the antitumor potency of adoptively transferred CD8(+) T cells. *Eur J Immunol* **50**, 1386-1399 (2020). https://doi.org:10.1002/eji.201948455
96 Zhang, Q. *et al.* Akt inhibition at the initial stage of CAR-T preparation enhances the CAR-positive expression rate, memory phenotype and in vivo efficacy. *Am J Cancer Res* **9**, 2379-2396 (2019).
97 Urak, R. *et al.* Ex vivo Akt inhibition promotes the generation of potent CD19CAR T cells for adoptive immunotherapy. *J Immunother Cancer* **5**, 26 (2017). https://doi.org:10.1186/s40425-017-0227-4
98 Klebanoff, C. A. *et al.* Inhibition of AKT signaling uncouples T cell differentiation from expansion for receptor-engineered adoptive immunotherapy. *JCI Insight* **2** (2017). https://doi.org:10.1172/jci.insight.95103
99 Zheng, W. *et al.* PI3K orchestration of the in vivo persistence of chimeric antigen receptor-modified T cells. *Leukemia* **32**, 1157-1167 (2018). https://doi.org:10.1038/s41375-017-0008-6
100 Xie, J., Wang, X. & Proud, C. G. mTOR inhibitors in cancer therapy. *F1000Res* **5** (2016). https://doi.org:10.12688/f1000research.9207.1
101 Nian, Z. *et al.* Rapamycin Pretreatment Rescues the Bone Marrow AML Cell Elimination Capacity of CAR-T Cells. *Clin Cancer Res* **27**, 6026-6038 (2021). https://doi.org:10.1158/1078-0432.CCR-21-0452
102 Lamarthee, B. *et al.* Transient mTOR inhibition rescues 4-1BB CAR-Tregs from tonic signal-induced dysfunction. *Nat Commun* **12**, 6446 (2021). https://doi.org:10.1038/s41467-021-26844-1
103 Han, C., Ge, M., Ho, P. C. & Zhang, L. Fueling T-cell Antitumor Immunity: Amino Acid Metabolism Revisited. *Cancer Immunol Res* **9**, 1373-1382 (2021). https://doi.org:10.1158/2326-6066.CIR-21-0459
104 Ye, L. *et al.* A genome-scale gain-of-function CRISPR screen in CD8 T cells identifies proline metabolism as a means to enhance CAR-T therapy. *Cell Metab* **34**, 595-614 e514 (2022). https://doi.org:10.1016/j.cmet.2022.02.009
105 Fultang, L. *et al.* Metabolic engineering against the arginine microenvironment enhances CAR-T cell proliferation and therapeutic activity. *Blood* **136**, 1155-1160 (2020). https://doi.org:10.1182/blood.2019004500
106 Panetti, S. *et al.* Engineering amino acid uptake or catabolism promotes CAR-T cell adaption to the tumour environment. *Blood Adv* (2022). https://doi.org:10.1182/bloodadvances.2022008272
107 Turkcan, S., Kiru, L., Naczynski, D. J., Sasportas, L. S. & Pratx, G. Lactic Acid Accumulation in the Tumor Microenvironment Suppresses (18)F-FDG Uptake. *Cancer Res* **79**, 410-419 (2019). https://doi.org:10.1158/0008-5472.CAN-17-0492

108 Brizel, D. M. *et al.* Elevated tumor lactate concentrations predict for an increased risk of metastases in head-and-neck cancer. *Int J Radiat Oncol Biol Phys* **51**, 349-353 (2001). https://doi.org:10.1016/s0360-3016(01)01630-3
109 Brand, A. *et al.* LDHA-Associated Lactic Acid Production Blunts Tumor Immunosurveillance by T and NK Cells. *Cell Metab* **24**, 657-671 (2016). https://doi.org:10.1016/j.cmet.2016.08.011
110 Harmon, C. *et al.* Lactate-Mediated Acidification of Tumor Microenvironment Induces Apoptosis of Liver-Resident NK Cells in Colorectal Liver Metastasis. *Cancer Immunol Res* **7**, 335-346 (2019). https://doi.org:10.1158/2326-6066.CIR-18-0481
111 Colegio, O. R. *et al.* Functional polarization of tumour-associated macrophages by tumour-derived lactic acid. *Nature* **513**, 559-563 (2014). https://doi.org:10.1038/nature13490
112 Geeraerts, X. *et al.* Macrophages are metabolically heterogeneous within the tumor microenvironment. *Cell Rep* **37**, 110171 (2021). https://doi.org:10.1016/j.celrep.2021.110171
113 Walenta, S. *et al.* High lactate levels predict likelihood of metastases, tumor recurrence, and restricted patient survival in human cervical cancers. *Cancer Res* **60**, 916-921 (2000).
114 Holroyde, C. P. *et al.* Lactate metabolism in patients with metastatic colorectal cancer. *Cancer Res* **39**, 4900-4904 (1979).
115 Qian, J. *et al.* Lactic acid promotes metastatic niche formation in bone metastasis of colorectal cancer. *Cell Commun Signal* **19**, 9 (2021). https://doi.org:10.1186/s12964-020-00667-x
116 Faubert, B. *et al.* Lactate Metabolism in Human Lung Tumors. *Cell* **171**, 358-371 e359 (2017). https://doi.org:10.1016/j.cell.2017.09.019
117 Gu, J. *et al.* Tumor metabolite lactate promotes tumorigenesis by modulating MOESIN lactylation and enhancing TGF-beta signaling in regulatory T cells. *Cell Rep* **39**, 110986 (2022). https://doi.org:10.1016/j.celrep.2022.110986
118 Fischer, K. *et al.* Inhibitory effect of tumor cell-derived lactic acid on human T cells. *Blood* **109**, 3812-3819 (2007). https://doi.org:10.1182/blood-2006-07-035972
119 Haas, R. *et al.* Lactate Regulates Metabolic and Pro-inflammatory Circuits in Control of T Cell Migration and Effector Functions. *PLoS Biol* **13**, e1002202 (2015). https://doi.org:10.1371/journal.pbio.1002202
120 Fischbeck, A. J. *et al.* Tumor Lactic Acidosis: Protecting Tumor by Inhibiting Cytotoxic Activity Through Motility Arrest and Bioenergetic Silencing. *Front Oncol* **10**, 589434 (2020). https://doi.org:10.3389/fonc.2020.589434
121 Rostamian, H. *et al.* Restricting tumor lactic acid metabolism using dichloroacetate improves T cell functions. *BMC Cancer* **22**, 39 (2022). https://doi.org:10.1186/s12885-021-09151-2
122 Qiao, T. *et al.* Inhibition of LDH-A by Oxamate Enhances the Efficacy of Anti-PD-1 Treatment in an NSCLC Humanized Mouse Model. *Front Oncol* **11**, 632364 (2021). https://doi.org:10.3389/fonc.2021.632364
123 Mane, M. M. *et al.* Lactate Dehydrogenase A Depletion Alters MyC-CaP Tumor Metabolism, Microenvironment, and CAR T Cell Therapy. *Mol Ther Oncolytics* **18**, 382-395 (2020). https://doi.org:10.1016/j.omto.2020.07.006
124 Quinn, W. J., 3rd *et al.* Lactate Limits T Cell Proliferation via the NAD(H) Redox State. *Cell Rep* **33**, 108500 (2020). https://doi.org:10.1016/j.celrep.2020.108500
125 Field, C. S. *et al.* Mitochondrial Integrity Regulated by Lipid Metabolism Is a Cell-Intrinsic Checkpoint for Treg Suppressive Function. *Cell Metab* **31**, 422-437 e425 (2020). https://doi.org:10.1016/j.cmet.2019.11.021
126 Shi, H. & Chi, H. Metabolic Control of Treg Cell Stability, Plasticity, and Tissue-Specific Heterogeneity. *Front Immunol* **10**, 2716 (2019). https://doi.org:10.3389/fimmu.2019.02716
127 Angelin, A. *et al.* Foxp3 Reprograms T Cell Metabolism to Function in Low-Glucose, High-Lactate Environments. *Cell Metab* **25**, 1282-1293 e1287 (2017). https://doi.org:10.1016/j.cmet.2016.12.018

128 Kumagai, S. *et al.* Lactic acid promotes PD-1 expression in regulatory T cells in highly glycolytic tumor microenvironments. *Cancer Cell* **40**, 201-218 e209 (2022). https://doi.org:10.1016/j.ccell.2022.01.001
129 Halestrap, A. P. & Wilson, M. C. The monocarboxylate transporter family--role and regulation. *IUBMB Life* **64**, 109-119 (2012). https://doi.org:10.1002/iub.572
130 Bonen, A. The expression of lactate transporters (MCT1 and MCT4) in heart and muscle. *Eur J Appl Physiol* **86**, 6-11 (2001). https://doi.org:10.1007/s004210100516
131 Fisel, P., Schaeffeler, E. & Schwab, M. Clinical and Functional Relevance of the Monocarboxylate Transporter Family in Disease Pathophysiology and Drug Therapy. *Clin Transl Sci* **11**, 352-364 (2018). https://doi.org:10.1111/cts.12551
132 Le Floch, R. *et al.* CD147 subunit of lactate/H+ symporters MCT1 and hypoxia-inducible MCT4 is critical for energetics and growth of glycolytic tumors. *Proc Natl Acad Sci U S A* **108**, 16663-16668 (2011). https://doi.org:10.1073/pnas.1106123108
133 Morrot, A. *et al.* Metabolic Symbiosis and Immunomodulation: How Tumor Cell-Derived Lactate May Disturb Innate and Adaptive Immune Responses. *Front Oncol* **8**, 81 (2018). https://doi.org:10.3389/fonc.2018.00081
134 Pisarsky, L. *et al.* Targeting Metabolic Symbiosis to Overcome Resistance to Anti-angiogenic Therapy. *Cell Rep* **15**, 1161-1174 (2016). https://doi.org:10.1016/j.celrep.2016.04.028
135 Payen, V. L., Mina, E., Van Hee, V. F., Porporato, P. E. & Sonveaux, P. Monocarboxylate transporters in cancer. *Mol Metab* **33**, 48-66 (2020). https://doi.org:10.1016/j.molmet.2019.07.006
136 Doyen, J. *et al.* Expression of the hypoxia-inducible monocarboxylate transporter MCT4 is increased in triple negative breast cancer and correlates independently with clinical outcome. *Biochem Biophys Res Commun* **451**, 54-61 (2014). https://doi.org:10.1016/j.bbrc.2014.07.050
137 Izumi, H. *et al.* Monocarboxylate transporters 1 and 4 are involved in the invasion activity of human lung cancer cells. *Cancer Sci* **102**, 1007-1013 (2011). https://doi.org:10.1111/j.1349-7006.2011.01908.x
138 Kim, H. K. *et al.* MCT4 Expression Is a Potential Therapeutic Target in Colorectal Cancer with Peritoneal Carcinomatosis. *Mol Cancer Ther* **17**, 838-848 (2018). https://doi.org:10.1158/1535-7163.MCT-17-0535
139 Perez-Escuredo, J. *et al.* Monocarboxylate transporters in the brain and in cancer. *Biochim Biophys Acta* **1863**, 2481-2497 (2016). https://doi.org:10.1016/j.bbamcr.2016.03.013
140 Curry, J. M. *et al.* Cancer metabolism, stemness and tumor recurrence: MCT1 and MCT4 are functional biomarkers of metabolic symbiosis in head and neck cancer. *Cell Cycle* **12**, 1371-1384 (2013). https://doi.org:10.4161/cc.24092
141 Leu, M. *et al.* Monocarboxylate transporter-1 (MCT1) protein expression in head and neck cancer affects clinical outcome. *Sci Rep* **11**, 4578 (2021). https://doi.org:10.1038/s41598-021-84019-w
142 Saulle, E. *et al.* Targeting Lactate Metabolism by Inhibiting MCT1 or MCT4 Impairs Leukemic Cell Proliferation, Induces Two Different Related Death-Pathways and Increases Chemotherapeutic Sensitivity of Acute Myeloid Leukemia Cells. *Front Oncol* **10**, 621458 (2020). https://doi.org:10.3389/fonc.2020.621458
143 Lopes-Coelho, F. *et al.* Monocarboxylate transporter 1 (MCT1), a tool to stratify acute myeloid leukemia (AML) patients and a vehicle to kill cancer cells. *Oncotarget* **8**, 82803-82823 (2017). https://doi.org:10.18632/oncotarget.20294
144 Noble, R. A. *et al.* Inhibition of monocarboxyate transporter 1 by AZD3965 as a novel therapeutic approach for diffuse large B-cell lymphoma and Burkitt lymphoma. *Haematologica* **102**, 1247-1257 (2017). https://doi.org:10.3324/haematol.2016.163030

145 Afonso, J. *et al.* Clinical significance of metabolism-related biomarkers in non-Hodgkin lymphoma - MCT1 as potential target in diffuse large B cell lymphoma. *Cell Oncol (Dordr)* **42**, 303-318 (2019). https://doi.org:10.1007/s13402-019-00426-2
146 Bola, B. M. *et al.* Inhibition of monocarboxylate transporter-1 (MCT1) by AZD3965 enhances radiosensitivity by reducing lactate transport. *Mol Cancer Ther* **13**, 2805-2816 (2014). https://doi.org:10.1158/1535-7163.MCT-13-1091
147 Ovens, M. J., Manoharan, C., Wilson, M. C., Murray, C. M. & Halestrap, A. P. The inhibition of monocarboxylate transporter 2 (MCT2) by AR-C155858 is modulated by the associated ancillary protein. *Biochem J* **431**, 217-225 (2010). https://doi.org:10.1042/BJ20100890
148 Nancolas, B., Sessions, R. B. & Halestrap, A. P. Identification of key binding site residues of MCT1 for AR-C155858 reveals the molecular basis of its isoform selectivity. *Biochem J* **466**, 177-188 (2015). https://doi.org:10.1042/BJ20141223
149 Quanz, M. *et al.* Preclinical Efficacy of the Novel Monocarboxylate Transporter 1 Inhibitor BAY-8002 and Associated Markers of Resistance. *Mol Cancer Ther* **17**, 2285-2296 (2018). https://doi.org:10.1158/1535-7163.MCT-17-1253
150 Braga, M. *et al.* Tracing Nutrient Flux Following Monocarboxylate Transporter-1 Inhibition with AZD3965. *Cancers (Basel)* **12** (2020). https://doi.org:10.3390/cancers12061703
151 Beloueche-Babari, M. *et al.* MCT1 Inhibitor AZD3965 Increases Mitochondrial Metabolism, Facilitating Combination Therapy and Noninvasive Magnetic Resonance Spectroscopy. *Cancer Res* **77**, 5913-5924 (2017). https://doi.org:10.1158/0008-5472.CAN-16-2686
152 Guan, X., Rodriguez-Cruz, V. & Morris, M. E. Cellular Uptake of MCT1 Inhibitors AR-C155858 and AZD3965 and Their Effects on MCT-Mediated Transport of L-Lactate in Murine 4T1 Breast Tumor Cancer Cells. *AAPS J* **21**, 13 (2019). https://doi.org:10.1208/s12248-018-0279-5
153 Curtis, N. J. *et al.* Pre-clinical pharmacology of AZD3965, a selective inhibitor of MCT1: DLBCL, NHL and Burkitt's lymphoma anti-tumor activity. *Oncotarget* **8**, 69219-69236 (2017). https://doi.org:10.18632/oncotarget.18215
154 Benyahia, Z. *et al.* In Vitro and In Vivo Characterization of MCT1 Inhibitor AZD3965 Confirms Preclinical Safety Compatible with Breast Cancer Treatment. *Cancers (Basel)* **13** (2021). https://doi.org:10.3390/cancers13030569
155 Polanski, R. *et al.* Activity of the monocarboxylate transporter 1 inhibitor AZD3965 in small cell lung cancer. *Clin Cancer Res* **20**, 926-937 (2014). https://doi.org:10.1158/1078-0432.CCR-13-2270
156 Mehibel, M. *et al.* Statin-induced metabolic reprogramming in head and neck cancer: a biomarker for targeting monocarboxylate transporters. *Sci Rep* **8**, 16804 (2018). https://doi.org:10.1038/s41598-018-35103-1
157 Guo, Y. *et al.* Oncogenic Chromatin Modifier KAT2A Activates MCT1 to Drive the Glycolytic Process and Tumor Progression in Renal Cell Carcinoma. *Front Cell Dev Biol* **9**, 690796 (2021). https://doi.org:10.3389/fcell.2021.690796
158 Doherty, J. R. *et al.* Blocking lactate export by inhibiting the Myc target MCT1 Disables glycolysis and glutathione synthesis. *Cancer Res* **74**, 908-920 (2014). https://doi.org:10.1158/0008-5472.CAN-13-2034
159 Lee, J. Y. *et al.* MCT4 as a potential therapeutic target for metastatic gastric cancer with peritoneal carcinomatosis. *Oncotarget* **7**, 43492-43503 (2016). https://doi.org:10.18632/oncotarget.9523
160 Hao, J. *et al.* Co-expression of CD147 (EMMPRIN), CD44v3-10, MDR1 and monocarboxylate transporters is associated with prostate cancer drug resistance and progression. *Br J Cancer* **103**, 1008-1018 (2010). https://doi.org:10.1038/sj.bjc.6605839
161 Jeon, J. Y. *et al.* Regulation of Acetate Utilization by Monocarboxylate Transporter 1 (MCT1) in Hepatocellular Carcinoma (HCC). *Oncol Res* **26**, 71-81 (2018). https://doi.org:10.3727/096504017X14902648894463

162 Miranda-Goncalves, V. *et al.* MCT1 Is a New Prognostic Biomarker and Its Therapeutic Inhibition Boosts Response to Temozolomide in Human Glioblastoma. *Cancers (Basel)* **13** (2021). https://doi.org:10.3390/cancers13143468
163 Puri, S. & Juvale, K. Monocarboxylate transporter 1 and 4 inhibitors as potential therapeutics for treating solid tumours: A review with structure-activity relationship insights. *Eur J Med Chem* **199**, 112393 (2020). https://doi.org:10.1016/j.ejmech.2020.112393
164 Beloueche-Babari, M. *et al.* Monocarboxylate transporter 1 blockade with AZD3965 inhibits lipid biosynthesis and increases tumour immune cell infiltration. *Br J Cancer* **122**, 895-903 (2020). https://doi.org:10.1038/s41416-019-0717-x
165 Guan, X., Bryniarski, M. A. & Morris, M. E. In Vitro and In Vivo Efficacy of the Monocarboxylate Transporter 1 Inhibitor AR-C155858 in the Murine 4T1 Breast Cancer Tumor Model. *AAPS J* **21**, 3 (2018). https://doi.org:10.1208/s12248-018-0261-2
166 Caslin, H. L., Abebayehu, D., Pinette, J. A. & Ryan, J. J. Lactate Is a Metabolic Mediator That Shapes Immune Cell Fate and Function. *Front Physiol* **12**, 688485 (2021). https://doi.org:10.3389/fphys.2021.688485
167 Wang, R. & Green, D. R. Metabolic reprogramming and metabolic dependency in T cells. *Immunol Rev* **249**, 14-26 (2012). https://doi.org:10.1111/j.1600-065X.2012.01155.x
168 Murray, C. M. *et al.* Monocarboxylate transporter MCT1 is a target for immunosuppression. *Nat Chem Biol* **1**, 371-376 (2005). https://doi.org:10.1038/nchembio744
169 Watson, M. J. *et al.* Metabolic support of tumour-infiltrating regulatory T cells by lactic acid. *Nature* **591**, 645-651 (2021). https://doi.org:10.1038/s41586-020-03045-2
170 Buyse, C. *et al.* Evaluation of Syrosingopine, an MCT Inhibitor, as Potential Modulator of Tumor Metabolism and Extracellular Acidification. *Metabolites* **12** (2022). https://doi.org:10.3390/metabo12060557
171 Benjamin, D. *et al.* Syrosingopine sensitizes cancer cells to killing by metformin. *Sci Adv* **2**, e1601756 (2016). https://doi.org:10.1126/sciadv.1601756
172 Cheng, G., Hardy, M., You, M. & Kalyanaraman, B. Combining PEGylated mito-atovaquone with MCT and Krebs cycle redox inhibitors as a potential strategy to abrogate tumor cell proliferation. *Sci Rep* **12**, 5143 (2022). https://doi.org:10.1038/s41598-022-08984-6
173 Takenaga, K. *et al.* MCT4 is induced by metastasis-enhancing pathogenic mitochondrial NADH dehydrogenase gene mutations and can be a therapeutic target. *Sci Rep* **11**, 13302 (2021). https://doi.org:10.1038/s41598-021-92772-1
174 Benjamin, D. *et al.* Dual Inhibition of the Lactate Transporters MCT1 and MCT4 Is Synthetic Lethal with Metformin due to NAD+ Depletion in Cancer Cells. *Cell Rep* **25**, 3047-3058 e3044 (2018). https://doi.org:10.1016/j.celrep.2018.11.043
175 Zarghi, A. & Arfaei, S. Selective COX-2 Inhibitors: A Review of Their Structure-Activity Relationships. *Iran J Pharm Res* **10**, 655-683 (2011).
176 Mayorek, N., Naftali-Shani, N. & Grunewald, M. Diclofenac inhibits tumor growth in a murine model of pancreatic cancer by modulation of VEGF levels and arginase activity. *PLoS One* **5**, e12715 (2010). https://doi.org:10.1371/journal.pone.0012715
177 Singer, K. *et al.* Topical Diclofenac Reprograms Metabolism and Immune Cell Infiltration in Actinic Keratosis. *Front Oncol* **9**, 605 (2019). https://doi.org:10.3389/fonc.2019.00605
178 Renner, K. *et al.* Restricting Glycolysis Preserves T Cell Effector Functions and Augments Checkpoint Therapy. *Cell Rep* **29**, 135-150 e139 (2019). https://doi.org:10.1016/j.celrep.2019.08.068
179 Bergstrom, J., Furst, P., Noree, L. O. & Vinnars, E. Intracellular free amino acid concentration in human muscle tissue. *J Appl Physiol* **36**, 693-697 (1974). https://doi.org:10.1152/jappl.1974.36.6.693
180 Jiang, J., Srivastava, S. & Zhang, J. Starve Cancer Cells of Glutamine: Break the Spell or Make a Hungry Monster? *Cancers (Basel)* **11** (2019). https://doi.org:10.3390/cancers11060804

181 Gao, P. *et al.* c-Myc suppression of miR-23a/b enhances mitochondrial glutaminase expression and glutamine metabolism. *Nature* **458**, 762-765 (2009). https://doi.org:10.1038/nature07823
182 Suzuki, S. *et al.* Phosphate-activated glutaminase (GLS2), a p53-inducible regulator of glutamine metabolism and reactive oxygen species. *Proc Natl Acad Sci U S A* **107**, 7461-7466 (2010). https://doi.org:10.1073/pnas.1002459107
183 Newsholme, P. Why is L-glutamine metabolism important to cells of the immune system in health, postinjury, surgery or infection? *J Nutr* **131**, 2515S-2522S; discussion 2523S-2514S (2001). https://doi.org:10.1093/jn/131.9.2515S
184 Loftus, R. M. *et al.* Amino acid-dependent cMyc expression is essential for NK cell metabolic and functional responses in mice. *Nat Commun* **9**, 2341 (2018). https://doi.org:10.1038/s41467-018-04719-2
185 Carr, E. L. *et al.* Glutamine uptake and metabolism are coordinately regulated by ERK/MAPK during T lymphocyte activation. *J Immunol* **185**, 1037-1044 (2010). https://doi.org:10.4049/jimmunol.0903586
186 Johnson, M. O. *et al.* Distinct Regulation of Th17 and Th1 Cell Differentiation by Glutaminase-Dependent Metabolism. *Cell* **175**, 1780-1795 e1719 (2018). https://doi.org:10.1016/j.cell.2018.10.001
187 Oh, M. H. *et al.* Targeting glutamine metabolism enhances tumor-specific immunity by modulating suppressive myeloid cells. *J Clin Invest* **130**, 3865-3884 (2020). https://doi.org:10.1172/JCI131859
188 Ma, G. *et al.* Reprogramming of glutamine metabolism and its impact on immune response in the tumor microenvironment. *Cell Commun Signal* **20**, 114 (2022). https://doi.org:10.1186/s12964-022-00909-0
189 Edwards, D. N. *et al.* Selective glutamine metabolism inhibition in tumor cells improves antitumor T lymphocyte activity in triple-negative breast cancer. *J Clin Invest* **131** (2021). https://doi.org:10.1172/JCI140100
190 Palmieri, E. M. *et al.* Pharmacologic or Genetic Targeting of Glutamine Synthetase Skews Macrophages toward an M1-like Phenotype and Inhibits Tumor Metastasis. *Cell Rep* **20**, 1654-1666 (2017). https://doi.org:10.1016/j.celrep.2017.07.054
191 Byun, J. K. *et al.* Inhibition of Glutamine Utilization Synergizes with Immune Checkpoint Inhibitor to Promote Antitumor Immunity. *Mol Cell* **80**, 592-606 e598 (2020). https://doi.org:10.1016/j.molcel.2020.10.015
192 Wang, L. *et al.* Immunosuppression Induced by Glutamine Deprivation Occurs via Activating PD-L1 Transcription in Bladder Cancer. *Front Mol Biosci* **8**, 687305 (2021). https://doi.org:10.3389/fmolb.2021.687305
193 Scalise, M., Pochini, L., Galluccio, M., Console, L. & Indiveri, C. Glutamine Transport and Mitochondrial Metabolism in Cancer Cell Growth. *Front Oncol* **7**, 306 (2017). https://doi.org:10.3389/fonc.2017.00306
194 Thomas, A. G. *et al.* Kinetic characterization of ebselen, chelerythrine and apomorphine as glutaminase inhibitors. *Biochem Biophys Res Commun* **438**, 243-248 (2013). https://doi.org:10.1016/j.bbrc.2013.06.110
195 Rahman, A., Smith, F. P., Luc, P. T. & Woolley, P. V. Phase I study and clinical pharmacology of 6-diazo-5-oxo-L-norleucine (DON). *Invest New Drugs* **3**, 369-374 (1985). https://doi.org:10.1007/BF00170760
196 Eagan, R. T., Frytak, S., Nichols, W. C., Creagan, E. T. & Ingle, J. N. Phase II study on DON in patients with previously treated advanced lung cancer. *Cancer Treat Rep* **66**, 1665-1666 (1982).
197 Lemberg, K. M., Vornov, J. J., Rais, R. & Slusher, B. S. We're Not "DON" Yet: Optimal Dosing and Prodrug Delivery of 6-Diazo-5-oxo-L-norleucine. *Mol Cancer Ther* **17**, 1824-1832 (2018). https://doi.org:10.1158/1535-7163.MCT-17-1148

198 Nabe, S. *et al.* Reinforce the antitumor activity of CD8(+) T cells via glutamine restriction. *Cancer Sci* **109**, 3737-3750 (2018). https://doi.org:10.1111/cas.13827
199 Shen, L. *et al.* Metabolic reprogramming by ex vivo glutamine inhibition endows CAR-T cells with less-differentiated phenotype and persistent antitumor activity. *Cancer Lett* **538**, 215710 (2022). https://doi.org:10.1016/j.canlet.2022.215710
200 Best, S. A. *et al.* Glutaminase inhibition impairs CD8 T cell activation in STK11-/Lkb1-deficient lung cancer. *Cell Metab* **34**, 874-887 e876 (2022). https://doi.org:10.1016/j.cmet.2022.04.003
201 Leone, R. D. *et al.* Glutamine blockade induces divergent metabolic programs to overcome tumor immune evasion. *Science* **366**, 1013-1021 (2019). https://doi.org:10.1126/science.aav2588
202 Rais, R. *et al.* Discovery of DRP-104, a tumor-targeted metabolic inhibitor prodrug. *Sci Adv* **8**, eabq5925 (2022). https://doi.org:10.1126/sciadv.abq5925
203 Lopes, C., Pereira, C. & Medeiros, R. ASCT2 and LAT1 Contribution to the Hallmarks of Cancer: From a Molecular Perspective to Clinical Translation. *Cancers (Basel)* **13** (2021). https://doi.org:10.3390/cancers13020203
204 Schulte, M. L. *et al.* Pharmacological blockade of ASCT2-dependent glutamine transport leads to antitumor efficacy in preclinical models. *Nat Med* **24**, 194-202 (2018). https://doi.org:10.1038/nm.4464
205 Kim, G. *et al.* Inhibition of Glutamine Uptake Resensitizes Paclitaxel Resistance in SKOV3-TR Ovarian Cancer Cell via mTORC1/S6K Signaling Pathway. *Int J Mol Sci* **23** (2022). https://doi.org:10.3390/ijms23158761
206 Luo, Z. *et al.* Co-delivery of 2-Deoxyglucose and a glutamine metabolism inhibitor V9302 via a prodrug micellar formulation for synergistic targeting of metabolism in cancer. *Acta Biomater* **105**, 239-252 (2020). https://doi.org:10.1016/j.actbio.2020.01.019
207 Osanai-Sasakawa, A. *et al.* An anti-ASCT2 monoclonal antibody suppresses gastric cancer growth by inducing oxidative stress and antibody dependent cellular toxicity in preclinical models. *Am J Cancer Res* **8**, 1499-1513 (2018).
208 Kasai, N. *et al.* Anti-tumor efficacy evaluation of a novel monoclonal antibody targeting neutral amino acid transporter ASCT2 using patient-derived xenograft mouse models of gastric cancer. *Am J Transl Res* **9**, 3399-3410 (2017).
209 Stowe, C. L. *et al.* Near-infrared dual bioluminescence imaging in mouse models of cancer using infraluciferin. *Elife* **8** (2019). https://doi.org:10.7554/eLife.45801
210 van der Windt, G. J. W., Chang, C. H. & Pearce, E. L. Measuring Bioenergetics in T Cells Using a Seahorse Extracellular Flux Analyzer. *Curr Protoc Immunol* **113**, 3 16B 11-13 16B 14 (2016). https://doi.org:10.1002/0471142735.im0316bs113
211 Silva, A. *et al.* In Vivo Anticancer Activity of AZD3965: A Systematic Review. *Molecules* **27** (2021). https://doi.org:10.3390/molecules27010181
212 Bonglack, E. N. *et al.* Monocarboxylate transporter antagonism reveals metabolic vulnerabilities of viral-driven lymphomas. *Proc Natl Acad Sci U S A* **118** (2021). https://doi.org:10.1073/pnas.2022495118
213 Davey, A. S., Call, M. E. & Call, M. J. The Influence of Chimeric Antigen Receptor Structural Domains on Clinical Outcomes and Associated Toxicities. *Cancers (Basel)* **13** (2020). https://doi.org:10.3390/cancers13010038
214 Philip, B. *et al.* A highly compact epitope-based marker/suicide gene for easier and safer T-cell therapy. *Blood* **124**, 1277-1287 (2014). https://doi.org:10.1182/blood-2014-01-545020
215 Frigault, M. J. *et al.* Identification of chimeric antigen receptors that mediate constitutive or inducible proliferation of T cells. *Cancer Immunol Res* **3**, 356-367 (2015). https://doi.org:10.1158/2326-6066.CIR-14-0186

216 Long, A. H. *et al.* 4-1BB costimulation ameliorates T cell exhaustion induced by tonic signaling of chimeric antigen receptors. *Nat Med* **21**, 581-590 (2015). https://doi.org:10.1038/nm.3838
217 Kirk, P. *et al.* CD147 is tightly associated with lactate transporters MCT1 and MCT4 and facilitates their cell surface expression. *EMBO J* **19**, 3896-3904 (2000). https://doi.org:10.1093/emboj/19.15.3896
218 Zhao, Y. *et al.* Targeted inhibition of MCT4 disrupts intracellular pH homeostasis and confers self-regulated apoptosis on hepatocellular carcinoma. *Exp Cell Res* **384**, 111591 (2019). https://doi.org:10.1016/j.yexcr.2019.111591
219 Tu, V. Y., Ayari, A. & O'Connor, R. S. Beyond the Lactate Paradox: How Lactate and Acidity Impact T Cell Therapies against Cancer. *Antibodies (Basel)* **10** (2021). https://doi.org:10.3390/antib10030025
220 Kishton, R. J., Sukumar, M. & Restifo, N. P. Metabolic Regulation of T Cell Longevity and Function in Tumor Immunotherapy. *Cell Metab* **26**, 94-109 (2017). https://doi.org:S1550-4131(17)30358-3 [pii]10.1016/j.cmet.2017.06.016
221 Blache, U. *et al.* Advanced Flow Cytometry Assays for Immune Monitoring of CAR-T Cell Applications. *Front Immunol* **12**, 658314 (2021). https://doi.org:10.3389/fimmu.2021.658314
222 Cullen, S. P., Brunet, M. & Martin, S. J. Granzymes in cancer and immunity. *Cell Death Differ* **17**, 616-623 (2010). https://doi.org:10.1038/cdd.2009.206
223 Fenton, S. E., Saleiro, D. & Platanias, L. C. Type I and II Interferons in the Anti-Tumor Immune Response. *Cancers (Basel)* **13** (2021). https://doi.org:10.3390/cancers13051037
224 Jiang, T., Zhou, C. & Ren, S. Role of IL-2 in cancer immunotherapy. *Oncoimmunology* **5**, e1163462 (2016). https://doi.org:10.1080/2162402X.2016.1163462
225 Rostamian, H. *et al.* A metabolic switch to memory CAR T cells: Implications for cancer treatment. *Cancer Lett* **500**, 107-118 (2021). https://doi.org:10.1016/j.canlet.2020.12.004
226 Romero, P. *et al.* Four functionally distinct populations of human effector-memory CD8+ T lymphocytes. *J Immunol* **178**, 4112-4119 (2007). https://doi.org:10.4049/jimmunol.178.7.4112
227 Ecker, C. & Riley, J. L. Translating In Vitro T Cell Metabolic Findings to In Vivo Tumor Models of Nutrient Competition. *Cell Metab* **28**, 190-195 (2018). https://doi.org:10.1016/j.cmet.2018.07.009
228 Muir, A., Danai, L. V. & Vander Heiden, M. G. Microenvironmental regulation of cancer cell metabolism: implications for experimental design and translational studies. *Dis Model Mech* **11** (2018). https://doi.org:10.1242/dmm.035758
229 Faubert, B., Solmonson, A. & DeBerardinis, R. J. Metabolic reprogramming and cancer progression. *Science* **368** (2020). https://doi.org:10.1126/science.aaw5473
230 Andrejeva, G. & Rathmell, J. C. Similarities and Distinctions of Cancer and Immune Metabolism in Inflammation and Tumors. *Cell Metab* **26**, 49-70 (2017). https://doi.org:10.1016/j.cmet.2017.06.004
231 Liu, Y. *et al.* The role of ASCT2 in cancer: A review. *Eur J Pharmacol* **837**, 81-87 (2018). https://doi.org:10.1016/j.ejphar.2018.07.007
232 Tang, Y. *et al.* Simultaneous glutamine metabolism and PD-L1 inhibition to enhance suppression of triple-negative breast cancer. *J Nanobiotechnology* **20**, 216 (2022). https://doi.org:10.1186/s12951-022-01424-7
233 Li, Q. *et al.* Inhibitor of glutamine metabolism V9302 promotes ROS-induced autophagic degradation of B7H3 to enhance antitumor immunity. *J Biol Chem* **298**, 101753 (2022). https://doi.org:10.1016/j.jbc.2022.101753
234 Suzuki, M., Toki, H., Furuya, A. & Ando, H. Establishment of monoclonal antibodies against cell surface domains of ASCT2/SLC1A5 and their inhibition of glutamine-dependent tumor

cell growth. *Biochem Biophys Res Commun* **482**, 651-657 (2017). https://doi.org:10.1016/j.bbrc.2016.11.089

235 Poffenberger, M. C. & Jones, R. G. Amino acids fuel T cell-mediated inflammation. *Immunity* **40**, 635-637 (2014). https://doi.org:10.1016/j.immuni.2014.04.017

236 Abraham, R. T. & Weiss, A. Jurkat T cells and development of the T-cell receptor signalling paradigm. *Nat Rev Immunol* **4**, 301-308 (2004). https://doi.org:10.1038/nri1330

237 Mercier-Letondal, P., Marton, C., Godet, Y. & Galaine, J. Validation of a method evaluating T cell metabolic potential in compliance with ICH Q2 (R1). *J Transl Med* **19**, 21 (2021). https://doi.org:10.1186/s12967-020-02672-7

238 Li, J. *et al.* Targeting Metabolism in Cancer Cells and the Tumour Microenvironment for Cancer Therapy. *Molecules* **25** (2020). https://doi.org:10.3390/molecules25204831

239 Ramachandran, I. *et al.* Systemic and local immunity following adoptive transfer of NY-ESO-1 SPEAR T cells in synovial sarcoma. *J Immunother Cancer* **7**, 276 (2019). https://doi.org:10.1186/s40425-019-0762-2

240 Sugiura, A. & Rathmell, J. C. Metabolic Barriers to T Cell Function in Tumors. *J Immunol* **200**, 400-407 (2018). https://doi.org:10.4049/jimmunol.1701041

241 Corrado, M. & Pearce, E. L. Targeting memory T cell metabolism to improve immunity. *J Clin Invest* **132** (2022). https://doi.org:10.1172/JCI148546

242 Ghassemi, S. *et al.* Enhancing Chimeric Antigen Receptor T Cell Anti-tumor Function through Advanced Media Design. *Mol Ther Methods Clin Dev* **18**, 595-606 (2020). https://doi.org:10.1016/j.omtm.2020.07.008

243 Mu, Q. *et al.* Metformin inhibits proliferation and cytotoxicity and induces apoptosis via AMPK pathway in CD19-chimeric antigen receptor-modified T cells. *Onco Targets Ther* **11**, 1767-1776 (2018). https://doi.org:10.2147/OTT.S154853

244 Zhang, Z. *et al.* Metformin Enhances the Antitumor Activity of CD8(+) T Lymphocytes via the AMPK-miR-107-Eomes-PD-1 Pathway. *J Immunol* **204**, 2575-2588 (2020). https://doi.org:10.4049/jimmunol.1901213

245 Ajina, A. & Maher, J. Strategies to Address Chimeric Antigen Receptor Tonic Signaling. *Mol Cancer Ther* **17**, 1795-1815 (2018). https://doi.org:10.1158/1535-7163.MCT-17-1097

246 Liu, X. *et al.* B cell lymphoma with different metabolic characteristics show distinct sensitivities to metabolic inhibitors. *J Cancer* **9**, 1582-1591 (2018). https://doi.org:10.7150/jca.24331

247 Hashimoto, T., Hussien, R., Oommen, S., Gohil, K. & Brooks, G. A. Lactate sensitive transcription factor network in L6 cells: activation of MCT1 and mitochondrial biogenesis. *FASEB J* **21**, 2602-2612 (2007). https://doi.org:10.1096/fj.07-8174com

248 Ron-Harel, N. *et al.* Mitochondrial Biogenesis and Proteome Remodeling Promote One-Carbon Metabolism for T Cell Activation. *Cell Metab* **24**, 104-117 (2016). https://doi.org:10.1016/j.cmet.2016.06.007S1550-4131(16)30293-5 [pii]

249 Kozlov, A. M., Lone, A., Betts, D. H. & Cumming, R. C. Lactate preconditioning promotes a HIF-1alpha-mediated metabolic shift from OXPHOS to glycolysis in normal human diploid fibroblasts. *Sci Rep* **10**, 8388 (2020). https://doi.org:10.1038/s41598-020-65193-9

250 Levine, L. S. *et al.* Single-cell analysis by mass cytometry reveals metabolic states of early-activated CD8(+) T cells during the primary immune response. *Immunity* **54**, 829-844 e825 (2021). https://doi.org:10.1016/j.immuni.2021.02.018

251 Ma, E. H. *et al.* Metabolic Profiling Using Stable Isotope Tracing Reveals Distinct Patterns of Glucose Utilization by Physiologically Activated CD8(+) T Cells. *Immunity* **51**, 856-870 e855 (2019). https://doi.org:10.1016/j.immuni.2019.09.003

252 Huang, T. *et al.* Tumor-Targeted Inhibition of Monocarboxylate Transporter 1 Improves T-Cell Immunotherapy of Solid Tumors. *Adv Healthc Mater* **10**, e2000549 (2021). https://doi.org:10.1002/adhm.202000549

253 Teijeira, A. *et al.* Mitochondrial Morphological and Functional Reprogramming Following CD137 (4-1BB) Costimulation. *Cancer Immunol Res* **6**, 798-811 (2018). https://doi.org:10.1158/2326-6066.CIR-17-0767
254 Wang, H. *et al.* Bcl-2 Enhances Chimeric Antigen Receptor T Cell Persistence by Reducing Activation-Induced Apoptosis. *Cancers (Basel)* **13** (2021). https://doi.org:10.3390/cancers13020197
255 Beckermann, K. E. *et al.* CD28 costimulation drives tumor-infiltrating T cell glycolysis to promote inflammation. *JCI Insight* **5** (2020). https://doi.org:10.1172/jci.insight.138729
256 Zhang, H. *et al.* A chimeric antigen receptor with antigen-independent OX40 signaling mediates potent antitumor activity. *Sci Transl Med* **13** (2021). https://doi.org:10.1126/scitranslmed.aba7308
257 Guedan, S. *et al.* ICOS-based chimeric antigen receptors program bipolar TH17/TH1 cells. *Blood* **124**, 1070-1080 (2014). https://doi.org:10.1182/blood-2013-10-535245
258 Sledzinska, A. *et al.* Regulatory T Cells Restrain Interleukin-2- and Blimp-1-Dependent Acquisition of Cytotoxic Function by CD4(+) T Cells. *Immunity* **52**, 151-166 e156 (2020). https://doi.org:10.1016/j.immuni.2019.12.007
259 Lopez-Cantillo, G., Uruena, C., Camacho, B. A. & Ramirez-Segura, C. CAR-T Cell Performance: How to Improve Their Persistence? *Front Immunol* **13**, 878209 (2022). https://doi.org:10.3389/fimmu.2022.878209
260 Gottfried, E. *et al.* New aspects of an old drug--diclofenac targets MYC and glucose metabolism in tumor cells. *PLoS One* **8**, e66987 (2013). https://doi.org:10.1371/journal.pone.0066987
261 Villalonga, N. *et al.* Immunomodulatory effects of diclofenac in leukocytes through the targeting of Kv1.3 voltage-dependent potassium channels. *Biochem Pharmacol* **80**, 858-866 (2010). https://doi.org:10.1016/j.bcp.2010.05.012
262 Gutting, B. W., Updyke, L. W. & Amacher, D. E. Diclofenac activates T cells in the direct popliteal lymph node assay and selectively induces IgG(1) and IgE against co-injected TNP-OVA. *Toxicol Lett* **131**, 167-180 (2002). https://doi.org:10.1016/s0378-4274(02)00029-2
263 Berry, G. J. *et al.* Genome-wide transcriptional analyses of islet-specific CD4+ T cells identify Idd9 genes controlling diabetogenic T cell function. *J Immunol* **194**, 2654-2663 (2015). https://doi.org:10.4049/jimmunol.1401288
264 La Rocca, C. *et al.* Immunometabolic profiling of T cells from patients with relapsing-remitting multiple sclerosis reveals an impairment in glycolysis and mitochondrial respiration. *Metabolism* **77**, 39-46 (2017). https://doi.org:10.1016/j.metabol.2017.08.011
265 Gemta, L. F. *et al.* Impaired enolase 1 glycolytic activity restrains effector functions of tumor-infiltrating CD8(+) T cells. *Sci Immunol* **4** (2019). https://doi.org:10.1126/sciimmunol.aap9520
266 Lin, Y. H. *et al.* An enolase inhibitor for the targeted treatment of ENO1-deleted cancers. *Nat Metab* **2**, 1413-1426 (2020). https://doi.org:10.1038/s42255-020-00313-3
267 Cho, H. *et al.* ENOblock, a unique small molecule inhibitor of the non-glycolytic functions of enolase, alleviates the symptoms of type 2 diabetes. *Sci Rep* **7**, 44186 (2017). https://doi.org:10.1038/srep44186
268 Merezhinskaya, N., Ogunwuyi, S. A., Mullick, F. G. & Fishbein, W. N. Presence and localization of three lactic acid transporters (MCT1, -2, and -4) in separated human granulocytes, lymphocytes, and monocytes. *J Histochem Cytochem* **52**, 1483-1493 (2004). https://doi.org:10.1369/jhc.4A6306.2004
269 Khalyfa, A. *et al.* Monocarboxylate Transporter-2 Expression Restricts Tumor Growth in a Murine Model of Lung Cancer: A Multi-Omic Analysis. *Int J Mol Sci* **22** (2021). https://doi.org:10.3390/ijms221910616

270 Pucino, V. *et al.* Lactate Buildup at the Site of Chronic Inflammation Promotes Disease by Inducing CD4(+) T Cell Metabolic Rewiring. *Cell Metab* **30**, 1055-1074 e1058 (2019). https://doi.org:10.1016/j.cmet.2019.10.004
271 Gopal, E. *et al.* Cloning and functional characterization of human SMCT2 (SLC5A12) and expression pattern of the transporter in kidney. *Biochim Biophys Acta* **1768**, 2690-2697 (2007). https://doi.org:10.1016/j.bbamem.2007.06.031
272 Peralta R, D. G. 669 Lactate uptake through MCT11, a novel monocarboxylate transporter, enforces dysfunction in terminally exhausted T cells. *Journal for ImmunotTherapy of Cancer* **9:doi: 10.1136/jitc-2021-SITC2021.669** (2021).
273 An, N. *et al.* Construction of a new anti-CD19 chimeric antigen receptor and the anti-leukemia function study of the transduced T cells. *Oncotarget* **7**, 10638-10649 (2016). https://doi.org:10.18632/oncotarget.7079
274 Comito, G. *et al.* Lactate modulates CD4(+) T-cell polarization and induces an immunosuppressive environment, which sustains prostate carcinoma progression via TLR8/miR21 axis. *Oncogene* **38**, 3681-3695 (2019). https://doi.org:10.1038/s41388-019-0688-7
275 Cazaux, M. *et al.* Single-cell imaging of CAR T cell activity in vivo reveals extensive functional and anatomical heterogeneity. *J Exp Med* **216**, 1038-1049 (2019). https://doi.org:10.1084/jem.20182375
276 Pinheiro, C. *et al.* The metabolic microenvironment of melanomas: Prognostic value of MCT1 and MCT4. *Cell Cycle* **15**, 1462-1470 (2016). https://doi.org:10.1080/15384101.2016.1175258
277 Pinheiro, C. *et al.* Expression of monocarboxylate transporters 1, 2, and 4 in human tumours and their association with CD147 and CD44. *J Biomed Biotechnol* **2010**, 427694 (2010). https://doi.org:10.1155/2010/427694
278 Navarro, F. *et al.* Overcoming T cell dysfunction in acidic pH to enhance adoptive T cell transfer immunotherapy. *Oncoimmunology* **11**, 2070337 (2022). https://doi.org:10.1080/2162402X.2022.2070337
279 Zenewicz, L. A. Oxygen Levels and Immunological Studies. *Front Immunol* **8**, 324 (2017). https://doi.org:10.3389/fimmu.2017.00324
280 Muz, B., de la Puente, P., Azab, F. & Azab, A. K. The role of hypoxia in cancer progression, angiogenesis, metastasis, and resistance to therapy. *Hypoxia (Auckl)* **3**, 83-92 (2015). https://doi.org:10.2147/HP.S93413
281 Mascanfroni, I. D. *et al.* Metabolic control of type 1 regulatory T cell differentiation by AHR and HIF1-alpha. *Nat Med* **21**, 638-646 (2015). https://doi.org:10.1038/nm.3868
282 Doedens, A. L. *et al.* Hypoxia-inducible factors enhance the effector responses of CD8(+) T cells to persistent antigen. *Nat Immunol* **14**, 1173-1182 (2013). https://doi.org:10.1038/ni.2714
283 Liikanen, I. *et al.* Hypoxia-inducible factor activity promotes antitumor effector function and tissue residency by CD8+ T cells. *J Clin Invest* **131** (2021). https://doi.org:10.1172/JCI143729
284 Bannoud, N. *et al.* Hypoxia Supports Differentiation of Terminally Exhausted CD8 T Cells. *Front Immunol* **12**, 660944 (2021). https://doi.org:10.3389/fimmu.2021.660944
285 Vignali, P. D. A. *et al.* Hypoxia drives CD39-dependent suppressor function in exhausted T cells to limit antitumor immunity. *Nat Immunol* **24**, 267-279 (2023). https://doi.org:10.1038/s41590-022-01379-9
286 Lequeux, A. *et al.* Targeting HIF-1 alpha transcriptional activity drives cytotoxic immune effector cells into melanoma and improves combination immunotherapy. *Oncogene* **40**, 4725-4735 (2021). https://doi.org:10.1038/s41388-021-01846-x
287 Wang, J. X. *et al.* Lactic Acid and an Acidic Tumor Microenvironment suppress Anticancer Immunity. *Int J Mol Sci* **21** (2020). https://doi.org:10.3390/ijms21218363

288 Erra Diaz, F. *et al.* Extracellular Acidosis and mTOR Inhibition Drive the Differentiation of Human Monocyte-Derived Dendritic Cells. *Cell Rep* **31**, 107613 (2020). https://doi.org:10.1016/j.celrep.2020.107613
289 Nasi, A. *et al.* Dendritic cell reprogramming by endogenously produced lactic acid. *J Immunol* **191**, 3090-3099 (2013). https://doi.org:10.4049/jimmunol.1300772
290 Paolini, L. *et al.* Lactic Acidosis Together with GM-CSF and M-CSF Induces Human Macrophages toward an Inflammatory Protumor Phenotype. *Cancer Immunol Res* **8**, 383-395 (2020). https://doi.org:10.1158/2326-6066.CIR-18-0749
291 Hahn, E. L., Halestrap, A. P. & Gamelli, R. L. Expression of the lactate transporter MCT1 in macrophages. *Shock* **13**, 253-260 (2000). https://doi.org:10.1097/00024382-200004000-00001
292 Li, B. *et al.* Expression of Monocarboxylate Transporter 1 in Immunosuppressive Macrophages Is Associated With the Poor Prognosis in Breast Cancer. *Front Oncol* **10**, 574787 (2020). https://doi.org:10.3389/fonc.2020.574787
293 Morrissey, S. M. *et al.* Tumor-derived exosomes drive immunosuppressive macrophages in a pre-metastatic niche through glycolytic dominant metabolic reprogramming. *Cell Metab* **33**, 2040-2058 e2010 (2021). https://doi.org:10.1016/j.cmet.2021.09.002
294 Li, Z. *et al.* Lactate in the tumor microenvironment: A rising star for targeted tumor therapy. *Front Nutr* **10**, 1113739 (2023). https://doi.org:10.3389/fnut.2023.1113739
295 Bonuccelli, G. *et al.* Ketones and lactate "fuel" tumor growth and metastasis: Evidence that epithelial cancer cells use oxidative mitochondrial metabolism. *Cell Cycle* **9**, 3506-3514 (2010). https://doi.org:10.4161/cc.9.17.12731
296 Andreucci, E. *et al.* Extracellular Lactic Acidosis of the Tumor Microenvironment Drives Adipocyte-to-Myofibroblast Transition Fueling the Generation of Cancer-Associated Fibroblasts. *Cells* **12** (2023). https://doi.org:10.3390/cells12060939
297 Linares, J. F. *et al.* The lactate-NAD(+) axis activates cancer-associated fibroblasts by downregulating p62. *Cell Rep* **39**, 110792 (2022). https://doi.org:10.1016/j.celrep.2022.110792
298 Kitamura, F. *et al.* Cancer-associated fibroblasts reuse cancer-derived lactate to maintain a fibrotic and immunosuppressive microenvironment in pancreatic cancer. *JCI Insight* **8** (2023). https://doi.org:10.1172/jci.insight.163022
299 Halestrap, A. P. & Meredith, D. The SLC16 gene family-from monocarboxylate transporters (MCTs) to aromatic amino acid transporters and beyond. *Pflugers Arch* **447**, 619-628 (2004). https://doi.org:10.1007/s00424-003-1067-2
300 Guan, X. & Morris, M. E. In Vitro and In Vivo Efficacy of AZD3965 and Alpha-Cyano-4-Hydroxycinnamic Acid in the Murine 4T1 Breast Tumor Model. *AAPS J* **22**, 84 (2020). https://doi.org:10.1208/s12248-020-00466-9
301 McNeillis, R. *et al.* A case of malignant hyperlactaemic acidosis appearing upon treatment with the mono-carboxylase transporter 1 inhibitor AZD3965. *Br J Cancer* **122**, 1141-1145 (2020). https://doi.org:10.1038/s41416-020-0727-8
302 Bisbach, C. M., Hass, D. T., Thomas, E. D., Cherry, T. J. & Hurley, J. B. Monocarboxylate Transporter 1 (MCT1) Mediates Succinate Export in the Retina. *Invest Ophthalmol Vis Sci* **63**, 1 (2022). https://doi.org:10.1167/iovs.63.4.1
303 Gerhart, D. Z., Leino, R. L. & Drewes, L. R. Distribution of monocarboxylate transporters MCT1 and MCT2 in rat retina. *Neuroscience* **92**, 367-375 (1999). https://doi.org:10.1016/s0306-4522(98)00699-x
304 Brudno, J. N. & Kochenderfer, J. N. Toxicities of chimeric antigen receptor T cells: recognition and management. *Blood* **127**, 3321-3330 (2016). https://doi.org:10.1182/blood-2016-04-703751

305 Karschnia, P. *et al.* Toxicities and Response Rates of Secondary CNS Lymphoma After Adoptive Immunotherapy With CD19-Directed Chimeric Antigen Receptor T Cells. *Neurology* **98**, 884-889 (2022). https://doi.org:10.1212/WNL.0000000000200608
306 Xiao, X. *et al.* Mechanisms of cytokine release syndrome and neurotoxicity of CAR T-cell therapy and associated prevention and management strategies. *J Exp Clin Cancer Res* **40**, 367 (2021). https://doi.org:10.1186/s13046-021-02148-6
307 Cappell, K. M. *et al.* Long-Term Follow-Up of Anti-CD19 Chimeric Antigen Receptor T-Cell Therapy. *J Clin Oncol* **38**, 3805-3815 (2020). https://doi.org:10.1200/JCO.20.01467
308 Kueberuwa, G., Zheng, W., Kalaitsidou, M., Gilham, D. E. & Hawkins, R. E. A Syngeneic Mouse B-Cell Lymphoma Model for Pre-Clinical Evaluation of CD19 CAR T Cells. *J Vis Exp* (2018). https://doi.org:10.3791/58492
309 Pennell, C. A. *et al.* Human CD19-Targeted Mouse T Cells Induce B Cell Aplasia and Toxicity in Human CD19 Transgenic Mice. *Mol Ther* **26**, 1423-1434 (2018). https://doi.org:10.1016/j.ymthe.2018.04.006
310 Kueberuwa, G., Kalaitsidou, M., Cheadle, E., Hawkins, R. E. & Gilham, D. E. CD19 CAR T Cells Expressing IL-12 Eradicate Lymphoma in Fully Lymphoreplete Mice through Induction of Host Immunity. *Mol Ther Oncolytics* **8**, 41-51 (2018). https://doi.org:10.1016/j.omto.2017.12.003
311 Kumar, A. & Chamoto, K. Immune metabolism in PD-1 blockade-based cancer immunotherapy. *Int Immunol* **33**, 17-26 (2021). https://doi.org:10.1093/intimm/dxaa046
312 Wang, Z. H., Peng, W. B., Zhang, P., Yang, X. P. & Zhou, Q. Lactate in the tumour microenvironment: From immune modulation to therapy. *EBioMedicine* **73**, 103627 (2021). https://doi.org:10.1016/j.ebiom.2021.103627
313 Kaymak, I. *et al.* Carbon source availability drives nutrient utilization in CD8(+) T cells. *Cell Metab* **34**, 1298-1311 e1296 (2022). https://doi.org:10.1016/j.cmet.2022.07.012
314 Barbieri, L. *et al.* Lactate exposure shapes the metabolic and transcriptomic profile of CD8+ T cells. *Front Immunol* **14**, 1101433 (2023). https://doi.org:10.3389/fimmu.2023.1101433
315 Feng, Q. *et al.* Lactate increases stemness of CD8 + T cells to augment anti-tumor immunity. *Nat Commun* **13**, 4981 (2022). https://doi.org:10.1038/s41467-022-32521-8
316 Macchi, C. *et al.* Monocarboxylate transporter 1 deficiency impacts CD8(+) T lymphocytes proliferation and recruitment to adipose tissue during obesity. *iScience* **25**, 104435 (2022). https://doi.org:10.1016/j.isci.2022.104435
317 Gudgeon, N. *et al.* Succinate uptake by T cells suppresses their effector function via inhibition of mitochondrial glucose oxidation. *Cell Rep* **40**, 111193 (2022). https://doi.org:10.1016/j.celrep.2022.111193
318 De Rosa, V. *et al.* Glycolysis controls the induction of human regulatory T cells by modulating the expression of FOXP3 exon 2 splicing variants. *Nat Immunol* **16**, 1174-1184 (2015). https://doi.org:10.1038/ni.3269
319 Shi, L. Z. *et al.* HIF1alpha-dependent glycolytic pathway orchestrates a metabolic checkpoint for the differentiation of TH17 and Treg cells. *J Exp Med* **208**, 1367-1376 (2011). https://doi.org:10.1084/jem.20110278
320 Schoeppe, R. *et al.* Glutamine synthetase expression rescues human dendritic cell survival in a glutamine-deprived environment. *Front Oncol* **13**, 1120194 (2023). https://doi.org:10.3389/fonc.2023.1120194
321 Liu, P. S. *et al.* alpha-ketoglutarate orchestrates macrophage activation through metabolic and epigenetic reprogramming. *Nat Immunol* **18**, 985-994 (2017). https://doi.org:10.1038/ni.3796
322 Cooray, S., Howe, S. J. & Thrasher, A. J. Retrovirus and lentivirus vector design and methods of cell conditioning. *Methods Enzymol* **507**, 29-57 (2012). https://doi.org:10.1016/B978-0-12-386509-0.00003-X

323 Sniegowski, T., Korac, K., Bhutia, Y. D. & Ganapathy, V. SLC6A14 and SLC38A5 Drive the Glutaminolysis and Serine-Glycine-One-Carbon Pathways in Cancer. *Pharmaceuticals (Basel)* **14** (2021). https://doi.org:10.3390/ph14030216
324 Lowman, X. H. *et al.* p53 Promotes Cancer Cell Adaptation to Glutamine Deprivation by Upregulating Slc7a3 to Increase Arginine Uptake. *Cell Rep* **26**, 3051-3060 e3054 (2019). https://doi.org:10.1016/j.celrep.2019.02.037
325 Ho, S. C. *et al.* Comparison of internal ribosome entry site (IRES) and Furin-2A (F2A) for monoclonal antibody expression level and quality in CHO cells. *PLoS One* **8**, e63247 (2013). https://doi.org:10.1371/journal.pone.0063247
326 Magill, G. B. *et al.* Pharmacological and initial therapeutic observations on 6-diazo-5-oxo-1-norleucine (DON) in human neoplastic disease. *Cancer* **10**, 1138-1150 (1957). https://doi.org:10.1002/1097-0142(195711/12)10:6<1138::aid-cncr2820100608>3.0.co;2-k
327 Zhong, L. *et al.* Small molecules in targeted cancer therapy: advances, challenges, and future perspectives. *Signal Transduct Target Ther* **6**, 201 (2021). https://doi.org:10.1038/s41392-021-00572-w
328 Lin, A. *et al.* Off-target toxicity is a common mechanism of action of cancer drugs undergoing clinical trials. *Sci Transl Med* **11** (2019). https://doi.org:10.1126/scitranslmed.aaw8412
329 Yoo, H. C. *et al.* A Variant of SLC1A5 Is a Mitochondrial Glutamine Transporter for Metabolic Reprogramming in Cancer Cells. *Cell Metab* **31**, 267-283 e212 (2020). https://doi.org:10.1016/j.cmet.2019.11.020
330 Zhang, Z. *et al.* ASCT2 (SLC1A5)-dependent glutamine uptake is involved in the progression of head and neck squamous cell carcinoma. *Br J Cancer* **122**, 82-93 (2020). https://doi.org:10.1038/s41416-019-0637-9
331 Broer, A., Fairweather, S. & Broer, S. Disruption of Amino Acid Homeostasis by Novel ASCT2 Inhibitors Involves Multiple Targets. *Front Pharmacol* **9**, 785 (2018). https://doi.org:10.3389/fphar.2018.00785
332 Gong, T. *et al.* Glutamine metabolism in cancers: Targeting the oxidative homeostasis. *Front Oncol* **12**, 994672 (2022). https://doi.org:10.3389/fonc.2022.994672
333 Jha, A. K. *et al.* Network integration of parallel metabolic and transcriptional data reveals metabolic modules that regulate macrophage polarization. *Immunity* **42**, 419-430 (2015). https://doi.org:10.1016/j.immuni.2015.02.005
334 Mestre-Farrera, A. *et al.* Glutamine-Directed Migration of Cancer-Activated Fibroblasts Facilitates Epithelial Tumor Invasion. *Cancer Res* **81**, 438-451 (2021). https://doi.org:10.1158/0008-5472.CAN-20-0622
335 Yang, L. *et al.* Targeting Stromal Glutamine Synthetase in Tumors Disrupts Tumor Microenvironment-Regulated Cancer Cell Growth. *Cell Metab* **24**, 685-700 (2016). https://doi.org:10.1016/j.cmet.2016.10.011
336 Reinfeld, B. I. *et al.* Cell-programmed nutrient partitioning in the tumour microenvironment. *Nature* **593**, 282-288 (2021). https://doi.org:10.1038/s41586-021-03442-1
337 Van Campenhout, R., Muyldermans, S., Vinken, M., Devoogdt, N. & De Groof, T. W. M. Therapeutic Nanobodies Targeting Cell Plasma Membrane Transport Proteins: A High-Risk/High-Gain Endeavor. *Biomolecules* **11** (2021). https://doi.org:10.3390/biom11010063
338 Ruiz-Lopez, E. *et al.* Nanobodies targeting ABCC3 for immunotargeted applications in glioblastoma. *Sci Rep* **12**, 22581 (2022). https://doi.org:10.1038/s41598-022-27161-3
339 Balaji, S. A., Udupa, N., Chamallamudi, M. R., Gupta, V. & Rangarajan, A. Role of the Drug Transporter ABCC3 in Breast Cancer Chemoresistance. *PLoS One* **11**, e0155013 (2016). https://doi.org:10.1371/journal.pone.0155013
340 Zhao, Y. *et al.* ABCC3 as a marker for multidrug resistance in non-small cell lung cancer. *Sci Rep* **3**, 3120 (2013). https://doi.org:10.1038/srep03120

341 Fumey, W. *et al.* Nanobodies effectively modulate the enzymatic activity of CD38 and allow specific imaging of CD38(+) tumors in mouse models in vivo. *Sci Rep* **7**, 14289 (2017). https://doi.org:10.1038/s41598-017-14112-6
342 Dwivedi, S., Rendon-Huerta, E. P., Ortiz-Navarrete, V. & Montano, L. F. CD38 and Regulation of the Immune Response Cells in Cancer. *J Oncol* **2021**, 6630295 (2021). https://doi.org:10.1155/2021/6630295
343 Lakhter, A. J. *et al.* Glucose-independent Acetate Metabolism Promotes Melanoma Cell Survival and Tumor Growth. *J Biol Chem* **291**, 21869-21879 (2016). https://doi.org:10.1074/jbc.M115.712166
344 Cheng, T. *et al.* Pyruvate carboxylase is required for glutamine-independent growth of tumor cells. *Proc Natl Acad Sci U S A* **108**, 8674-8679 (2011). https://doi.org:10.1073/pnas.1016627108
345 Biancur, D. E. *et al.* Compensatory metabolic networks in pancreatic cancers upon perturbation of glutamine metabolism. *Nat Commun* **8**, 15965 (2017). https://doi.org:10.1038/ncomms15965
346 Tajan, M. *et al.* A Role for p53 in the Adaptation to Glutamine Starvation through the Expression of SLC1A3. *Cell Metab* **28**, 721-736 e726 (2018). https://doi.org:10.1016/j.cmet.2018.07.005